A Cascade of Molecular Events During Neural Induction

Katherine Elizabeth Trevers

University College London

2015

Thesis submitted in fulfilment of the
requirements for the degree of
Doctor of Philosophy in Developmental Biology.

‘I, Katherine Elizabeth Trevers, confirm that the work presented in this thesis is my own. Where information has been derived from other sources, I confirm that this has been indicated in the thesis.'

Acknowledgements

I must begin by acknowledging the guidance of Professor Claudio Stern, from whom I have learnt so much. Thank you for letting me contribute to a project which has been such a big part of your academic career.

I am indebted to the many colleagues who have supported me along the way. I share a great deal of the credit for my research with Mohsin Khan, who spent endless and often futile hours rooted to one computer. This project would also not have been possible without the ever-cheerful Nidia de Oliveira, who always went out of her way to solve so many of our problems.

To the "Stern chicks"; Claire, Lizzy, Nati, Matt and Irene -thank you for being constant sources of advice, encouragement and entertainment. I can't imagine how I ever would have managed without you, but also the many others who have passed through our doors; notably Božka, Angela, Jackie, Anna, Ana, Ingrid and Sharon. I feel compelled to mention BBC Radio 2 for getting us through those long hours of embryology.

To my family, especially Anna and Matt -thank you for sharing this mad world with me. Remember, what doesn't kill you makes you stronger. Also not to forget Charlie -for making me smile without saying anything at all, the way only a dog can.

However I owe my deepest gratitude to Tom. For putting up with the late nights and early mornings, for always finding a way to calm my nerves and encouraging me to stop and celebrate my achievements. You're the best distraction I could have asked for.

In memory of Oma and Dziadzia

Abstract

Neural induction is the process by which a region of ectoderm acquires a neural identity and forms the neural plate. A popular explanation for neural induction is the “default model”. This proposes that non-neural cells are specified as epidermal by BMP expression and that inhibition of this signal at the end of gastrulation is sufficient to induce neural fate. Although this model is attractive in its simplicity, accumulating evidence suggests a more complex scenario, where neural induction comprises a series of sequential events and multiple signals. However the details of this hierarchy are unclear, as are the specific contributions of different signalling pathways.

Using a range of known markers, we first characterised the progression of neural induction. The earliest responses occur in competent cells within 3h of exposure to a grafted organizer, but 9-12h are required before cells become committed to a neural fate. To identify all transcriptional responses to neural induction during this time-course, an RNA-Seq screen was conducted. It identified 482 differentially expressed transcriptional regulators. After verifying the expression of 166, we confirm that the screen accurately predicts events that occur in the normal embryo during neural induction. Distinct markers define the specification of key states before cells adopt neural commitment. Furthermore, transitions between these states are probably regulated by multiple layers of transcriptional repression and activation. Therefore neural induction must occur as a cascade of molecular events.

We also demonstrate that FGF signalling makes a major contribution to the onset of neural induction by inducing transcription factors and chromatin modifiers. These are normally expressed in the pre-streak embryo, providing further evidence that neural induction begins before gastrulation. This pre-neural state is transcriptionally similar to the neural plate border but is also heavily associated with pluripotency -perhaps suggesting that FGFs function to induce a multipotent “pre-neural/pre-border” state.

List of Abbreviations

AP	Alkaline phosphatase
AVE	Anterior Visceral Endoderm
BCIP	5-Bromo-4-chloro-3-indolyl phosphate
BMP	Bone morphogenetic protein
BRA	Brachyury
BSA	Bovine serum albumin
ChEST	Chicken expressed sequence tags
DAB	3,3'-Diaminobenzidine
DIG	Digoxigenin
DPP	Decapentaplegic
EGF	Epidermal growth factor
EGK	Eyal-Giladi and Kochav stage
EMT	Epithelial-mesenchymal transition
ESC	Embryonic stem cell
FGF	Fibroblast growth factor
FLU	Fluorescein
GSC	Goosecoid
HGF	Hepatocyte growth factor
HGF/SF	Hepatocyte growth factor/scatter factor
HH	Hamburger Hamilton stage
HRP	Horseradish peroxidase
HYB	Hybridisation buffer
IGF	Insulin growth factor
NBT	4-Nitro blue tetrazolium chloride
NICD	Notch intracellular domain
NOG	Noggin
NPB	Neural pate border
PBS	Phosphate-buffered saline
PBTW	Phosphate buffered saline containing tween
PFA	Paraformaldehyde
PKC	Protein kinase C
PPR	Pre-placodal region
Pre-streak	Pre-primitive streak stage
SHH	Sonic hedgehog
TBST	Tris-buffered saline containing tween
WNT	Wingless/INT

Contents

Figures and Tables

Chapter 1: Introduction

1.1 Early embryonic development in chick

Chicken eggs are laid 20h post fertilisation when the blastoderm already consists of 20,000 cells generated after rounds of meroblastic, equatorial and vertical cleavage (Arendt and Nubler-Jung, 1999, Stern, 2004a). At these early stages, embryonic development is described according to the system defined by Eyal-Giladi and Kochav (EGK) using roman numerals between I-XIV (Eyal-Giladi and Kochav, 1976). Upon laying, the embryo is already at around EGKIX-X and can be divided into two domains: the area opaca, an outer ring of cells whose edges are attached to the vitelline membrane and within this, the area pellucida (Eyal-Giladi and Kochav, 1976). The epiblast, a single cell thick epithelium, is continuous across both regions and several layers of opaque yolky cells underlie the epiblast of the area opaca (Bancroft and Bellairs, 1974, Bellairs *et al.*, 1975). In contrast, the area pellucida is more translucent, although initially (at EGK IX-X) it too is populated sparsely by islands of yolky cells (Eyal-Giladi and Kochav, 1976, Kochav *et al.*, 1980, Fabian and Eyal-Giladi, 1981, Eyal-Giladi, 1984). The marginal zone marks the boundary between the area pellucida and area opaca (Stern and Ireland, 1981, Stern, 1990). Koller's sickle, a crescent-shaped ridge of cells, projects ventrally from the epiblast and marks the posterior border between the area pellucida and marginal zone (Koller, 1882, Callebaut and Van Nueten, 1994).

After further incubation, dramatic cellular and tissue rearrangements take place. First, the sparse yolky cells of the area pellucida fuse in a wave starting posteriorly. This forms a continuous layer called the hypoblast (Vakaet, 1970, Stern, 1990) which is equivalent to the mouse anterior visceral endoderm (AVE) (Bachvarova *et al.*, 1998, Foley *et al.*, 2000, Bertocchini and Stern, 2002). At EGKXII the hypoblast has only made a layer over the posterior half the area pellucida, but by EGKXIII this is almost complete anteriorly such that the area pellucida is now two-layered (Eyal-Giladi and Kochav, 1976, Kochav *et al.*, 1980). Following this, the hypoblast starts to become displaced anteriorly by the endoblast which forms from the posterior germ wall, a layer of yolky cells firmly attached to the area opaca epiblast (Stern, 1990). However, neither the hypoblast nor endoblast contributes to the embryo proper; later they only contribute to the yolk sac (Rosenquist, 1972, Lawson and Pedersen, 1987). At EGKXIV, a thickening referred to as the "posterior bridge", projects behind Koller's sickle and the primitive streak forms shortly thereafter (Stern, 2004a).

1.2 Gastrulation in chick

Gastrulation, which generates the three germ layers, (ectoderm, mesoderm and endoderm) is characterised by the formation and elongation of the primitive streak. Once this begins, chick embryonic development is described using Arabic numerals, according to the scheme devised by Hamburger and Hamilton (HH) (Hamburger and Hamilton, 1951). Fate mapping experiments demonstrate that the streak forms from Koller's sickle and a population of cells local to the site of streak formation (Bachvarova *et al.*, 1998, Wei and Mikawa, 2000) but also incorporates cells that ingress from the epiblast over a wide area (Stern and Canning, 1990, Voiculescu *et al.*, 2014). It starts at HH2 as a triangular structure at the posterior edge of the area pellucida, between the epiblast and endoblast. The streak then lengthens to form a distinctive rod of mesenchymal cells which defines HH3 (Hamburger and Hamilton, 1951, Eyal-Giladi and Kochav, 1976, Kochav *et al.*, 1980). Recently the large scale tissue movements that occur during streak formation have been shown to result from local cell interactions (Voiculescu *et al.*, 2014). Epiblast cells fated to form the streak, first intercalate along the prospective midline to extend into the centre of the embryo. Starting posteriorly, cells behind the extending tip of the prospective streak undergo epithelial-mesenchymal transition and then ingress between the epiblast and hypoblast to form streak mesenchyme. Together these two processes can account for the characteristic "polonaise" movements that occur in the epiblast either side of the forming streak (Voiculescu *et al.*, 2007, Voiculescu *et al.*, 2014).

At HH3+, the primitive groove develops longitudinally in the epiblast layer of the primitive streak, through which streak mesenchyme migrates laterally to form the lateral plate mesoderm (Vakaet, 1970). Now, the epiblast of the anterior area pellucida which will later give rise to neural tissue is referred to as the "prospective neural plate" (Rudnick, 1935, Spratt, 1952, Rosenquist, 1981). However, some of these epiblast cells actually migrate through the primitive streak to form mesoderm and endoderm between HH3+ and HH4+ (Bellairs, 1953a, Bellairs, 1953b, Bellairs, 1957, Vakaet, 1962, Nicolet, 1967, Selleck and Stern, 1991, Schoenwolf *et al.*, 1992, Psychoyos and Stern, 1996a, Joubin and Stern, 1999, Kimura *et al.*, 2006). At HH4, Hensen's node forms from all three tissue layers as a swelling at the tip of the primitive streak (Hensen, 1876) and the neural plate proper arises as a thickening of epiblast cells surrounding the node (Bancroft and Bellairs, 1975). The head process emerges anteriorly from the node at HH4+ (Spratt, 1947, Bellairs, 1953b), to form the prechordal mesendoderm (Seifert *et al.*, 1993, Foley *et al.*, 1997, Joubin and Stern, 1999). Gastrulation is complete by HH5 when ingression movements through the streak have ended (Vakaet, 1962, Selleck and Stern, 1991, Schoenwolf *et al.*, 1992, Joubin and Stern, 1999). From HH5, the embryo and neural plate lengthen posteriorly as Hensen's node regresses (Spratt, 1947) and starting at

HH7, somites bud off sequentially in a rostro-caudal manner from the presomitic mesoderm either side of the midline (Keynes and Stern, 1988). The neural folds at the lateral edges of the neural plate start to elevate and fuse dorsally by HH9, a process that extends progressively down the dorsal midline to form a neural tube (Schoenwolf and Smith, 1990).

1.3 The organizer and neural induction

During gastrulation in chick the neural plate proper arises as an ectodermal thickening around Hensen's node at HH4, by a process known as neural induction. Embryonic induction was defined by Gurdon as *"... an interaction between one (inducing) tissue and another (responding) tissue, as a result of which the responding tissue undergoes a change in its direction of differentiation"* (Gurdon, 1987). Therefore, embryonic neural induction refers the process by which ectodermal cells acquire a neural fate in response to neuralising signals, and form the neural plate rather than give rise to other structures such as epidermis or mesoderm (Stern, 2004a).

In 1924, the ground-breaking experiments of Spemann and Mangold demonstrated that transplanting the dorsal lip of the amphibian blastopore to the ventral side of a gastrula stage host embryo, generates a secondary axis (Spemann and Mangold, 1924). By using inter-species grafts between three species of newt with different pigmentation, they showed that these axes include almost the entire early central nervous system derived from the host. In contrast the graft differentiated into mesodermal derivatives and contributed some cells to the induced floor plate (Spemann, 1921, Spemann and Mangold, 1924, Gimlich and Cooke, 1983). Therefore, when transplanted into a region fated to become epidermis, the dorsal blastopore lip has the ability to induce a secondary neural axis. It was the first demonstration that instructive signals from the dorsal lip of the blastopore, now famously known as the Spemann's Organizer, are capable of neural induction.

Subsequently, equivalent regions were discovered in all other classes of vertebrates. Hensen's node (Hensen, 1876), at the tip of the primitive streak, is the functional equivalent in birds and mammals (Waddington, 1932, Waddington, 1933, Waddington, 1936, Waddington, 1937, Beddington, 1994). In teleosts it is known as the embryonic shield; a thickening at the dorsal edge of the embryo during the formation of the germ ring (Luther, 1935, Oppenheimer, 1936b, Shih and Fraser, 1996). Inter-specific grafts (even across vertebrate classes) can also induce secondary axes, suggesting that the mechanisms of neural induction are conserved (Waddington, 1934, Oppenheimer, 1936a, Kintner and Dodd, 1991, Blum *et al.*, 1992, Hatta and Takahashi, 1996).

1.4 The search for neural inducing signals

After the organizer's ability to induce a nervous system was demonstrated (Spemann and Mangold, 1924), began the search for the responsible inductive signals. For more than six decades, embryos and ectodermal explants were exposed to a wide variety of substances including: dead organizers boiled in alcohol, methylene blue, high and low pH, guinea pig bone marrow, blue jay liver, sterols, fatty acids, grains of sand, steroids and protein extracts. This search failed to identify any specific neural inducing signals as all substances were able to neuralise embryonic ectoderm as effectively as an organizer graft (reviewed in (Nakamura and Toivonen, 1978)). Eventually it was realised that newt ectoderm, which was frequently used, could be neuralised in the absence of an inducer just by culturing animal caps in inadequate saline, suggesting that newt tissue was unsuitable for these experiments (Barth, 1941, Holtfreter, 1944).

It wasn't until the mid-90s that several, apparently unrelated, observations started to shed light on the molecular basis of neural induction. First, in *Xenopus,* which is more resistant to neuralisation than newt, it was observed that neural tissue can be induced merely by transient cell disaggregation of gastrula stage animal caps (Born *et al.*, 1989, Godsave and Slack, 1989, Grunz and Tacke, 1989, Sato and Sargent, 1989). With the onset of the molecular era came the finding that inhibition of "Activin" signalling by injection of a dominant-negative Activin receptor (XAR1, now known as Activin Receptor Type 2B), also generates neural tissue in isolated animal caps (Hemmati-Brivanlou and Melton, 1992, Hemmati-Brivanlou *et al.*, 1992, Hemmati-Brivanlou and Melton, 1994). Then, three genes which encode proteins with neural inducing ability were isolated from the organizer; Noggin (Smith and Harland, 1992, Lamb *et al.*, 1993, Smith *et al.*, 1993), Follistatin (Hemmati-Brivanlou *et al.*, 1994) and Chordin (Sasai *et al.*, 1994, Sasai *et al.*, 1995). Although a specific function linking these observations was not clear, it was suggested that neuralisation might occur by the removal of an inhibitory substance in each assay, rather than by an instructive signal (Hemmati-Brivanlou and Melton, 1994).

Several other findings began to reinforce the idea of a permissive signal. At around the same time, misexpression of BMP4 -a member of the TGFβ superfamily, was found to severely ventralise *Xenopus* embryos (Dale *et al.*, 1992, Jones *et al.*, 1992) by inducing epidermis at the expense of neural fated tissue (Hawley *et al.*, 1995, Wilson and Hemmati-Brivanlou, 1995). Then, Noggin, Chordin and Follistatin, which have the opposite dorsalising and neuralising effect, were found to antagonise BMP signalling by binding to BMPs such as BMP4 (Piccolo *et al.*, 1996, Zimmerman *et al.*, 1996, Fainsod *et al.*, 1997). Furthermore, the dominant-negative Activin receptor XAR1 was found to inhibit both TGFβ and BMP pathways (Hemmati-Brivanlou

and Melton, 1992). Together these findings hinted that neural induction might involve the inhibition of BMP signalling.

1.5 BMPs, BMP antagonism and the "default model"

These observations were finally reconciled by the "default model" of neural induction (Hemmati-Brivanlou and Melton, 1997), which suggested that ectodermal cells will autonomously acquire a neural fate in the absence of signals. However, *in vivo*, BMP4 is expressed throughout the ectoderm where it potently inhibits the formation of the neural plate and instead specifies cells to become epidermis (Fainsod *et al.*, 1994). The model implies that the secretion of BMP antagonists from the organizer overcomes this inhibition to effectively create a "default" neural state (Hemmati-Brivanlou and Melton, 1997). In agreement with this, BMP4 transcripts are initially expressed throughout the ectoderm before gastrulation and clear from the neural plate as it forms (Fainsod *et al.*, 1994).

Consistent with the "default" model's predictions, animal caps from embryos injected with mRNA for BMP pathway targets MSX1 (Suzuki *et al.*, 1997b), SMAD1 (Wilson *et al.*, 1997) or SMAD5 (Suzuki *et al.*, 1997a) cannot be neuralised by dissociation, leading to the suggestion that dissociation causes neuralisation by diluting away BMPs present in the animal hemisphere (Munoz-Sanjuan and Brivanlou, 2002). Conversely, inhibition of BMP signalling by expression of dominant-negative BMP receptors (Hemmati-Brivanlou and Melton, 1994), non-cleavable forms of BMP4 or BMP7 (Hawley *et al.*, 1995), or antisense BMP RNA (Sasai *et al.*, 1995) can neuralise animal caps without dissociation. It seemed that finally a molecular mechanism existed to describe neural induction, more than 70 years after Spemann and Mangold first discovered the organizer.

Since then, homologues for Noggin (Valenzuela *et al.*, 1995, Tonegawa and Takahashi, 1998, Furthauer *et al.*, 1999), Chordin (Schulte-Merker *et al.*, 1997, Pappano *et al.*, 1998, Streit *et al.*, 1998) and Follistatin (Albano *et al.*, 1994, Connolly *et al.*, 1995, Bauer *et al.*, 1998) have been identified in chick, mouse, zebrafish and many other organisms. The importance of endogenous BMP antagonists is further reinforced by the discovery of various other secreted factors that inhibit the BMP pathway. Several are also expressed in or around the organizer in a number of organisms, including Cerberus (Bouwmeester *et al.*, 1996, Belo *et al.*, 1997), Caronte (Rodriguez Esteban *et al.*, 1999, Yokouchi *et al.*, 1999), Dante (Pearce *et al.*, 1999) and Xnr3 (Smith *et al.*, 1995, Hansen *et al.*, 1997). A comprehensive summary of secreted BMP inhibitors, their expression and targets can be found in (Ozair *et al.*, 2013).

Other evidence for the evolutionary conservation of BMP antagonists in neural *versus* epidermal fate decisions come from studies of *Drosophila* Chordin homologue; short gastrulation (SOG) (Francois *et al.*, 1994, Francois and Bier, 1995), which was identified from a screen for genes involved in dorsoventral patterning (Zusman *et al.*, 1988). Even in the Protostome clade, where dorsal territories give rise to epidermis and ventral territories form neuroectoderm (the reversal of blastopore fate, from mouth in Protostomes to anus in Deuterostomes, caused a reversal of the oral/aboral axis and consequently also of dorsoventral orientation (Geoffroy Saint-Hilaire, 1822)), the separation of these fates still requires BMP inhibition (De Robertis and Sasai, 1996). Here, ventral SOG promotes neural fate by directly antagonising dorsal Decapentaplegic (DPP) (Holley *et al.*, 1995, Biehs *et al.*, 1996), a BMP4 homologue (Padgett *et al.*, 1993), which generates a dorsoventral gradient of DPP activity (Ferguson and Anderson, 1992, Wharton *et al.*, 1993, Ashe and Levine, 1999) which is lowest ventrally in the future neural domain. The similarities between these proteins is further demonstrated by the promotion of dorsal and neural structures by SOG mRNA in *Xenopus* (Holley *et al.*, 1995, Schmidt *et al.*, 1995) and ventral structures by Chordin mRNA in *Drosophila* or DPP in *Xenopus* (Holley *et al.*, 1995). Furthermore vertebrate BMP ligands can replace DPP in null mutants (Padgett *et al.*, 1993), confirming the conservation function of these proteins (De Robertis and Sasai, 1996, Ferguson, 1996).

Arthropods such as spiders (Akiyama-Oda and Oda, 2006) and beetles (van der Zee *et al.*, 2006) also rely on SOG to ventralise their ectoderm. Inhibition of HrBMPb -a BMP2/4 homologue, is required for the formation of anterior neural fate in *Halocynthia* so it appears to function as a neural inhibitor (Miya *et al.*, 1997), however BMP inhibition is not the neural inducer in *Ciona*, another urochordate (Bertrand *et al.*, 2003). Another exception is Acorn worms (hemichordates), where BMP misexpression does not inhibit neural markers and BMP inhibition does not promote neuralisation, although the ectoderm of this species does not normally segregate into distinct neural and epidermal domains (Lowe *et al.*, 2006).

Together, this body of literature strongly suggests that BMP inhibition is required for neural fate specification across a wide range of metazoans. But is it sufficient?

1.6 Challenging the "default model"; is BMP inhibition sufficient for neural induction?

The "default model" implies two things; that neural induction occurs during gastrulation and that a single stimulus; BMP inhibition by endogenous BMP antagonists in the organizer, is sufficient to induce neural fate. Despite considerable evidence supporting the role of BMP antagonists in neural induction the "default model" has been challenged by a number of observations.

In chick, neither Noggin or Follistatin are expressed in the organizer when the neural plate forms; Follistatin is expressed at HH4 in a ring around Hensen's node (Levin, 1998) while Noggin is first expressed in the head process at HH4+/5, and later in the notochord (Streit and Stern, 1999a). They are similarly absent from the embryonic shield in zebrafish (Bauer *et al.*, 1998). Chordin is expressed in Hensen's node at HH3 (Streit *et al.*, 1998) so it could contribute to neural induction, but it alone is unlikely to function as the "neural inducer" because its expression continues beyond HH4 when the node has lost its neural inducing ability (Dias and Schoenwolf, 1990, Storey *et al.*, 1992). Furthermore, BMP4 (Streit *et al.*, 1998) and the BMP signalling component phospho-SMAD1 (Faure *et al.*, 2002), are already absent from the epiblast at HH2-3; before Hensen's node arises and later they are only expressed in the neural plate border at HH4+ (Streit *et al.*, 1998, Faure *et al.*, 2002). As the "default model" (Hemmati-Brivanlou and Melton, 1997) implies that BMP antagonists present in the organizer are sufficient to inhibit BMP expression in the ectoderm during gastrulation, these BMPs and antagonists are not expressed in the appropriate tissues or at the appropriate stages in chick to fit with this model.

Loss- and gain-of-function experiments also do not produce the expected results in chick. Misexpression of Chordin or Noggin in competent epiblast (see Chapter 1.10) is not sufficient to induce an ectopic neural plate or the neural markers SOX3 or SOX2 in cells that can respond to signals from a grafted organizer (Streit *et al.*, 1998, Streit and Stern, 1999g). Even a combination of several potent BMP inhibitors (SMAD6, dominant-negative BMP receptor, Noggin and Chordin) to inhibit BMP signalling as strongly as possible, is still unable to induce SOX2 expression (Linker and Stern, 2004). In addition, misexpression of BMP4 or BMP7 in the epiblast at EGKXIII or prospective neural plate at HH3+ has no effect on the expression of SOX3 by HH5, but it can inhibit the expression of SOX2, a later neural marker (Streit *et al.*, 1998, Linker and Stern, 2004). However, although it cannot induce SOX3, Chordin can maintain its expression after it has been induced by 5h of signals from an organizer graft (Streit *et al.*, 1998). Together, these results suggest that BMP inhibition is not sufficient for neural induction and that BMP signalling can only prevent expression of late but not early neural markers. The

interpretation of this is that other signals are required before BMP inhibition, which is only required as a later step, perhaps to maintain markers that have already been induced.

In agreement with this suggestion, zebrafish and mouse mutants are not grossly affected by the absence of BMP antagonism. Although ventralised, zebrafish *chordino* mutants still form a slightly smaller neural plate and a relatively normal nervous system (Kishimoto *et al.*, 1997, Schulte-Merker *et al.*, 1997, Bauer *et al.*, 1998). In mouse, Noggin (Brunet *et al.*, 1998, McMahon *et al.*, 1998) or Cerberus (Belo *et al.*, 2000) mutants still form a neural plate, BMP2 (Zhang and Bradley, 1996) and BMP7 (Dudley *et al.*, 1995) mutants do not display an early epidermal phenotype while BMP4 (Winnier *et al.*, 1995) mutants die of more generalised developmental defects. More severe defects are observed in Noggin/Chordin double mutants, but these still form a distinct neural plate (Bachiller *et al.*, 2000). Therefore, loss of one or two BMPs or BMP antagonists does not significantly affect epidermal *versus* neural cell choices. Severe loss of neural tissue is only observed in *Xenopus* (Khokha *et al.*, 2005) and zebrafish (Dal-Pra *et al.*, 2006) Chordin/Noggin/Follistatin triple morphants, and almost complete loss of epidermal differentiation in *Xenopus* BMP2/4/7 triple morphants (Reversade *et al.*, 2005). However, these embryos also display severe phenotypes that could be caused by the abolition of dorsoventral patterning (reviewed in (De Robertis and Kuroda, 2004)). The considerable redundancy between the large number of BMPs and BMP antagonists and their requirement for multiple functions at different times during embryonic development makes it difficult to dissect their specific contribution to neural induction by these loss-of-function approaches.

1.7 Other signals are required for neural induction

BMP inhibition is certainly important for neural induction, but further questions about its sufficiency have arisen from experiments considering other signalling pathways. There is increasing support for contributions from FGF, IGF, WNT, Retinoic acid, Calcium, Notch and Hedgehog signals in neural induction. The evidence for these either individually, in combination with BMP inhibition or each other is summarised in the following sections.

1.7.1 FGF signals

The default model implies that BMP inhibition is sufficient for ectodermal cells to acquire a neural fate. Therefore much controversy surrounded observations that FGF signals might also be required for neural induction. The earliest suggestion that FGF signals are required for neural induction in *Xenopus* included the finding that neural induction was blocked in embryos treated with suramin, a chemical that inhibits ligand binding to tyrosine kinase receptors

including FGF/FGFRs (Grunz, 1992). However other evidence from *Xenopus* suggested that FGF signals did not contribute to neural induction. Inhibition of FGF signalling using a dominant negative FGFR1 receptor (ΔXFD) in *Xenopus* embryos or explants demonstrated that it is required for mesoderm formation but that neural structures still form (Amaya *et al.*, 1991, Cox and Hemmati-Brivanlou, 1995, Lamb and Harland, 1995, Kroll and Amaya, 1996, Holowacz and Sokol, 1999, Ishimura *et al.*, 2000, Ribisi *et al.*, 2000, Pownall *et al.*, 2003) (Kengaku and Okamoto, 1993, Godsave and Durston, 1997). However neural structures were often disorganized and lacking posterior markers in these experiments. In some cases anterior markers were still expressed (Ribisi *et al.*, 2000), leading to the suggestion that FGFS are not required for neural induction, but only for the formation and patterning of posterior neural tissue.

Other studies came to different conclusions. Young animal caps were induced to express anterior neural markers when treated with FGFs or co-cultured with FGF expressing tissues (notochord and somites), a response which was blocked by the introduction of ΔXFD into animal caps (Barnett *et al.*, 1998). Expression of ΔXFD in whole embryos or animal caps was also shown to prevent neural induction by Noggin (Launay *et al.*, 1996), and a greater proportion of embryos demonstrated anterior defects when dorso-animal blastomeres were targeted, compared to dorso-vegetal blastomeres. These anterior-deficient embryos demonstrated loss of NCAM staining and only very small neural structures, suggesting FGFs are important anteriorly as well as posteriorly (Launay *et al.*, 1996). In animal caps, co-injection of Noggin RNA was unable to rescue NCAM expression when cells expressed ΔXFD (Launay *et al.*, 1996). Similarly, Chordin is unable to induce neural tissue in animal caps where FGF signalling is inhibited (Sasai *et al.*, 1996). ΔXFD also inhibited neural induction in animal caps cultured with grafts of Spemann's organizer or Hensen's node, suggesting FGF secretion by both organizers is necessary for neural induction in *Xenopus* (Launay *et al.*, 1996).

A possible explanation for some of the discrepancies regarding the contributions of FGF in *Xenopus* might arise from different contributions of FGF receptors during development. FGF8 overexpression in *Xenopus* embryos causes the formation of ectopic neurons in the absence of mesoderm, an effect that can only be blocked efficiently by expression of ΔFGFR4 rather than ΔFGFR1 (Hardcastle *et al.*, 2000). Similarly, dominant negative FGFR4 constructs are more effective than ΔXFD (which lacks the intracellular tyrosine kinase domain of FGFR1) at inhibiting neural induction in the embryo, but also the expression of anterior and posterior markers in animal caps co-cultured with organizer cells, or animal caps subjected to prolonged dissociation (Hongo *et al.*, 1999).These observations suggest that FGF signalling via FGFR4 is required for neural induction and that previous experiments relying on ΔXFD, may not have

blocked the FGF signals specific for neural induction effectively enough. Furthermore, FGFR1 is only expressed at low levels between stages 10-15 in *Xenopus*, compared to FGFR4 which is expressed at much higher levels (Hongo *et al.*, 1999). In fact FGFR1 is associated more closely with mesoderm formation and caudalisation which may account for the varying responses observed and the stronger effect of ΔXFD on posterior rather than anterior structures (Umbhauer *et al.*, 2000).

Indeed when *Xenopus* embryos are treated with SU5402, a broad FGF receptor chemical inhibitor, neural induction is blocked in a dose-dependent manner (Delaune *et al.*, 2005). The most severely affected embryos do not express the neural plate marker SOX2 and only form epidermis, cement gland and endodermal tissues. This tissue loss is not due to cell death, suggesting that broad FGF inhibition promotes epidermis formation at the expense of neural and mesodermal tissues (Delaune *et al.*, 2005).

Evidence for FGF signalling in neural induction also comes from other organisms. In ascidians such as *Ciona* or *Halocynthia*, FGFs are responsible for neural induction (Inazawa *et al.*, 1998, Hudson and Lemaire, 2001, Kim and Nishida, 2001, Bertrand *et al.*, 2003, Hudson *et al.*, 2003), whereas BMPs and BMP antagonists contribute to neural patterning and differentiation (Darras and Nishida, 2001). This suggests an ancient role for FGFs in neural induction.

However, some of the most widely accepted evidence for FGFs in vertebrate neural induction comes from experiments in chick. Early work involving beads grafted into the prospective neural plate showed that FGF signals could induce ectopic neural axes from epiblast, without induction of mesodermal markers such as Brachyury (Rodriguez-Gallardo *et al.*, 1997, Alvarez *et al.*, 1998). These axes expressed markers of anterior-posterior neural tube patterning including HOXB9, KROX20 and OTX2. Although this might indicate sufficiency of FGFs for neural induction, beads were grafted in close proximity to the embryo so these structures might form through the recruitment of cells already fated to contribute to the neural plate.

Other studies have taken advantage of the extra-embryonic epiblast of the area opaca. The inner third of the area opaca can respond to neuralising signals from a node graft (see Chapter 1.10), but does not contribute to the embryo proper (Gallera and Ivanov, 1964, Storey *et al.*, 1992, Streit *et al.*, 1995). In this way the assay avoids recruitment of pre-specified cells from the embryo's own neural plate. Here, grafted beads soaked in FGFs were shown to induce neural markers including SAX1 and CASH4, but not anterior markers EN-2 or KROX20 (Storey *et al.*, 1998). Therefore FGFs tend to induce posterior markers; however this is accompanied by Brachyury expression, suggesting that the effect of FGFs may be indirect.

Other studies in the extra-embryonic epiblast reveal that BMP inhibition is insufficient to induce neural markers. Instead the epiblast can only respond to BMP inhibition after receiving 5h of signals from Hensen's node -at this point, Chordin can maintain the otherwise transient induction of SOX3 (Streit *et al.*, 1998). This suggests that other organizer signals are necessary for neural induction before BMP inhibition. This observation became the basis of a differential screen to identify genes induced within 5h of signals from a grafted node (see Chapter 1.11). Of the ten genes induced by a node graft, the earliest responses; ERNI, SOX3 (Streit *et al.*, 2000) and Calfacilitin (Papanayotou *et al.*, 2013) can all be induced within 5h of signals from Hensen's node or a bead soaked in FGF8 (in the absence of mesoderm). Several other genes identified by the screen, namely Churchill (Sheng *et al.*, 2003), UBII (Gibson *et al.*, 2011), Asterix and Obelix (Pinho *et al.*, 2011), are induced slightly later but also in response to FGFs. These findings suggest that FGFs rather than BMP inhibitors are sufficient to induce some of the earliest neural responses. However, they are insufficient to induce a neural plate or the definitive neural marker SOX2, suggesting that other signals are also required for neural induction (Streit and Stern, 1999a, Streit *et al.*, 2000, Linker and Stern, 2004, Linker *et al.*, 2009).

Strikingly, the earliest known FGF-induced responses to neural induction (ERNI, SOX3 and Calfacilitin) are first expressed throughout the epiblast at EGKXII-XIII (Streit *et al.*, 2000, Papanayotou *et al.*, 2013). At these stages, Hensen's node has not yet formed and the BMP antagonists Noggin (Streit and Stern, 1999a) and Follistatin (Levin, 1998) are not expressed. Chordin is detected, but only weakly in Koller's sickle (Streit *et al.*, 1998, Wilson *et al.*, 2000), whereas FGFs are more appropriately expressed in the hypoblast underlying the epiblast (Streit *et al.*, 2000) to induce early markers (see also Chapter 1.14).

Similar suggestions were made based on experiments using cultured ectodermal chick explants. Epiblast tissue taken from the centre of the area pellucida at EGKVIII, expresses the BMP target genes MSX1 and MSX2 after 40h of culture (Wilson *et al.*, 2000). When explants are taken later from EGKXII embryos (but still before gastrulation), they do not express MSX genes, suggesting that BMPs are expressed very early but are already downregulated by EGKXII. Only these later explants go on to express neural markers including SOX2, SOX3, PAX6 and OTX2 (Wilson *et al.*, 2000), but this is prevented when FGF signalling is blocked using SU5402 and instead explants express epidermal markers. In fact, FGF signalling inhibits the transcription of BMP4 and BMP7 -providing further evidence that FGF signals are required for neural induction before gastrulation (Wilson *et al.*, 2000).

1.7.2 IGFs, the MAPK pathway and FGFs as BMP inhibitors

Although FGFS are now considered an important neuralising signal in chick and amphibians, it was initially disputed how their contributions might fit within the "default model". One suggestion came from observations that IGFs were also important for neural induction in *Xenopus*. Misexpression of IGF or IGFBP5 in ectodermal explants induces anterior neural markers in the absence of mesoderm, while knockdown of IGF inhibits neural induction by Chordin (Pera *et al.*, 2001). Since IGF, FGF, EGF and HGF ligands signal through tyrosine kinase receptors to commonly activate the MAPK pathway, the involvement of this pathway in neural induction was studied further. Earlier work showed that MAPK pathway activation by EGFs or HGFs leads to Serine-phosphorylation of the SMAD1-linker domain at four sites that contain the PXSP amino-sequence (Kretzschmar *et al.*, 1997a, Kretzschmar *et al.*, 1999). This modification prevents nuclear translocation, unlike BMP signalling which phosphorylates the carboxy- terminus of SMAD1 (Kretzschmar *et al.*, 1997d) to activate nuclear translocation and target gene expression. Mutations in these PXSP sites or treatment with a MEK inhibitor renders SMAD1 insensitive to MAPK activity, and the latter can be rescued by recombinant phosphorylated ERK (Kretzschmar *et al.*, 1997a, Kretzschmar *et al.*, 1999). In this way, the effects of IGFs and FGFs but also EGFs and HGFs can be incorporated into the default model based on their ability to inhibit BMP signalling via SMAD1 (Pera *et al.*, 2003).

The finding that FGFs can antagonise BMP via SMAD1 might explain observations that FGF mediated downregulation of BMPs between EGKVIII and XII, causes chick epiblast explants to switch from an epidermal to neural cell fate (Wilson *et al.*, 2000). However, the integration of FGF signalling with BMP inhibition cannot account for all responses during neural induction. A mouse line carrying mutations that prevent phosphorylation of the SMAD1-linker region, displays only mild phenotypes and no gross nervous system defects (Aubin *et al.*, 2004). This contrasts with the finding that expression of a linker-mutated SMAD1 in *Xenopus* results in a severely ventralised phenotype, although it is possible that SMAD5/8 may compensate in the mouse mutant (Pera *et al.*, 2003). Furthermore, BMP inhibition is not sufficient to rescue neural induction when FGF signalling is inhibited, suggesting a role for SMAD1-independent FGF signalling (Delaune *et al.*, 2005). This is also consistent with earlier findings that neither Chordin (Sasai *et al.*, 1996) nor Noggin (Launay *et al.*, 1996) can induce neural markers in *Xenopus* embryos where FGF has been inhibited (see also Chapter 1.7.1). Additionally, no combination of FGF signalling and BMP inhibition is sufficient to induce definitive neural markers in either chick or *Xenopus* (Linker and Stern, 2004), suggesting that other signals remain to be discovered.

1.7.3 WNT signals

WNT inhibition has also been associated with neural induction because a number of WNT antagonists, including FRZB, SFRP2 (Ladher *et al.*, 2000), Crescent (Pfeffer *et al.*, 1997), and DKK1 (Foley *et al.*, 2000) and Cerberus (Zhu *et al.*, 1999) are expressed in or around the organizer. Early interest came from experiments which found that overexpression of BMP and WNT inhibitors in *Xenopus* was able to induce complete secondary axes, including head structures (Bouwmeester *et al.*, 1996, Glinka *et al.*, 1997, Glinka *et al.*, 1998, Piccolo *et al.*, 1999).

In chick, it was found that WNT inhibition promotes neural fates at the expense of epidermal differentiation in explants taken from the centre of the epiblast at EGKXII. Furthermore, explants taken earlier at EGKX express WNT3A and WNT8C and are specified as epidermis (Wilson *et al.*, 2000, Wilson *et al.*, 2001). These observations led to a model (Wilson and Edlund, 2001) where WNT signals render epiblast cells insensitive to FGF signals, thereby permitting BMP signalling to specify epidermis. In this system, WNT inhibition allows epiblast cells to respond to FGF signals and induce neural markers and therefore the status of WNT signalling was considered to regulate choices between epidermal and neural fates. Further evidence for WNT inhibition came from a screen which identified the WNT antagonist SFRP2 as important for the differentiation of neural progenitors from ES cells, a process which is blocked by WNT agonists lithium chloride or WNT1 (Aubert *et al.*, 2002). WNT inhibition has also been implicated in the induction of anterior neural markers by IGFs which, in addition to inhibiting BMP signalling, are potent inhibitors of the WNT pathway at the level of β-catenin (Pera *et al.*, 2001, Richard-Parpaillon *et al.*, 2002, Pera *et al.*, 2003).

Yet, there are also reports that canonical WNT signalling can have the opposite effect. Overexpression of WNT pathway agonists including WNT8, β-catenin, or dominant-negative GSK3 can induce NRP1 expression in animal caps, possibly by repressing BMP4 expression in the ectoderm (Baker *et al.*, 1999). In fact, WNT signalling was shown to be a more potent dorsal specifier and downregulator of BMP4 than Noggin in these experiments. Yet upregulation of canonical WNT signals interferes with neural plate formation while canonical WNT inhibition can expand the neural plate (Heeg-Truesdell and LaBonne, 2006). It has been suggested that these contradictory observations can be explained by differences in the timing of WNT requirement (Stern, 2005) as early WNTs might be necessary to establish dorsoventral identity (Baker *et al.*, 1999) but their inhibition may be required later to promote neural induction by FGF signals (Wilson *et al.*, 2001, Heeg-Truesdell and LaBonne, 2006). Certainly, no combination of FGF signalling plus BMP and WNT inhibition in chick is sufficient to induce the

definitive neural marker SOX2, suggesting other signals must be required (Linker and Stern, 2004).

1.7.4 Retinoic acid signals

Retinoic acid, the biological derivative of vitamin A, has not been so widely studied in relation to neural induction. Instead it is generally known for its contributions to neuronal differentiation, neurite outgrowth and axonal regeneration (reviewed in (Maden, 2002, Maden, 2007)).

In the early embryo, retinoic acid has mostly been studied in regard to anterior-posterior patterning of the nervous system (Durston *et al.*, 1989, Sharpe, 1991, Simeone *et al.*, 1995, Maden *et al.*, 1996, Papalopulu and Kintner, 1996). It is synthesised by RALDH2 which is expressed in the posterior mesoderm. In chick, a diverse range of tissues have the potential to respond to retinoic acid as retinoic acid receptors are expressed in overlapping domains throughout the embryo from HH4 onwards (Blentic *et al.*, 2003, Cui *et al.*, 2003, Reijntjes *et al.*, 2004, Reijntjes *et al.*, 2005), while CYP26A1 and CYP26C1 (retinoic acid catabolising enzymes) are expressed in the anterior neural plate and its underlying mesoderm respectively.

These and similar observations in other organisms, have led to a gradient model which proposes that retinoic acid controls patterning in the neural tube and that its concentrations are lower anteriorly (reviewed in (Maden, 2002)). Certainly high retinoic acid levels are important for patterning the hindbrain; retinoic acid deficiency causes dose-dependent loss of rhombomere identity and boundaries (Durston *et al.*, 1989, Sharpe, 1991, Simeone *et al.*, 1995, Maden *et al.*, 1996, Papalopulu and Kintner, 1996). Certainly in mouse and chick, retinoic acid levels do appear to be higher in the spinal cord but low or undetectable in the early forebrain, midbrain and hindbrain (Mendelsohn *et al.*, 1991, Reynolds *et al.*, 1991, Balkan *et al.*, 1992, Wagner *et al.*, 1992, LaMantia *et al.*, 1993, Maden *et al.*, 1998), suggesting the presence of a concentration gradient. Similar evidence was found in neurula stage *Xenopus* embryos using a luciferase reporter of retinoic acid (Chen *et al.*, 1994).

Contradicting these, are observations that 9-cis-retinoic acid, rather than all-trans retinoic acid, is present at equally high levels anteriorly and posteriorly, so anterior territories may not be completely devoid of retinoids (Kraft *et al.*, 1994). This correlates better with the anterior expression of CYP26A1 (Reijntjes *et al.*, 2005, Albazerchi and Stern, 2007), which can be induced by high concentrations of retinoic acid (White *et al.*, 1996, Loudig *et al.*, 2000). It also raises the possibility that separate retinoid isomers may have distinct roles within discrete

spatio-temporal domains. However, the expression of CYP26A1 should be interpreted with caution as it can also be induced by FGFs (Diez del Corral *et al.*, 2003, Olivera-Martinez and Storey, 2007), FGF or WNT inhibition (Kudoh *et al.*, 2002) and Notch (Echeverri and Oates, 2007) signalling, in different contexts.

Despite this, the expression of RALDH3 (Blentic *et al.*, 2003) and presence of retinoids in Hensen's node (Chen *et al.*, 1992, Chen and Solursh, 1992) has previously implicated retinoic acid signalling earlier during neural induction, especially since beads of retinoic acid are able to induce secondary axes when grafted next to the primitive streak (Chen and Solursh, 1992). Furthermore, in pre-primitive streak stage (pre-streak) chick embryos, retinoic acid secretion by the hypoblast has been implicated in NOT1 and NOT2 expression but also in controlling the position of the primitive streak (Knezevic *et al.*, 1995, Knezevic and Mackem, 2001). In addition, hypoblast grafts can transiently induce expression of early neural and forebrain markers by different combinations of signals (Foley *et al.*, 2000, Albazerchi and Stern, 2007). FGF8 induces expression of SOX3 and ERNI, while low levels of FGF8 with WNT and BMP antagonists can induce OTX2 and retinoic acid can induce CYP26A1 (Albazerchi and Stern, 2007). Although the hypoblast can induce an early pre-forebrain character, other signals are required to maintain them and no combination can induce the definitive neural marker SOX2 or a mature neural plate, suggesting that even these signals are insufficient for neural induction (Foley *et al.*, 2000, Albazerchi and Stern, 2007).

The contribution of retinoic acid and FGFs to the expression of early neural markers is particularly surprising given that they both act as caudalising factors during spinal cord formation (reviewed in (Diez del Corral and Storey, 2004)). Here, the caudal stem zone which lies lateral to the regressing Hensen's node, contributes cells to the forming neuroepithelium (Diez del Corral *et al.*, 2003). In these cells, mutual inhibition occurs between FGFs which maintain stem zone precursors and retinoic acid which drives precursor differentiation. FGFs inhibit retinoic acid signalling and differentiation by promoting expression of CYP26A1 and repressing RALDH2, an enzyme that synthesises retinoic acid and RARB, a retinoic acid receptor. Retinoic acid limits FGF signalling and promotes differentiation by repressing FGF8 transcription (Diez del Corral *et al.*, 2003) and may even induce expression of a MAPK phosphatase (Moreno and Kintner, 2004). Within this mutually antagonistic environment, caudal stem zone cells transition from FGF maintenance to retinoic acid differentiation via a WNT mediated switch (Olivera-Martinez and Storey, 2007). Initially FGF signalling in neural precursors promotes WNT8C expression which weakly maintains cells in an undifferentiated state. Then, as cells enter the neuroepithelium and their exposure to FGFs declines, WNT8C promotes retinoic acid synthesis via RALDH2. Increasing retinoic acid levels serve to abolish

FGF and WNT8C, finally committing cells to neural differentiation. In this way, balancing the exposure of cells to FGF and retinoic acid allows some cells in the caudal stem zone to differentiate, while maintaining a precursor pool (Olivera-Martinez and Storey, 2007).

In vitro experiments suggest that cross-talk between FGF and retinoic acid is a general theme during neural differentiation (Stavridis *et al.*, 2010). Similar signalling events are observed, and reveal that embryonic stem cell (ESC) neural differentiation actually begins with retinoic acid mediated stimulation of the FGF/MAPK pathway on day 1 but FGF inhibition from day 2 (Stavridis *et al.*, 2010). This initial FGF stimulation appears to be crucial in priming cells for differentiation, since retinoic acid cannot drive differentiation when cells are treated with an FGFR inhibitor (Stavridis *et al.*, 2007, Stavridis *et al.*, 2010). In fact, despite generally antagonising FGFs, retinoic acid is capable of stimulating FGF8 in *Xenopus* embryos at neurula stages (Moreno and Kintner, 2004) and RARs can bind to the FGF8 promoter to activate its expression (Brondani *et al.*, 2002, Zhao *et al.*, 2009). A strikingly similar situation occurs during chick neural induction, where cells must first be primed by FGF signals (Streit *et al.*, 2000, Stavridis *et al.*, 2007). It raises the possibility that some parallels may exist between the contributions of FGF and retinoic acid to ESC and spinal cord neural differentiation, and the initiation of neural induction in the early embryo -especially given that both signals are present in the hypoblast at the earliest stages of neural induction (Knezevic *et al.*, 1995, Streit *et al.*, 2000, Knezevic and Mackem, 2001).

Despite this, the contribution of retinoic acid to neural induction must be relatively minimal, or can be compensated for, given that vitamin A deficient (VAD) embryos still form a neural tube (Maden *et al.*, 1996) and SOX2 expression is only delayed in RALDH2 mutant mice (Ribes *et al.*, 2009). It may be more important later to promote neural differentiation since SOX1 transcripts are reduced in the neural tube of VAD quail embryos as a consequence of excess FGF signalling (Stavridis *et al.*, 2010). Indeed the authors suggest that retinoic acid is important to limit FGF exposure and drive neural differentiation later. In agreement with this, retinoic acid controls the numbers of primary neurons and the timing of their differentiation in fish and amphibians (Papalopulu and Kintner, 1996, Franco *et al.*, 1999, Sharpe and Goldstone, 2000a), while genes involved in early neural differentiation including GLI3, ZIC2 (Franco *et al.*, 1999) and SHH (Sharpe and Goldstone, 2000b) are under the control of retinoic acid in vertebrates. Retinoic acid may encourage cross-talk and refine the action of signalling pathways during neural induction, but it is difficult to argue for its fundamental importance if neural plate formation occurs even in its absence.

1.7.5 Calcium signals

Calcium was first implicated in neural induction by experiments in *Rana pipiens*, where it was considered to mediate a choice between epidermal and neural cell fates (Barth and Barth, 1964). This was reinforced by experiments in *Xenopus laevis* and *Pleurodeles waltl*, where the dissociation of animal caps in Ca^{2+}/Mg^{2+} free medium caused them to adopt a neural fate (Grunz and Tacke, 1989, Saint-Jeannet *et al.*, 1990). Although this neuralisation is now attributed to the diffusion of BMPs (Munoz-Sanjuan and Brivanlou, 2002) or activation of the FGF pathway (Kuroda *et al.*, 2005), the extracellular release of calcium from internal stores was also considered to trigger this fate change. Certainly, the increase in extracellular calcium and neural induction is abolished when animal caps are dissociated in the presence of a calcium chelator (Leclerc *et al.*, 2001). Furthermore, other compounds including caffeine, which stimulate calcium release, also behave as strong neuralisers (Moreau *et al.*, 1994, Batut *et al.*, 2005). Protein kinase C (PKC); a target of calcium signalling, has also been implicated in *Xenopus* neural induction (Otte *et al.*, 1988, Otte *et al.*, 1989, Kuriyama and Mayor, 2009).

In zebrafish and amphibian embryos, spontaneous calcium fluxes coincide spatio-temporally with neural induction (Webb and Miller, 2007) and never occur ventrally in ectoderm fated to form epidermis. These transients begin during blastula stages, but increase in frequency and intensity until they peak around mid- gastrula stage, when neural induction occurs (Leclerc *et al.*, 1997, Leclerc *et al.*, 2000). In amphibian and newt embryos, calcium channels comprised of pore-forming Ca_V subunits are believed to mediate these fluxes by transporting calcium into cells. The expression of voltage-gated DHP-Ca^{2+} channels closely mirrors the appearance of calcium fluxes; they are first expressed at blastula stages, but are present at the highest levels during mid-gastrulation. Shortly after, as tissue competence to neural induction reduces, so does the expression of DHP-Ca^{2+} channels (Drean *et al.*, 1995, Leclerc *et al.*, 1995). Their specific contribution to neural induction is demonstrated by treatment with DHP-Ca^{2+} channel antagonists which abolish calcium transients and downregulate expression of two early neural genes, ZIC3 and Geminin. Such embryos also demonstrate severe anterior nervous system defects (Leclerc *et al.*, 1997, Leclerc *et al.*, 2000, Leclerc *et al.*, 2001).

Recently a mechanism to regulate these types of voltage-gated channels was uncovered in chick (Papanayotou *et al.*, 2013). Calfacilitin, a transmembrane calcium channel facilitator, was identified by a screen for responses to neural induction (see Chapter 1.11). It is expressed in the neural plate where it is required for neural plate formation and the expression of neural markers including Geminin and SOX2. Calfacilitin functions by increasing calcium flux by slowing L-type $Ca_V1.2$ channel inactivation. Calfacilitin loss-of-function of can be rescued by

increasing intracellular calcium, providing further evidence for the importance of calcium in neural induction (Papanayotou *et al.*, 2013).

It seems that calcium signals converge at multiple levels with FGF and BMP pathways during neural induction. DHP-Ca^{2+} channels can be activated by membrane depolarisation after FGF signalling or BMP antagonism, and the resulting calcium fluxes can be prevented by treatment with FGF or DHP-Ca^{2+} channel inhibitors (Lee *et al.*, 2009). Increased intracellular calcium also activates the MAPK pathway by phosphorylating ERK (Kuroda *et al.*, 2005). Therefore calcium can be integrated into the SMAD1-linker model (Kretzschmar *et al.*, 1997a, Kretzschmar *et al.*, 1999, Pera *et al.*, 2003), whereby calcium indirectly inhibits epidermis formation by activating ERK which in turn phosphorylates and inactivates SMAD1 (Leclerc *et al.*, 2001, Batut *et al.*, 2005, Kuroda *et al.*, 2005, Lin *et al.*, 2010, Leclerc *et al.*, 2011). Recent evidence for more direct targeting of the BMP pathway comes from Calcineurin; a Ca^{2+}/calmodulin-dependent serine/threonine phosphatase, which is essential for neural induction in human and murine embryonic stem cells (Cho *et al.*, 2014). Calcineurin prevents BMP target gene transcription by directly dephosphorylating SMAD1/5 to prevent their translocation to the nucleus. Furthermore calcineurin is activated in a calcium and FGF-dependent manner, further demonstrating the considerable cross-talk between these signals (Cho *et al.*, 2014).

1.7.6 Notch signals

Notch signalling has been widely studied in relation to neuronal determination via lateral inhibition. Early suggestions that it might be important for specification came from studies in *Drosophila* which showed that mutations at the Notch locus alter cell fate, such that epidermal precursors are converted to neuroblasts (Hoppe and Greenspan, 1986). Other studies of the *Xenopus* Xotch homologue showed similar results; deletion of the Xotch extracellular domain causes expansion of neural territories in the absence of cell division (Coffman *et al.*, 1990, Coffman *et al.*, 1993). In mouse and human ESC cultures, inhibition of Notch signalling prevents cells from differentiating into SOX1 expressing neurons, while Notch activation is a potent promoter of neuronal differentiation (Lowell *et al.*, 2006).

Evidence for Notch in neural rather than neuronal specification comes from evidence showing Notch is important for determining cell fate in the caudal stem zone -a domain of undifferentiated proliferating cells at the caudal end of the somites (Akai *et al.*, 2005). Here FGF signalling maintains stem cell self-renewal and is required for expression of the Notch ligand Delta1, via expression of ASCL2 (CASH4). Active Notch/Delta1 signalling between these cells is also required for cell proliferation though unlike FGF, it is not required to retain cells in

the stem zone. However, while loss of Notch signalling causes cells to exit the cell cycle, these cells do not undergo neuronal differentiation. This is because as they leave the stem zone and enter the caudal neural tube, FGF signalling declines and Notch signalling becomes important to specify individual Delta1 expressing neurons by lateral inhibition. Therefore Notch is required at two distinct phases; initially to maintain a neural precursor pool and later to specify neuronal identity (Akai *et al.*, 2005).

Evidence implicating Notch in neural specification also comes from experiments demonstrating that the neural plate and its border can be expanded by BMP inhibition, but only when targeting ectodermal cells in a continuous trail extending from the neural plate border (Linker *et al.*, 2009). One interpretation of this is that homeogenetic neural inducing signals can travel between BMP-inhibited cells to expand neural territories (Linker *et al.*, 2009). As a juxtacrine signal, Notch is a promising candidate especially as it has been implicated in establishing the neural plate border (Kintner, 1992, Cornell and Eisen, 2002, Endo *et al.*, 2002, Glavic *et al.*, 2004). Preliminary Notch gain- and loss-of-function experiments have not produced clear results but do not rule out its involvement (C. Linker, A. Rolo, C. D. Stern; unpublished observations). More direct evidence for cross-talk between Notch and BMP pathways comes from interactions between the Notch intracellular domain (NICD) and SMAD1 (Dahlqvist *et al.*, 2003, Takizawa *et al.*, 2003, Itoh *et al.*, 2004), SMAD2 (Abe *et al.*, 2005) or SMAD3 (Blokzijl *et al.*, 2003). These studies suggest positive co-operation between BMP and Notch signalling, but NICD and SMAD1 could also be incorporated into a model where SIP1, which only interacts with active phosphorylated SMAD1, provides a readout of BMP pathway activity (see also Chapter 1.8.1) (Sheng *et al.*, 2003).

1.7.7 Hedgehog signals

Despite the expression of Sonic hedgehog (SHH) in Hensen's node from HH4 (Levin *et al.*, 1995), the hedgehog pathway has barely been considered in regard to neural induction. This is probably because it was assumed to be expressed too late, as neural induction was believed to occur before HH4 (see Chapter 1.12). Instead much focus has revolved around the role of SHH signals in patterning ventral motor neurons in the neural tube (reviewed in (Ericson *et al.*, 1995, Dessaud *et al.*, 2008)).

Early indications that hedgehog signalling may be implicated in epidermal *versus* neural fate decisions came from studies of banded hedgehog (X-BHH), a *Xenopus* homologue of Indian hedgehog (Ekker *et al.*, 1995, Lai *et al.*, 1995). Injection of X-BHH mRNA expanded anterior neural (HESX1) and cement gland markers (AG1) and could induce ectopic cement glands in

10% of cases. Furthermore, X-BHH overexpresion in animal caps induced OTX2 weakly as well as AG1 expression and cement gland morphology; a characteristic of the BMP antagonists Noggin and Follistatin (Lamb *et al.*, 1993, Hemmati-Brivanlou *et al.*, 1994). However X-BHH is unable to induce later neural markers such as NCAM. Although X-BHH can be induced by Activin, its expression in animal caps is neither induced by nor induces Noggin and Follistatin, suggesting that it acts independently of these BMP antagonists which can be Activin-induced (Ekker *et al.*, 1995, Lai *et al.*, 1995).

Furthermore, misexpression of hedgehog ligands or GLI1, their downstream transcriptional activator, can expand neural plate and anterior neural markers such as SOX2 and OTX2 in *Xenopus* embryos (Min *et al.*, 2011). Conversely, hedgehog loss-of-function expands cytokeratin expression at the expense of SOX2 and OTX2, (Min *et al.*, 2011).The authors conclude that this occurs due to SUFU mediated cross-talk between hedgehog and WNT pathways, since SUFU can inhibit β-catenin. However, neural plate expansion is also a characteristic of BMP antagonism, which they cannot rule out as SUFU knockdown weakly induces Chordin in these experiments (Min *et al.*, 2011).

1.8 Other perspectives on neural induction

Other studies have provided new insights into the nature of neural induction in terms of cell fate choices and specification states involved, as well as the timing and requirement of critical signals. These studies are summarised here as they inform the experiments discussed above, demonstrate novel techniques and pose new questions relevant to our understanding of neural induction.

1.8.1 A view from the primitive streak

Churchill is a zinc-finger transcriptional activator that was first identified from a screen for responses induced after 5h of neural inducing signals from Hensen's node (see also Chapter 1.11). Consistent with a role in neural induction Churchill is first expressed in the prospective neural plate at HH3-4, where it later persists in a SOX2-like pattern. In contradiction with the "default" model, Churchill is not induced by BMP inhibition, instead it can be induced after 5h by a grafted bead soaked in FGF8 (Sheng *et al.*, 2003).

Functional analyses reveal that Churchill misexpression in the embryonic epiblast causes downregulation of the mesodermal marker Brachyury and actually inhibits the formation of mesoderm by FGFs by preventing the ingression of epiblast cells through the primitive streak.

Churchill achieves this indirectly, initially by binding to CGGGRR motifs in SIP1 regulatory sequences to induce its expression. SIP1, which is also expressed in the neural plate, then blocks expression of the mesoderm markers Brachyury and TBX6. In this way, Churchill regulates epiblast fate by mediating a choice between whether cells ingress through the streak to form mesoderm, or remain in the epiblast where they will contribute to the neural plate (Sheng *et al.*, 2003). Interestingly, SOX3 (Acloque *et al.*, 2011) and SOX2 (Takemoto *et al.*, 2011) themselves have been shown to be involved in a similar switch between neural and mesodermal fates in both chick and mouse embryos by preventing epithelial to mesenchymal transition (EMT). TBX6 is also involved in this process by favouring mesoderm formation - strikingly, mouse mutants lacking functional TBX6 possess three neural tubes (the supernumerary ones lie on either side of the endogenous neural tube and form at the expense of somitic mesoderm (Chapman and Papaioannou, 1998)).

Induction of Churchill after 5h may also regulate a crucial switch in signal requirements. SIP1, a SMAD1 interacting protein, only associates with SMAD1 when the BMP pathway is active and SMAD1 is phosphorylated (Verschueren *et al.*, 1999, Postigo *et al.*, 2003). Therefore SIP1 expression is suggested to provide a readout of BMP pathway activity, depending on whether it associates with SMAD1. This could neatly explain the observation that chick ectodermal cells must be exposed to 5h of signals from an organiser before they can respond to BMP inhibition (Streit *et al.*, 1998). So the induction of Churchill by FGFs not only mediates mesodermal *versus* ectodermal cell fate choices, but it can also account for the switch to epiblast sensitivity to BMP inhibition after 5h. Therefore Churchill neatly illustrates how neural induction is not simply a choice between epidermal or neural cell fates governed by BMP and BMP inhibition, as is suggested by the default model.

1.8.2 A view from the neural plate border

The same screen that identified Churchill also identified nine other responses to an organizer graft. Of these ERNI and SOX3 are both are induced within 1-3h of signals from an organizer graft by FGFs. Unlike Churchill, they are expressed much earlier in the epiblast at pre-streak stages EGKXII-XIII; before gastrulation and earlier than neural induction was previously considered to occur (Streit *et al.*, 2000). Expression of both markers continues in the prospective neural plate at HH3-4. Soon after, their expression patterns diverge: SOX3 remains in the neural plate, whereas ERNI expression clears and instead shifts to the pre-placodal region (PPR) by HH5 (Streit *et al.*, 2000). The PPR is a domain that derives from the anterior neural plate border and later gives rise to the sensory placodes (Streit, 2008, Schlosser, 2010).

Based on the expression patterns of ERNI and SOX3, it has been proposed that the neural plate and the neural plate border might derive from a common “pre-neural” border-like domain which exists in the epiblast at EGKXII-XIII and is induced by FGFs (Stern, 2004e, Streit, 2008). Consistent with this, fate maps reveal that some central epiblast cells at these stages are fated to contribute to the neural plate and neural plate border (Hatada and Stern, 1994).

There are also several functional similarities between the pre-streak epiblast and neural plate border which further reinforce this idea. Unlike non-neural ectoderm or the neural plate (Streit *et al.*, 1998, Linker and Stern, 2004), the neural plate border is highly responsive to BMP signalling as neural and border markers can be expanded when BMP antagonists are misexpressed in a continuous line from the neural plate border (Streit and Stern, 1999a, Linker *et al.*, 2009). Similarly, explants of chick pre-streak epiblast cells can be readily neuralised by BMP inhibition (Wilson *et al.*, 2000, Wilson *et al.*, 2001). Furthermore, when such explants are cultured in the absence of signals for 40h, they express neural plate and border markers, including SOX3, SOX2, PAX7, MSX1 and SLUG (Linker *et al.*, 2009) as well as DLX5, GATA3, SIX4, EYA2 and ERNI (Stower, 2012). These explants never express the definitive neural marker SOX1, the mesoderm marker TBX6 or the non-neural ectoderm marker GATA2, suggesting that they are generally specified as neural plate border. When such explants are cultured up to 6 days, they continue to express SLUG, but also acquire the pan-PPR marker PAX6 and lens markers δ-Crystallin and MAFA in addition to forming distinctive morphological lenses on the culture plate (Stower, 2012). The same dramatic transformation to lens is also observed when PPR explants from HH5-6 embryos are cultured in the absence of signals (Bailey *et al.*, 2006).

These observations demonstrate that the pre-streak epiblast not only expresses neural plate border markers, but it also behaves the same way in response to BMP pathway modulation and ultimately shares the same default specification fate as the neural plate border/PPR, as both tissues differentiate into lens after culture in the absence of signals. Given that ERNI and SOX3 are the earliest induced markers of this state, it suggests that one of the first steps in neural induction might be the specification of “pre-neural” border/PPR- like state by FGFs (Stern, 2004e). Since the default specification fate of this tissue seems to be lens, other signals must be required after FGFs to specify neural plate, neural crest and the other placodes (olfactory, trigeminal, otic and epibranchial) from this territory (Streit, 2008).

1.8.3 A view from the animal cap

Despite the finding that inter-species organizer grafts can induce secondary axes, some consider the molecular basis of neural induction to differ between *Xenopus* and chick due to the apparent differences for BMP inhibition in these organisms. In chick, BMP inhibition cannot induce neural plate markers in ectoderm, compared to *Xenopus* ectodermal explants which are readily neuralised (Linker and Stern, 2004). The only region in chick that is sensitive to BMPs is the neural plate border, which can be readily expanded by BMP inhibition, but only when inhibited cells form a continuous trail to the neural plate or its border, suggesting that homeogenetic neural inducing signals can travel between BMP inhibited cells (Streit and Stern, 1999a, Linker *et al.*, 2009).

Yet, neural induction in amphibians may not be so different to chick, which appears to begin with the induction of a "border-like" state. Fate maps of early (32-64 cell) amphibian embryos suggest that blastomeres A2 and A3 contribute progeny to the neural plate border (Jacobson and Hirose, 1981, Moody, 1987, Moury and Jacobson, 1989, Moody and Kline, 1990, Moury and Jacobson, 1990, Saint-Jeannet and Dawid, 1994, Delarue *et al.*, 1997). Furthermore, fate maps of animal caps reveal that the cells within them contribute to the neural plate itself, and even the smallest animal caps contribute to the neural plate border (Linker *et al.*, 2009). As most functional experiments in *Xenopus* involve animal caps or these blastomeres, prospective neural plate border cells are being targeted -the only ones which can express neural plate markers in response to BMP inhibition..

In agreement with this observation, BMP inhibition in cells that never contribute to the neural plate or neural plate border is unable to induce neural markers in *Xenopus* animal caps or in ventral epidermis (Delaune *et al.*, 2005, Linker *et al.*, 2009). This result is the same as BMP inhibition experiments in chick extra-embryonic ectoderm, where neural markers cannot be induced (Streit *et al.*, 1998, Streit and Stern, 1999g, Linker and Stern, 2004, Linker *et al.*, 2009). This contrasts sharply with experiments targeting the A1-A3 blastomeres (and therefore neural border cells) which can expand neural markers, as at the neural plate border in chick (Linker and Stern, 2004, Delaune *et al.*, 2005, Linker *et al.*, 2009). Therefore these observations go some way to reconciling the different results for neural induction by BMP inhibition in chick and *Xenopus*. Since homeogenetic neural inducing signals can travel between BMP inhibited cells, animal caps or blastomeres A1-A3 are unsuitable for studying true neural induction because they cannot distinguish between *de novo* induction of neural markers as opposed to the expansion of fates that have already been specified (Linker *et al.*, 2009).

Studies of neural induction in cells normally fated to form ventral epidermis or extra-embryonic tissue in *Xenopus* and chick respectively, offer a more stringent test for true instructive induction, as a change of fate. Such assays reveal that BMP inhibition is not sufficient to induce neural markers, in both species. This result is observed even when BMP is inhibited thoroughly using high concentrations of BMP antagonists and when combinations of antagonists (e.g. SMAD6, DN-BMPRs, Noggin and Chordin) are used (Linker and Stern, 2004, Delaune *et al.*, 2005, Linker *et al.*, 2009). Careful reanalysis of the contributions of FGF, BMP inhibition and WNT inhibition in *Xenopus* and chick now confirms that FGF signalling before gastrulation is required for neural induction but FGFs are not sufficient to induce definitive neural markers (Streit *et al.*, 1998, Streit *et al.*, 2000, Linker and Stern, 2004, Delaune *et al.*, 2005, Linker *et al.*, 2009). High levels of BMP inhibition cannot rescue FGF inhibition even when multiple antagonists are used, suggesting that although FGFs may act to inhibit BMPs, they also contribute to neural induction in a BMP/SMAD1-independent manner (Delaune *et al.*, 2005). BMP inhibition is required for SOX2, but not for the initial phase of SOX3 expression, suggesting that it is required but probably as a later step in neural induction (Linker and Stern, 2004). BMP inhibition is also required to maintain SOX3 thereafter (Streit *et al.*, 1998). However some differences still remain between the two model species. FGF plus weak BMP inhibition is reported to induce SOX2 in *Xenopus* ventral epidermis (Delaune *et al.*, 2005), whereas these signals, with or without WNT inhibition, were insufficient to induce SOX2 in *Xenopus* or chick extra-embryonic ectoderm, suggesting that yet more signals are required (Linker and Stern, 2004, Linker *et al.*, 2009).

1.8.4 A view from the genome

Biological development is determined by the precise spatio-temporal expression of genes in response to combinations of regulatory signals. Whether a gene is transcribed depends on the integration of multiple factors including its location in the genome, local chromatin structure and its associated transcriptional regulatory elements; promoters, enhancers, silencers, and insulators (Maston *et al.*, 2006, Vogelmann *et al.*, 2011). In the systems biology era, new bioinformatics tools are now available to explore gene regulation by identifying cis-regulatory elements in the genome (Khan *et al.*, 2013).

One powerful approach has been the identification of conserved promoters and enhancer elements and the transcription factor binding sites contained within them. This can identify specific motifs responsible for gene expression. For example, thorough analysis has discovered over 40 enhancers located up and downstream of the chicken SOX2 gene (Uchikawa *et al.*,

2003, Uchikawa *et al.*, 2004, Okamoto *et al.*, 2015). Not only are these conserved in mouse and human homologues of SOX2 but they were confirmed experimentally using reporter analysis (Streit *et al.*, 2013).

The overall expression of SOX2 in the neural plate and neural tube is regulated by the coordinated integration of five enhancers, each with discrete regional coverage. Two enhancers; referred to as N1 and N2, specifically regulate the onset of SOX2 expression in the neural plate at around HH4-5 (Uchikawa *et al.*, 2003, Uchikawa *et al.*, 2004). The N1 enhancer is located 13kb downstream of SOX2. Its activity is first detected at HH5 around Hensen's node and later follows the node as it regresses caudally. This suggested that N1 activity provides a readout of Hensen's node induced SOX2 expression and accordingly, grafts of Hensen's node can induce N1-reporter expression in the extra-embryonic area opaca. It also confirms that ectopic SOX2 induction by a node graft requires that same enhancer usage as SOX2 expression in the neural plate. The N2 enhancer is located 4kb upstream of SOX2. N2 activity initially covers a broad domain anterior to the node at HH5 and later becomes restricted to the future prosencephalon, mesencephalon, and rostral rhombencephalon. Therefore N2 represents a good specifier of anterior neural plate development (Uchikawa *et al.*, 2003, Uchikawa *et al.*, 2004).

Analysis of transcription factor binding sites in these enhancers has identified conserved motifs. The N1 enhancer contains binding sites for a SOX-related protein (possibly SOX3, which is expressed earlier than SOX2 in the neural plate), a TCF/LEF homeodomain protein (WNT pathway target), and an E-box sequence known to be a target of ZEB/ZFHX family proteins (Verschueren *et al.*, 1999, Uchikawa *et al.*, 2003, Uchikawa *et al.*, 2004). SIP1 (ZEB2) shares overlapping expression domains in the neural plate with SOX2, so its location is consistent with SIP1 potentially regulating SOX2 (Sheng *et al.*, 2003). Mutational analysis of the N1 core, a 56bp region within the 420bp enhancer, reveals that it is activated synergistically by WNT and FGF signals (Takemoto *et al.*, 2006). Consistent with the absence of BMP or BMP pathway-related binding sites, the N1 core enhancer does not respond to BMP agonism or antagonism (Takemoto *et al.*, 2006). This suggests that WNT and FGF, but not BMP signals converge on the N1 enhancer to induce SOX2 in the vicinity of Hensen's node.

Functional analysis of the anteriorly active N2 enhancer reveals that it contains binding sites for ZIC2, OTX and several POU proteins (Iwafuchi-Doi *et al.*, 2011, Iwafuchi-Doi *et al.*, 2012). Its activity is regulated by different combinations of transcription factors in different states. When epiblast stem cell differentiation was used as model for neural specification, N2-dependant SOX2 expression in an "epiblast-like" state requires just ZIC2 and POU5F1 (OCT3/4) binding.

Later in a more “anterior neural plate-like” state, SOX2 expression via N2 involves occupancy of the OTX binding site and a switch from POU5f1 to POU3fs at the POU site (Iwafuchi-Doi *et al.*, 2011, Iwafuchi-Doi *et al.*, 2012). This suggests that SOX2 expression in the anterior neural plate requires inputs from OTX2, ZIC2 and POU proteins, consistent with the differences in SOX2 expression anteriorly and posteriorly.

In this way, bioinformatics approaches can identify putative enhancers and the binding sites within them to provide a guide for functional techniques. Certainly, the analysis of SOX2 to date reveals that its expression in the neural plate integrates information from spatially restricted cues such as WNTs, FGFs and specific transcription factors including OTX2 which are appropriately expressed in the embryo. These types of analyses reveal the regulatory elements necessary for the expression of individual genes and can link transcriptional states by converging gene expression on the cis-regulatory elements of downstream targets.

However, transcription factor binding to the relevant enhancers is not enough to account for the spatio-temporal expression of SOX2, as has been demonstrated for the N2 enhancer (Papanayotou *et al.*, 2008). Here, an interplay between the SWI/SNF chromatin remodelling factor Brahma, the heterochromatin protein repressors HP1α and HP1γ and coiled-coil proteins ERNI, Geminin and BERT regulate when this enhancer becomes active (Papanayotou *et al.*, 2008). Specifically, it was proposed that in the “basal” state the N2 enhancer is constitutively occupied by Brahma, whose activity as a transcriptional activator is blocked by the binding of HP1α. At early stages of development, FGF signalling induces ERNI and Geminin, which bind to each other through their coiled-coil domains. Geminin also binds to Brahma at the same site as HP1α to displace the latter. However, ERNI recruits the related repressor HP1γ to a specific sequence at its C-terminal end, which continues to repress N2 enhancer expression. At later stages, BERT starts to be expressed and its coiled-coil domain binds to those of both ERNI and Geminin and thus disrupts their association, which effectively removes HP1γ from this site. This finally allows activation of N2 expression by Brahma, which may act by its chromatin-unwinding activity (Papanayotou *et al.*, 2008). It was proposed that this mechanism allows cells to build up a “memory” of their signalling history (encoded by transcription factors bound to the enhancer, each induced by a different set of signals) before removing repression and allowing cells to express a key neural commitment gene like SOX2. An important function of this mechanism may be to separate, in time and space, incompatible functions of the same signals, such as FGF, which are required for both mesodermal and neural induction (Papanayotou *et al.*, 2008).

1.9 A screen for secreted signals from the organizer

In an effort to identify other neural inducing signals, a genetic screen was conducted to isolate secreted factors from Hensen's node between HH3+/4, when it is most potent. It used a yeast signal sequence trap vector consisting of a modified yeast invertase gene lacking both its methionine start codon and signal peptide, under control of a yeast dehydrogenase promoter (Jacobs *et al.*, 1997). The invertase gene mutations mean that yeast colonies transformed with the vector are normally unable to grow under invertase selection. However, colony survival can be rescued by introduction of native invertase or other cDNAs containing signal sequences into a cloning site between the promoter and mutant invertase. A cDNA library of mRNA extracted from Hensen's node at HH3+/4 was transformed into yeast containing the vector and screened for secreted proteins by extracting plasmids from colonies that survived invertase selection. This screen isolated 137 sequences, including three that were expressed in Hensen's node at the appropriate stages based on in situ hybridisation and confirmed as secreted. Functional neural induction analyses have suggested roles for Calreticulin; a calcium regulator and nhbr90; a probable non-coding RNA, while a third candidate (Fibulin2) did not have any effect in neural induction assays (Marta de Almeida, 2012).

1.10 Competence for neural induction

The outcome of inductive events depends not only on the signals a tissue receives but whether the tissue is competent to respond. For example, grafts of Hensen's node to the area opaca are able to induce ectopic secondary axes but only between HH2-4 when the tissue is competent to respond. Between HH4-4+, grafted nodes become unable to induce ectopic neural tissue as competence is progressively lost (Gallera and Ivanov, 1964, Storey *et al.*, 1992).

The dawn of the molecular era enabled this problem to be investigated. The $L5^{220}$ epitope, an N-glycoside linked carbohydrate modification related to the Lewis-X antigen (Streit *et al.*, 1996), was initially described as an early neural marker (Streit *et al.*, 1990, Roberts *et al.*, 1991). It starts to be expressed weakly in the posterior area pellucida at EGKXIII and in scattered cells of the more central area pellucida. By HH3+, $L5^{220}$ is expressed strongly around the anterior region of the streak, extending to cover the inner third of the area opaca by HH4. Shortly after, its expression domain narrows until it is confined to the neural plate at HH6 and neural tube at HH9- (Streit *et al.*, 1995). Therefore the spatio-temporal expression of $L5^{220}$ correlates closely with regions competent to respond to neural induction.

Gain- and loss-of function experiments confirm a role for the $L5^{220}$ epitope in neural competence. Grafts of Hensen's node are able to enhance its expression in the area opaca

(Roberts *et al.*, 1991) via HGF/SF signals (Streit *et al.*, 1995). HGF/SF can also delay the loss of to $L5^{220}$ to maintain, but not induce, competence long after it would normally have been lost (Streit *et al.*, 1997). Conversely there was a marked decrease in ectopic inductions when cell pellets secreting an antibody against the $L5^{220}$ epitope were grafted together with Hensen's node (Roberts *et al.*, 1991). Despite the finding that the $L5^{220}$ epitope is of critical importance for ectodermal tissue to respond to neural induction, the protein that carries this proteoglycan modification remains unknown.

1.11 A screen for transcriptional responses to neural induction

To establish the molecular processes that occur during neural induction before BMP inhibition, a screen was conducted to identify genes that are differentially expressed following 5h of a Hensen's node graft (Streit *et al.*, 2000). This time period was chosen because of the observation that chick ectodermal cells cannot respond to BMP signalling by maintaining SOX3 expression unless they have first been primed by 5h of signals from the organizer (Streit *et al.*, 1998). Quail nodes were grafted to the inner third of the area opaca, a region which is competent to respond to organizer signalling, but which does not contribute cells to the embryo proper. After 5h, induced ectoderm from underneath the graft was isolated as well as uninduced ectoderm from the contralateral side of the same embryo. From these tissues, cDNA libraries were constructed and screened for differentially expressed genes (Streit *et al.*, 2000).

The expression of 10 genes was found to be upregulated in induced tissue, including the novel genes ERNI (Streit *et al.*, 2000), Churchill (Sheng *et al.*, 2003), Calfacilitin (Papanayotou *et al.*, 2013), Asterix and Obelix (Pinho *et al.*, 2011) and previously characterised genes: SOX3 (Streit *et al.*, 2000), DAD1, UBII, FTH1 (Gibson *et al.*, 2011) and TRKC (Pinho *et al.*, 2011). Consistent with a role in neural induction, each gene is expressed in the neural plate at some stage. ERNI, SOX3 and Calfacilitin are first expressed in the pre-streak epiblast at EGKXIII and this continues in the prospective neural plate at HH3-4, when Churchill, DAD1, UBII, FTH1, Asterix and Obelix can also be detected (Pinho *et al.*, 2011).

SOX3, a transcription factor of the SRY-related HMG-box family has been extensively studied in terms of cell fate determination during embryonic development (Stevanovic *et al.*, 1993) and is considered to be an early marker of ectoderm that is competent to form nervous tissue (Rex *et al.*, 1997). Functional analysis of several other markers reveals their specific contributions to neural induction. The role of the zinc-finger transcriptional activator Churchill in regulating the ingression of epiblast cells through the primitive streak has already been described (see

Chapter 1.8.1). Likewise, the function of Calfacilitin, a transmembrane calcium channel facilitator, which is required for neural plate formation, has also been covered (see Chapter 1.7.5). ERNI seems to function mainly to repress premature neural fate acquisition at least partly by controlling the activity of the SOX2 enhancer N2, and has also been discussed above (see Chapter 1.8.4).

DAD1, UBII (UBB) and FTH1 are expressed in the neural plate and have previously been implicated in programmed cell death. Although they do not seem to affect neural cell fate, their expression appears to protect cells from apoptosis and to restrict this to the neural plate border and non-neural ectoderm (Gibson *et al.*, 2011).

The specific functions of Asterix and Obelix are less clear. Obelix protein mainly localises to the nucleus and does not appear to be secreted. Sequence analysis suggests that it shares homology to the oligonucleotide/oligosaccharide-binding (OB) domain of eIF1A, a highly conserved translation initiation factor (Pinho *et al.*, 2011). The OB domain comprising a five-stranded beta-sheet which is coiled to form a beta-barrel, specifically imparts the RNA-binding properties of eIF1A. Therefore Obelix is predicted to bind RNA but is unlikely to function as an elongation initiation factor as it does not share any other homology with eIF1A (Pinho *et al.*, 2011). Although Asterix is also highly conserved across vertebrates and invertebrates, it belongs to a family of as yet uncharacterised proteins (Pinho *et al.*, 2011).

1.12 The timing of neural induction

Before the molecular era, careful grafting experiments revealed that grafts of Hensen's node can only consistently induce secondary axes up to HH4. Between HH4 to HH4+, it progressively loses the ability to induce neural tissue (Gallera and Ivanov, 1964, Gallera and Nicolet, 1969, Gallera, 1971, Storey *et al.*, 1992, Storey *et al.*, 1995), at the same time as regions competent to respond to these neural inducing signals lose the expression of the $L5^{220}$ epitope (Streit *et al.*, 1997). One interpretation of these observations is that neural induction normally occurs during gastrulation and that it ends completely by the onset of neurulation at HH4+. Similar suggestions have been made for neural induction in *Xenopus*, which is considered to end by stage 12/13 (Waddington and Needham, 1936, Gurdon, 1987, Sharpe and Gurdon, 1990, Servetnick and Grainger, 1991).

However, assessment of the tissue induced by grafts of the organizer into the area opaca reveals that a "neuroid" response is elicited after 6h of grafting, and a morphological neural plate appears by 8.5h (Gallera, 1965). Yet, morphology was lost when grafts were removed

before 13h (Gallera and Ivanov, 1964, Gallera, 1971). So although initial inductive events may occur earlier, it is only later that cells acquire neural plate morphology and become committed to a neural fate. In addition, the use of molecular markers enabled the observation that older nodes (between HH5-6), which have a greater tendency to self-differentiate, can still induce but only posterior neural tissue (Storey *et al.*, 1992, Storey *et al.*, 1995) -leaving open the possibility that some inductive events might continue even after HH4+.

It has sometimes been assumed that neural induction can only begin once the organizer has formed, which in chick occurs at around HH4 (Connolly *et al.*, 1995, Hemmati-Brivanlou and Melton, 1997, Streit *et al.*, 1998, Streit and Stern, 1999a). More recent results suggest that, the earliest responses to neural inducing signals from a grafted node (ERNI, SOX3 and Calfacilitin) are normally first expressed in response to FGF signals in the epiblast of EGKXII-XIII embryos (Streit *et al.*, 2000, Papanayotou *et al.*, 2013). Fate mapping experiments reveal that this territory contains cells which contribute to multiple lineages, including the future neural plate (Hatada and Stern, 1994). Taken together, this suggests that neural induction begins well before gastrulation - much earlier than previously considered. Furthermore, timed node graft experiments reveal that ERNI, SOX3 and Calfacilitin can be induced within 3h of neural inducing signals, while Churchill, DAD1, UBII, Asterix and Obelix which require 5h of signals, are not expressed until HH3-4 in the prospective neural plate (Sheng *et al.*, 2003, Gibson *et al.*, 2011, Pinho *et al.*, 2011). Therefore even the earliest responses to neural induction appear to occur in two distinct sequential steps, both ectopically and in the normal embryo.

Although a number of signals and responses to neural induction have been identified at different times, it is difficult to determine precisely when neural induction begins and ends. Morphological, functional and spatio-temporal observations hint that neural induction might occur as a sequence of events spanning a long period, at least between EGKXII and HH4-5. This begs the questions: if neural induction comprises a hierarchy of responses, which step represents the inductive step? Is it an early, but reversible bias towards a neural fate, or the final step which might confer commitment to neural specification? The node graft assay represents a useful tool for studying the entire process. The time of grafting represents a clear starting for neural induction and since ectopic induction appears to proceed via similar morphological and molecular events to the mature neural plate, it also allows later events to be dissected.

1.13 Is the organizer required for neural induction?

Although grafting experiments demonstrate that the organizer is an important source of neuralising signals, it has been argued that it may not be necessary for neural induction particularly since the organizer is never adjacent to the most anterior regions of the neural plate in chick or mouse (Stern, 2005). Hensen's node ablation does not affect nervous system formation, although these experiments do not completely remove organizer activity because Hensen's node regenerates (Psychoyos and Stern, 1996c). Even genetic ablations such as mouse homozygous HNF3β mutants, lack a node but still form a rudimentary neural tube as do zebrafish one-eyed pinhead mutants, which are defective in dorsal mesoderm and organizer development (Gritsman *et al.*, 1999, Klingensmith *et al.*, 1999). In addition, zebrafish and mouse mutants lacking organizer markers such as the BMP antagonists Noggin, Chordin, Follistatin and Cerberus still form nervous tissue (Matzuk *et al.*, 1995, Schulte-Merker *et al.*, 1997, McMahon *et al.*, 1998, Simpson *et al.*, 1999, Bachiller *et al.*, 2000, Belo *et al.*, 2000, Mukhopadhyay *et al.*, 2001).

1.14 Other sources of neural inducing signals in the embryo

The lack of dependence of neural induction on Hensen's node might also be explained by observations that the organizer is not the only source of neuralising signals in the embryo. The earliest responses to a grafted node (ERNI, SOX3 and Calfacilitin) are induced by FGF signals, including FGF8 which is first expressed in the hypoblast of normal embryos at EGKXII-XIII (Streit *et al.*, 2000) and perhaps FGF3 which is expressed in the epiblast at even earlier stages (Wilson *et al.*, 2000). The hypoblast is also an important source of signals including retinoic acid (Knezevic *et al.*, 1995, Knezevic and Mackem, 2001) and WNT antagonists DKK1 and Crescent, as well as Cerberus (Foley *et al.*, 2000) which can inhibit TGFβ and WNT signalling. Functional experiments have revealed a role for the hypoblast in positioning the primitive streak and inhibiting the formation of multiple streaks (Foley *et al.*, 2000, Bertocchini and Stern, 2002). Like the mouse AVE to which is it equivalent, grafts of the hypoblast are able to induce early neural markers transiently, including SOX3 and ERNI by FGFs, CYP26A1 possibly by retinoic acid, and OTX2 by FGF together with WNT and BMP antagonism (Foley *et al.*, 2000, Albazerchi and Stern, 2007). However, neither can induce later neural markers such as SOX2 or HESX1 nor a morphological axis, suggesting that although the hypoblast contains some of the same neural inducing signals, it cannot compensate for all signals secreted from the organizer (Foley *et al.*, 2000, Albazerchi and Stern, 2007). Therefore the hypoblast is a source of the earliest signals during neural induction but Hensen's node takes over once the hypoblast no longer persists.

Signals from the node must continue to be important as the node regresses if, as suggested (see Chapter 1.12), neural induction proceeds as a sequence of events continuing beyond HH4. Certainly older nodes remain important for the induction of posterior markers (Storey *et al.*, 1992, Storey *et al.*, 1998). The head process forms at HH4+ from the middle layer of Hensen's node, so its derivatives (the prechordal mesendoderm and notochord) may be important sources of signals at later stages (Selleck and Stern, 1991, Psychoyos and Stern, 1996a). Certainly the contributions of SHH from the notochord to neural tube dorsoventral patterning are well known (Dessaud *et al.*, 2008). This is further reinforced by observations that Hensen's node grafts differentiate into NOT1-expressing, notochord-like structures after longer culture, as well as contributing cells to the floor plate of ectopic neural axes (Storey *et al.*, 1992, Storey *et al.*, 1995).

1.15 Thesis aims

The "default model" proposes that neural induction occurs during gastrulation in response to BMP antagonists secreted from the organizer, which are sufficient to induce neural markers. Although attractive in its simplicity, numerous studies now suggest a far more complicated picture where neural induction seems to occur as a series of sequential events that begins before gastrulation and involves inputs and cross-talk between multiple signalling pathways at different time points. However the overall time-course of such a hierarchy is unclear, as are the specific contributions of relevant signalling pathways to this process.

Presented here is a body of work that aims to shed new light on the entire process of neural induction. First, we characterise the progression of neural induction using a range of other markers already known to be expressed in the neural plate at different stages. Second, we conduct a differential screen to identify the full repertoire of transcriptional responses to neural inducing signals from Hensen's node. Finally we begin to determine the precise timing and signals responsible for inducing these markers.

Chapter 2: Materials and Methods

2.1 Eggs

Fertile hens' eggs (Brown Bovan Gold; Henry Stewart & Co., UK), Japanese quails' eggs (B.C. Potter, Rosedean Farm, UK) or cytoplasmic GFP-transgenic chick eggs (Transgenic Chick Facility, Roslin Institute UK), were incubated at 38°C in a humidified chamber to the desired stages. Embryos were staged according to (Hamburger and Hamilton, 1951) in Arabic numerals or (Eyal-Giladi and Kochav, 1976) in Roman numerals for pre-primitive streak (pre-streak) stages. Embryos were dissected in physiological saline: Pannett-Compton, Tyrode's or 1x PBS (Ca^{2+}/Mg^{2+} free) and fixed in 4% Paraformaldehyde (PFA).

Pannett-Compton saline was made by combining 40mL of solution A, 900mL of distilled H_20 and 60mL of solution B immediately before use. Solution A contains 121g NaCl, 15.5g KCl, 10.42g $CaCl_2{\cdot}2H_2O$ and 12.7g $MgCl_2{\cdot}6H_2O$, dissolved in H_2O to 1L. Solution B contains 2.365g $Na_2HPO_4.2H_2O$ and 0.188g $NaH_2PO_4{\cdot}2H_2O$, dissolved in H_2O to 1L (Pannett and Compton, 1924). Both solutions were autoclaved prior to use and stored at 4°C once opened.

A 10x stock of Tyrode's saline was made by combining 80g NaCl, 2g KCl, 2.71g $CaCl_2{\cdot}2H_2O$, 0.5g $NaH_2PO_4{\cdot}2H_2O$, 2g $MgCl_2{\cdot}6H_2O$ and 10g glucose dissolved in H_2O to 1L. This was autoclaved and stored at 4°C once opened (Voiculescu *et al.*, 2008). Immediately prior to use the stock was diluted to a 1x working concentration with H_2O.

A 20x stock of phosphate buffered saline (PBS) was made by dissolving 160g NaCl, 4g KCl, 28.8g Na_2HPO_4 and 4.8g KH_2PO_4 in H_2O to 1L. This was autoclaved and stored at room temperature. The pH of each batch was tested after diluting to a 1x working concentration; batches should measure pH7.4.

Fresh 4% PFA was made each week by dissolving 2g of Paraformaldehyde pellets (Sigma) in 50mL of 1xPBS containing 2mM EGTA. The pH was adjusted to pH7.4 using 1M NaOH. This mixture was heated in a water bath at 70°C until the PFA dissolved and was then stored at 4°C.

2.2 Harvesting chicken embryos

Eggs were opened by cracking the shell at one end and windowing with blunt forceps. Albumin surrounding the yolk was removed and the opening widened to allow access. The yolk was positioned with the embryo uppermost by gently stroking the surface of the vitelline membrane with forceps. Dissecting scissors were used to make parallel incisions either side of

the embryo and again at right angles, to isolate a square of membrane with the embryo attached. A small spoon was used to scoop out the embryo with a little yolk and transfer it to a large 10cm Petri dish containing Pannett-Compton, Tyrode's or 1xPBS (Ca^{2+}/Mg^{2+} free). Using fine forceps, the membrane was first peeled away from the yolk and then the embryo was separated from the membrane. Embryos were cleaned of excess yolk and fixed flat in 4% PFA for 1h at room temperature or overnight at 4°C.

2.3 *Ex ovo* culture

Chicken embryos were cultured *ex ovo* using a modified New culture method (New, 1955, Stern and Ireland, 1981). In brief, eggs were opened with blunt forceps. The albumin surrounding the yolk was removed using forceps and a small quantity of thin albumin was collected to serve as culture medium. Intact yolks were carefully transferred to a large dish containing physiological saline, either Pannett-Compton or Tyrode's. Any remaining albumin was aspirated from the yolks using a fire-polished glass Pasteur pipette. The vitelline membrane was cut around the equator of the yolk, keeping the embryo central. The membrane was then carefully peeled away from the underlying yolk, while keeping the embryo attached. While remaining submerged, membranes were then placed on a watch glass with the embryo orientated ventral side up. A glass ring (about 3mm high, cut from glass tubing of 27mm diameter) was positioned centrally over the embryo and the edges of the membrane wrapped over the ring. This assembly was then lifted out of the dish and adjusted under a dissecting microscope while keeping the embryo submerged in a small pool of saline. The vitelline membrane was gently pulled taut around the glass ring before the excess was trimmed. Excess yolk was dislodged from the membrane and embryo by gently pipetting a stream of saline. Finally the saline was removed and replaced with fresh liquid, leaving the embryo on an optically clear membrane. At this point, embryos can be cultured as they are or with the addition of node or bead grafts (see Chapter 2.4 and 2.5) which were transferred to the ring and positioned while the embryo remained submerged.

To complete the culture, saline was removed from around and within the ring without disturbing the embryo and any grafts. The dry ring was then transferred to a 35mm Petri dish containing a shallow pool of thin albumin. The edges of the ring were pressed down to prevent it from floating, leaving the embryo supported by a shallow bubble of albumin beneath the membrane. Dishes were sealed by coating the lid with thin albumin and covering. Completed cultures were incubated in a humidified chamber at 38°C for the desired length of time.

After culture, embryos were fixed on the membrane with 4% PFA or submerged with ice-cold saline to allow tissue dissection.

2.4 Neural induction assays

Neural induction assays were performed according to (Stern, 2008, Streit and Stern, 2008). For Hensen's node grafts, chick donors at Hamburger Hamilton (HH) 3+/4- and chick hosts at HH3, 3+, 4-, 4 or 4+ were used and New cultures incubated for 1, 3, 5, 7, 9, 12 or 15h at 38°C in a humidified chamber.

One or two nodes were grafted contra-laterally per embryo, within the inner third of the area opaca and at or above the level of the host node. This region is competent to respond to neural inducing signals but only contributes to the extra-embryonic membranes and not the embryo proper (Streit *et al.*, 1997). Nodes were grafted with their endodermal surface in contact with the host epiblast.

2.5 Bead graft assays

Heparin acrylic (Sigma), Affi-gel Blue (Biorad) or AG1X2 formate (Biorad) beads were used to deliver proteins or chemicals, depending on their binding specificity and charge. Beads were rinsed 3 times in PBS before soaking for at least 6h or overnight at 4°C in the appropriate factor. Immediately prior to use, beads were rinsed twice in PBS to remove excess factor and were grafted in the same manner as node tissue.

For gain-of-function assays, beads were loaded with the following factors at the specified concentrations and a single bead was grafted to the area opaca.

Assay	Factor	Stock	Loading Concentration	Bead Type
FGF	Mouse recombinant FGF8b R&D Systems Cat. No: 423-F8	100µg/mL in 0.1% BSA/PBS	25µg/mL in 0.1% BSA/PBS	Heparin acrylic
Retinoic Acid	All-trans Retinoic acid Sigma Cat. No: R2625	5mg/mL in 100% DMSO	5µg/mL in 0.1% DMSO/PBS	AG1X2
BMP Inhibition	Human recombinant Noggin R&D Systems Cat. No: 6057-NG	125µg/mL in 0.1% BSA/PBS	91µg/mL in 0.1% BSA/PBS	Heparin acrylic

Assay	Factor	Stock	Loading Concentration	Bead Type
WNT Inhibition	IWR-1 Sigma Cat. No: I0161	2.44mM in 100% DMSO	100µM in 4.1% DMSO/PBS	AG1X2
SHH	Human recombinant SHH-N R&D Systems Cat. No: 1845-SH	1mg/mL in 0.1% BSA/PBS	1mg/mL in 0.1% BSA/PBS	Affi-gel Blue

Table 2.1: The preparation of secreted factors and chemicals for gain-of-function assays.

At these concentrations each factor elicited the appropriate functional response. FGF8b induced the target gene SOX3 (Appendix 9) but without inducing the mesodermal marker Brachyury (BRA) (Streit *et al.*, 2000). All-trans Retinoic Acid induced CYP26A1 (Albazerchi and Stern, 2007). Beads of Noggin grafted at HH4 expanded the domain of SOX2 expression after 9h (Linker *et al.*, 2009). IWR-1 beads grafted at HH8-10, lateral to Hensen's node caused a delay in RALDH2 expression in the pre-somitic mesoderm and somites after 8h (Olivera-Martinez and Storey, 2007). Bilateral Nodal expression was induced by beads of SHH-N grafted adjacent to Hensen's node on the embryonic right side (Levin *et al.*, 1995).

For loss-of-function assays, 6 beads loaded with the following factors were positioned around a Hensen's node graft in the area opaca. Where specified, the host or graft tissue was pre-incubated in the factor for 20min prior to grafting.

Assay	Factor	Stock	Loading Concentration	Additional Notes	Bead Type
Node + FGF Inhibition	SU5402 Calbiochem Cat. No: 572630	3mM in 100% DMSO	25µM in 0.83% DMSO/PBS	Host soaked in 2.5µM SU5402 in 0.083% DMSO/PBS	AG1X2
Node + FGF Inhibition	FIIN-1-Hydrochloride Tocris Cat. No: 4002	10mM in 100% DMSO	10mM in 100% DMSO	-	AG1X2
Node + Retinoic Acid Inhibition	Citral Sigma Cat. No: C83007	58mM in 100% DMSO	100µM in 0.17% DMSO/PBS	Grafts soaked in 10µM Citral in 0.017% DMSO/PBS	AG1X2
Node + BMP	Recombinant Human BMP4 R&D Systems Cat. No: 314-BP	50µg/mL in 0.1% BSA/PBS	25µg/mL in 0.1% BSA/PBS	-	Affi-gel Blue

Assay	Factor	Stock	Loading Concentration	Additional Notes	Bead Type
Node + WNT	BIO Tocris Cat. No: 3194	5mM in 100% DMSO	5µM in 0.1% DMSO/PBS	Host soaked in 0.5µM BIO in 0.01% DMSO/PBS	AG1X2
Node + HH Inhibition	Cyclopamine Abcam Cat. No: 120392	11.2mM in 100% DMSO	100µM in 0.89% DMSO/PBS	1µL of the 100µM solution was pipetted directly around grafts	

Table 2.2: The preparation of secreted factors and chemicals for loss-of-function assays.

At these concentrations each factor elicited the appropriate functional response. SU5402 reduced or abolished the induction of SOX3 (Appendix 9) by a node graft after 5h (Streit *et al.*, 2000). Beads of FIIN-1-hydrochloride reduced Sox3 expression when grafted to the prospective neural plate at HH2-3 for 6h. Citral reduced or abolished the expression of CYP26A1 induced by a node graft after 5h (Streit *et al.*, 2000). Beads of BMP4 grafted into the prospective neural plate at HH4-, abolished SOX2 expression after 9h (Linker and Stern, 2004). Beads of BIO grafted into the prospective neural plate at HH4- shifted the mid-hindbrain boundary anteriorly based on OTX2 expression at HH11 (Nordstrom *et al.*, 2002). Treatment with 2µL of a 100µM stock of cyclopamine pipetted directly onto HH4 embryos completely abolished Nodal expression after 9h compared to a vehicle control (Levin *et al.*, 1995, Cooper *et al.*, 1998).

The following factors were also used to assess the regulation of TRKC; 2µg/ml mouse recombinant Noggin (R&D) on heparin acrylic beads, 2µM Ionomycin (Sigma) and 1mM somatostatin (Tocris) on AG1X2 beads.

2.6 Node and bead graft removal

Node and bead grafts were removed after culture by submerging the embryo in saline while still attached to the membrane. Fine syringe needles (27g or 30g, B D Microlance) were used to peel yolky cells away from the grafted tissue. Grafts were gently lifted away from the underlying epiblast by working from the edges. Where grafts were firmly attached, 0.1% trypsin dissolved in saline was gently pipetted over the graft site to assist in removal. After dissection, trypsin-treated embryos were washed with fresh saline and rinsed briefly with heat-inactivated goat serum to neutralise trypsin activity (Stern, 1993). This was then replaced with fresh saline and the experimental tissue directly underneath the graft was isolated using syringe needles and mounted insect pins.

2.7 Tissue collection for RNA-Seq

For RNA-Seq, HH4- chick nodes were grafted to the area opaca of HH4- chick hosts. A single node was grafted to the left or right side per host, and embryos were cultured for 5, 9 or 12h. Node grafts were removed as described previously (Chapter 2.6) and the induced epiblast directly underneath the graft, which appeared greyish and thickened, was dissected. Uninduced epiblast tissue from same position on the contralateral side was also dissected. Tissue samples per condition were pooled, frozen on dry ice and stored at -80°C. For each time point (5, 9 or 12h) a total of 50 induced and corresponding uninduced pieces of tissue were collected. Additionally, 50 pieces of uninduced tissue were collected from HH4- embryos that had not been cultured, representing a 0h control. Tissue samples for each condition were then pooled and lysed in 1mL TRIzol® (Invitrogen) for RNA extraction.

2.8 RNA-Sequencing

Transcriptome sequencing was conducted by ARK Genomics (Roslin Institute, University of Edinburgh). Total RNA was extracted from Trizol by adding 200µL of 1-bromo-3-chloro-propane (BCP), mixed and centrifuged for 15min at maximum speed. The solution divided into two phases, and 500µL of the upper aqueous phase was removed to a fresh RNAse free tube containing 1µL of Linear Acrylamide (Ambion: AM9520). A further 100µL of BCP were added and the sample mixed prior to centrifuging for 15min at maximum speed. Of this, 450µL of the upper aqueous phase was transferred to a fresh tube and 450µL of isopropanol was added. Each sample was allowed to precipitate at room temperature for 20min then centrifuged at maximum speed for 30min. The supernatant was removed from the RNA pellet which was then washed twice with 70% ethanol. The pellet was allowed to air dry for 10min before being re-suspended in 15µL of RNAse free water. RNA quality was assessed using the Agilent 2100 Bioanalyzer. RNA samples should have a RNA Integrity Number (RIN) >7. All samples registered a RIN value between 9.2-10.0 (Appendix 2).

From these, labelled RNA libraries were constructed using the Illumina® Truseq mRNA library preparation kit. In brief, mRNAs were selected from total RNA using oligo-dT conjugated magnetic beads to select transcripts with polyA tails. Following purification, mRNAs were chemically fragmented to an average size of 180-200 bases. Fragments were then transcribed using short random primers and reverse transcriptase to produce single-stranded cDNA. This was then used to produce double-stranded cDNA using DNA polymerase I and RNaseH. After synthesis the cDNA was blunt-ended and a single A-base added to the 3' end. Molecularly barcoded sequencing adapters were ligated to fragments via a T-base overhang at their 3' end,

to uniquely label separate RNA samples. Adapter-ligated fragments were then purified to remove unincorporated adapters before being enriched by 10 cycles of PCR. Library quality was checked by electrophoresis and quantified by qPCR. The 7 RNA libraries were sequenced over 2 lanes via 100-cycle, paired-end sequencing using the Illumina® HiSeq 2000 system.

2.8.1 Galgal3 RNA-Seq analysis

RNA-Seq analysis was conducted by M. Khan.

2.8.1.1 Quality control of raw data

Raw sequencing data for each condition were provided as FASTQ files. Before aligning reads to the chicken genome, sequencing reads underwent quality control analysis using the pipeline published by (Blankenberg *et al.*, 2010). First, files were converted to FASTQSanger format using the "FASTQ Groomer" algorithm. The quality scores of reads were calculated using the "FASTQ Summary Statistics" algorithm. Quality scores were measured as phred =-10 $\log_{10}(p)$, where "p" is the estimated probability of a base being called incorrectly. Reads with a phred score of equal to or greater than 20 (i.e. 99% probability of a base being correctly identified) were kept, while poor quality reads with phred scores of less than 20 were filtered out using the "FASTQ Quality Filter" algorithm. Quality statistics for the remaining paired-end reads were summarised as box plots of the average phred scores across bases 1-100 (Appendix 3, 4 and 5). Based on these, the reads in each condition were trimmed by 10 base pairs to remove lower quality regions which occur at the 3' ends (where the phred score drops below 20).

2.8.1.2 Alignment of reads to the chicken genome

All reads that passed quality control analysis were aligned to the chicken genome (assembly version Gallus_gallus-2.1, GenBank Assembly ID GCA_000002315.1). Paired reads were aligned using the "TopHat" algorithm (Trapnell *et al.*, 2009) to produce spliced alignments as BAM files.

2.8.1.3 Differential expression analysis of transcripts

Differential expression analysis was performed by comparing the counts for each transcript between uninduced and induced tissue at each time point (5, 9 and 12h) using two separate methods.

The first method followed the protocol published by (Trapnell *et al.*, 2012). The "Cufflinks" algorithm was used to assemble transcripts from aligned paired reads. Once assembled, the transcripts for each pair of experimental and control samples were merged using the "Cuffmerge" algorithm. Differential expression analysis for constructed transcripts was then performed using "Cuffdiff". Transcripts that were upregulated or downregulated with a $\log_2$ fold change of at least 1.2 were extracted, and these formed the first data set.

The second method used the "DESeq" algorithm to calculate differential expression. Initially the "easyRNASeq" algorithm (Delhomme *et al.*, 2012), together with the Ensembl Galgal3 Gene Transfer File (GTF) were used to assemble and count transcripts from aligned paired reads. Differential expression analysis for constructed transcripts was then performed using the "DESeq" algorithm (Anders and Huber, 2010), which is available as a package in R. Transcripts that were upregulated or downregulated with a $\log_2$ fold change of at least 1.2 were extracted and these formed the second data set.

Both data sets were then compared in an Excel spreadsheet and categorised as follows: transcripts commonly identified as significant by both methods (with a $\log_2$ fold change cut-off of 1.2 and a P-value cut-off of 0.05) were displayed as red, transcripts identified as significant by either method were displayed as orange and those identified as insignificant by both methods were displayed as yellow.

2.8.1.4 Gene annotations and chromosome locations

For both Cufflinks and DESeq analyses, gene annotations and chromosome locations were added to constructed transcripts using the Ensembl Galgal3 GTF. These analyses identified a total of 7745 differentially expressed transcripts across all 3 time points. Gene annotations could be assigned to 4508 of these, corresponding to 2333 unique genes. Due to the incomplete nature of the Galgal3 chicken genome, 3237 transcripts were left unannotated (Appendix 6).

2.8.2 Galgal4 RNA-Seq reanalysis

After analysing the RNA sequencing against the Galgal3 build of the chicken genome, the more complete Galgal4 assembly was released in 2013. We used this opportunity to reassess our data and increase the annotation coverage of transcripts. Reanalysis was conducted by M. Khan.

2.8.2.1 Alignment of reads to the chicken genome

Reads that passed quality control analysis (Appendix 3, 4 and 5) were aligned to the chicken genome (assembly version Gallus_gallus-4.0, GenBank Assembly ID GCA_000002315.2). Paired reads were aligned using the "TopHat" algorithm as previously described (Chapter 2.8.1.2).

2.8.2.2 Differential expression analysis of transcripts

Due to the unstable nature of the Cufflinks suite of algorithms we decided to calculate differential expression in the Galgal4 reanalysis by DESeq alone. The "easyRNASeq" and "DESeq" algorithms were used as previously described (Chapter 2.8.1.3), only this time using the Ensembl Galgal4 GTF instead of Galgal3. The process was then repeated using the UCSC Galgal4 GTF to ensure that all available transcripts were constructed and extracted from both sets of annotations.

2.8.2.3 Gene annotations and chromosome locations

For the Ensembl constructed transcripts, gene annotations and chromosome locations were added using Ensembl Biomart data. For UCSC constructed transcripts, gene annotations and chromosome locations were added using UCSC Galgal4 GTF and annotation data from the UCSC table browser. In this way, two different lists of differentially expressed genes were generated based on Ensembl or UCSC annotations. Fully annotated transcripts from either Ensembl or UCSC lists were combined to provide the most comprehensive set of annotations. Unannotated transcipts with chromosome co-ordinates as well as transcripts belonging to unknown loci were also extracted from either list, to provide the most comprehensive list of differentially expressed transcripts based on currently available Ensembl and UCSC data.

This reanalysis identified 8673 differentially expressed transcripts across the 3 time points. Gene annotations could be assigned to 7184 of these, corresponding to 4145 unique genes (1812 more than the initial Galgal3 analysis). Due to the incomplete nature of the chicken genome, 989 transcripts still remain unannotated; many less than the Galgal3 analysis (Appendix 8).

2.8.3 Gene ontology analysis

Gene ontology (GO) analysis was conducted on the annotated genes from both Galgal3 and Galgal4 analyses using the DAVID Bioinformatics Resources 6.7 (Huang *et al.*, 2009a, Huang *et al.*, 2009b). Gene symbols for differentially expressed genes at each time point were uploaded

onto the DAVID browser GO terms were assigned and downloaded into Microsoft Excel files. These were only used to extract genes with GO terms associated with transcriptional regulation.

2.8.4 Identifying transcriptional regulators

Of the differentially expressed candidates identified by Galgal3 and Galgal4 analysis, we were most interested in the transcriptional regulators. These were extracted in several ways from each data set. First, they were compared to lists of known transcriptional regulators available from transcription factor databases (e.g. JASPAR, Clover, RSAT and Transfac). Second, they were compared to all genes identified from gene ontology analysis as being associated with transcriptional regulation. Finally, all remaining genes were manually filtered based on full gene name, and their function verified using NCBI AceView (Thierry-Mieg and Thierry-Mieg, 2006). Bar graphs representing $\log_2$ of the induced and uninduced base mean at each time point were plotted for all differentially expressed transcriptional regulators identified by Galgal3 and Galgal4 analyses (by M. Khan).

2.9 Selecting chicken expressed sequence tag clones

Chicken Expressed Sequence Tag (ChEST) clones were selected to serve as templates for riboprobe synthesis. First, the UCSC browser (www.genome.ucsc.edu) was searched using chromosome locations from the DE-Seq results, to confirm gene annotations in the Galgal3 or Galgal4 build of the chicken genome. The corresponding nucleotide sequences for coordinates were then extracted and double-checked with the NCBI BLASTn algorithm (http://blast.ncbi.nlm.nih.gov/Blast.cgi) using the nucleotide collection as the reference database. The nucleotide sequence from the RNA-Seq was then annotated using NCBI and Ensembl (http://www.ensembl.org/index.html) to distinguish exons, introns and untranslated regions (UTRs) of transcripts. Finally the annotated transcript was used to search the ChEST database (www.chick.manchester.ac.uk) for possible clones using the BLAST function (Boardman *et al.*, 2002, Hubbard *et al.*, 2005). Clones with the longest alignment coverage across exons and UTRs of the target region were selected. Clones that did not align well or which targeted intronic regions were avoided. Where possible, clones were picked to target known UTRs. Lastly, chosen ChEST clones were BLASTed against NCBI's nucleotide collection to check that they corresponded to the target gene alone. Clones that showed cross-homology to other genes were discarded and more specific clones were picked instead.

Selected ChEST clones were ordered from Source Bioscience or ARK Genomics as fragments cloned into the pBluescriptKS+ vector. They arrived as sequence verified plasmid preparations or stab cultures which were used to prepare DNA and glycerol stocks, and served as the template from which to generate antisense riboprobes by PCR. A list of all clones obtained is provided in Chapter 2.16.2 and 2.16.3.

2.10 RNA extraction

Chicken tissue from HH14-18 embryos was dissected in sterile, ice-cold PBS and collected on ice. Tissue was centrifuged briefly and excess PBS removed. RNA was extracted using TRIzol® Reagent (Life Technologies) and following manufacturer's instructions. Extracted RNA was re-suspended in 20µL of RNase-free water, the concentration was measured and samples stored at -80°C.

2.11 First-strand cDNA synthesis

Single-stranded cDNA was synthesised from extracted RNA using the SuperScript® II First-Strand Synthesis kit (Life Technologies, Cat. No: 11904-018). The basic manufacturer's protocol was adapted as follows to generate single-stranded cDNA alongside a minus reverse transcriptase control.

For each reaction the following were combined in a sterile PCR tube; 2µg extracted RNA, 1µL of oligo-dT primers (0.5µg/µL), 1µL random hexamers (50ng/µL) and DEPC water added to a total volume of 10µL. Tubes were mixed well and incubated at 65°C for 5min and 4°C for 1min.

In two separate tubes the following were combined; 2µL of 10x reverse transcriptase buffer, 4µL of 25mM $MgCl_2$, 2µL of 0.1M DTT and 1µL of RNaseOUT™ (40U/µL). This mixture was added to the RNA and primer reaction, mixed well and incubated at 42°C for 2min. To one tube, 1µL of SuperScript™ II reverse transcriptase was added, while 1µL of DEPC water was added to the second tube as a minus reverse transcriptase control. The mixture was incubated at 42°C for 50min, 70°C for 15min and stopped at 4°C. The reactions were briefly centrifuged and 1µL of RNase H was added to each tube and incubated at 37°C for 20min. A sample of each reaction was run on an agarose gel to check for cDNA product. The remaining single-stranded cDNA was diluted 1:5 in DEPC water and stored at -20°C.

2.12 Cloning cDNA templates for riboprobes

Appropriate ChEST templates could not be identified for some candidates identified by RNA-Seq. Instead, templates for these were cloned by PCR from single-stranded cDNA using primers designed to amplify approximately 1kb regions of the target cDNA. Primers were designed using Primer3 software (Koressaar and Remm, 2007, Untergasser *et al.*, 2012) and checked for their specificity in Primer-BLAST (Ye *et al.*, 2012).

The following primers were designed to clone the specified regions of each cDNA target:

Target cDNA	Forward and Reverse Primers	Primer T_a	Product Size	Coverage
PRDM1 ENSGALT00000024824	F: CAACGTTTGCTCCAAGACCT R: TTAGTAACTGGCGAGGCAAC	58°C	958bp	Partial exon 7-3'UTR
GRHL2 ENSGALT00000022978	F: TGACCCCACAAGCACACTAT R: AGAGAACTGGCTGGGAATCC	60°C	924bp	Partial exons 4-11
STOX1 ENSGALT00000006552	F: AGTACCTCGGCTGAAGTGTC R: TTGTCACTATCATCACGCGC	58°C	998bp	Partial exons 2-3
TRIM3 ENSGALT00000029931	F: CCATCCTCAACCTGGGAGTT R: TCCATCCGCATTGTACACCT	58°C	1028bp	Partial exons 6-11

Table 2.3: Primers targeting chick PRDM1, GRHL2, STOX1 and TRIM3 cDNA fragments.

Primers (Invitrogen) were re-suspended in sterile water to a concentration of 100µM. A 10µM working stock was made for each primer. Fragments were cloned by PCR using GoTaq® Flexi DNA Polymerase (Promega, Cat. No: M829) and following manufacturer's instructions.

A 2µL sample of each reaction was run on an agarose gel to check the product size. Where a single band of the appropriate size was generated, the remaining reaction was purified using the QIAquick PCR Purification Kit (Qiagen) and following manufacturer's instructions. Where multiple bands were generated, the remaining reaction was run on a fresh gel and the appropriate sized bands excised and the DNA extracted using the QIAquick Gel Extraction Kit (Qiagen) and following manufacturer's instructions. The final concentration of the purified product was measured.

2.13 Ligation of cloned fragments into plasmids

Cloned fragments were ligated into the pGEM®-T Easy vector (Promega) via their overhanging A base at the 3' end. Ligation reactions were set up following the manufacturer's instructions and incubated for 2h at room temperature or overnight at 14°C.

Ligation products were transformed into competent bacterial cells (see Chapter 2.14) and plated onto LB agar plates supplemented with ampicillin, IPTG and X-gal. Plates were incubated overnight at 37°C and 6-10 white colonies were inoculated into 5mL of LB medium supplemented with ampicillin.

Plasmids were extracted using the QIAprep Spin Miniprep Kit (Qiagen) and diagnostic digests were used to generate specific fragments by cleaving at one site within the vector and at one site within the predicted insert. Plasmids that produced appropriate digest products were sequenced by Source Bioscience using T7 or SP6 sequencing primers to confirm clone identity.

2.14 Chemical transformation of competent cells

Competent cells were produced via chemical transformation using the following protocol (Walhout *et al.*, 2000), modified from (Chung and Miller, 1988).

2.15 Plasmid transformation and DNA preparation

Plasmids were acquired as DNA preparations suspended in water or spotted onto filter paper. DNA was recovered from filter paper by soaking it in 50µL of sterile water and incubating for 2h at 37°C.

Chemically transformed competent cells were thawed on ice. To these, 10µL of the recovered DNA or 1-5µL of DNA from a plasmid preparation was added, mixed gently and incubated on ice for 30min. Cells were heat-shocked for 2min at 42°C. Tubes were then returned to ice and 500µL of SOC medium added. Cells were then incubated for 30min at 37°C while shaking, and 200µL plated onto LB agar plates supplemented with the appropriate antibiotic resistance (100µg/mL ampicillin, 50µg/mL kanamycin, 100µg/mL carbenicillin or 10µg/mL tetracycline). Where blue/white colony selection was required, plates were treated with 100µL of 100mM IPTG and 20µL of 50mg/mL X-Gal prior to plating.

Plated colonies were grown overnight and a single colony was inoculated into 5, 50 or 200mL (depending on mini, midi or maxi preparation requirements) of LB medium supplemented with

the appropriate antibiotic. Plasmids were extracted using the appropriate mini-, midi- or maxi-prep kits (Qiagen) and following the manufacturer's instructions.

Glycerol stocks were generated by adding 500 µL of the bacterial culture suspension to 500µL of sterile glycerol. Tubes were flicked to mix, snap-frozen on dry ice and stored at -80°C.

2.16 Synthesis of labelled riboprobes for in situ hybridisation

Antisense riboprobes were generated from plasmid templates containing a cDNA clone of the gene of interest either by initial digest or PCR.

2.16.1 Riboprobe synthesis by restriction enzyme digest

To generate probes by digest, 10µg of plasmid was linearised by using the appropriate restriction enzyme to cut 5' of the insert in the sense orientation. Digest reactions were then run on an agarose gel to confirm complete linearisation. DNA was extracted into the top phase after adding an equal volume of phenol:chloroform. It was then precipitated overnight at -20°C by adding sodium acetate and absolute ethanol. DNA was pelleted by centrifugation for 15min at 13.2rpm in a chilled centrifuge and washed with 70% ethanol. The pellet was spun again for 15min and the alcohol removed. The pellet was allowed to air-dry completely, before being re-suspended in 8µL of ultrapure water to give an approximate concentration of 1µg/mL.

This linearised template was used to transcribe probes in the antisense direction using the appropriate T7, T3 or SP6 polymerase (Promega) and following manufacturer's instructions. Reactions were set up for 3h at 37°C using 1µL or 3µL of template and digoxigenin (DIG) or fluorescein (FLU) labelled nucleotides to generate antisense labelled riboprobes. Next, RNase-free DNase was added for 45min at 37°C to digest the DNA template. To check that a probe had been synthesised and the template digested, 2µL of the reaction was run on an agarose gel. The reaction was stopped by adding EDTA and the RNA precipitated overnight at -20°C using lithium chloride and absolute ethanol. RNA was pelleted by centrifugation for 15min at 4°C and then washed with 70% ethanol and spun again. Finally the pellet was washed with 100% ethanol, spun and left to air-dry completely. Pellets were dissolved in 50µL of ultrapure water and the concentration measured. To this, Hybridisation (HYB) solution was added to give a 1:1 ratio of water:HYB and the probe stored at -20°C. Working probes were diluted to approximately 1µg/mL in HYB.

2.16.1.1 List of riboprobes synthesised by digest

The following riboprobes were generated by restriction digest and transcription.

Gene	Kind gift of	Linearised	Transcribed	Reference
BMI1	T. Sauka-Spengler	XhoI	SP6	(Fraser and Sauka-Spengler, 2004)
BRACHYURY (T)	V. Cunliffe	XbaI	T3	(Smith *et al.*, 1991)
CBFA2T2 (MTGR1)	N. Koyano-Nakagawa	NotI	T7	(Koyano-Nakagawa and Kintner, 2005)
CCND1	F. Pituello	HindIII	T7	(Lobjois *et al.*, 2004)
CDX2	A. Fainsod	ClaI	T3	(Marom *et al.*, 1997)
CDX4	G. Sheng	ApaI	SP6	(Alev *et al.*, 2010)
CHORDIN	-	EcoRI	SP6	(Streit *et al.*, 1998)
CYP26A1	M. Maden	BamHI	T7	(Swindell *et al.*, 1999)
DACH1	C. Tabin	SmaI	T7	(Heanue *et al.*, 2002)
DLX3	E. Pera	HindIII	SP6	(Pera and Kessel, 1999)
DLX5	G. Lizarraga	BamHI	T3	(Ferrari *et al.*, 1995)
EOMES	B. Pain	SalI	T7	(Pernaute *et al.*, 2010) (Jean *et al.*, 2015)
ERNI	-	KpnI	T3	(Streit *et al.*, 2000)
ETS2 (ETV3)	A. Mey	NheI	T3	(Mey *et al.*, 2012)
ETV1 (ER81)	K. Storey	NotI	T7	(Lunn *et al.*, 2007)
ETV4 (PEA3)	K. Storey	NotI	T7	(Lunn *et al.*, 2007)
EYA2	S. Tomarev	NotI	T7	(Mishima and Tomarev, 1998)
GATA2	-	NdeI	T7	(Sheng and Stern, 1999)
GATA4	B. Pain	ApaI	SP6	(Chapman *et al.*, 2007) (Jean *et al.*, 2015)
GATA5	B. Pain	ApaI	SP6	(Chapman *et al.*, 2007) (Jean *et al.*, 2015)
GATA6	B. Pain	NcoI	SP6	(Chapman *et al.*, 2007) (Jean *et al.*, 2015)
GBX2	A. Streit	BglII	T3	(Shamim and Mason, 1998)
GLI2	J. Briscoe	HindIII	T3	(Marigo *et al.*, 1996)
GLI3	J. Briscoe	EcoRV	T3	(Schweitzer *et al.*, 2000)
GOOSECOID	-	NotI	T7	(Izpisua-Belmonte *et al.*, 1993)
HAND1	D. Srivastava	BamHI	T7	(Srivastava *et al.*, 1995)
HESX1	S. Mackem	XhoI	T3	(Hermesz *et al.*, 1996)
HEY1	M. Gessler	EcoRI	T3	(Leimeister *et al.*, 2000)
HNF1B (vHNF1)	C. Pujades	SacII	T7	(Aragon and Pujades, 2009)

Gene	Kind gift of	Linearised	Transcribed	Reference
HOXB1	V. Prince	XbaI	T7	(Paxton *et al.*, 2010)
ID2	M. Bronner	EcoRI	T7	(Martinsen *et al.*, 2004)
IRX2	T. Ogura	XhoI	T3	(Matsumoto *et al.*, 2004)
KLF2	P. Antin	EcoRI	T7	(Antin *et al.*, 2010)
KLF4	P. Antin	NotI	T3	(Antin *et al.*, 2010)
KLF5 *ChEST429a18*	P. Antin	NotI	T3	(Antin *et al.*, 2010)
KLF6 *ChEST837d22*	P. Antin	NotI	T3	(Antin *et al.*, 2010)
LIN28A	B. Pain	ApaI	SP6	(Yokoyama *et al.*, 2008) (Jean *et al.*, 2015)
LMO7 *ChEST860d14*	D. Burt	NotI	T3	-
LMX1B	C. Tabin	SpeI	T7	(Riddle *et al.*, 1995)
MAFA (L-MAF)	H. Ogino	XbaI	T7	(Ogino and Yasuda, 1998)
MSX1	K. Liem	BglII	T3	(Suzuki *et al.*, 1991)
MSX2	C. Tickle	SacI	T7	(Brown *et al.*, 1997)
NANOG	B. Pain	ApaI	SP6	(Lavial *et al.*, 2007) (Jean *et al.*, 2015)
NKX6-2	J. Ericson	XbaI	T7	(Pattyn *et al.*, 2003)
NODAL	M. Kuehn	NotI	T7	(Levin *et al.*, 1995)
NOT1	M. Kessel	EcoRI	T7	(Stein *et al.*, 1996)
NOT2	M. Kessel	HindIII	T7	(Stein *et al.*, 1996)
OTX2	L. Bally-Cuif	XhoI	T3	(Bally-Cuif *et al.*, 1995)
PITX2	M. Levin	PstI	T7	(Zhu *et al.*, 1999)
RUNX1T1 (MTG8)	N. Koyano-Nakagawa	NotI	T7	(Koyano-Nakagawa and Kintner, 2005)
SIX3	P. Bovolenta	ClaI	T3	(Bovolenta *et al.*, 1998)
SMAD6	P. Szendro	XbaI	T7	(Vargesson and Laufer, 2001)
SMAD7	E. Laufer	EcoRI	T3	(Vargesson and Laufer, 2001)
SMAD9 (SMAD8)	J. Hurle	SacI	T7	(Zuzarte-Luis *et al.*, 2004)
SNAI1 *ChEST366k21*	ARK Genomics	NotI	T3	(Garcia-Castro *et al.*, 2000)
SOX1	H. Kondoh	XhoI	T7	(Kamachi *et al.*, 1998)
SOX11	M. Bronner	BamHI	T3	-
SOX2	P. Scotting	PstI	T7	(Rex *et al.*, 1997)
SOX3	P. Scotting	PstI	T7	(Rex *et al.*, 1997)
SP5	S. Kuratani	EcoRI	T7	(Kuraku *et al.*, 2005)

Gene	Kind gift of	Linearised	Transcribed	Reference
STOX2 *ChEST851g13*	A. Streit	NotI	T3	-
TBX3	C. Tickle	XhoI	T3	(Isaac *et al.*, 1998)
TBX6	S. Mackem	XbaI	T7	(Knezevic *et al.*, 1997)
TGIF1	J. Hurle	SacI	T7	(Lorda-Diez *et al.*, 2009)
TRKC	C. Kalcheim	BamHI	T7	(Kahane and Kalcheim, 1994)
ZEB2 (SIP1)	-	SacII	SP6	(Sheng *et al.*, 2003)
ZIC2	K. Storey	NcoI	SP6	(Warner *et al.*, 2003)

Table 2.4: The source and preparation of riboprobes synthesised by digest.

2.16.2 Riboprobe synthesis by PCR

Where cDNA plasmids contained M13F and M13R promoter sites flanking the insert and RNA polymerase sites (e.g. ChEST clones and other pBluescript or pGEM-T-easy vectors), the insert was first amplified by PCR. This approach was quicker than the digest method as it requires much less starting material (5ng as opposed to 10µg of DNA) and so mini-prep DNA is sufficient. In addition, ChEST plasmids tend to comprise 600-1000bp cDNA fragments cloned into the same pBluescriptKS+ (Stratagene) vector, so it is simple to set up the same PCR reaction for different templates.

Primers for M13F (GTAAAACGACGGCCAGT) and M13R (GCGGATAACAATTTCACACAGG) promoter sites were used to amplify the insert and flanking T3/T7/SP6 polymerase sites. PCR reactions were set up on ice using the following reagents and cycling conditions. Control reactions were set up by omitting the plasmid and substituting with H_20.

Reagents	Volume (µL)
Ultrapure H_20	4.6
GoTaq® Flexi Buffer (5x)	2.0
$MgCl_2$ (25mM)	1.0
dNTP mix (10mM)	0.2
M13F (10µM)	0.5
M13R (10µM)	0.5
Plasmid DNA (5ng/µL)	1.0
GoTaq® Polymerase	0.2
Total	10.0

Step	Purpose	Conditions
1	Hot start	95°C for 5min
2	Denature	95°C for 1min
3	Annealing	50°C for 1min
4	Extension	72°C for 1min/kb
5	Return to step 2	34 times
6	Final extension	72°C for 5min
7	Hold	4°C forever

Table 2.5: PCR recipe and conditions for riboprobe amplification from cDNA plasmids.

Upon completion, 1µL of each reaction was run on an agarose gel to check that a single band had been amplified. A very faint, larger band may also be observed for the plasmid template. Reaction products were used directly as the transcription template, without the need for purification. Transcription reactions were set up as described for riboprobes generated by digest (Chapter 2.16.1), using 1µL or 3µL of the PCR reaction as a template from which to directly to synthesise labelled antisense riboprobes. RNA was precipitated and re-suspended in HYB as before.

2.16.2.1 List of riboprobes synthesised by PCR

The following riboprobes were generated by PCR followed by transcription.

Gene	Obtained from/Kind gift of	Linearised	Transcribed	Reference
AHR *ChEST355d19*	Source Bioscience	M13F/R	T3	-
AXIN2 *ChEST755b16*	C. Kiecker	M13F/R	T3	(Quinlan *et al.*, 2009)
ARID5B *ChEST60e17*	Source Bioscience	M13F/R	T3	-
ATF3 *ChEST425m11*	Source Bioscience	M13F/R	T3	-
BACH1 *ChEST761e22*	Source Bioscience	M13F/R	T3	-
BACH2 *ChEST593g13*	Source Bioscience	M13F/R	T3	-
BHLHE40 (BHLHB2) *ChEST258o16*	Source Bioscience	M13F/R	T3	-
CDCA7 *ChEST252j12*	Source Bioscience	M13F/R	T3	-
CEBPB *ChEST664e19*	Source Bioscience	M13F/R	T7	-
CITED4 (CITED3) *ChEST150g1*	Source Bioscience	M13F/R	T3	(Andrews *et al.*, 2000)
CREB3L1 *ChEST441l21*	Source Bioscience	M13F/R	T3	-
CREG1 *ChEST368d4*	Source Bioscience	M13F/R	T3	-
CRIP2 *ChEST741k5*	Source Bioscience	M13F/R	T3	-
CSRP2 *ChEST77p7*	Source Bioscience	M13F/R	T3	-

Gene	Obtained from/Kind gift of	Linearised	Transcribed	Reference
DMBX1 *ChEST244g19*	Source Bioscience	M13F/R	T3	(Ferran *et al.*, 2007)
DNMT3A *ChEST425j12*	A. Streit	M13F/R	T3	(Hu *et al.*, 2012)
DNMT3B *ChEST405f22*	A. Streit	M13F/R	T3	
ELF1 *ChEST188c18*	Source Bioscience	M13F/R	T3	-
ELF3 *ChEST546f17*	Source Bioscience	M13F/R	T3	-
ENC1 *ChEST689f18*	Source Bioscience	M13F/R	T3	-
EPAS1 (HIF2A)	G. Sheng	M13F/R	SP6	(Ota *et al.*, 2007)
ESRRG *ChEST593B16*	ARK Genomics	M13F/R	T3	-
ETV5 (ERM) *ChEST337i4*	M. Bronner	M13F/R	T3	(Lunn *et al.*, 2007)
EZH2 *ChEST511d7*	Source Bioscience	M13F/R	T3	-
FKHR (FOXO1A) *ChEST232b16*	Source Bioscience	M13F/R	T3	-
FOXO3 *ChEST558l10*	Source Bioscience	M13F/R	T3	-
FRY *ChEST309m11*	Source Bioscience	M13F/R	T3	-
GRHL1 *ChEST301e4*	Source Bioscience	M13F/R	T3	-
GRHL2	Cloned by K. Trevers	M13F/R	T7	-
GRHL3 *ChEST664c10*	Source Bioscience	M13F/R	T3	-
HIC2 *ChEST902c20*	Source Bioscience	M13F/R	T3	-
HIPK2 *ChEST436n24*	Source Bioscience	M13F/R	T3	-
HIVEP2 *ChEST8c12*	Source Bioscience	M13F/R	T3	-
HIVEP3 *ChEST341h23*	Source Bioscience	M13F/R	T3	-
HOXA1 *ChEST1010d14*	Source Bioscience	M13F/R	T3	(McClintock *et al.*, 2003)
HOXA2 *ChEST671c8*	Source Bioscience	M13F/R	T3	(Prince and Lumsden, 1994)

Gene	Obtained from/Kind gift of	Linearised	Transcribed	Reference
ID3 *ChEST2M18*	ARK Genomics	M13F/R	T3	(Kee and Bronner-Fraser, 2001)
ING5 *ChEST696i13*	A. Streit	M13F/R	T3	-
IRF7 (IRF3) *ChEST45h21*	Source Bioscience	M13F/R	T3	-
ISX *ChEST595l5*	Source Bioscience	M13F/R	T3	-
IVNS1ABP *ChEST452o4*	Source Bioscience	M13F/R	T3	-
JMJD4 *ChEST427j1*	Source Bioscience	M13F/R	T3	-
KAT2B *ChEST481p23*	Source Bioscience	M13F/R	T3	-
KDM4A *ChEST121j8*	Source Bioscience	M13F/R	T3	-
LHX5 *ChEST455n21*	Source Bioscience	M13F/R	T3	-
LIN28B *ChEST770i7*	Source Bioscience	M13F/R	T3	-
LMO1 *ChEST410h4*	Source Bioscience	M13F/R	T3	-
MAML2 *ChEST243a24*	Source Bioscience	M13F/R	T3	-
MBNL2 *ChEST476i5*	Source Bioscience	M13F/R	T3	-
MEF2D *ChEST535j15*	Source Bioscience	M13F/R	T3	-
MEIS1 *ChEST397o24*	Source Bioscience	M13F/R	T3	(Mercader *et al.*, 1999)
MEIS2	A. Streit	M13F/R	SP6	(Mercader *et al.*, 1999)
MTA1 *ChEST87a11*	Source Bioscience	M13F/R	T3	-
MYC (C-MYC) *ChEST895e1*	M. Bronner	M13F/R	T3	(Khudyakov and Bronner-Fraser, 2009)
MYCN (N-MYC) *ChEST442N13*	M. Bronner	M13F/R	T3	(Khudyakov and Bronner-Fraser, 2009)
NCOA2 *ChEST304i18*	Source Bioscience	M13F/R	T3	-
NFKBIZ *ChEST142K1*	ARK Genomics	M13F/R	T3	-
NKX1-2 *ChEST427n5*	Source Bioscience	M13F/R	T3	(Bertrand *et al.*, 2000)

Gene	Obtained from/Kind gift of	Linearised	Transcribed	Reference
NRIP1 *ChEST97g15*	Source Bioscience	M13F/R	T3	-
NSD1 *ChEST995e21*	A. Streit	M13F/R	T3	-
OVOL2 *ChEST627k2*	Source Bioscience	M13F/R	T3	-
PDCD4 *ChEST132g13*	Source Bioscience	M13F/R	T3	-
PDLIM1 *ChEST982m14*	Source Bioscience	M13F/R	T3	-
PDLIM4 *ChEST384d10*	Source Bioscience	M13F/R	T3	-
PDLIM5 *ChEST594j18*	Source Bioscience	M13F/R	T3	-
PITX3 *ChEST292n23*	Source Bioscience	M13F/R	T3	-
PPARGC1A *ChEST999p5*	Source Bioscience	M13F/R	T3	-
PRDM1 (BLIMP1)	Cloned by K. Trevers	M13F/R	T7	(Ha and Riddle, 2003)
PTRF *ChEST224k9*	Source Bioscience	M13F/R	T3	-
RARB *ChEST392d11*	Source Bioscience	M13F/R	T3	-
RASSF7 *ChEST733e13*	Source Bioscience	M13F/R	T3	-
RB1 *ChEST613e5*	Source Bioscience	M13F/R	T3	-
RFX3 *ChEST399m9*	Source Bioscience	M13F/R	T3	-
RREB1 *ChEST262i21*	ARK Genomics	M13F/R	T3	-
SALL1 *ChEST818L4*	ARK Genomics	M13F/R	T3	(Sweetman *et al.*, 2005)
SCML2 *ChEST818b24*	Source Bioscience	M13F/R	T3	-
SERTAD2 *ChEST464c24*	Source Bioscience	M13F/R	T3	-
SETD2 *ChEST525a17*	A. Streit	M13F/R	T3	-
SMARCA2 *ChEST885f13*	Source Bioscience	M13F/R	T3	-
SOX13 *ChEST103b23*	Source Bioscience	M13F/R	T3	-

Gene	Obtained from/Kind gift of	Linearised	Transcribed	Reference
STOX1	Cloned by K. Trevers	M13F/R	SP6	-
TAF1A *ChEST580f1*	Source Bioscience	M13F/R	T3	-
TBL1XR1 *ChEST921d17*	Source Bioscience	M13F/R	T3	-
TCF12 *ChEST101h2*	Source Bioscience	M13F/R	T3	-
TCF7L1 (TCF3)	A. Munsterberg	M13F/R	T3	(Schmidt *et al.*, 2004)
TCF7L2 (TCF4) *ChEST583d9*	Source Bioscience	M13F/R	T3	(Hartmann and Tabin, 2000)
TFAP2A *ChEST765g1*	Source Bioscience	M13F/R	T3	(Khudyakov and Bronner-Fraser, 2009)
TFAP2C *ChEST712l8*	Source Bioscience	M13F/R	T3	(Qiao *et al.*, 2012)
TFAP2E *ChEST104e8*	Source Bioscience	M13F/R	T3	-
TFCP2L1 *ChEST831a6*	Source Bioscience	M13F/R	T3	-
TRIM3	Cloned by K. Trevers	M13F/R	T7	-
TRIM9 *ChEST850f24*	Source Bioscience	M13F/R	T3	-
TRIM24 *ChEST401k15*	A. Streit	M13F/R	T3	-
VGLL1 *ChEST869b3*	Source Bioscience	M13F/R	T3	-
WWTR1 *ChEST1024a14*	Source Bioscience	M13F/R	T3	-
YEATS4 (GAS41) *ChEST9i5*	A. Streit	M13F/R	T3	-
ZBTB46 *ChEST22g17*	Source Bioscience	M13F/R	T3	-
ZFHX3 *ChEST472L4*	A. Streit	M13F/R	T3	-
ZFPM1 *ChEST999l13*	Source Bioscience	M13F/R	T3	-
ZIC3 *ChEST289o16*	Ark Genomics	M13F/R	T3	-
ZMYND11 *ChEST675h24*	Source Bioscience	M13F/R	T3	-
ZNF185 *ChEST630j23*	Source Bioscience	M13F/R	T3	-

Gene	Obtained from/Kind gift of	Linearised	Transcribed	Reference
ZNF423 *ChEST39g7*	A. Streit	M13F/R	T3	-
ZNF462 *ChEST236b12*	A. Streit	M13F/R	T3	-
ZNF469 *ChEST231n23*	Source Bioscience	M13F/R	T3	-

Table 2.6: The source and preparation of riboprobes synthesised by PCR.

2.17 Whole-mount in situ hybridisation

Whole-mount in situ hybridization using DIG- or FLU-labelled riboprobes was performed as previously described (Stern, 1998, Streit and Stern, 2001). This protocol is mainly based on those by D. Henrique and D. Ish-Horowicz, who in turn modified protocols from R. Conlon, R. Harland, P. Ingham and D. Wilkinson.

In brief, embryos were fixed in 4% PFA for 1h at room temperature or overnight at 4°C and stored in 100% methanol at -20°C for up to one week. They were then progressively rehydrated through a 75%, 50%, 25% series of methanol in 1x PBS containing 0.1% Tween-20 (PBTW) before being washed on a rocker for 2 x 10min in PBTW. Embryos were then incubated in 10µg/mL of Proteinase K (Sigma) diluted in PBTW to permeabilise tissue and digest RNAses. Tubes were gently rotated to coat the entire tube with Proteinase K and the length of incubation varied depending on the stage of embryo and whether it had been New cultured. Typical times include 3-5min for EGK XII-HH3, 8min for HH3-5 and, 12min for HH6-8 and 15min or more for HH9 onwards. New cultures embryos were never incubated for longer than 8min due to their fragile nature. Embryos were then rinsed briefly in PBTW and post-fixed for 30min with 4% PFA containing 0.1% Tween-20 and 0.1% glutaraldehyde. Finally they were rinsed twice briefly in PBTW to remove fixative and stored until required at -20°C in hybridisation (HYB) solution. HYB contains final concentrations of 50% formamide, 1.3x SSC pH4.5, 5mM EDTA pH8.0, 50µg/mL Torula Yeast RNA (Sigma), 100µg/mL Porcine Heparin (Sigma), 0.5% CHAPS, 0.2% Tween-20 dissolved to a final volume of 1L in autoclaved H_2O.

Prior to hybridisation, embryos and riboprobes were pre-heated in a water bath to 70°C for 2-3h. Probes were then added to embryos and hybridised overnight at 70°C. For probes shorter than 400nt, the hybridisation temperature was reduced to allow annealing; 65-68°C for 200-350nt and 62-65°C for 100-200nt. For double-labelled in situ hybridisation, a mixture of 2 probes was added to embryos, each labelled with DIG or FLU.

The following day, probes were removed and saved for re-use. Embryos were rinsed 3x and washed for 2x 30min with preheated HYB at 70°C. Next, they were washed for 20min with a preheated 1:1 mixture of HYB:TBST. TBST was diluted 1:10 from a 10x stock containing 80g NaCl, 2g KCl, 250mL 1M Tris-HCl pH7.5, 110g Tween-20, dissolved to a final volume of 1L with H_2O. Embryos were then rinsed 3x followed by 3x 30min washes with 1xTBST before being blocked for 3h at room temperature. Blocking buffer contained 5% heat inactivated goat serum with 1mg/mL Bovine Serum Albumin (BSA) dissolved in TBST. Embryos were then incubated overnight at 4°C on a rocking platform in fresh blocking buffer containing sheep anti-DIG-AP conjugated Fab fragments, or anti-FLU-AP conjugated Fab fragments (Roche) at a 1:5000 concentration.

On day 3, the antibody solution was removed and embryos were rinsed 3x TBST and washed 3x 1h TBST before being returned to the 4°C rocker overnight. On day 4 embryos were washed in NTMT for 2x 10min. NTMT contains a final concentration of 100mM NaCl, 100mM Tris-HCl pH9.5, 50mM MgCl2 and 1% Tween-20. Colour staining was developed at room temperature by adding colour buffer containing 2.3µL of 5-Bromo-4-chloro-3-indolyl phosphate (BCIP) and 3µL of 4-Nitro-blue-tetrazolium chloride (NBT) (Roche) per mL of NTMT. Embryos were protected from the light and left rocking. Staining was stopped by rinsing embryos in NTMT at 4°C for several days before washing 2x 10min in PBTW and storing in 4% PFA.

For double-labelled in situ hybridisation, embryos were fixed for at least 24h at 4°C. Then, they were rinsed 3x and washed 5x 30min in TBST containing 0.1% Tween-20 rather than 1%. Remaining alkaline phosphatase activity was quenched by incubating embryos at 70°C for 1h before washing 3x 15min in TBST containing 0.1% Tween and 3x 15min in TBST containing 1% Tween. Embryos were blocked for 2h at room temperature as before and then incubated overnight at 4°C with anti-DIG or anti-FLU to reveal the second probe.

After removing the antibody, embryos were washed as before; 3x rinses followed by 3x 1h washes with TBST and 2x 10min washes in NTMT. Colour was developed by adding NTMT containing 7.5µL INT-BCIP (Roche) per mL and stopped by washing in NTMT at 4°C for several days before washing 2x 10min in PBTW and fixing in 4% PFA.

2.18 Whole-mount antibody staining

Antibody staining was performed after in situ hybridisation. Embryos were re-fixed in 4% PFA overnight at 4°C and then rinsed 3x 10min and washed 3x 1h in PBTW. They were then blocked for 1h at room temperature in blocking buffer containing 1mg/mL BSA, 5% heat inactivated goat serum in PBTW before being incubated for 2 nights at 4°C with primary antibody diluted in blocking buffer as previously described (Streit *et al.*, 1995, Streit *et al.*, 1997). Next, embryos were rinsed 3x 10min and washed 3x 1h with PBTW before being incubated in Horse radish peroxidase (HRP)-conjugated secondary antibody in blocking buffer overnight at 4°C. Again, embryos were rinsed 3x 10min and washed 3x 1h with PBTW before being washed 2x 20min with 0.1M Tris-HCl pH7.4. HRP activity was revealed using 0.5mg/mL 3, 3'-diaminobenzidine (DAB) in 0.1M Tris-HCl pH7.4 containing 0.003% hydrogen peroxide.

To reveal quail graft tissue, mouse monoclonal QCPN IgG; 1:5 (Developmental Studies Hybridoma Bank) followed by goat anti-mouse-HRP IgG; 1:1000 (Jackson Immunoresearch). For staining GFP-chick graft tissue, rabbit polyclonal anti-GFP IgG; 1:2000 (Molecular Probes) followed by goat anti-rabbit-HRP IgG; 1:2000 (Santa-Cruz).

2.19 Paraffin embedding and sectioning of embryos

Where necessary, embryos were sectioned after whole-mount imaging. They were prepared for paraffin embedding by processing with the following solutions; absolute methanol for 10min, propan-2-ol for 5min and tetrahydronaphthalene for 30min. To this, melted paraffin wax was added to give a 1:1 mixture of tetrahydronaphthalene:wax and embryos were left to equilibrate at 60°C. Fresh wax was then replaced 3x 1h and then left overnight at 60°C. The following day embryos were embedded into small plastic trays and the wax left to cool gently. Wax blocks were trimmed and orientated before being sectioned to 10-12µm on a microtome. Sections were mounted on slides treated with glycerin-albumin. Slides were left to dry overnight at 37°C before subsequent dewaxing with histoclear. The first histoclear wash was left overnight and the second for several hours. Coverslips were mounted using a 3:1 mixture of Canada Balsam:histoclear and left to dry completely before imaging.

2.20 Imaging of whole-mount and sectioned embryos

Whole-mount embryos were imaged on a white background and illuminated with transmitted and reflected light. All images were taken from the dorsal perspective unless otherwise stated. Embryos were oriented on an Olympus SZH10 Stereomicroscope with an Olympus DF PlanApo 1X objective and an Olympus NFK 3.3x LD 125 photo eyepiece.

Sections were imaged on an Olympus Vanox-T optical microscope using either Olympus SPlan 20x (0.46 PL 160/0.17) or Olympus SPlan 10x (0.30 PL 160/0.17) objectives.

Images were captured using the QImaging Retiga 2000R Fast 1394 camera and QCapture Pro software. They were saved as 24-bit, colour TIFF files with dimensions of 1600 x 1200 pixels, at 300dpi.

2.21 NanoString nCounter

2.21.1 A custom NanoString probe set for neural induction

NanoString experiments were run on the nCounter Analysis System, using a custom probe set and following NanoString guidelines. The probe set was designed to include the following:

1. Upregulated genes at 5, 9 and 12h with a fold change of 1.2 $\log_2$ and RNA-Seq induced base mean of at least 45.
2. Downregulated candidates at 5, 9 and 12h with a fold change of 1.2 $\log_2$ and RNA-Seq uninduced base mean of at least 200.
3. All candidate genes from the original 5h neural induction screen.
4. Standard housekeeping genes (ACTB, GAPDH and LDHA) and endogenous controls identified from the RNA-Seq screen, which show no variation between samples.
5. Markers of apoptosis and proliferation
6. Transcriptional readouts of FGF, BMP, WNT, Retinoic acid, Notch and Hedgehog signalling.
7. Markers of other cell fates: epithelial, mesodermal, endodermal, neural plate border, pre-placodal region, neural crest and Hensen's node.
8. Standard NanoString control probes: 6 positive and 8 negative.

2.21.2 Tissue collection for NanoString analysis

Uninduced tissue or induced epiblast that had been exposed to node and bead grafts was dissected as previously described (Chapter 2.6). Per condition, 4-12 pieces of tissue were dissected in ice-cold PBS and collected in triplicate. Tissue was collected on ice and promptly processed by adding 4µL of lysis buffer from the RNAqueous®-Micro Total RNA Isolation Kit (Ambion). Where fewer pieces of tissue were collected, these were processed in 2µL of lysis buffer and later combined with other samples to make up the numbers and volume. After the addition of lysis buffer, tubes were immediately snap-frozen on dry ice and stored at -80°C.

Tissue for all NanoString experiments was collected in this way. To refine the time-course of induction, induced and uninduced tissue was collected after Hensen's node grafts for 1, 3, 5, 7, 9 and 12h. The contributions of particular signalling pathways to neural induction were assessed by perturbation. Tissue from FGF, BMP inhibition, WNT inhibition, retinoic acid and Sonic Hedgehog gain- and loss-of-function experiments was collected after 5 and 9h.

2.21.3 Tissue processing for NanoString analysis

Tissue samples were processed using the provided NanoString kit and following manufacturer's instructions. Samples were processed in batches of 12. In brief, cell lysates were defrosted on ice, together with a single vial of custom reporter probes and capture probes. Once defrosted, 130µL of hybridisation buffer and 13µL of RNase-free water was added to the reporter probes to make a master mix. Of this, 21µL was gently pipetted into a strip of 12 sterile PCR tubes. To each tube, 1-4µL of cell lysate was added (depending on the number of lysed pieces of dissected tissue) and topped up to a total of 4µL with lysis buffer (Ambion). Finally 5uL of capture probes were added to give a total volume of 30µL in each PCR tube. Tubes were flicked gently to mix well and vortexed gently, to prevent probe shearing. Probes were hybridised to cell lysates overnight for 17h at 65°C.

Next, samples were transferred to the NanoString prep-station robot, which was set up to process the hybridised samples using the following materials. Two high sensitivity (50ng) prep-plates were defrosted for 30min at room temperature and centrifuged for 2min at 1000 rpm. One NanoString cartridge was defrosted at room temperature and placed on the robot with the electrodes in each well. One rack of tips, two racks of tip sheaths and two strips of sterile PCR tubes were also added. Lastly, the hybridised samples at 65°C were added to the prep-station and the standard processing programme was run for around 3h. During this time probe-target complexes are purified from the hybridisation mix and immobilised on the cartridge. Any unbound probes are removed and finally complexes are aligned.

Once processing was complete, the underside of the cartridge was treated with immersion oil and placed on the NanoString Analyzer, where the standard programme was used to digitally count probe-target complexes for each experiment from 600 fields of view.

2.21.4 Raw NanoString data quality control analysis

Raw NanoString data were imported into Microsoft Excel and analysed according to NanoString guidelines with some minor adjustments. Firstly, data for each assay were checked to ensure 600 (or very close to) fields of view were counted and that binding density values fell within the 0.05-2.25 range. Next, the sum of the 6 positive controls probes was calculated for each assay, and then averaged across the entire data set. From these, a positive lane normalisation factor (PLNF) was calculated by dividing the average sum of all assays by the total sum for each assay. This value should fall between 0.3-3.0. For each lane, negative and endogenous probe raw counts were multiplied by their respective PLNF to normalise data across the entire set of assays. The mean, standard deviation, and mean plus two times standard deviation (M+(2xSD)) was calculated from the 8 normalised negative control probes. Each sample was adjusted to remove background binding levels by subtracting the (M+(2xSD)) from normalised endogenous gene counts. Any transcript counts that became negative as a result, were reset to zero. Next, the data were transformed by adding 1 to all counts in each assay. These normalised and adjusted raw values were used to calculate the total sum of RNAs in each assay. Individual transcript counts were divided by their assay total, to quantify transcript expression as a proportion of the total transcripts counted.

2.21.5 Differential expression analysis

Data from paired experimental and control conditions were compared to calculate transcript differential expression. The mean and standard deviation was calculated from each triplicate of assays. Transcript fold change was calculated by dividing the mean for experimental conditions by the corresponding control mean. Fold change thresholds of ≥1.2 or ≤0.75 were used to define transcripts as upregulated or downregulated in the experimental condition respectively. The statistical significance of these results was calculated using a Two-tailed Type 2 T-Test with a P-value of 0.05. Using Excel, the results for selected markers and readouts were plotted as bar graphs comparing experimental and control means. Graphs were saved in Microsoft Powerpoint as JPEG files at a resolution of 300dpi.

Chapter 3: Neural induction proceeds as a cascade of events

3.1 Introduction

Neural induction is the process by which a region of embryonic ectoderm acquires a neural identity, and in vertebrates, culminates in the formation of the neural plate. Investigating its molecular basis established the "default model" (Hemmati-Brivanlou and Melton, 1997), which proposes that ectodermal cells will automatically acquire a neural fate in the absence of signalling (see Chapter 1.5). However, in chick expression patterns of BMPs and BMP antagonists do not fit with the predictions of the "default model" (Streit *et al.*, 1998, Streit and Stern, 1999). Furthermore BMP inhibition is not sufficient to induce neural markers (Streit and Stern, 1999, Linker and Stern, 2004), in fact chick ectoderm can only respond to BMP inhibition if it has first been exposed to 5h of organizer signals (Streit *et al.*, 1998). Additionally, there are reports that neural induction requires FGFs (Lamb and Harland, 1995, Launay *et al.*, 1996, Linker and Stern, 2004, Delaune *et al.*, 2005), but many other signals have also been implicated (see Chapter 1.7). Together, these findings indicate that the "default model" is too simplistic, and that other signals must be required in addition to BMP inhibitors for neural induction.

Chick is a powerful model in which to study this problem. Grafts of the organizer, Hensen's node (Hensen, 1876), to a region of competent extra-embryonic ectoderm can induce ectopic neural tubes derived from the host ectoderm (Waddington, 1933, Waddington and Schmidt, 1933, Waddington, 1934, Waddington, 1936, Gallera and Ivanov, 1964, Storey *et al.*, 1992). Using this technique, a differential screen identified 10 genes that are induced following 5h of a graft (Streit *et al.*, 2000). The earliest responses (ERNI, SOX3 (Streit *et al.*, 2000) and Calfacilitin (Papanayotou *et al.*, 2013)) are induced within 3h of a node graft and are normally expressed in the EGKXII-XIII epiblast. Others, (Churchill (Sheng *et al.*, 2003), DAD1, UBII (Gibson *et al.*, 2011), Asterix and Obelix (Pinho *et al.*, 2011)) require 5h of exposure to a node and are first detected in the prospective neural plate at HH3-4. Furthermore, a number of markers were found to be induced by FGFs, rather than BMP antagonists (see Chapter 1.11).

To date, the relative timing of markers induction correlates with the sequence of their expression in the embryo (Pinho *et al.*, 2011), suggesting that neural induction in an ectopic region mimics the endogenous process and that it might occur as a sequence of events (see Chapter 1.12). However the screen did not identify many other neural markers. For example, NOT1, NOT2 (Knezevic *et al.*, 1995, Knezevic and Mackem, 2001), OTX2 (Bally-Cuif *et al.*, 1995) (Foley *et al.*, 2000) and CYP26A1 (Albazerchi and Stern, 2007) could also be early responses to neural induction as they are expressed in either the epiblast at EGKXII-XIII or the prospective

neural plate at HH3+/4-. Definitive neural markers such as SOX2 (Rex *et al.*, 1997) and SOX1 (Pevny *et al.*, 1998), which are normally expressed even later than the markers identified by the screen, were also not detected. To determine whether these are also responses to neural induction, we investigated their expression following grafts of Hensen's node in time course.

Expression of TRKC (or NTRK3), the last remaining candidate identified from the original differential screen, has also been observed at primitive streak stages (Bernd and Li, 1999, Li and Bernd, 1999). To confirm whether TRKC is also expressed as a response to neural induction, we verified its earliest expression and then tested whether it is induced by signals from Hensen's node.

We find that each of these markers is induced by grafts of Hensen's node, but at different time points. At least 9h of signals are required before definitive neural markers are induced, but cells require 12h of signals before they are committed to a neural fate. This suggests that neural induction must occur as a sequence of molecular events that occur between 0-12h of a node graft.

3.2 Results

3.2.1 TRKC is expressed in the neural plate

(Part of Pinho *et al*., 2011)

Whole-mount in situ hybridisation was used to confirm the expression of TRKC in chick embryos between EGKXII and HH8 (Fig. 3.1). Weak TRKC expression is first evident anterior to the node in the prospective neural plate at HH3+ (Fig. 3.1B). This expression intensifies in the anterior neural plate as the head process emerges between HH4+ to 6 (Fig. 3.1D-F). By HH8, TRKC is strongly expressed in the anterior neural tube and neural folds, extending caudally as far as the somites (Fig. 3.1G). Expression of TRKC at primitive streak stages is consistent with the published expression pattern (Bernd and Li, 1999) and was never observed in the primitive streak, neighbouring ectoderm or notochord. In addition, no specific staining was observed prior to gastrulation in pre-streak embryos (Fig. 3.1A). Therefore TRKC is expressed at the appropriate time in the neural plate to be a response to neural induction.

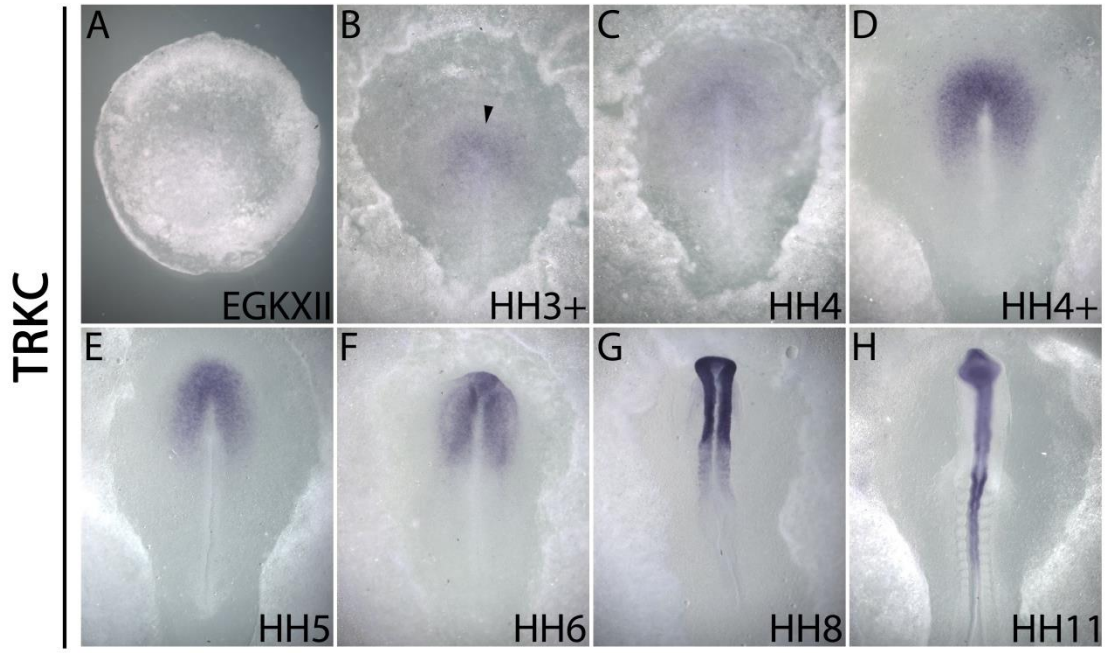

Figure 3.1: TRKC expression during early chick development.

TRKC expression was assessed at a range of stages by in situ hybridisation. Expression is first observed at HH3+ in the prospective neural plate (B; arrow). TRKC expression continues in the anterior neural plate (C-F) and later in the neural folds and neural tube (G and H). No TRKC expression was detected in pre-streak embryos (A).

3.2.2 TRKC is induced by grafts of Hensen's node

(Part of Pinho *et al*., 2011)

The presence of TRKC in the neural plate during gastrulation, together with its identification from the differential screen, suggests that TRKC may be induced by Hensen's node during neural induction. To test this, its induction was studied in time course, by grafting a quail Hensen's node at HH3+/4- into a chick host at HH3+/4- followed by incubation for different periods of time (Fig. 3.2A).

In situ hybridisation for TRKC reveals that it is induced to differing extents in response to timed quail node grafts (Fig. 3.2). Very weak induction of TRKC was detected after 3h of incubation but only by a proportion of grafts (Fig. 3.2B; 6/8). Slightly stronger expression was seen at 4h by 3/3 grafts (Fig. 3.2C). Robust expression was observed after 6h (Fig. 3.2D; 5/5) and this persisted after 9h (Fig. 3.2E; 4/4). These results confirm that TRKC expression can be induced robustly within 4-6h of signals from a grafted organizer. It suggests that TRKC can be induced

by grafts of Hensen's node and that its expression, which first arises in the ectoderm adjacent to Hensen's node, is likely a response to signals from the organizer.

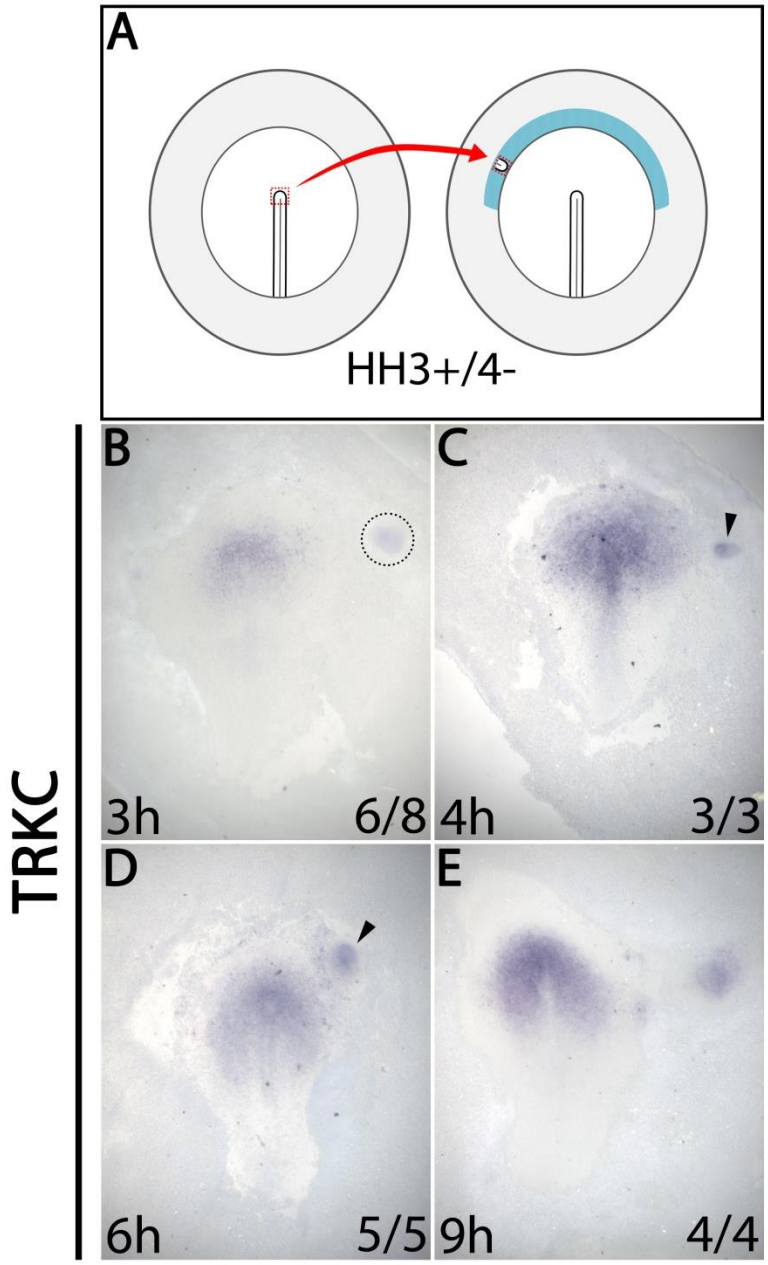

Figure 3.2: A time-course of TRKC induction by grafts of Hensen's node.

Grafts of quail Hensen's node at HH3+/4- into chick hosts at HH3+/4- (A) were analysed in time-course after in situ hybridisation (B-E). Very weak TRKC expression is observed after 3h in 6/8 grafts (B). Slightly stronger expression is observed in the extra-embryonic ectoderm after 4h (C; 3/3). TRKC is strongly induced 6-9h after grafting (D; 5/5 and E; 4/4).

3.2.3 The regulation of TRKC by chemical and secreted factors

(Part of Pinho *et al*., 2011, conducted in collaboration with M. Stower)

Having demonstrated that TRKC expression is induced robustly within 6h of organizer signals, we sought to establish which factors might be involved. FGF8 is sufficient to induce ERNI, SOX3 (Streit *et al.*, 2000), Churchill (Sheng *et al.*, 2003), Calfacilitin (Papanayotou *et al.*, 2013), DAD1, UBII (Gibson *et al.*, 2011) and Asterix (Pinho *et al.*, 2011). Furthermore, it is expressed by the hypoblast and Hensen's node at stages relevant to the induction of early responses to neural induction (Streit *et al.*, 2000). To test whether FGF8 signalling regulates TRKC expression, gain- and loss-of-function experiments were performed. Heparin beads soaked in FGF8b were grafted to a competent region of the area opaca, or beads of the FGF inhibitor SU5402, were grafted together with a node (Fig. 3.3A).

Beads of FGF8b failed to induce TRKC expression after 6 or 14h of incubation (Fig. 3.3B and C). Furthermore, beads of SU5402 did not inhibit TRKC induction by a node graft after 6h (Fig. 3.3D; 6/6). This suggests that FGF8 signalling is neither sufficient nor necessary for the induction of TRKC by Hensen's node. Other factors were tested in an attempt to discover which might be involved. Retinoids are known to be present in Hensen's node (Chen and Solursh, 1992) (Chen *et al.*, 1992) but beads of retinoic acid (Fig. 3.3E; 0/4) were also unable to induce TRKC. Similarly TRKC was not induced by ionomycin, a calcium ionophore (Fig. 3.3F; 0/4), the BMP inhibitor noggin (Fig. 3.3G; 0/3) nor the neuropeptide somatostatin have any effect (Fig. 3.3H; 0/8). As none of these signals is able to induce TRKC, other factors or combinations of factors must be responsible for inducing TRKC.

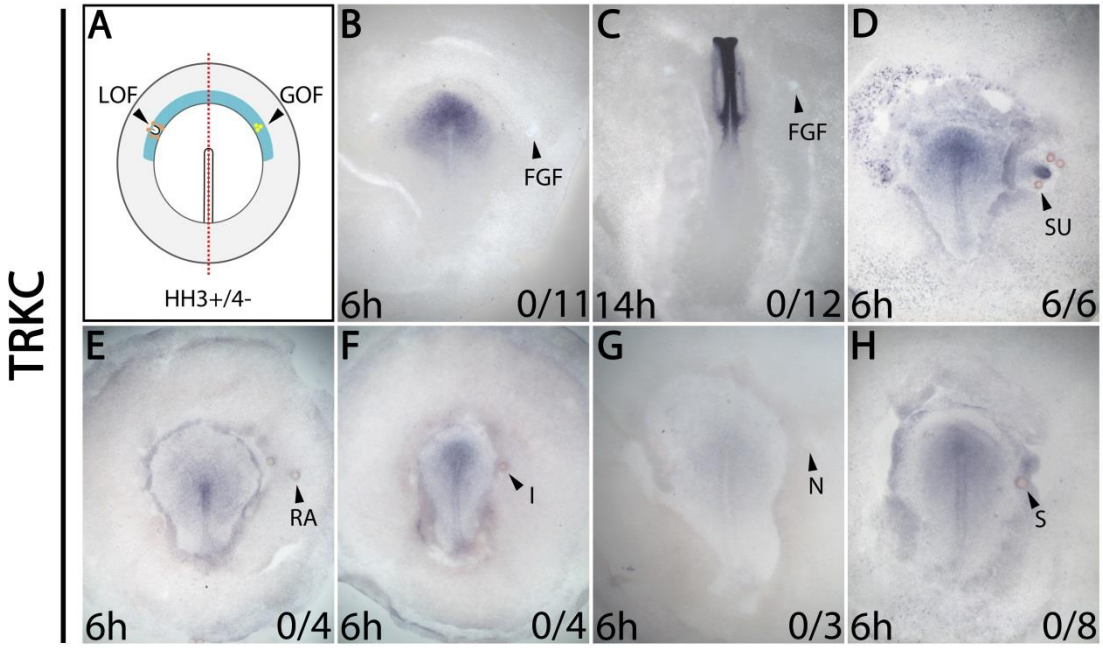

Figure 3.3: Regulation of TRKC induction by chemical and secreted factors.

Gain or loss-of-function experiments were used to assess which signals might be responsible for regulating TRKC (A). TRKC was not induced by beads of FGF8b after 6 or 14h (B; 0/11 and C; 0/12; black arrows). TRKC was induced after 6h in the presence of SU5402 (D; 6/6). After 6h beads of retinoic acid (E; 0/4), ionomycin (F; 0/4), noggin (G; 0/3) and somatostatin (0/8) were also unable to induce TRKC. (Arrows show bead placement).

3.2.4 Is the neural plate responsive to NT-3 signalling during neural induction?

(Part of Pinho *et al*., 2011)

TRKC is a receptor tyrosine kinase responsible for specific, high affinity binding of Neurotrophin 3, a factor involved in neuronal survival and differentiation (Arévalo and Wu, 2006). Although TRKC is present in the neural plate as early as HH3+/4, it is unknown whether it mediates neurotrophin signalling at these stages. RT-PCR has previously detected NT-3 mRNA from whole embryos in the chick at stages 5-8 but this does not reveal where NT-3 is localised at these stages (Yao *et al.*, 1994, Baig and Khan, 1996). To explore whether tissues expressing TRKC might be responsive to NT-3 signalling during early development, NT-3 expression was assessed by in situ hybridisation (Fig. 3.4).

The expression of NT-3 was examined over a range of stages. It is not expressed before primitive streak formation at EGKXII or even at HH4 (Fig. 3.4 A-B), when TRKC is present in the

neural plate. The earliest NT-3 expression was detected at HH9-10 (Fig. 3.4C) so it is possible that NT-3 signalling may occur via TRKC from HH9-10 onwards when they are co-expressed in the anterior neural tube. However, NT-3 expression does not seem to coincide with TRKC expression during neural induction, so any function of TRKC at these stages could be independent of NT-3.

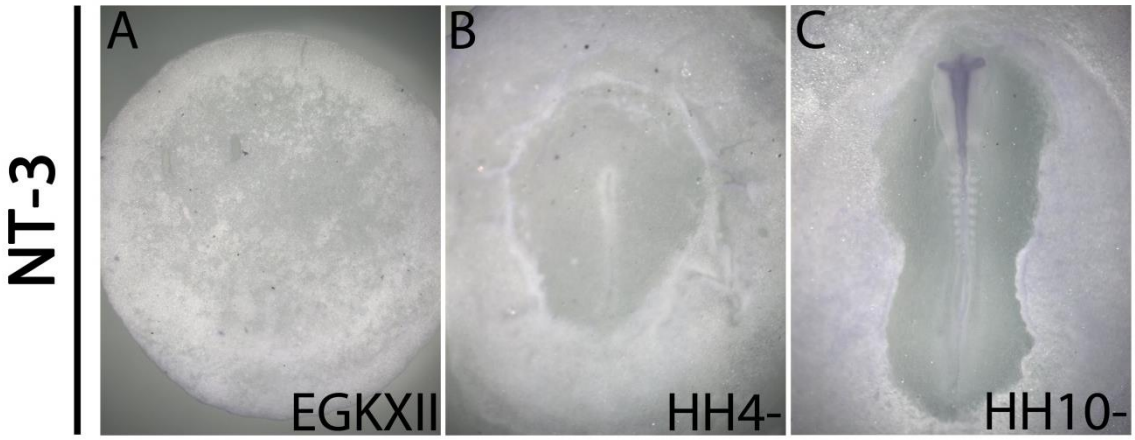

Figure 3.4: NT-3 expression in the early embryo.

NT-3 expression cannot be detected prior to gastrulation in EGKXII embryos (A), or at HH4 during gastrulation (B). Weak NT-3 expression is first observed in the anterior neural tube at HH9-10 extending caudally as far as the somites (C).

3.2.5 NOT1 and NOT2 can be induced by grafts of Hensen's node

NOT1 and NOT2 are CCR4-Not complex transcription factors that are expressed in the axial mesoderm from HH4+ (Stein and Kessel, 1995, Stein *et al.*, 1996), but prior to this they are expressed in the pre-streak epiblast at EGKXII-XIII (Knezevic *et al.*, 1995, Knezevic and Mackem, 2001). Given the similarity of their early expression to ERNI and SOX3 (Streit *et al.*, 2000), we tested whether these transcription factors might also be induced by grafts of Hensen's node.

Like TRKC, there is no evidence of NOT1 or NOT2 induction after 1h (Fig. 3.5A and D). After receiving 3h of signals, NOT1 and NOT2 are induced but only in a proportion of cases (Fig. 3.5B; 8/18, E; 8/13). After 5h, incomplete induction of both genes is still observed (Fig. 3.5C; 8/13, F; 10/16). Therefore grafts of Hensen's node do provide signals which induce NOT1 and NOT2 after 5h, but are not able to induce them in all cases. It is possible that more than 5h of signals are required for complete induction. Alternatively, since the expression of NOT1 and NOT2 in the endogenous prospective neural tissue is only transient -by HH4+ they are only expressed in

the head process (Fig. 3.5C and F); they might only be induced very transiently by a node with subtle variations in timing between grafts.

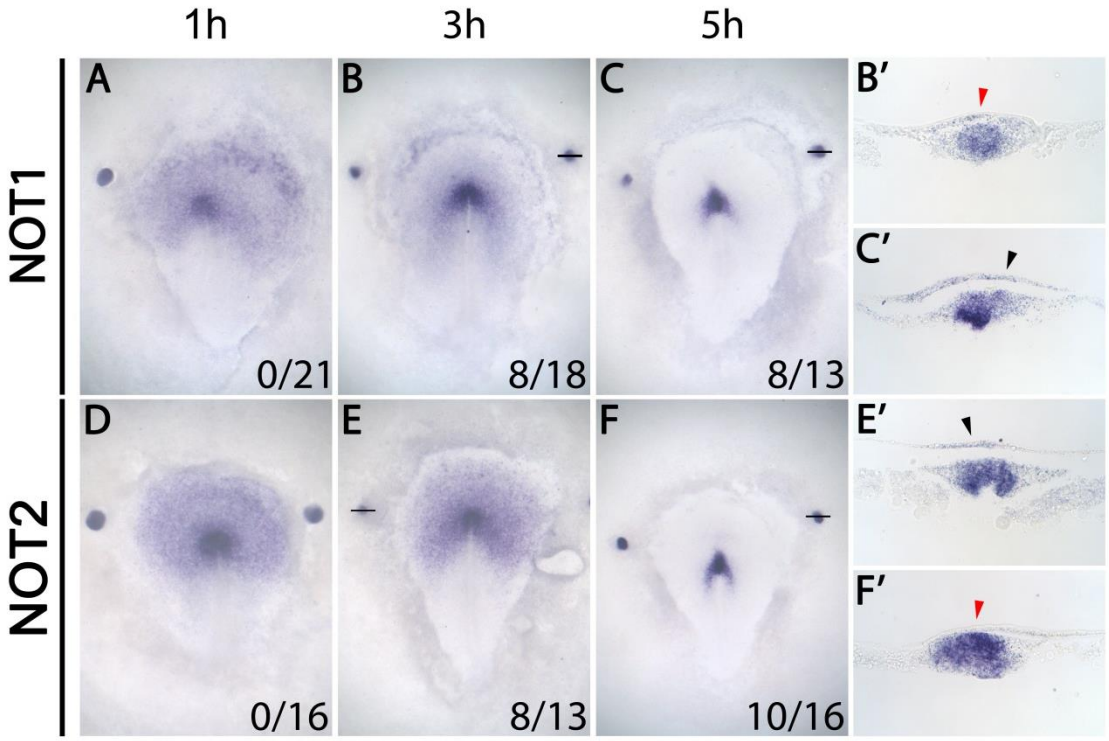

Figure 3.5: A time-course of NOT1 and NOT2 induction by grafts of Hensen's node.

The induction of NOT1 and NOT2 was studied in time-course by grafts of Hensen's node. No induction of either NOT1 or NOT2 is observed after 1h (A; 0/21, D; 0/16) when expression is observed only in the node graft itself. After 3 and 5h, both NOT1 (B, B', C, C') and NOT2 (E, E', F, F') are induced, but only by a proportion of grafts. Presence (black arrows) or absence (red arrows) of NOT1 and NOT2 induction is shown in closer detail (B', C' E', F'). Horizontal lines show where sections through grafts were taken (B, C, E, F).

3.2.6 OTX2 is also induced by grafts of Hensen's node

The anterior neural markers OTX2 (Bally-Cuif *et al.*, 1995) and CYP26A1 (Swindell *et al.*, 1999, Blentic *et al.*, 2003) are also expressed appropriately in the prospective neural plate to be involved in neural induction. Both can be induced by grafts of the hypoblast: CYP26A1 by retinoic acid and OTX2 by a combination of FGFs with BMP and WNT antagonists (Albazerchi and Stern, 2007). Although these signals are also present in Hensen's node, neither gene was detected in the original 5h screen. To test whether these might also be induced in response to

organizer signals, chick nodes were grafted to the area opaca to determine a time-course for their possible induction (Fig. 3.6)

OTX2 induction by a node graft is similar to SOX3 (Streit *et al.*, 2000). No induction was observed in the adjacent epiblast after 1h (Fig. 3.6A; 0/8); the only detectable staining is restricted to the node graft itself. After 3 and 5h, OTX2 was induced in all cases (Fig. 3.6B; 7/7 and C; 6/6). After 1h there was also no induction of CYP26A1 (Fig. 3.6D; 0/21) but unlike OTX2, it was only induced by a proportion of grafts after 3 and 5h (Fig. 3.6E; 8/13, F; 7/13). Where expression was observed, it always appeared as a trail (red arrow) or patch (black arrows) of cells extending between the host expression domain and the grafted node. Grafts placed even slightly further away from the embryo, but still in a region competent to respond to neural induction, were never associated with CYP26A1 expression. This suggests that CYP26A1 expression can only be readily expanded from the neural plate after 3-5h, but not induced ectopically.

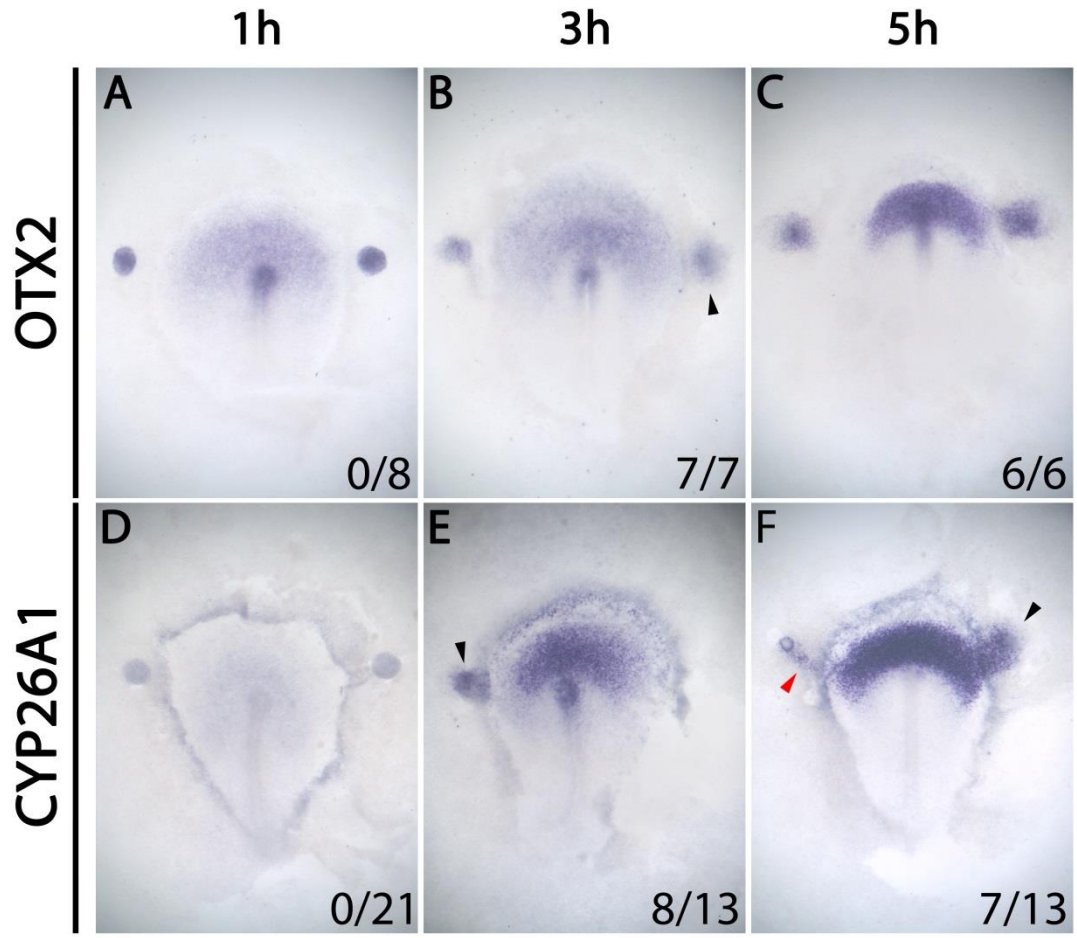

Figure 3.6: Time-course of OTX2 and CYP26A1 induction by node grafts.

Grafts of chick Hensen's node into chick hosts were analysed in time course for the induction of OTX2 (A-C) and CYP26A1 (D-F). OTX2 is not induced in the epiblast after 1h (A; 0/8) and staining is only visible in node tissue. However, OTX2 is fully induced after 3h (B; 7/7, arrow) and 5h (C; 6/6). CYP26A1 induction is not observed after 1h (D; 0/21) and is only associated with a proportion of grafts after 3h (E; 8/13) and 5h (F; 7/13), when it only appears as a patch (black arrows) or trail of cells (red arrow) connected to the host expression domain.

3.2.7 The definitive neural marker SOX2 can be induced within 9h

The neural induction screen successfully identified early responses to grafts of Hensen's node. These markers are all expressed in the prospective neural plate at HH3+/4- (Pinho *et al.*, 2011); prior to formation of the neural plate proper. Therefore, no later neural markers were detected.

SOX2 is first expressed anterior to the node in the forming neural plate between HH4/4+ (Rex *et al.*, 1997). Its expression persists throughout the neural plate and later in the neural tube, where it is considered a marker of neural specification (Rex *et al.*, 1997). Since 5h of signals are insufficient to induce definitive neural markers or a neural plate, we sought to determine the period of signals required to induce SOX2 by studying the timing of its ectopic induction.

In situ hybridisation for SOX2 shows that it is induced to different extents in response to timed node grafts. No SOX2 expression was detected after 3h of incubation (Fig. 3.7B; 0/8). Weak expression was observed after 5h, but only by a proportion of grafts (Fig. 3.7C; 7/12). Robust induction could be seen after 9h in all cases (Fig. 3.7D; 8/8). This continued over 12-15h of incubation when the induced domains lengthen to form secondary axes which strikingly resemble the host (Fig. 3.7E-F). This suggests that 9h of signals from a grafted node are required before SOX2 expression is fully induced.

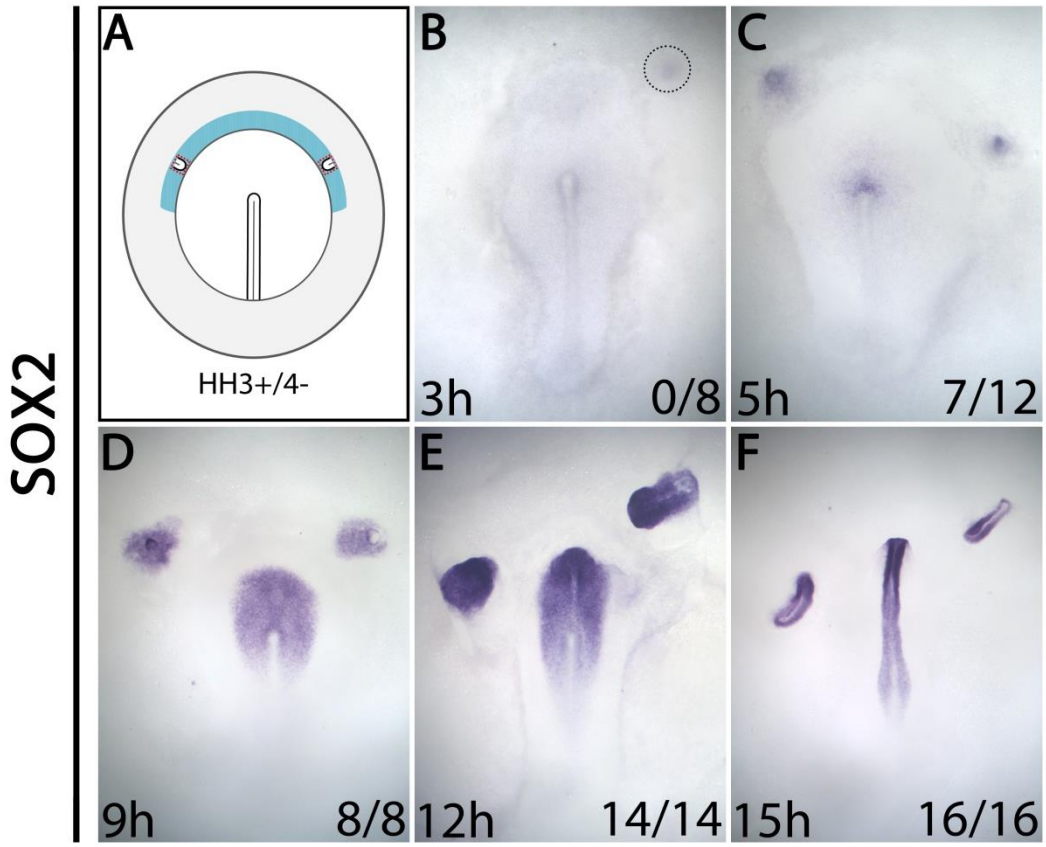

Figure 3.7: A time-course of SOX2 induction by grafts of Hensen's node.

Grafts of chick Hensen's node into chick hosts were analysed in time-course for induction of SOX2 (A). No induction in the epiblast is observed after 3h (B) and weak expression is observed after 5h but only in 7/12 grafts (C). Robust expression is induced after 9h (D) by all grafts. This progressively strengthens over 12 and 15h (E-F).

3.2.8 Does host age influence the timing of ectopic induction?

Our observation that SOX2 is induced after 9h, is consistent with some previous experiments (Streit and Stern, 1999) but differs from suggestions that 12h are necessary (Pinho *et al.*, 2011).Therefore we considered factors which might influence the timing of induction

Earlier work established that expression of the L5 epitope defines the region of epiblast which is competent to respond to neural inducing signals (Streit *et al.*, 1995). At HH3+/4 this domain extends anteriorly and laterally as far as the inner third of the area opaca. After HH4 the epiblast simultaneously loses L5 expression and neural competence (Gallera and Ivanov, 1964, Storey *et al.*, 1992, Streit *et al.*, 1995). Although the timing of grafting is important in terms of competence, we wondered whether stage differences within this window could account for

variation in the timing of SOX2 induction. To test this, HH3+ chick nodes were grafted to hosts between HH3 and HH4+ and the timing of SOX2 induction assessed (Fig. 3.8).

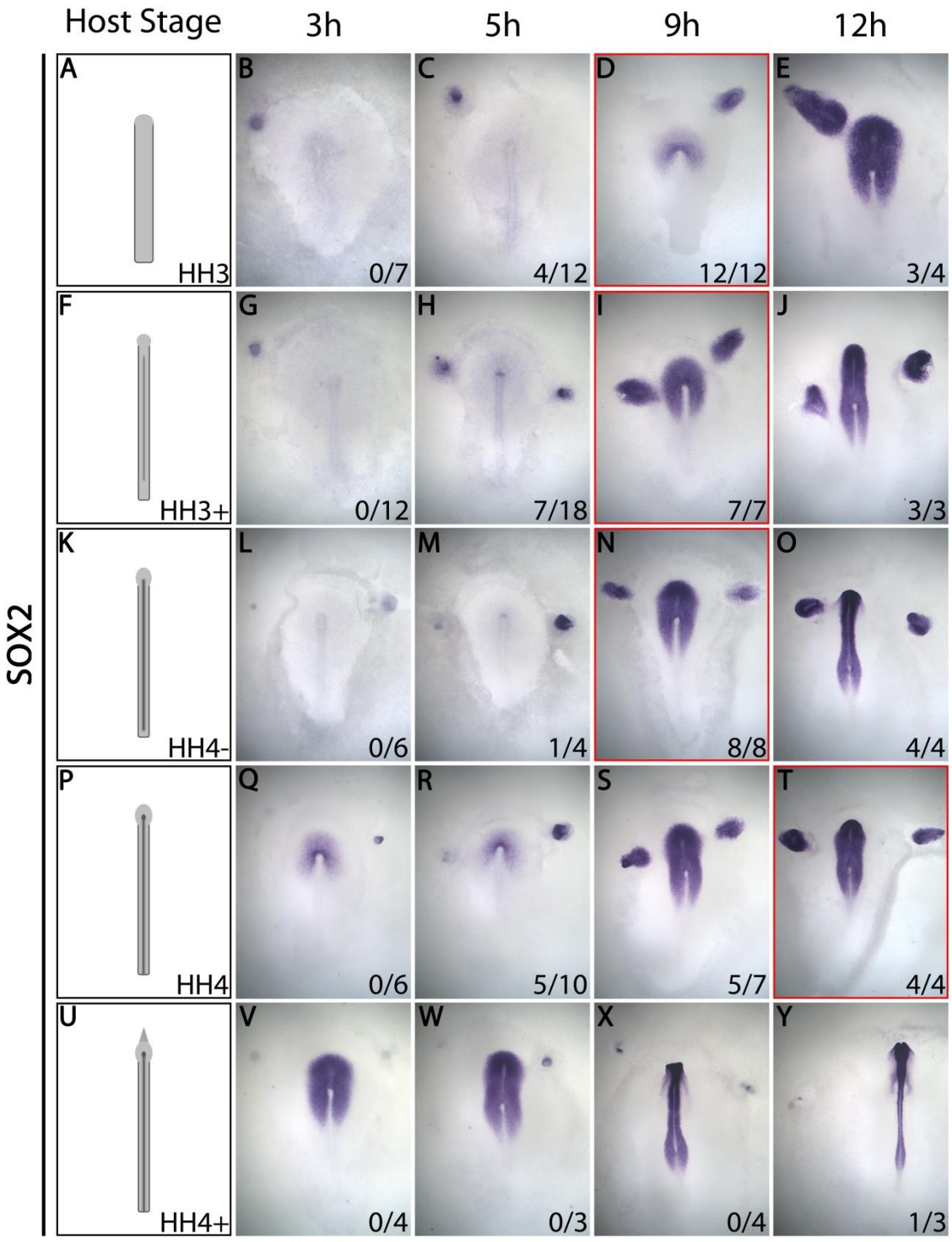

Figure 3.8: The timing of SOX2 induction varies with host age.

HH3+ chick nodes were grafted to hosts at HH3, 3+, 4-, 4 and 4+ and incubated for 3, 5, 9 or 12h (A, F, K, P, U). Irrespective of whether nodes were grafted into hosts at HH3 (A-E), 3+ (F-J) and 4- (K-O), the same time-course of induction was observed. No expression was observed

after 3h (B, G, L) and only weak induction in 25-40% of node grafts after 5h (C, H, M). Complete SOX2 induction was observed after 9h (D, I, N), which strengthened after 12h (E, J, O). Nodes grafted into HH4+ hosts did not induce SOX2 expression in the host epiblast at any time point (U-Y). Nodes grafted into HH4 embryos did induce SOX2 fully after 12h (T; 4/4), but only by a proportion of grafts after 5h (R; 5/10) and 9h (S; 5/7). At 3h no SOX2 induction was observed, only self-differentiation (Q; 0/7). (Red boxes highlight the timing of complete induction.)

As expected, nodes grafted into HH4+ hosts did not induce SOX2 expression in the majority of cases at any time point; staining was mainly observed in the nodes themselves as they self-differentiated (Fig. 3.8U-Y). This is in agreement with observations that the host epiblast is unable to respond to neural inducing signals after HH4 (Storey *et al.*, 1992). Nodes grafted into HH4 embryos did induce SOX2 fully, but only after 12h (Fig. 3.8T 4/4). Induction was only observed by a proportion of grafts after 5 and 9h (Fig. 3.8R; 5/10, S; 5/7). No SOX2 induction was observed after 3h, only self- differentiation (Fig. 3.8Q; 0/7).

At stages where the host epiblast is competent to respond to a node graft (HH3, 3+ and 4-) the same time-course of induction was observed (Fig. 3.8 A-E, F-J, K-O). Induction was never detected after 3h (Fig. 3.8B, G, L) and only weak induction in 25-40% of node grafts after 5h (Fig. 3.8C, H, M). SOX2 was induced robustly by all grafts after 9h (Fig. 3.8D, I, N) and persisted after 12h (Fig. 3.8E, J, O).

This confirms the initial observation that SOX2 can be fully induced within 9h; 3h earlier than previously considered. It also demonstrates that differences in host age between HH3, 3+ and 4- when the epiblast is competent (Storey *et al.*, 1992, Streit *et al.*, 1997) do not influence the timing of induction. When HH4 hosts were used, complete SOX2 induction was only observed after 12h so host age does influence the timing of SOX2 expression between HH4- and HH4 as the epiblast begins to lose competence.

3.2.9 The initial induction of SOX2 after 9h is transient

The neural induction screen was designed to identify genes induced within the first 5h of signals from Hensen's node because chick ectodermal cells must be sensitised by 5h of signals from the organizer before they can respond to BMP antagonists. Specifically, SOX3 expression induced after 5h can be maintained by Chordin-secreting cells (Streit *et al.*, 1998), but is otherwise lost after the node is removed.

Having demonstrated that 9h of signals are required to induce SOX2 expression, we next questioned whether this expression is stable or if, like SOX3, further signals are required to maintain it. To test this, chick nodes at HH3+/4- were grafted to the area opaca of chick hosts and incubated for 5, 9 or 12h. Node grafts were removed and the embryos incubated for a further 12h before SOX2 expression was assessed (Fig. 3.9A).

Normally 5h of incubation only induces weak SOX2 by a proportion of grafts while 9h is sufficient to induce SOX2 robustly in all cases (Fig. 3.7C and D). Node removal after 5h causes complete loss of SOX2 expression (Fig. 3.9B), while SOX2 expression remained but only very faintly in 4/8 cases after 9h (Fig. 3.9C). However, when the epiblast receives node signals for 12h, SOX2 expression is expressed strongly after node removal, in almost all cases (Fig. 3.9D; 4/5). As node removal earlier than 12h causes significant reduction or loss of SOX2 expression, it suggests that the initial induction of SOX2 expression by a node graft is transient and that it is only stabilised after 9-12h.

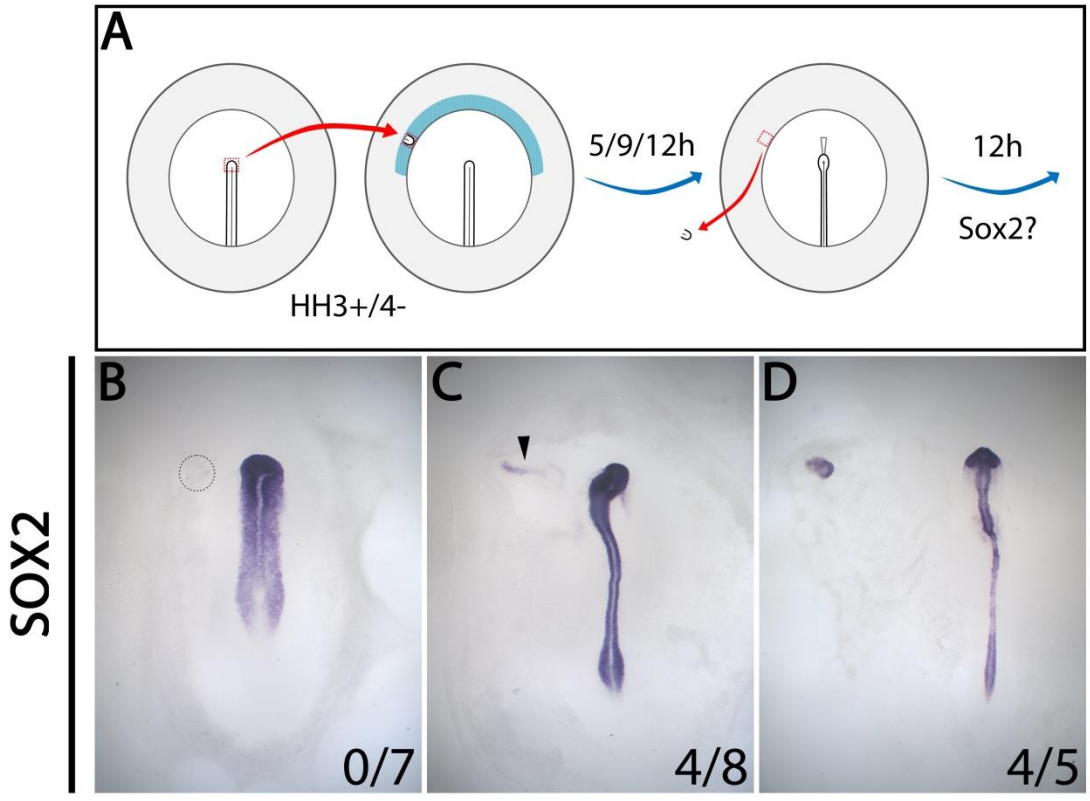

Figure 3.9: SOX2 expression is lost if grafted nodes are removed before 12h.

Nodes grafted to HH3+/4- embryos were removed after 5, 9 or 12h of incubation and host embryos cultured for a further 12h. When nodes are removed after 5h, there is no evidence of SOX2 expression in the region that received the graft (B; 0/7). When nodes are removed after

9h weak SOX2 expression persisted in 4/8 cases (C; arrow); SOX2 remains in almost all cases after 12h (D; 4/5).

3.2.10 Establishing a time-course for SOX1 induction

SOX1, another SOXB1 family transcription factor, is considered to be a definitive neural marker. SOX1 expression in neural progenitors has been associated with their commitment and differentiation to a neural fate (Pevny *et al.*, 1998). Previously, SOX1 has been predicted to be induced within 13-14h of a node graft, but this was based upon the assumption that SOX2 was first induced after 12h (Pinho *et al.*, 2011). The exact timing of its expression in the neural plate and its induction by a node has not been examined.

Initially the normal expression of SOX1 was confirmed by in situ hybridisation. No expression was detected at EGKXIII or at streak stages HH4- and HH5 (Fig. 3.10A-C). The earliest SOX1 expression was detected in the neural tube of HH8-9 embryos, where it extends posteriorly to the regressing node (Fig. 3.10D). SOX1 can also be induced by grafts of Hensen's node. It is induced in the majority of cases after 12h (Fig. 3.10E; 10/13), and almost completely after 15h (Fig. 3.10F; 11/12). Therefore SOX1 expression begins later than SOX2 in the endogenous neural plate and in a time-course of node induction.

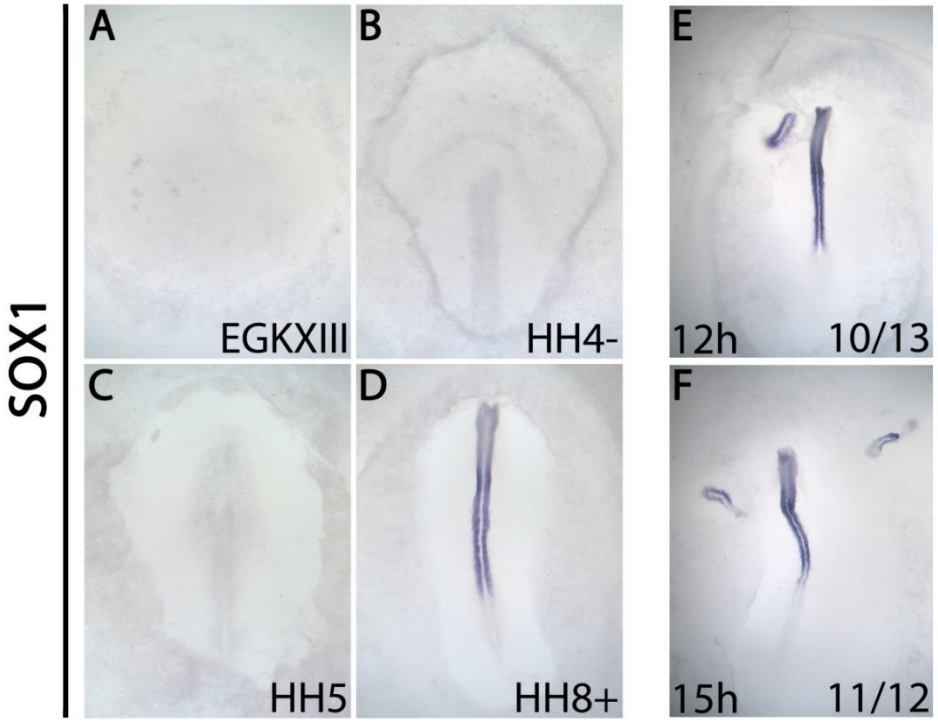

Figure 3.10: The normal expression of SOX1 and its induction by node grafts.

In the normal embryo, SOX1 expression could not be detected in pre-streak (A), during gastrulation (B), or in the neural plate at HH5 (C). It is first expressed in the neural tube from HH8-9 (D). It is induced by the majority of node grafts after 12h (E; 10/13) and 15h (F; 11/12).

3.3 Discussion

Described here are a group of genes that mark neural tissue at different stages during its development. Despite differences in the onset of their normal expression, we show that all are induced as responses to the neural induction by signals from Hensen's node. These differences are reflected in the timing of their induction by node grafts, suggesting that they are not co-regulated and revealing greater complexity to neural induction.

TRKC was one of ten genes upregulated in a screen (Streit *et al.*, 2000) designed to identify genes induced within 5h of an ectopic node graft (Pinho *et al.*, 2011). It belongs to a family of Tropomyosin-related kinase (TRK) neurotrophin receptors and is a well-studied membrane receptor for NT-3 (Arévalo and Wu, 2006). Although its expression in the neural plate has been studied previously, it had not been implicated as a response to neural induction (Bernd and Li, 1999, Li and Bernd, 1999). We verify that TRKC is first expressed weakly in the neural plate at around HH3+/4-. This expression broadens until it is expressed strongly throughout the anterior neural plate, and later the neural tube. The absence of NT-3 expression during gastrulation and neural induction suggests that whatever the function of TRKC at these stages, it is unlikely to involve NT-3. Our findings contradict observations that NT-3, as well as other TRK receptors (TRKA, TRKB) and ligands (NTF, BDNF) are expressed in avian embryos at HH5-8 (Yao *et al.*, 1994, Baig and Khan, 1996, Zhang *et al.*, 1996). However these were probably detected at much lower levels by RT-PCR, a more sensitive approach than in situ hybridisation.

OTX2 is a transcription factor known to be expressed in the epiblast at EGKXII-XIII (Foley *et al.*, 2000) and in the future neural plate at HH3+/4- (Bally-Cuif *et al.*, 1995, Albazerchi and Stern, 2007). Later its expression is restricted anteriorly and confers regional identity to the neural axis, including an important function in defining the mid-hindbrain boundary (Millet *et al.*, 1999). Given its early SOX3-like expression, we might have expected it to be identified as an early response by the neural induction screen. Likewise, the CCR4-Not transcription factors NOT1 and NOT2 also share this early pre-streak expression domain (Knezevic *et al.*, 1995, Knezevic and Mackem, 2001).

In contrast, SOX2 and SOX1 are absent from epiblast tissue at EGKXII-XIII and the prospective neural plate at HH3+/4-. Instead they are detected much later in the normal embryo. SOX2

expression begins between HH4/4+ just anteriorly to the node, but it is only expressed robustly throughout the neural plate by HH5 (Rex *et al.*, 1997). SOX1 expression begins later still; the first transcripts can be detected weakly in the neural tube at HH8-9 (Pevny *et al.*, 1998).

3.3.1 Responses to neural induction occur at different times

Analysing the ectopic induction of these markers reveals that they are all induced by grafts of Hensen's node. OTX2 is expressed in a similar time course to SOX3, ERNI and Calfacilitin (Pinho *et al.*, 2011), which are expressed in the epiblast at EGKXII-XIII as well as being induced within 3h of grafting (Streit *et al.*, 2000, Papanayotou *et al.*, 2013). TRKC more closely resembles markers such as Churchill, DAD1, UBII, Asterix and Obelix which are all induced within the first 5h of grafting and are first expressed in the neural plate by HH3+/4 (Pinho *et al.*, 2011). Therefore even within the first 5h, we can begin to separate the earliest neural responses based on their temporal expression dynamics.

Although grafts of Hensen's node have the ability to induce NOT1 and NOT2, their responses differ from OTX2 and TRKC as they are never completely induced within 3-5h. It is possible that this could happen after longer exposure to a node graft. However, we suspect that incomplete induction occurs because they are only transiently induced in neural territories. In the early embryo; both NOT1 and NOT2 are expressed in the EGKXII-XIII epiblast (Knezevic *et al.*, 1995, Knezevic and Mackem, 2001) and prospective neural plate at HH3+/4-, but do not persist in the neural plate at HH4+ (Stein and Kessel, 1995, Stein *et al.*, 1996). By sampling node grafts after 3h and 5h, we might detect their initial induction but also their imminent downregulation. Subtle differences between embryos in the exact window when this occurs, would explain why complete induction is never achieved at either time point. Therefore the incomplete induction observed, may actually reflect the normal transient nature of their expression. If so, it demonstrates that the node graft assay accurately represents the timing and dynamics of events that occur in the embryo.

Apart from these early responses, we also investigated the timing of later neural markers. Secondary axes induced by Hensen's node grafts not only exhibit the same columnar epithelial morphology as the neural plate (Gallera, 1968), but they express neural plate (SOX2) and neural tube specific markers (SOX1) (Rex *et al.*, 1997, Pevny *et al.*, 1998). However these markers require more than 5h of signals from a grafted node before they are induced; SOX2 can be induced within 9h and SOX1 almost completely within 12h. Even at these later time points, the relative timing of their induction reflects their temporal expression in the neural

plate, as SOX2 is expressed robustly in the neural plate at HH5, while SOX1 is expressed later in the neural tube at HH8-9.

Since all markers identified by the screen are earliest co-expressed in the prospective neural plate, it suggests that ectopic neural induction after 5h closely resembles the endogenous process at HH3+/4-, before the neural plate has formed. Therefore, it is not surprising that markers of the neural plate (SOX2) and neural tube (SOX1) were not identified. As signals secreted from the organizer are sufficient to induce mature neural tissue and the time of grafting represents a clear starting point, the node graft assay is a useful tool to study the entire process of neural induction. These experiments, together with those conducted previously (Sheng and Stern, 1999, Streit *et al.*, 2000, Papanayotou *et al.*, 2008, Gibson *et al.*, 2011, Pinho *et al.*, 2011) suggest that responses to neural induction do not occur at the same time. Even the earliest events proceed as a sequence and consequently it is difficult to distinguish a single "inductive" event.

3.3.2 Host age does not affect the timing of induction while the epiblast is competent

In the above experiments, chick nodes were always grafted into chick hosts at HH3+/4-. This turns out to be particularly important as subtle differences in host age can influence the timing of induction. SOX2 can be induced consistently after 9h, when nodes were grafted to hosts at HH3, 3+ and 4-, but when HH4 hosts are used; 12h of a node graft are required before SOX2 is completely induced. Therefore, differences in the timing of SOX2 induction observed by Pinho *et al*. 2011 and Streit *et al*., 1998, could be due to the former having used slightly older embryos as hosts. Although we do not test precisely why this occurs, it is likely due to the effect of competency. At HH4+ the epiblast is not competent to respond due to absence of the $L5^{220}$ epitope (Streit *et al.*, 1997). $L5^{220}$ expression starts to be lost from HH4, so it is possible that reduced competence at HH4 already hinders neuralisation, which occurs more easily at HH4-. However, as long as hosts receive grafts when the epiblast is competent to respond (between HH3 and HH4-), host age does not influence the timing of SOX2 induction. To ensure consistency of timing, future experiments should never use hosts older than HH4-.

Our conclusions differ from those of Gallera, who suggested that host age does influence ectopic induction by a node graft (Gallera, 1968). In these experiments, a morphological neural plate was induced simultaneously by a HH4 node grafted to a host at HH2, and a HH4 node grafted to the same embryo later at HH4 (i.e. the first graft took longer to induce than the second). In contrast, we observe that HH4 hosts actually take longer to respond to a node

graft. These differences can probably be explained based on the timing of the competency window. As the L5^{220} epitope confers competency between HH3-4 (Streit *et al.*, 1997), the initial graft was probably unable to neuralise the area opaca until the HH2 host was older. Therefore the first graft seemed to take longer because the two grafts could only induce neural tissue simultaneously once competency was acquired. This would fit with Gallera's interpretation that the timing of neural induction is linked to an intrinsic property of the epiblast (Gallera, 1968).

However, Gallera also suggests that an embryo-wide mechanism synchronises the onset of induction across the whole embryo, as he observes ectopic neural induction to occur at the same time as the endogenous process in the host (Gallera, 1968). With the benefit of specific temporal markers, as opposed to relying just on morphology, we have observed SOX2 expression in the host when it is absent ectopically, and vice-versa (data not shown). Therefore our experiments argue against a more clock-type mechanism that regulates precisely when tissue responds. Certainly the timing of ectopic and endogenous induction events is intimately linked by the brief window of L5^{220} expression which spans the prospective neural plate and area opaca. This permits induction by a graft to occur within the same period as the host, but not necessarily at exactly the same time.

3.3.3 Cells are only committed to a neural fate 12h after a node graft

We also demonstrate that although cells express SOX2 after 9h, a further 3h of exposure to a node graft are required before its expression is maintained. This is strikingly similar to SOX3, which can be induced within 5h but expression is lost if a node is removed earlier than 12h (Streit *et al.*, 1998, Streit and Stern, 1999). Taken together, these observations suggest that 12h of signals from Hensen's node are required to commit cells to a neural fate. This is roughly consistent with classical grafting experiments which suggest that 8.5h of signals from a node are required to form a morphological neural plate (Gallera, 1965) but 13h are necessary before cells are committed to a neural fate (Gallera and Ivanov, 1964, Gallera, 1971).

SOX1 has previously been implicated in neural precursor commitment and differentiation *in vitro* (Pevny *et al.*, 1998). Its induction after 12h of grafting places it appropriately at the time when cells become committed to a neural fate. Consequently, SOX1 may represent a better marker of the definitive neural state than SOX2, which confers neural specification to progenitors (Graham *et al.*, 2003).

3.3.4 Hensen's node and the hypoblast as sources of neuralising signals

Grafts of Hensen's node must contain at least the minimal information required to impart normal neural identity, to induce definitive neural markers. As our analyses, and those of others, suggest that neural induction must occur as a sequence of events and that FGFs and BMP inhibition are not sufficient for these, neural induction must be regulated by additional signals at different times.

Although Hensen's node contains all the signals required for neural induction, it is yet to form when the earliest markers (e.g. ERNI, SOX3 and OTX2) are induced in the pre-streak epiblast. At these stages the hypoblast, which is equivalent to the mouse anterior visceral endoderm, is an important source of early neural signals (Foley *et al.*, 2000, Albazerchi and Stern, 2007). For example SOX3 and ERNI expression are regulated by FGF8 from the underlying hypoblast (Streit *et al.*, 2000). The hypoblast is also important for the early expression of OTX2, NOT1 and NOT2. Although their regulation has not been tested here, retinoids from the hypoblast have been implicated in regulating NOT1 and NOT2 expression in the pre-streak epiblast (Knezevic *et al.*, 1995, Knezevic and Mackem, 2001). However this response seems to occur synergistically with other factors including Activin and FGFs. Similarly, hypoblast grafts can induce OTX2 within 3-4h in response to FGF signalling combined with BMP and WNT inhibition, but this effect is only transient as OTX2 expression is lost completely after 10-12h (Albazerchi and Stern, 2007), suggesting that further signals are required for its maintenance.

Unlike these early responses, TRKC is not expressed in the pre-streak epiblast. Its expression begins at HH3+/4-, when the hypoblast has been displaced (Rosenquist, 1972, Lawson and Pedersen, 1987). As TRKC expression is first observed adjacent to Hensen's node, it is the likely endogenous source of signals regulating TRKC. However, TRKC cannot be induced by FGFs, nor are they required for its expression. Retinoic acid, Noggin, and calcium signalling, which also contribute to neural induction are similarly insufficient to induce TRKC. Nor does it respond to somatostatin, a neuropeptide which is expressed in the prechordal mesendoderm and has been implicated in inducing PAX6 expression in the anterior neural plate border (Lleras-Forero *et al.*, 2013). Therefore we predict that as yet unidentified signals from the node are responsible for its expression (Pinho *et al.*, 2011).

Similarly, grafts of the hypoblast are insufficient to induce the forebrain marker HESX1, or SOX2 (Foley *et al.*, 2000, Albazerchi and Stern, 2007), the latter can only be induced by node grafts. Even though FGFs together with BMP and WNT antagonists are required for neural induction, no combination of these is sufficient to induce SOX2 (Linker and Stern, 2004). This indicates that SOX2 also requires as yet unidentified signals from the node. It will be

particularly important to identify new signals secreted from the node or its derivatives that coincide with SOX2 expression between HH4-5 (or after 5-9h of grafting). Since 12h of grafting are required to induce SOX1 expression and stabilise SOX2, these responses may need longer exposure to factors that that are already present after 9h. Alternatively they could also require additional signals that are secreted between HH5-8 in the normal embryo or from a graft after 9-12h.

CYP26A1 differs from these other markers as node grafts can only expand its endogenous domain but never induce it ectopically. A similar response is observed after grafts of the hypoblast or beads soaked in retinoic acid, which expand CYP26A1 from the neural plate and can even shift endogenous expression towards the graft (Albazerchi and Stern, 2007). CYP26A1 is known to be induced by retinoic acid as a means of regulating its own concentration (White *et al.*, 1996, Loudig *et al.*, 2000), and therefore its expression may provide a readout of high retinoid levels (Reijntjes *et al.*, 2005). It would be reasonable to expect node grafts to induce CYP26A1 consistently given that retinoids are present in Hensen's node (Chen *et al.*, 1992, Chen and Solursh, 1992, Blentic *et al.*, 2003), but perhaps the concentration of retinoids in node grafts is not sufficient to induce CYP26A1 expression ectopically. Instead nodes grafted closer to the neural plate might expand CYP26A1 expression because they contribute to an existing domain that already has high retinoic acid levels. This might explain why CYP26A1 expression was only associated with node grafts in close proximity to the host CYP26A1 expression domain.

Alternatively, grafts of Hensen's node or hypoblast may only expand, but not induce CYP26A1, if other signals in the embryo contribute to its normal expression in the prospective neural plate, or if signals in the area opaca might prevent its induction. Certainly there are reports that CYP26A1 can be induced by WNT inhibition (Kudoh *et al.*, 2002), and FGF inhibition (Kudoh *et al.*, 2002) or activity (Wahl *et al.*, 2007) in different contexts. However, only beads of retinoic acid and not FGF8 are able to induce CYP26A1 in the area opaca (Albazerchi and Stern, 2007). Other reports suggest that CYP26A1 also responds to Notch signalling (Echeverri and Oates, 2007). If juxtacrine signalling via Notch is involved in our context, it might explain why CYP26A1 could only be expanded as a patch or trail of cells extending from the host. What these studies do suggest is that CYP26A1 regulation is probably more complex than just retinoic acid. While reasons for the specific response of CYP26A1 to a node graft remains unclear, it seems that despite being expressed in the prospective neural plate, it may not be required during the equivalent stages of ectopic neural induction as it is not induced by all grafts.

3.3.5 Neural induction proceeds as a sequence of events

Although we are not yet able to define molecularly the entire process of neural induction, it is possible to illustrate it as a simple cascade of responses based on the markers analysed to date (Fig. 3.11). It follows the same temporal cascade of responses ectopically and in the embryo. The earliest responses are expressed in the epiblast of EGKXIII embryos; prior to gastrulation. They are induced robustly within the first 3h of a node graft, and include markers such as ERNI, SOX3, Calfacilitin and OTX2. NOT1 and NOT2 are also induced although possibly only transiently. Additional markers are acquired after 5h of a node graft, including Churchill, DAD1, UBII, Asterix, Obelix and TRKC. These are first expressed in the HH3+/4- prospective neural plate at around the time that NOT1 and NOT2 are downregulated. These early markers (red and blue) are expressed before the neural plate proper forms and therefore we consider them to define a pre-neural state. FGF signalling contributes significantly to these early responses but does not regulate them all. It is only after these first 5h of signalling from a node, or at approximately HH3+, that induced tissue is able respond to BMP inhibition (Streit and Stern, 1999). SOX2 can be induced completely after 9h and is expressed robustly in the neural plate proper by HH5, where we consider it to mark neural specification. Later, SOX1 expression is acquired later at around the time that cells become committed to a neural fate.

In this way, the period of neural induction in the normal embryo can be defined according to the time-course of the earliest and latest neural markers. The earliest responses occur within 3h of a graft or in the embryo before gastrulation, where they define a pre-neural state. However cells do not acquire SOX2 expression and neural specification until 9h or HH5, but even then, they are not committed to a neural fate until 12h, the same time they express SOX1. This scheme fits nicely with classical experiments suggesting that a “neuroid” response can be induced after 6h of a node graft, but that 8.5h are required to induce a morphological neural plate (Gallera, 1965) and 13h for cells to commit to a neural fate (Gallera and Ivanov, 1964, Gallera, 1968, Gallera, 1971). As none of these steps in isolation is sufficient for cells to acquire a neural fate, it is difficult to identify a single neural “inductive” event. Therefore, we must consider that neural induction proceeds as a cascade of responses to multiple signals between 0-12h of a Hensen’s node graft, or in the embryo between EGKXII and HH8-9. These findings contrast with the “default model” of neural induction, which predicts that neural induction occurs during gastrulation in response to a single stimulus; BMP antagonists from the organizer (Hemmati-Brivanlou and Melton, 1997).

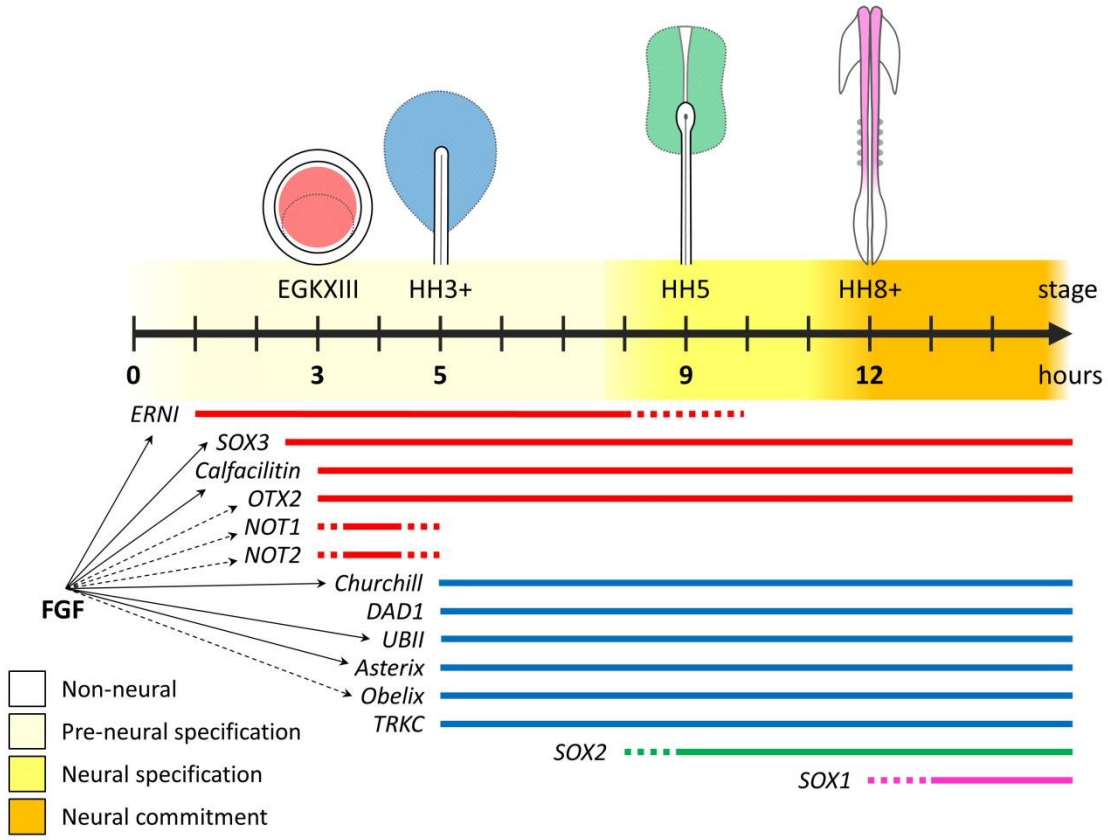

Figure 3.11: Neural induction proceeds as a cascade in response to different signals.

A temporal cascade of neural markers is expressed in response to neural induction. Coloured bars represent the expression period of each gene in relation to the timing of induction by a node graft (hours) and the stage of their expression in the normal embryo. (Solid lines, complete induction; dashed lines, incomplete induction.) Genes can be grouped into 4 "epochs" based on the timing of their expression. The earliest responses (red) can be induced by a node graft within 3h and are expressed in the pre-streak epiblast. A second set of markers (blue) is first expressed at HH3+/4- or after 5h of a node graft. Red and blue markers define a pre-neural state that exists prior to the formation of the neural plate. Many of these early markers are regulated by FGFs (solid arrow; FGF sufficiency, dashed arrow; FGFs necessary). Later expression of SOX2 after 9h of a node graft or approximately HH5 marks the onset of definitive neural specification but commitment to neural fate and differentiation only begins around 12h when SOX1 is induced. The approximate expression domain of markers is shown in the embryo at EGKXIII, HH3+, HH5 and HH8+ (adapted from (Pinho *et al.*, 2011)).

3.4 Conclusions

The emerging picture illustrated by these experiments, is that 9-12h of signals from a grafted node are required before definitive neural markers and cells are irreversibly committed to a neural fate. The responses identified within the first 5h correspond closely to events that occur in the normal embryo prior to the formation of the definitive neural plate. As such they specify the induction of a pre-neural territory.

Ectopic induction proceeds according to the same molecular events as the host neural plate, so the node graft assay is a useful tool to study the entire process of neural induction. Since we demonstrate that neural induction must proceed as a sequence of responses and BMP antagonists are not sufficient to regulate all these events, our results dispute the widely accepted “default model” of neural induction.

Although the duration of neural induction can now be better defined, it is evident from just these markers, that the formation of a definitive neural plate requires additional factors and responses at different time points. FGF signalling contributes to the regulation of early markers, but we know little about events that occur or signals that are required after more than 5h of a node graft.

Chapter 4: A time-course of responses to neural induction, analysed by RNA-Seq

4.1 Introduction

In the previous chapter we investigated the process of neural induction using a group of selected markers. Node graft assays revealed that the earliest responses are upregulated within 1-3h and include genes such as ERNI, SOX3 (Streit *et al.*, 2000), Calfacilitin (Papanayotou *et al.*, 2013), OTX2 (Bally-Cuif *et al.*, 1995), NOT1 and NOT2 (Knezevic *et al.*, 1995, Knezevic and Mackem, 2001), which are normally expressed in the pre-streak embryo. Following this, a second wave of responses is induced after 5h including Churchill (Sheng *et al.*, 2003), Asterix, Obelix, TRKC (Pinho *et al.*, 2011), DAD1 and UBII (Gibson *et al.*, 2011), whose expression is first detected in the prospective neural plate at around HH3-4. After these early responses, SOX2 is induced after 9h and SOX1 after 12h.

Although we have not focused on the specific function of these markers, they clearly illustrate previously unappreciated characteristics of neural induction. First, the earliest markers are expressed in the pre-streak epiblast, indicating that neural induction begins before gastrulation. Second, at least for the markers where this was tested, BMP antagonism is not sufficient to induce their expression. In several cases, FGFs and possibly retinoic acid are responsible (Knezevic *et al.*, 1995, Foley *et al.*, 2000, Streit *et al.*, 2000, Knezevic and Mackem, 2001, Sheng *et al.*, 2003, Gibson *et al.*, 2011, Pinho *et al.*, 2011, Papanayotou *et al.*, 2013), consistent with the proposal that BMP antagonists function later in the neural induction process (Linker and Stern, 2004). These data suggest that neural induction proceeds as a cascade of sequential responses to signals from Hensen's node (Pinho *et al.*, 2011) including FGFs. This contrasts with the accepted "default model" of neural induction which proposes that ectodermal cells will automatically (by "default") acquire a neural fate in the absence of signals (Hemmati-Brivanlou and Melton, 1997) and implies that BMP antagonists secreted from the organizer effectively create a "default" neural state by inhibiting BMPs which are expressed in the ectoderm (Lamb *et al.*, 1993, Hemmati-Brivanlou *et al.*, 1994, Sasai *et al.*, 1994, Sasai *et al.*, 1995).

Of the responses studied to date, most were identified by a differential screen which compared uninduced epiblast to tissue exposed to a node graft for 5h (Streit *et al.*, 2000). This successfully identified 10 early neural markers, each of which is expressed in the prospective neural plate in response to signals from Hensen's node (Streit *et al.*, 2000, Sheng *et al.*, 2003,

Gibson *et al.*, 2011, Pinho *et al.*, 2011, Papanayotou *et al.*, 2013). However, it now seems that these markers only define the earliest stages of neural induction (Pinho *et al.*, 2011), and that they are not the only early responses (see Chapter 3). More than 5h of exposure to a node graft are required to induce the definitive neural markers SOX2 (9h) and SOX1 (at least 12h) and we know almost no other genes that mark these or the intermediate steps in the cascade. In addition, it is surprising that the original screen did not identify markers that are downregulated in response to a graft of Hensen's node, which could function normally to repress neural fates in non-neural regions of the ectoderm.

The preceding observations suggest that neural induction is more complex than previously considered. It proceeds as a temporal cascade of multiple responses and signals between 0-12h of a node graft or stages EGKXII-HH9 in the embryo. However many of the transcription factors which describe the process and the signals which regulate it are unknown. Next generation sequencing now provides the opportunity to reinvestigate the neural induction cascade with greater sensitivity. To uncover all genes that change during this period, an RNA-Seq analysis of induced and uninduced tissue at key time points was conducted. We decided to begin by studying responses to a grafted node after 5h; to seek genes that may have been missed by the previous screen and after 9h; to characterise the unexplored gap between early responses and genes leading to induction of SOX2 and neural plate specification. Lastly, to detect responses that coincide with the induction of SOX1 and commitment to a neural fate, we also chose to study markers after 12h following a node graft.

4.2 Methods

4.2.1 RNA-Seq analysis of responses to neural induction

Chick HH4- Hensen's nodes were grafted into chick hosts at the same stage and incubated for 5, 9 or 12h. To minimise the possible contribution of embryonic asymmetries, nodes were grafted to either the left or right side of the embryo. At each time point, 50 pieces of induced epiblast were dissected from underneath the graft, as well as 50 pieces of uninduced epiblast from the contralateral side. Uninduced epiblast was also isolated from HH4- embryos to serve as a 0h control (Fig. 4.1A). Tissue from each condition was pooled, the RNA extracted and its quality assessed (Appendix 2). Library samples were prepared using the Illumina mRNA TruSeq system and analysed by 100-cycle paired-end RNA-Seq (Fig. 4.1B).

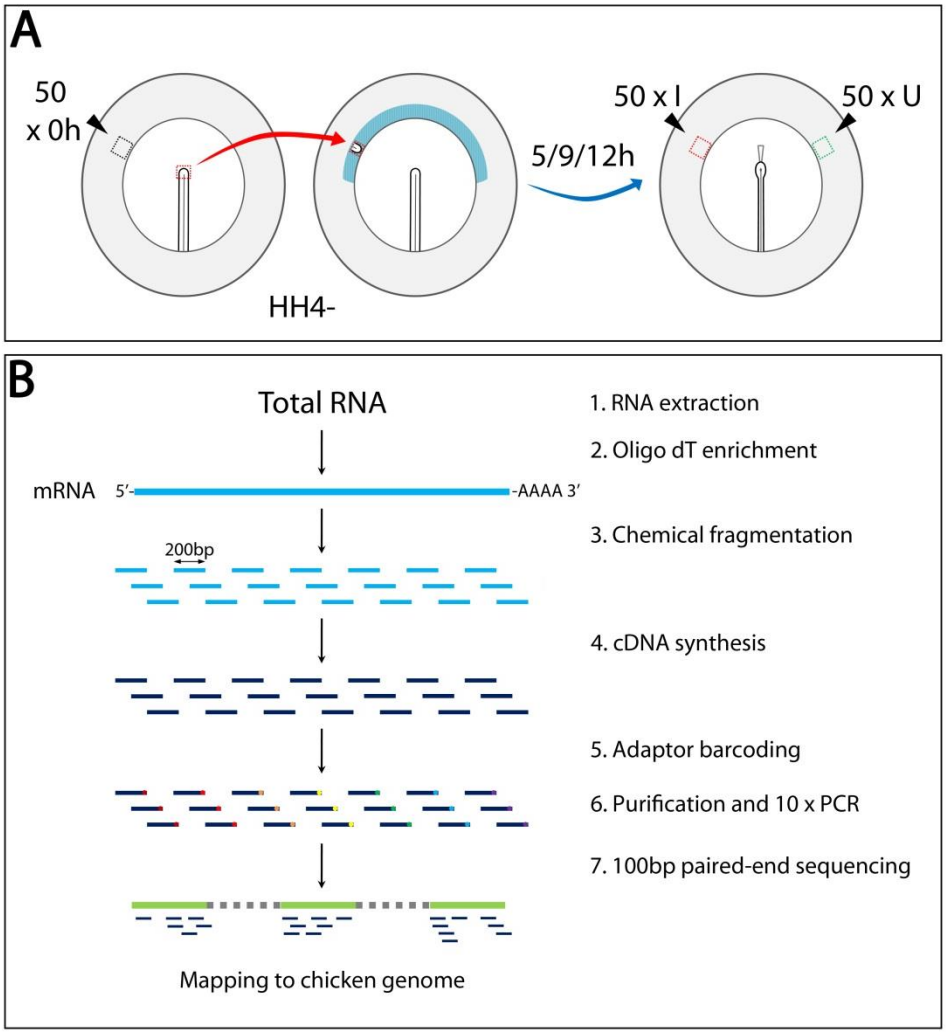

Figure 4.1: RNA-Seq screen experimental set-up and RNA processing.

For the RNA-Seq screen, Hensen's nodes at HH4- were grafted to a competent region of the area opaca (the inner third, at the level of the host node shown in blue) of hosts at HH4- (A). Nodes were grafted to the left or right side, and embryos cultured for 5, 9 or 12h. At each time point, 50 pieces of induced epiblast in contact with the graft and of contralateral (uninduced) tissue were collected. In addition, 50 pieces of tissue were taken from the area opaca of HH4- embryos to serve as a 0h time point. For each condition RNA was extracted and cDNA libraries constructed as follows (B). First, mRNA was enriched using oligo-dT and chemically fragmented into approximately 200bp fragments. From these, cDNA was synthesised using random primers and then adaptors ligated to barcode each sample. Barcoded libraries were purified to remove unincorporated adaptors, and enriched using 10 cycles of PCR. Finally these were processed using 100bp paired-end sequencing.

For each library sequenced, raw reads underwent quality control assessment (Appendix 3, 4 and 5). Low quality reads were filtered out and the remainder were trimmed at the 3' end to remove lower quality regions over the last 10bp (Blankenberg *et al.*, 2010). High quality paired (forward and reverse) reads remained, which overlapped by 80bp. These were mapped to the chicken genome (Trapnell *et al.*, 2009), annotated and their expression levels quantified. Finally differential expression of transcripts was determined by comparing induced and uninduced reads at 5, 9 and 12h.

4.3 Results

4.3.1 RNA-Seq Analysis

Conducted by M. Khan in collaboration with K.E. Trevers

Initially, reads were mapped to the available Galgal3 version of the chicken genome (assembly version Gallus_gallus-2.1, GenBank Assembly ID GCA_000002315.1) and annotated using the Ensembl database. Differential expression was calculated using two separate methods, the first used the Cufflinks suite of algorithms and the second used DE-Seq (Anders and Huber, 2010, Delhomme *et al.*, 2012, Trapnell *et al.*, 2012). In both cases a threshold $\log_2$ fold change of 1.2 was used to define differential expression. The results of Cufflinks and DE-Seq analyses were compared and transcripts were categorised depending on whether they were statistically significant ($P \leq 0.05$) in both analyses (red), either analysis (orange), or in neither (yellow) (Appendix 6). This approach identified 7745 differentially expressed transcripts across all three experimental time points (Appendix 7). Gene annotations could be assigned to 4508 of these, corresponding to 2333 unique genes. Due to the incomplete nature of the Galgal3 chicken genome, 3237 transcripts were left unannotated (Appendix 6).

Upon release of the Galgal4 version of the chicken genome (assembly version Gallus_gallus-4.0, GenBank Assembly ID GCA_000002315.2) the RNA-Seq data was reanalysed to obtain extra annotations. This time, differential expression was calculated only using DE-Seq and using a threshold $\log_2$ fold change of 1.2, while annotations were obtained using both Ensembl and UCSC databases (Anders and Huber, 2010, Delhomme *et al.*, 2012). Cufflinks was not used due to the unstable nature of the algorithm, which gives different results each time it is used. With this approach, the Galgal4 reanalysis identified 8673 differentially expressed transcripts across all three experimental time points (Appendix 8). Gene annotations could be assigned to 7184 of these, corresponding to 4145 unique genes (1812 more than the initial Galgal3 analysis). These data are summarised using volcano plots comparing fold change and P-value

and heat maps representing the expression levels of transcripts from induced and uninduced tissue at each time point (Fig. 4.2, 4.3, 4.4). Despite the incomplete nature of the chicken genome only 989 transcripts remained unannotated -many fewer than the Galgal3 analysis (Appendix 8).

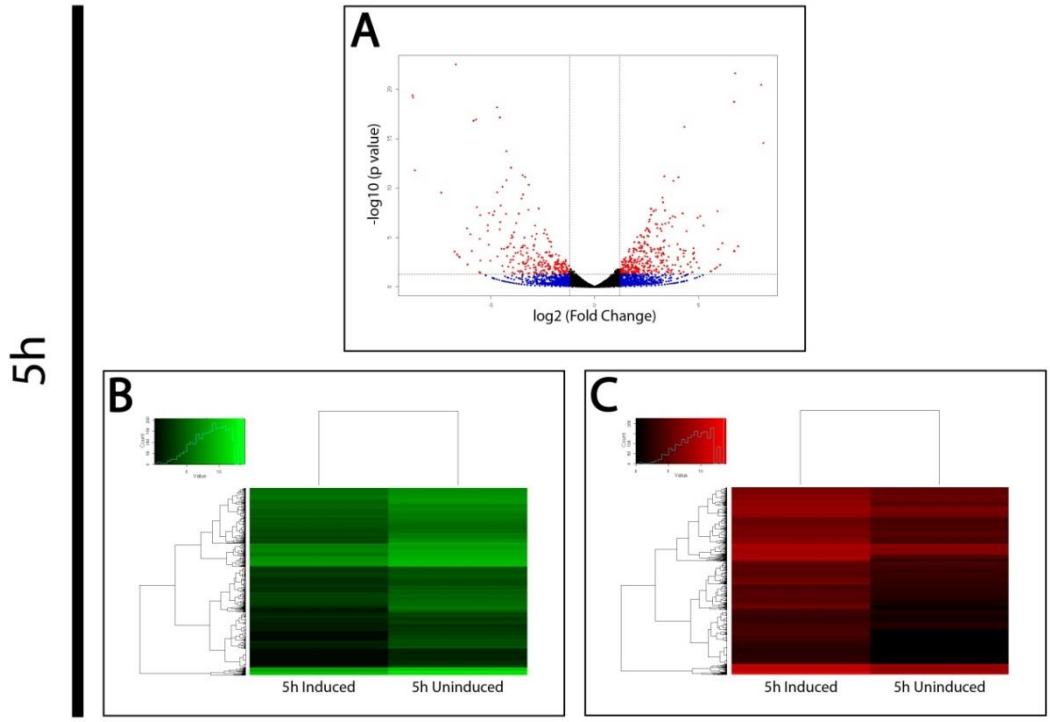

Figure 4.2: DE-Seq analysis of 5h induced vs. uninduced transcripts.

Differentially expressed genes were identified using DE-Seq analysis to compare transcripts from uninduced and induced tissue at the 5h time point. The results shown here are based on the Galgal4 version of the chicken genome. A volcano plot of P-value and fold change for all transcripts in the 5h induced vs. 5h uninduced comparison (A). The X axis represents $\log_2$ fold change and the Y axis represents $-\log_{10}$ of the P-value. Transcripts that pass a P-value threshold of 0.05 and a fold change cut-off of $\log_2$ 1.2 are shown in red. Those that don't pass the P-value threshold of 0.05 but pass the fold change cut-off of $\log_2$ 1.2 are in blue. Transcripts that are not differentially expressed are shown in black. Heat map visualisations with hierarchical clustering of differentially expressed transcripts based on a $\log_2$ fold change of 1.2, in 5h induced tissue compared to 5h uninduced control tissue. Downregulated transcripts (green) are expressed lower in the induced condition compared to the uninduced control (B). Upregulated transcripts (red) are expressed higher in the induced condition compared to the uninduced control (C).

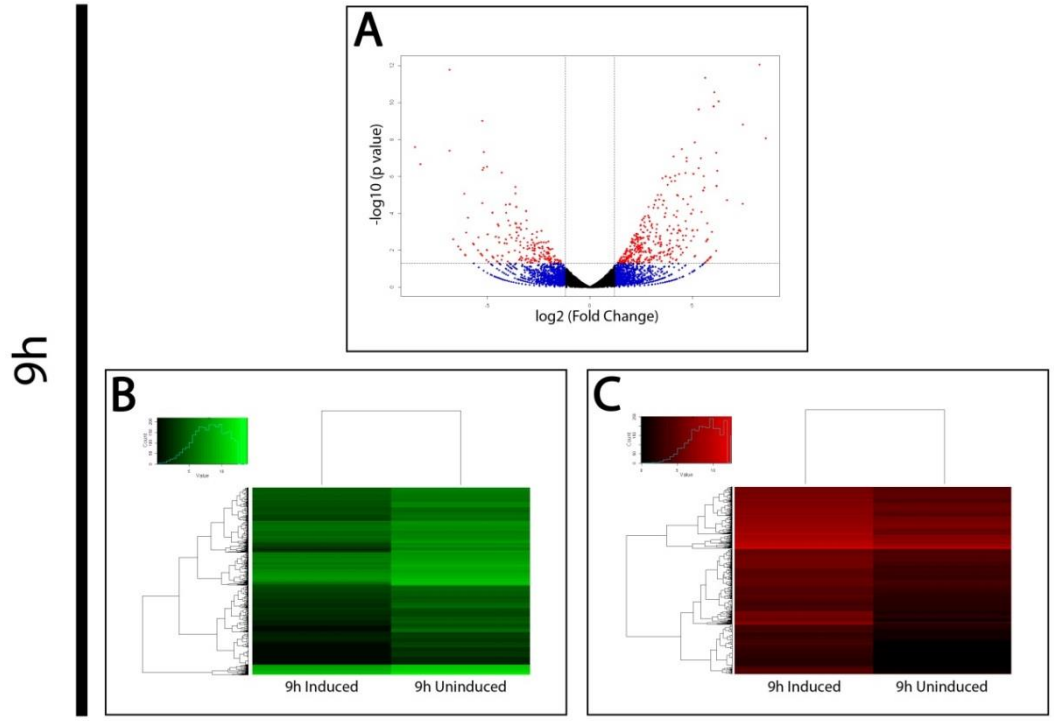

Figure 4.3: DE-Seq analysis of 9h induced vs. uninduced transcripts.

Differentially expressed genes were identified using DE-Seq analysis to compare transcripts from uninduced and induced tissue at the 9h time point. For details, see Fig. 4.2.

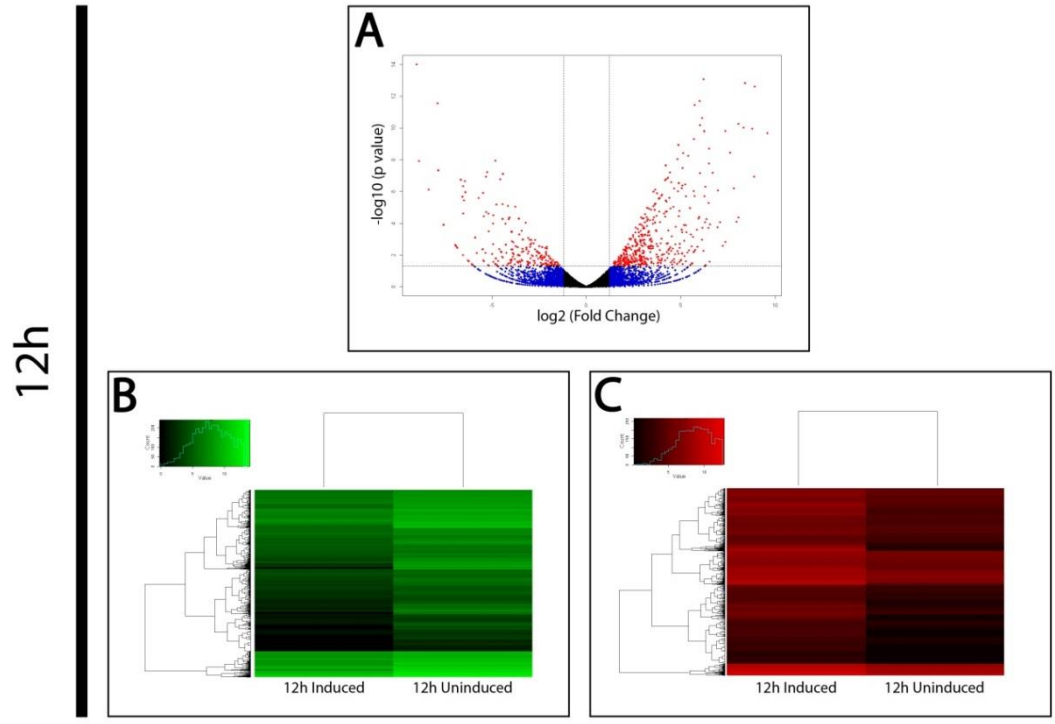

Figure 4.4: DE-Seq analysis of 12h induced vs. uninduced transcripts.

Differentially expressed genes were identified using DE-Seq analysis to compare transcripts from uninduced and induced tissue at the 12h time point. For details, see Fig. 4.2.

4.3.2 The screen detects anticipated transcriptional responses to neural induction

To assess whether the RNA-Seq screen successfully identified responses associated with neural induction, we looked for the differential expression of responses already known, or predicted to be involved with this process (Table 4.1).

	5h		9h		12h		
	UP	DOWN	UP	DOWN	UP	DOWN	
Transcription Factors	SOX3 OTX2	GATA2 MSX1 SMAD6 SMAD7	SOX2 OTX2 GBX2	GATA2 MSX1 SMAD6 SMAD7	SOX1 SOX2 OTX2 HOXB1 NEUROG2	GATA2 MSX1 SMAD6 SMAD7	↑ Neural ↓ Non-neural
Other Markers	ERNI	KRT7 KRT19	NCAM1	KRT7 KRT19	NCAM1	KRT7 KRT19	
Signalling Readouts	SPRY1 SPRY2 SPRED1 FRZB SFRP1 LFNG HEY1 PTCH2	BMP2 BMP7 AXIN2 RARB	SPRY1 SPRY2 SPRED1 FRZB SFRP1 CYP26A1 LFNG HEY1 PTCH2 PTCH1	BMP2 BMP7 AXIN2 RARB	SPRY1 SPRY2 FRZB SFRP1 CYP26A1 LFNG HEY1 PTCH2 PTCH1	BMP2 BMP7 AXIN2 RARB	↑ FGF ↑ RA ↑ Notch ↑ HH ↓ BMP ↓ WNT

Table 4.1: Anticipated responses to neural induction, as identified by RNA-Seq.

The following markers and signalling readouts were identified as being either up- or down-regulated after 5, 9 or 12h. Known responses to neural induction include the upregulation of ERNI, SOX3, SOX2 and SOX1 at the appropriate time points, in addition to downregulation of non-neural ectoderm and epidermal markers such as GATA2, MSX1, KRT7 and KRT19. These are accompanied by readouts of signalling events associated with neural induction including FGF signalling, plus BMP inhibition and WNT inhibition. Also detected are readouts of retinoic acid, Notch and hedgehog pathways.

The neural markers SOX3, SOX2 and SOX1 are upregulated at the appropriate time points: 5, 9 and 12h respectively (Streit *et al.*, 2000). Markers of neural tube anterior-posterior patterning are progressively acquired, including OTX2 (Bally-Cuif *et al.*, 1995) at each time point, GBX2 (Shamim and Mason, 1998) after 9h and HOXB1 (Paxton *et al.*, 2010) after 12h. Upregulation of the proneural gene NEUROG2 (Perez *et al.*, 1999), is also detected at the 12h time point. Epidermal markers including KRT7 (Heller *et al.*, 1998) and KRT19 (McLarren *et al.*, 2003) are downregulated at each time point, while the neural marker NCAM1 (Chuong and Edelman, 1985) is upregulated after 9 and 12h.

Also identified, are transcriptional readouts of signalling pathways previously associated with neural induction. We detect early and persistent upregulation of FGF signalling targets including SPRY1, SPRY2 and SPRED1 (Sivak *et al.*, 2005). BMP signalling is generally inhibited. BMP2 (Francis *et al.*, 1994) and BMP7 (Monroe *et al.*, 2000) are downregulated at each time point, as is the BMP signalling component SMAD6 (Vargesson and Laufer, 2001) and BMP target genes GATA2 (Sheng *et al.*, 2003) and MSX1 (Suzuki *et al.*, 1991). WNT inhibition is also prevalent; the WNT antagonists SFRP1 (Esteve *et al.*, 2000) and FRZB (Ladher *et al.*, 2000) are consistently upregulated, while AXIN2 (Quinlan *et al.*, 2009) -an endogenous reporter of WNT signalling, is downregulated. In addition, we also identify distinct readouts of other signalling pathways. The upregulation of CYP26A1 (Swindell *et al.*, 1999, Albazerchi and Stern, 2007) after 9 and 12h might suggest high levels of retinoic acid, but the retinoic acid receptor RARB (Cui *et al.*, 2003) is simultaneously downregulated. Transcriptional targets of Notch signalling such as LFNG (Sakamoto *et al.*, 1997) and HEY1 (Leimeister *et al.*, 2000) are consistently upregulated. There is also evidence of hedgehog signalling as the receptors PTCH1 and PTCH2 (Pearse *et al.*, 2001) are consistently upregulated at 5, 9 and 12h.

Therefore the screen successfully identified upregulation of factors known to be expressed in neural tissue together with downregulation of factors associated with non-neural ectoderm. These changes coincide at the appropriate time points with signalling events that are required for neural induction, namely early upregulation of FGF signalling together with general WNT and BMP inhibition. Since the screen detects the precise types of markers and signalling readouts we would anticipate, it gives confidence that other newly identified markers within the data should also be relevant to neural induction.

4.3.3 Differentially expressed transcriptional regulators accompanying neural induction

Within these RNA-Seq data, the differential expression of transcriptional regulators is of particular interest because these determine tissue specification by exerting global control over gene transcription during neural induction. In total, the Galgal3 analysis identified 284 unique differentially expressed transcriptional regulators (Appendix 6 and 7) while the Galgal4 reanalysis identified 482 (Fig. 4.3 and Appendix. 8). These are depicted as heat maps and Venn diagrams representing their differential expression across the three experimental time points. They reveal that transcriptional regulators are expressed at a wide range of levels (Fig. 4.5A). Some are consistently up- or downregulated, others are unique to a time point or span two time points (Fig. 4.5B), while 24 are up- and downregulated but at different time points. Therefore differentially expressed transcriptional regulators vary in terms of the levels and the timing of their expression and differential expression, during neural induction.

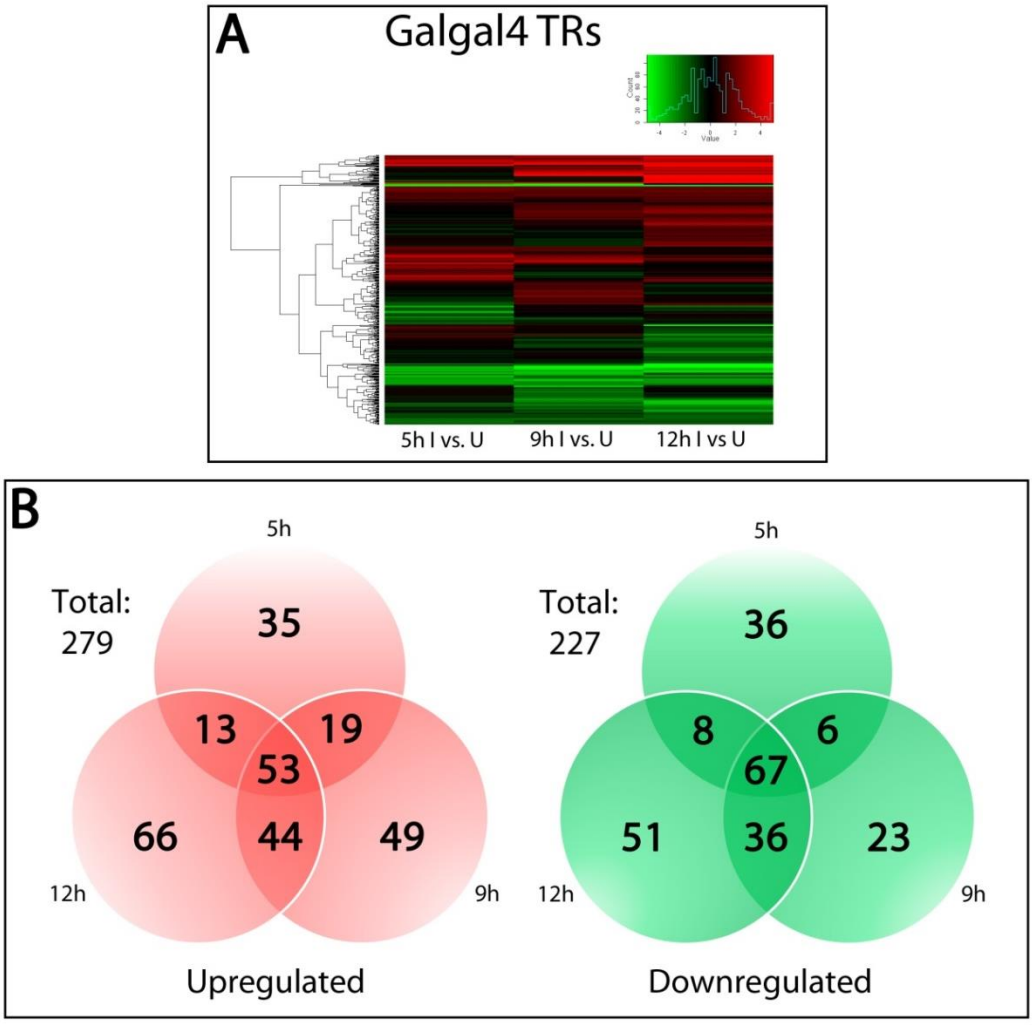

Figure 4.5: Differentially expressed transcriptional regulators from Galgal4 RNA-Seq.

Differentially expressed genes were identified using DE-Seq analysis to compare transcripts from uninduced and induced tissue at each time point, using the Galgal4 version of the chicken genome and a $\log_2$ fold change cut-off of 1.2. Extracted from this analysis are 1009 transcripts coding for 482 unique transcriptional regulators. These are represented as heat maps with hierarchical clustering of upregulated (red) and downregulated (green) transcriptional regulators across the 3 time points (A). The same data are displayed as Venn diagrams of up- and downregulated transcriptional regulators, split according to the time points at which they are differentially expressed (B).

4.3.4 The normal expression of differentially expressed transcriptional regulators

To confirm whether these transcriptional regulators are expressed appropriately for a role in neural induction, their expression was determined in the normal embryo. The original intention was to confirm the expression of all differentially expressed transcriptional regulators, but the screen identified more candidates than expected. Therefore we decided to confirm a proportion of these by in situ hybridisation. Beginning with the Galgal3 analysis, we chose to verify the expression of 135 transcriptional regulators that were categorised as red or orange; those calculated as being significantly differentially expressed by Cufflinks, DE-Seq, or both (Appendix 6). When the new assembly and annotations (Galgal4) were released, we added candidates that showed significant differential expression in DE-Seq (Appendix 8), colour coded red in the volcano plots (Fig. 4.2A, Fig. 4.3A and Fig. 4.4A). This generated a shortlist of 138, of which 97 were common to the Galgal3 analysis. Therefore in total 176 candidates were picked across both versions of the analysis: 88 upregulated and 88 downregulated.

We are mainly interested in these transcriptional regulators as markers of specification states rather than their specific function during neural induction. To date, the expression of 166 transcriptional regulators has been verified by in situ hybridisation at four embryonic stages equivalent to key time points in the screen. To test whether candidates are induced earlier than 5h, their expression was assessed prior to gastrulation at EGKXII-XIII. Then, expression was verified in the prospective neural plate at HH3-4 for candidates induced after 5h. Later, expression was confirmed between HH5-7, roughly corresponding to induction of SOX2 after 9h, and at HH8-9, equivalent to the induction of SOX1 after 12h.

Of the 166 genes assessed so far, 86 have been previously characterised in chick but not always at stages relevant to neural induction. These are highlighted in **bold**, and a brief

description of their expression and the relevant references in chick are provided. A further 80 transcriptional regulators have not been previously studied in the chicken embryo. These are highlighted as **underlined** and are formally described here. References to these genes or the proteins they encode in other organisms or experimental systems are provided.

4.3.4.1 Upregulated transcriptional regulators

The expression of 83 transcription factors which were upregulated after 5, 9 or 12h was verified by in situ hybridisation. These included many known markers of neural fate, but also numerous markers which have not previously been implicated in neural induction and 31 not previously studied in chick.

BMI1 (Fig. 4.6A-E) is expressed in the pre-streak epiblast, prospective neural plate and forming mesoderm at HH3-4, in the neural plate proper but also in the axial and lateral plate mesoderm at HH5-7 and the anterior neural tube at HH8-10 (Fraser and Sauka-Spengler, 2004).

CBFAT2T2 (Fig. 4.6F-J) is expressed weakly in the neural plate at HH3-4 and mainly in the forming mesoderm. This continues at HH5-7 and HH8-10, where it is upregulated anteriorly in the future lens placode (Koyano-Nakagawa and Kintner, 2005).

CCND1 (Fig. 4.6K-O) is expressed in the area opaca, weakly in the prospective neural plate at HH3-4 but also across the posterior streak. Later it is expressed in the neural plate and pre-somitic mesoderm at HH5-7 and the neural tube, somites, lateral plate and pre-somitic mesoderm at HH8-10 (Lobjois *et al.*, 2004).

CDCA7 encodes a transcriptional regulator which associates with MYC (Goto *et al.*, 2006, Gill *et al.*, 2013). It was identified as upregulated at all screen time points. Consistent with this, CDCA7 is expressed in the prospective neural plate at HH4, the neural plate proper at HH7 and in the neural tube at HH9. At these stages it is also expressed weakly in the primitive streak but there is no specific CDCA7 expression at EGKXIII (Fig. 4.6P-T).

CITED4 (Fig. 4.6U-Y) is upregulated only at the 5h time point and is expressed in the pre-streak epiblast at EGKXII-XIII and the prospective neural plate at HH3-4. It is downregulated in the neural plate by HH5-7, when it is expressed weakly in the neural plate border. By HH8-10 it is only expressed anteriorly in the neural folds and head surface ectoderm (Andrews *et al.*, 2000).

CRIP2 encodes a putative LIM domain transcription factor (Weiskirchen *et al.*, 1995). It was identified as upregulated after 5 and 9h. In the embryo, CRIP2 is expressed strongly in the neural plate at HH4, HH5 and HH8-. It is also weakly expressed in the epiblast at EGKXIII (Fig. 4.6Z-AD).

DACH1 (Fig. 4.7A-E) is expressed weakly in the epiblast and more strongly in the prospective and neural plate proper at HH3-4 and HH5-7. By HH8-10 it is expressed broadly in the embryo and throughout the forming neural tube (Heanue *et al.*, 2002).

DMBX1 (Fig. 4.7F-J) expression is absent from the early embryo and the prospective neural plate. Instead expression is first detected at HH5-7 in the anterior neural plate border and pre-placodal domain. The expression continues at HH8-10 in the anterior neural folds (Ferran *et al.*, 2007).

DNMT3A (Fig. 4.7K-O) is expressed strongly at all stages assessed. It is present in the pre-streak epiblast, prospective neural plate, neural plate proper and forming neural tube (Hu *et al.*, 2012).

DNMT3B (Fig. 4.7P-T) is expressed strongly at all stages assessed. It is present in the pre-streak epiblast, prospective neural plate, neural plate proper and forming neural tube (Rengaraj *et al.*, 2011).

ENC1 regulates the transcription factor NRF2 (Wang and Zhang, 2009). It was identified as upregulated in each time point. By in situ hybridisation, ENC1 is expressed weakly in the epiblast at EGKXIII and in the prospective neural plate and mesoderm at HH4. By HH6 it is expressed strongly in the neural plate, primitive streak and the underlying mesoderm. Expression continues in the caudal mesoderm at HH8+, when it becomes restricted to the anterior neural folds (Fig. 4.7U-Y).

EOMES (Fig. 4.7Z-AD) is expressed broadly throughout the area opaca but also posteriorly in the area pellucida at EGKXII-XIII. By HH3-4 it is expressed strongly in the prospective neural plate and the mesoderm exiting the streak. Expression then decreases such that it is only expressed weakly in the neural plate at HH5-7 and cannot be detected by HH8-10 (Jean *et al.*, 2015).

ERNI (Fig. 4.8A-E) is expressed strongly in the pre-streak epiblast at EGKXII-XIII and prospective neural plate at HH3-4. Then its expression clears from the neural plate at HH5-7 and shifts to the neural plate border and pre-placodal region. By HH8-10 it is expressed strongly in the anterior neural folds and head surface ectoderm (Streit *et al.*, 2000).

ETV1 (Fig. 4.8F-J) is expressed weakly in the posterior epiblast at EGKXII-XIII and in the epiblast around Hensen's node at HH3-4. Later it is absent from the neural plate and neural tube, instead being expressed in the axial and lateral plate mesoderm at HH5-7 and HH8-10 (Lunn *et al.*, 2007).

ETV4 (Fig. 4.8K-O) is expressed strongest in the epiblast and prospective neural plate at EGKXII-XII and HH3-4 respectively. Later it is mainly expressed posteriorly in the mesoderm but also weakly in the posterior neural plate at HH5-7 and in the anterior neural folds and the future hindbrain at HH8-10 (Lunn *et al.*, 2007).

ETV5 (Fig. 4.8P-T) is expressed weakly in the epiblast at EGKXII-XIII but more strongly in the prospective neural plate at HH3-4. By HH5-7 it is expressed throughout the neural plate and at HH8-10 it is expressed anteriorly to the somites in the forming neural tube but also in the paraxial mesoderm (Lunn *et al.*, 2007).

EYA2 (Fig. 4.8U-Y) is weakly expressed in the epiblast at EGKXII-XIII, but it cannot be detected in the prospective neural plate at HH3-4. By HH5-7 it is expressed in the forming head fold and by HH8-10 it is detected in the anterior neural tube, neural folds and head surface ectoderm (Mishima and Tomarev, 1998).

EZH2 belongs to the polycomb group of transcriptional repressors (Vire *et al.*, 2006). EZH2 was upregulated only at the 12h time point, and no specific expression was detected in the embryo at EGKXII or HH4-. At HH7 it appears to be upregulated in small groups of cells in the head fold and heart forming region and by HH9- it is only weakly upregulated in the neural tube (Fig. 4.8Z-AD).

GBX2 (Fig. 4.9A-E) is expressed in the hypoblast layer but not the epiblast at EGKXII-XIII. By HH3-4 it is expressed broadly throughout the area pellucida ectoderm including the prospective neural plate. By HH5-7, GBX2 expression clears from the anterior neural plate but remains in the neural plate border and in the future hindbrain, pre-cardiac and paraxial mesoderm. This expression continues at HH8-10 when it is expressed in the forming neural tube, but is upregulated in the hindbrain where it forms a boundary with the midbrain (Shamim and Mason, 1998).

GLI2 (Fig. 4.9F-J) and **GLI3** (Fig. 4.9K-O) are not detected at EGKXII-XIII or HH3-4. Instead both are expressed in the anterior neural plate at HH5-7 and forming neural tube at HH8-10 (Schweitzer *et al.*, 2000).

HESX1 (Fig. 4.9P-T) cannot be detected at EGKXII-XIII or at HH3-4. It is expressed weakly in neural plate anterior to Hensen's node at HH5-7 and more strongly in the anterior neural folds at HH8-10 (Chapman *et al.*, 2002).

HEY1 (Fig. 4.9U-Y) expression cannot be detected at EGKXII-XIII, HH3-4 or HH5-7. It is only weakly expressed in the neural tube at HH8-10 (Leimeister *et al.*, 2000).

HIVEP3 encodes a zinc finger protein of the human immunodeficiency virus type 1 enhancer-binding protein family (Hicar *et al.*, 2001). HIVEP3 is upregulated at the 5h time point but there is only broad low level expression detected throughout the embryo at all stages (Fig. 4.10A-E).

HOXB1 (Fig. 4.10F-J) is absent from the pre-streak embryo at EGKXII-XIII. By HH3-4 it is expressed strongly in the axial mesoderm exiting the posterior primitive streak. This continues at HH5-7, and by HH8-10 it is also expressed posteriorly in the neural tube, but remains absent from the neural tube anterior to the somites (Paxton *et al.*, 2010).

ING5 may function as a component of the histone acetyltransferase complex (Doyon *et al.*, 2006). In the screen, it is upregulated after 5 and 9h and similar expression dynamics are observed by in situ hybridisation. ING5 is expressed strongest at early stages, in the epiblast at EGKXIII and prospective neural plate at HH4. By HH6, expression clears anteriorly from the neural plate and is restricted to a band across the anterior border and pre-placodal region. Expression continues weakly at HH8+ throughout the neural tube (Fig. 4.10K-O)

IRX2 (Fig. 4.10P-T) cannot be detected at EGKXII-XIII and HH3-4. Expression is observed in the neural plate and at HH5-7 and in the forming neural tube and somites at HH8-10 (Matsumoto *et al.*, 2004).

IVNS1ABP modifies the Aryl hydrocarbon receptor (AHR) pathway, to increase the concentration of AHR available to activate transcription (Dunham *et al.*, 2006). In the screen, it is upregulated after 5 and 9h. By in situ, IVNS1ABP expression is first detected in the prospective neural plate at HH4. It remains in the neural plate and neural tube at HH6 and HH8+ (Fig. 4.10U-Y).

KAT2B encodes a protein with histone acetyltransferase activity. In association with p300/CBP it interacts with core histones and nucleosomes to regulate transcription (Zhang and Bieker, 1998). KAT2B is upregulated after 5h in the screen but expression is not detected early at EGKXIII or HH4. There appears to be ubiquitous low level expression

throughout the embryo at HH5. It is only upregulated in the neural tube at HH9 (Fig. 4.10Z-AD).

KDM4A encodes a protein with histone demethylase activity (Zhang *et al.*, 2005) which is upregulated after 9 and 12h in the screen. It is detected in the epiblast at EGKXIII and the prospective neural plate at HH4. Later, it is expressed robustly in the neural plate at HH5 and the neural tube at HH8 (Fig. 4.11A-E).

LHX5 belongs to a large family of LIM homeobox proteins (Zhao *et al.*, 2000). It was only identified as upregulated after 12h. In the embryo LHX5 is not observed at EGKXIII and by HH4 there is only weak expression in the neural plate. At HH6 it is strongly expressed in the anterior neural plate, extending into the pre-placodal region. This continues in the neural tube at HH8-, when it is also expressed in the notochord (Fig. 4.11F-J).

LIN28A (Fig. 4.11K-O) is expressed strongly in the epiblast at EGKXII-XIII. At HH3-4 it is expressed in the prospective neural plate but is absent from regions closest to the primitive streak. Later at HH5-7 and HH8-10 it is expressed broadly and strongly throughout the embryo, including the neural plate and neural tube (Jean *et al.*, 2015).

LIN28B (Fig. 4.11P-T) is expressed weakly in the epiblast and prospective neural plate at EGKXII-XIII and HH3-4. No expression is detected at HH5-7, but it is expressed strongly in the neural tube at HH8-10 (Bobbs *et al.*, 2012, Jean *et al.*, 2015).

LMO1 encodes a putative transcriptional regulator that contains two zinc finger domains (McGuire *et al.*, 1991). It was detected as an upregulated candidate after 9 and 12h. In the embryo expression can first be detected at HH4 in the ectodermal cells overlying the node. By HH6, LMO1 is expressed strongly in the neural plate but is specifically absent from the anterior neural plate border and pre-placodal region surrounding the neural plate. At HH8 it is expressed strongly throughout the neural tube (Fig. 4.11U-Y).

LMX1B (Fig. 4.11Z-AD) is not expressed at EGKXII-XIII or HH3-4. Strong expression is detected in the neural plate and neural plate border at HH5-7, but is absent from the most anterior domains. By HH8-10 it is expressed throughout the forming neural tube and the migrating neural crest (Riddle *et al.*, 1995).

MAFA (Fig. 4.12A-E) is expressed strongly in the epiblast at EGKXII-XIII and prospective neural plate at HH3-4. Its expression weakens in the neural plate at HH5-7 and neural tube at HH8-10 (Ogino and Yasuda, 1998).

MAML2 functions as a transcriptional co-activator by interacting with the Notch intracellular domain (NICD) (Wu *et al.*, 2002). It is upregulated after only 9 and 12h and consistent with this, expression was not observed at EGKXIII or HH4 or HH5. However, by HH8 it is strongly expressed throughout the forming neural tube, but also the lateral plate mesoderm and somites (Fig. 4.12F-J).

MEIS1 (Fig. 4.12K-O) expression cannot be detected at EGKXII-XIII or HH3-4. By HH5-7 it is expressed strongly in the caudal neural plate but also in the mesoderm emerging from the posterior streak. This expression continues in the caudal neural tube at HH8-10 (Mercader *et al.*, 1999).

MEIS2 (Fig. 4.12P-T) is also absent at early stages, but is expressed in the caudal neural plate and neural tube and lateral plate mesoderm at HH5-7 and HH8-10 (Mercader *et al.*, 1999).

MTA1 is predicted to regulate transcription via HDAC1 (Yoo *et al.*, 2006). It is upregulated after 5 and 9h and is strongly expressed in prospective neural tissue at all stages examined. Expression is first detected in the epiblast at EGKXIII and in the prospective neural plate at HH4. This continues in the neural plate and lateral plate mesoderm at HH6 and HH9- (Fig. 4.12U-Y).

MYCN, or N-MYC, (Fig. 4.12Z-AD) is also expressed strongly at all stages assessed. It is detected in the epiblast and prospective neural plate at EGKXII-XIII and HH3-4. Later, at HH5-7 and HH8-10 expression persists in the neural plate and neural tube, but also in lateral plate mesoderm (Khudyakov and Bronner-Fraser, 2009).

NKX1-2 (Fig. 4.13A-E) expression is not detected at EGKXII-XIII and HH3-4. Instead it is expressed in the posterior lateral plate mesoderm at HH5-7. This continues at HH8-10, when it is also expressed in the caudal neural tube (Bertrand *et al.*, 2000).

NKX6-2 (Fig. 4.13F-J) is expressed ubiquitously at low levels at EGKXII-XIII and HH3-4. Later at HH5-7 and HH8-10 it is expressed only weakly in the neural plate and forming neural tube (Pattyn *et al.*, 2003).

NOT1 (Fig. 4.13K-O) is expressed at all stages assessed. Transcripts are present in the epiblast at EGKXII-XIII and prospective neural plate at HH3-4, when it is expressed strongest around Hensen's node. Later at HH5-7 and HH8-10 it is expressed in the neural plate directly adjacent to the regressing node, as well as in the notochord (Knezevic *et al.*, 1995, Stein *et al.*, 1996).

NOT2 (Fig. 4.13P-T) is also expressed strongly in the epiblast at EGKXII-XIII and in the ectoderm around Hensen's node at HH3-4. Later it is expressed strongly in the notochord, but weakly in the caudal ectoderm surrounding the regressing node (Stein *et al.*, 1996, Knezevic and Mackem, 2001).

NRIP1 modulates transcription by interacting with nuclear receptors (Subramaniam *et al.*, 1999). It was detected as upregulated only at the 5h time point. In the embryo, NRIP1 is expressed weakly in the epiblast at EGKXIII and more strongly in the prospective neural plate at HH4. However it is absent from the neural plate at HH6 and by HH9- it is mainly expressed in the lateral plate and pre-somitic mesoderm (Fig. 4.13U-Y).

NSD1 encodes a SET domain histone methyltransferase (Qiao *et al.*, 2011). It was identified by the screen as upregulated at each time point and strong NSD1 expression is observed at all stages assessed. It is detected in the epiblast at EGKXIII and the prospective neural plate at HH4. This continues in the neural plate and neural tube at HH7 and HH9+ (Fig. 4.13Z-AD).

OTX2 (Fig. 4.14A-E) is expressed strongly in the epiblast and EGKXII-XIII and prospective neural plate HH3-4. Later at HH5-7 it is restricted to the anterior neural plate extending outwards to cover the pre-placodal region. This continues at HH8-10 when OTX2 is expressed in the anterior neural tube and neural folds (Bally-Cuif *et al.*, 1995).

PDCD4 is a tumour suppressor that interacts with eIF4A to prevent transcription (Schlichter *et al.*, 2001, Palamarchuk *et al.*, 2005). In the screen, it was upregulated at the 12h time point only. By in situ, PDCD4 transcripts are detected in the epiblast at EGKXIII and in the prospective neural plate at HH4-. By HH6 it is strongly expressed in the neural plate and lateral plate mesoderm. At HH8 it is expressed throughout the neural plate and in the head surface ectoderm (Fig. 4.14F-J).

PDLIM4 contains PDZ and LIM domains. It was upregulated in the screen at each time point. No specific expression was detected at EGKXIII, but by HH4 it is expressed in the prospective neural plate. This continues in the neural plate proper at HH6 when it is also expressed in lateral plate mesoderm. By HH8+ it is expressed in the dorsal neural folds and posteriorly in the neural plate and its border (Fig. 4.14K-O).

PRDM1 (Fig. 4.14P-T) is expressed in the epiblast at EGKXII-XIII and prospective neural plate at HH3-4. Later at HH5-7 and HH8-10, it is absent from the neural plate and neural tube. Instead it is expressed in the pre-placodal region surrounding the anterior neural plate and later in the future lens, otic and epibranchial placodes (Ha and Riddle, 2003).

RB1 is a negative regulator of the cell cycle and acts as a transcriptional repressor of E2F1 target genes (Feinstein *et al.*, 1994, Rubin *et al.*, 2005). It was identified as an upregulated target, but only in the Galgal3 version of the RNA-Seq analysis. RB1 expression is not detected at EGKXIII, HH4 or HH5. However by HH8 it is strongly expressed throughout the neural plate (Fig. 4.14U-Y).

RFX3 is a transcriptional factor of the RFX family (Nakayama *et al.*, 2003). It was identified as upregulated at each time point but specific expression was not observed at EGKXIII, HH4 or HH7. Weak expression is only detected in the neural tube at HH8+ (Fig. 4.14Z-AD).

RUNX1T1 (Fig. 4.15A-E) is expressed strongest in the epiblast at EGKXII-XIII. Expression continues, but only weakly in the prospective neural plate, neural plate proper and neural tube at HH3-4, HH5-7 and HH8-10 respectively (Koyano-Nakagawa and Kintner, 2005).

SALL1 (Fig. 4.15F-J) is expressed broadly throughout the area opaca and area pellucida at EGKXII-XIII, except in the posterior marginal zone. By HH3-4 it is expressed weakly in the prospective neural plate and Hensen's node. Later at HH5-7 and HH8-10 it is expressed throughout the neural plate and neural tube, but also in lateral plate mesoderm (Sweetman *et al.*, 2005).

SETD2 is a H3K36 methyltransferase (Yoh *et al.*, 2008). In the screen it is upregulated at all stages. Strong SETD2 expression is also detected by in situ hybridisation at all stages. It is one of the strongest expressed markers in the epiblast at EGKXIII. This continues in the prospective neural plate at HH4, the neural plate proper at HH7 and forming neural tube at HH9- (Fig. 4.15K-O).

SIX3 (Fig. 4.15P-T) expression cannot be detected at EGKXII-XIII or HH3-4. By HH5-7 SIX3 is expressed strongly in the anterior neural plate extending to cover the pre-placodal region. This continues in the neural tube and neural folds at HH8-10, in the region contributing to the future forebrain (Bovolenta *et al.*, 1998).

SNAI1 (Fig. 4.15U-Y) is expressed broadly throughout the area opaca and hypoblast at EGKXII-XIII, but is also expressed posteriorly in the epiblast. By HH3-4, expression is detected weakly in Hensen's node and at HH5-7 and HH8-10 it is present in the somites, paraxial mesoderm and lateral plate (Garcia-Castro *et al.*, 2000).

SOX1 (Fig. 4.15Z-AD) expression cannot be detected at EGKXII-XIII, HH3-4 or HH5-7. It is first expressed in the neural plate and neural tube at HH8-10 (Pevny *et al.*, 1998).

SOX2 (Fig. 4.16A-E) is not expressed at EGKXII-XIII or HH3-4. Instead it is first expressed in the neural plate at HH5-7 and this continues in the forming neural tube at HH8-10 (Rex *et al.*, 1997).

SOX3 (Fig. 4.16F-J) is expressed strongly in the epiblast at EGKXII-XIII and prospective neural plate at HH3-4. By HH5-7 expression continues in the neural plate proper but clears from a region just anterior to Hensen's node. At HH8-10 it is expressed throughout the forming neural tube (Rex *et al.*, 1997).

SOX11 (Fig. 4.16K-O) is also expressed strongly in the epiblast at EGKXII-XIII and prospective neural plate at and HH3-4, when it is also detected in the primitive streak and Hensen's node. By HH5-7 it is expressed throughout the neural plate and pre-placodal region, but also in the lateral plate mesoderm. This continues at HH8-10 (Uwanogho *et al.*, 1995).

SOX13 is another member of the SOX (SRY-related HMG-box) family of transcription factors (Roose *et al.*, 1999). Like SOX11 it is also upregulated at each time point in the screen. Expression is observed weakly in the epiblast at EGKXIII, but much stronger in the prospective neural plate at HH4. This continues in the neural plate proper at HH5 and HH8 (Fig. 4.16P-T).

SP5 (Fig. 4.16U-Y) is only expressed posteriorly, in Koller's sickle at EGKXII-XIII. At HH3-4 it is absent from the prospective neural plate but is expressed posteriorly in the early mesoderm and primitive streak. Mesodermal expression continues at HH5-7, but transcripts are also detected in the caudal neural plate. By HH8-10 it is expressed throughout the neural tube as well as in the cardiac mesoderm and lateral plate (Kuraku *et al.*, 2005).

STOX1 is a transcription factor of the storkhead-box domain family (Rigourd *et al.*, 2009). It was identified as upregulated at each time point, but expression was not observed at any stage between EGKXIII-HH9 (Fig. 4.16Z-AD).

STOX2 is another storkhead-box domain protein (Fenstad *et al.*, 2010). It was identified as upregulated at the 9 and 12h time points. In the embryo, STOX2 is detected at all stages. Transcripts are weakly expressed in the epiblast at EGKXIII, but stronger in the prospective neural plate at HH4. By HH7 it is observed throughout the neural plate but

also in the pre-somitic and lateral plate mesoderm. This continues at HH8+ (Fig. 4.17A-E).

T (Brachyury) (Fig. 4.17F-J) is not expressed at EGKXII-XIII. At HH3-4 it is expressed in the primitive streak and emerging early mesoderm. By HH5-7 it is expressed strongly in the notochord but also in the lateral plate and weakly in the caudal neural plate. This continues at HH8-10 (Smith and Eichele, 1991).

TAF1A encodes a TATA box-binding protein-associated factor that plays a role in the assembly of the RNA polymerase I preinitiation complex (Friedrich *et al.*, 2005). It is only detected in the screen as an upregulated gene after 12h. In the embryo, TAF1A expression was not observed at any stage assessed (Fig. 4.17K-O).

TBL1XR1 acts as a component of the N-Cor co-repressor complex (Perissi *et al.*, 2004). It was identified as upregulated at each time point in the screen. In situ hybridisation reveals that it is expressed broadly throughout the embryo at all stages assessed, but is mildly upregulated in the neural tube at HH8-10 (Fig. 4.17P-T).

TBX6 (Fig. 4.17U-Y) is expressed posteriorly in the epiblast at EGKXII-XIII and in the ectoderm of the primitive streak and early mesoderm at HH3-4. Later, expression continues posteriorly in the streak ectoderm and lateral plate mesoderm (Knezevic *et al.*, 1997).

TCF7L1 (Fig. 4.17Z-AD) is expressed weakly at EGKXII-XIII and in the prospective neural plate at HH3-4. By HH5-7 it is strongly expressed in the neural plate proper and this continues in the forming neural tube at HH8-10 (Schmidt *et al.*, 2004).

TCF7L2 (Fig. 4.18A-E) is expressed ubiquitously at low levels at EGKXII-XIII and HH3-4, but it is upregulated it is expressed in the anterior neural plate at HH5-7 and in the anterior neural tube and folds by HH8-10 (Hartmann and Tabin, 2000).

TCF12 (Fig. 4.18F-J) also shows no specific expression at the earlier stages, but is upregulated in the neural plate at HH5-7. By HH8-10 it is strongly expressed in the neural tube (Helms *et al.*, 1994).

TGIF1 (Fig. 4.18K-O) is weakly expressed in the epiblast at EGKXII-XIII but is expressed much more strongly in the ectoderm including the prospective neural plate at HH3-4. Expression weakens in the neural plate proper at HH5-7, but it is detected throughout the forming neural tube at HH8-10 (Lorda-Diez *et al.*, 2009).

TRIM9 is a member of the tripartite motif (TRIM) family (Reymond *et al.*, 2001). In the screen it was detected as upregulated at each time point. TRIM9 expression was not detected at EGKXIII and at HH4 it is only weakly expressed in the mesoderm. By HH7 it is expressed strongly in the neural plate but is absent from the anterior lateral edge of the neural plate. At HH9-, TRIM9 is expressed along the inner wall of the neural tube (Fig. 4.18P-T).

TRIM24 is another TRIM family member which regulates transcription by interacting with the AF2 region of nuclear receptors (Tsai *et al.*, 2010). It was identified as being upregulated, but only at the 5h time point. In the embryo it is expressed strongly in the epiblast at EGKXIII and also in the prospective neural plate at HH4. By HH6 it is expressed along the lateral edges of the neural plate and by HH9+ it is only expressed weakly in the neural tube (Fig. 4.18U-Y).

YEATS4 is putative transcription factor (Zimmermann *et al.*, 2002). It is upregulated consistently in the screen and is expressed strongly at all stages assessed. Transcripts are detected in the epiblast and prospective neural plate at EGKXIII and HH4. By HH5 it is expressed in the neural plate and this continues in the neural tube at HH10 (Fig. 4.18Z-AD).

ZEB2 (Fig. 4.19A-E) expression is not detected at EGKXII-XIII and it is only expressed weakly in the early mesoderm at HH3-4. By HH5-7 it is expressed more strongly in the neural plate and throughout the forming neural tube by HH8-10 (Sheng *et al.*, 2003).

ZIC2 (Fig. 4.19F-J) is expressed at low levels throughout the embryo between pre-streak and HH5-7. Even by HH8-10, it is only expressed weakly in the forming neural tube (Warner *et al.*, 2003).

ZIC3 (Fig. 4.19K-O) is expressed strongly in the epiblast at EGKXII-XIII and in the prospective neural plate and primitive streak at HH3-4. At HH5-7 and HH8-10 it is expressed strongly in the anterior neural plate and neural tube and in the lateral plate mesoderm (Warner *et al.*, 2003).

ZNF423 (also known as OAZ) belongs to the family of Kruppel-like C2H2 zinc finger proteins and functions as a DNA-binding transcription factor (Hata *et al.*, 2000). In the screen it is upregulated, but only at the 9 and 12h time points. Accordingly, expression is not observed at EGKXIII or HH4. It is strongly expressed in the neural plate at HH6 and HH8+. Therefore it resembles the expression profile of SOX2 (Fig. 4.19P-T).

ZNF462 is a nuclear zinc finger protein predicted to function as a chromatin modifier or transcription factor (Masse *et al.*, 2011). In the screen it is upregulated at each time point and in the embryo ZNF462 is expressed in the epiblast at EGKIII and prospective neural plate at HH4. Later at HH6 and HH8+, it is expressed in the neural plate and lateral plate mesoderm (Fig. 4.19U-Y).

ZNF469 is also a predicted zinc finger transcription factor (Abu *et al.*, 2008). It was identified as upregulated, but only at the 5h time point. In the embryo, expression is not observed at EGKXIII, HH4 or HH5+. At HH8 it is expressed broadly but seems to be upregulated in the neural plate (Fig. 4.19Z-AD).

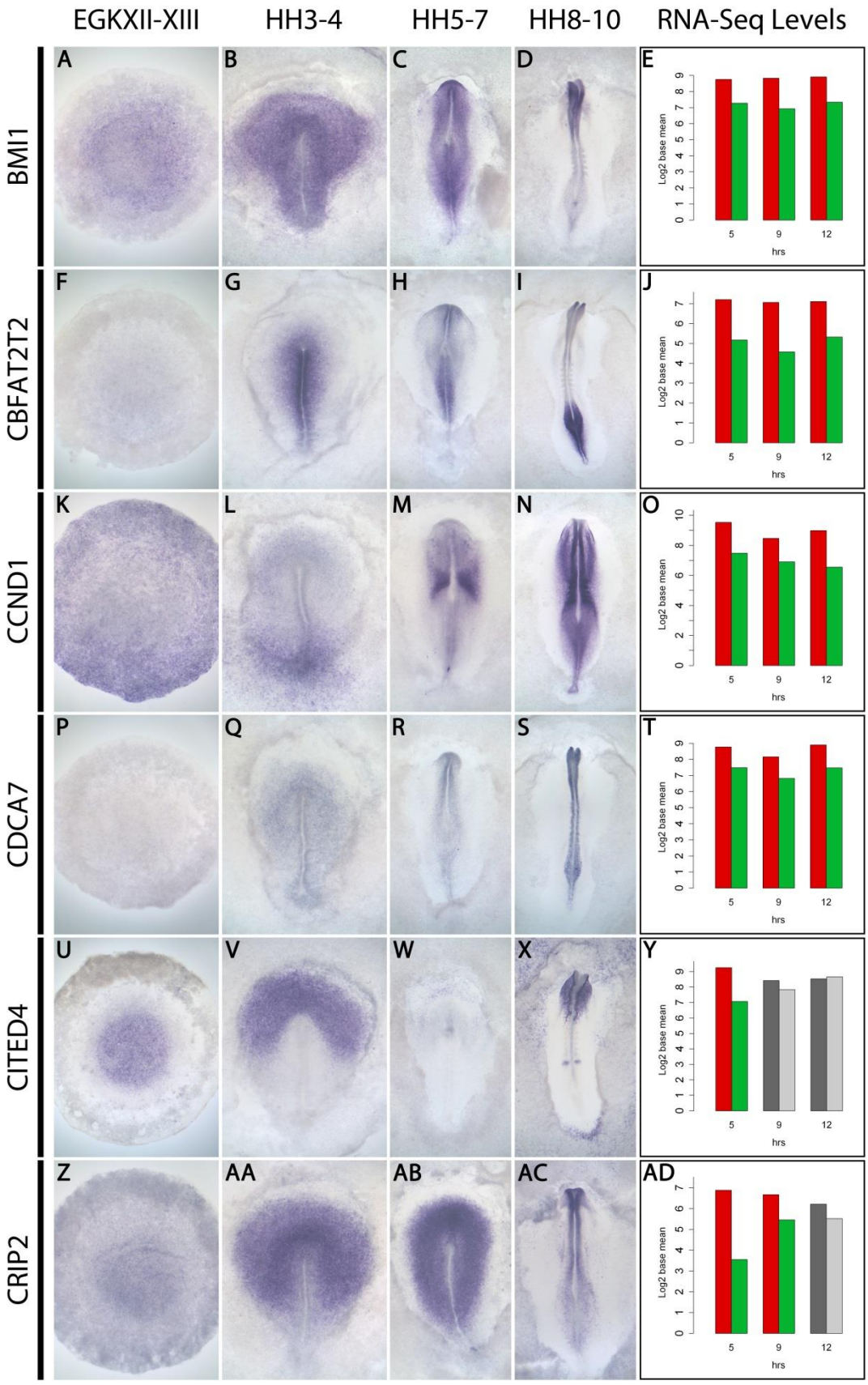

Figure 4.6: Expression of BMI1, CBFAT2T2, CCND1, CDCA7, CITED4 and CRIP2.

The expression of upregulated markers was assessed by in situ hybridisation at four key stages: pre-streak at EGKXII-XIII (A, F, K, P, U, Z), during gastrulation at HH3-4 (B, G, L, Q, V, AA), at neural plate stages HH5-7 (C, H, M, R, W, AB) and neural tube stages HH8-10 (D, I, N, S, X, AC). Expression patterns are compared to the absolute transcript counts as quantified by RNA-Seq (E, J, O, T, Y, AD). Expression levels at each time point are plotted as bar graphs of $\log_2$ of the base mean for induced (red or dark grey) and uninduced (green or light grey) tissues at each time point. Where columns are coloured red and green, induced and uninduced values differ by at least $\log_2$ 1.2 and markers are differentially expressed. Columns coloured dark and light grey distinguish when markers are not differentially expressed.

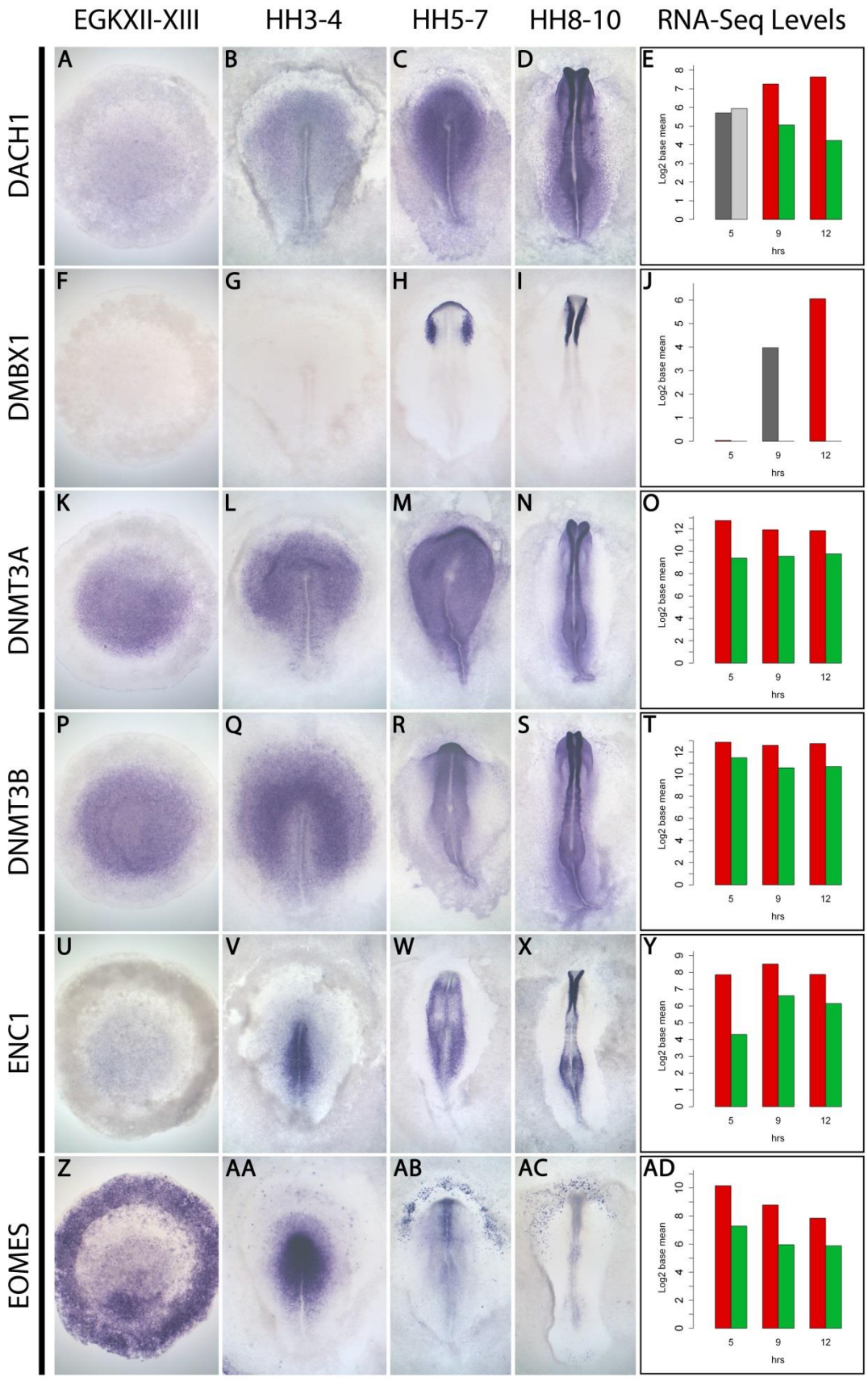

Figure 4.7: Expression of DACH1, DMBX1, DNMT3A, DNMT3B, ENC1 and EOMES.

For details, see Fig. 4.6.

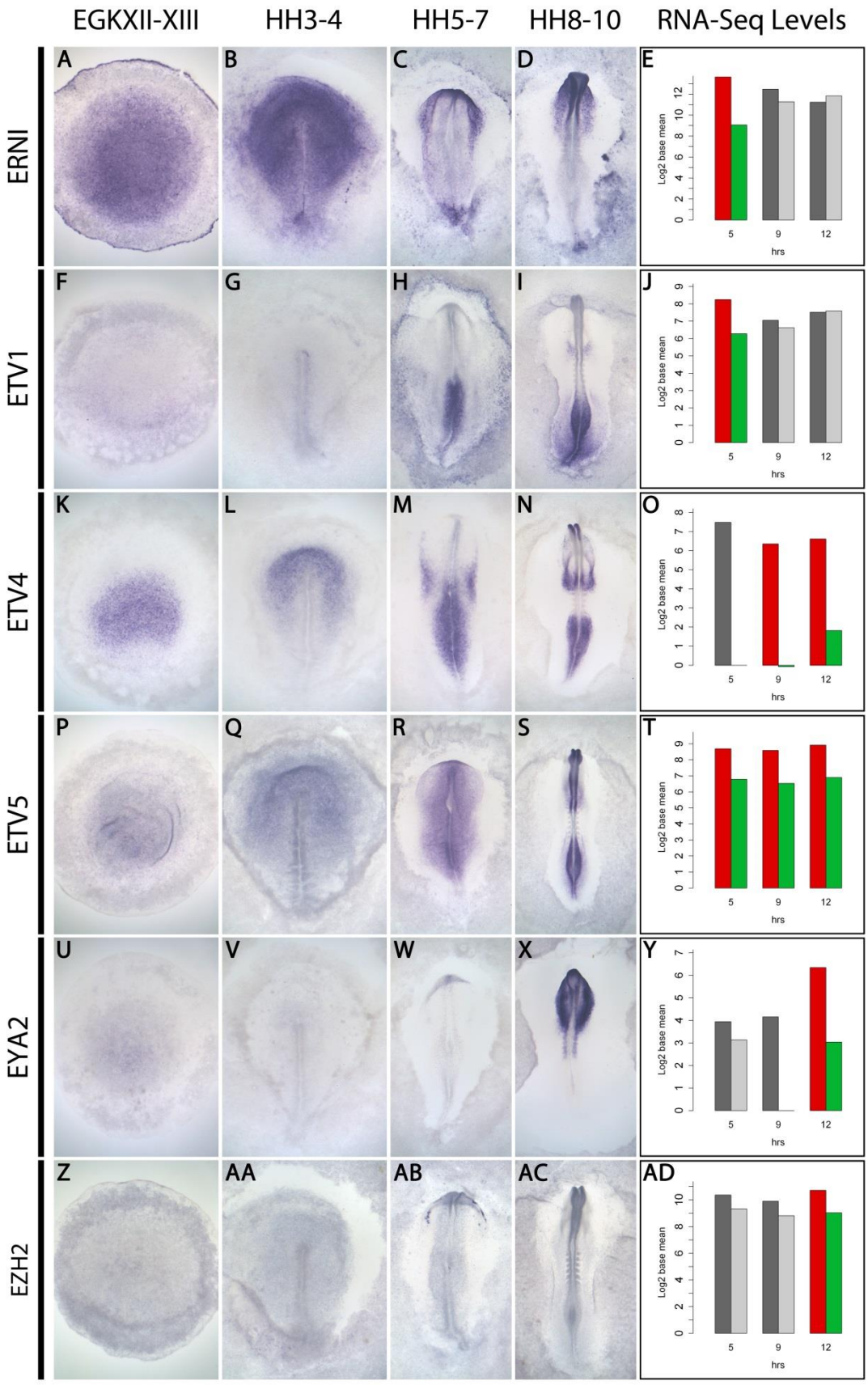

Figure 4.8: Expression of ERNI, ETV1, ETV4, ETV5, EYA2 and EZH2.

For details, see Fig. 4.6.

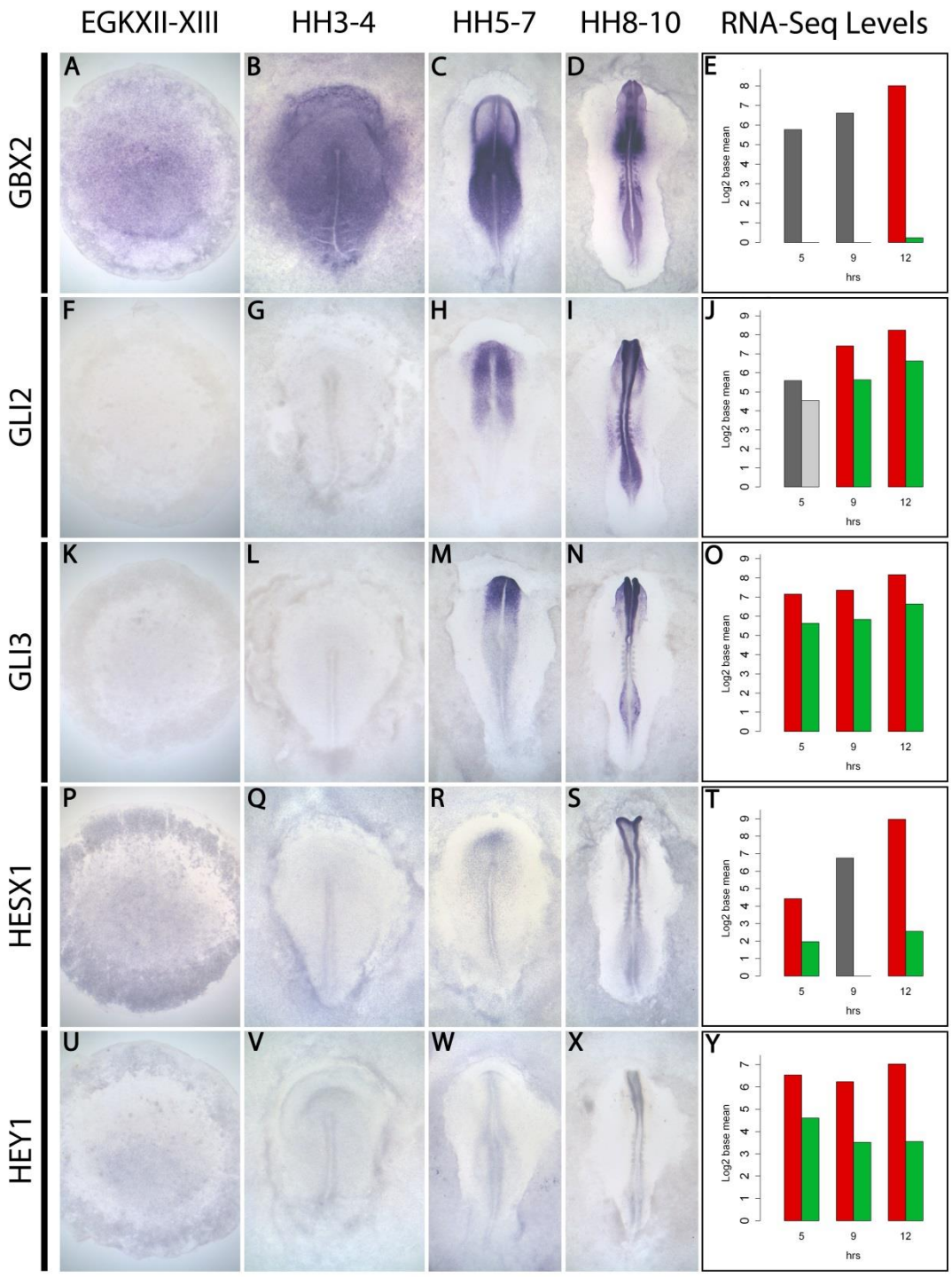

Figure 4.9: Expression of GBX2, GLI2, GLI3, HESX1 and HEY1.

For details, see Fig. 4.6.

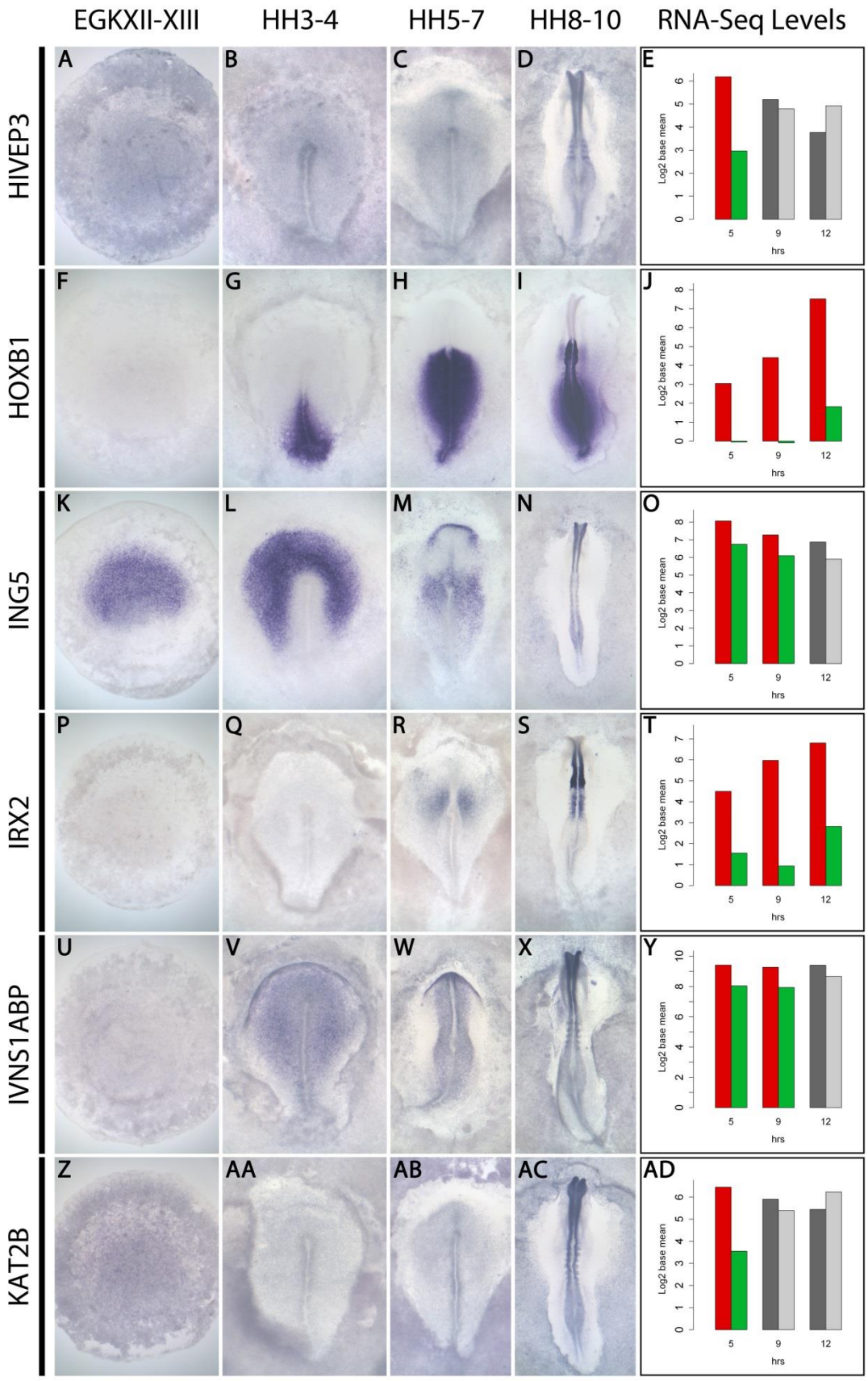

Figure 4.10: Expression of HIVEP3, HOXB1, ING5, IRX2, IVNS1ABP and KAT2B.

For details, see Fig. 4.6.

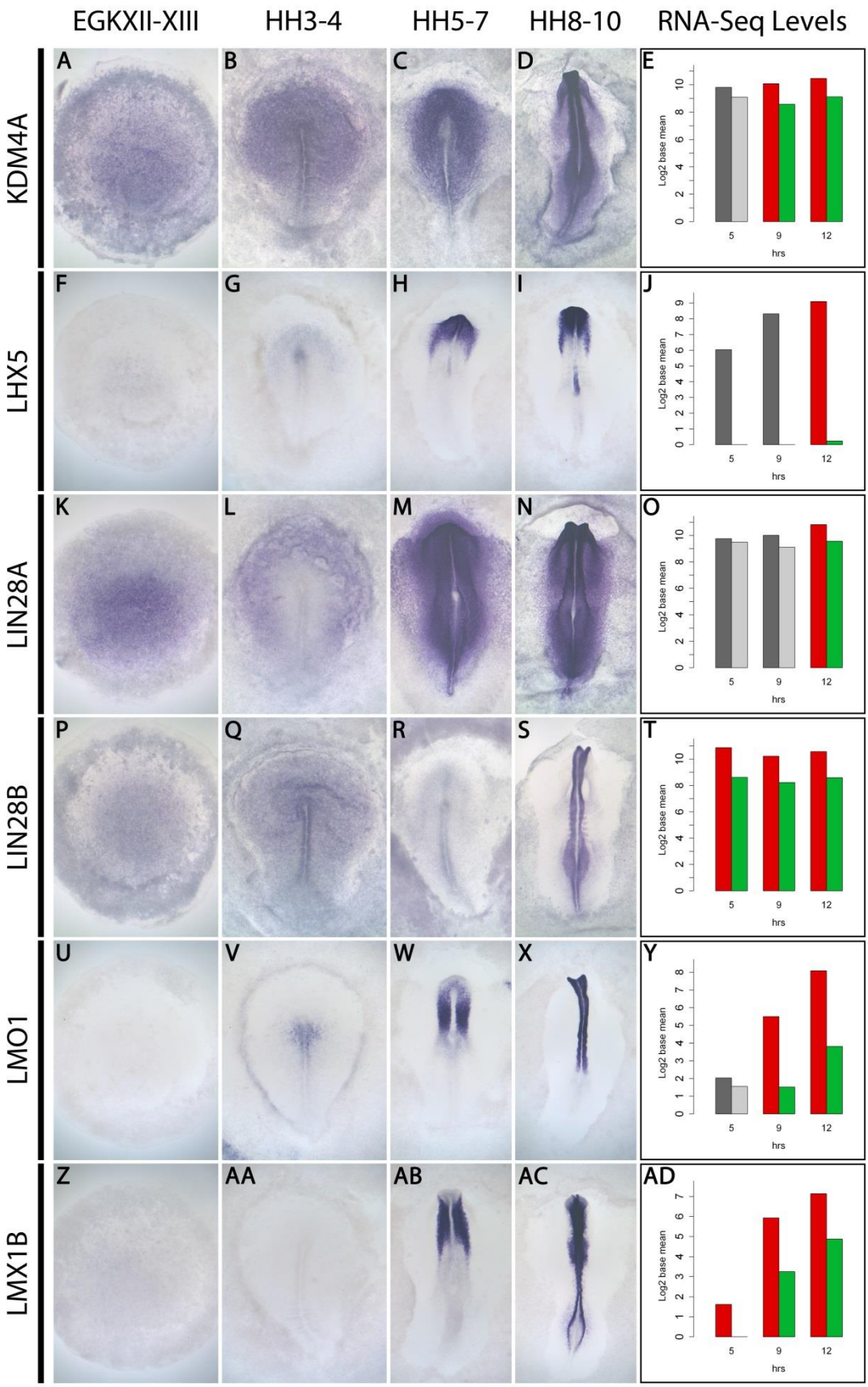

Figure 4.11: Expression of KDM4A, LHX5, LIN28A, LIN28B, LMO1 and LMX1B.

For details, see Fig. 4.6.

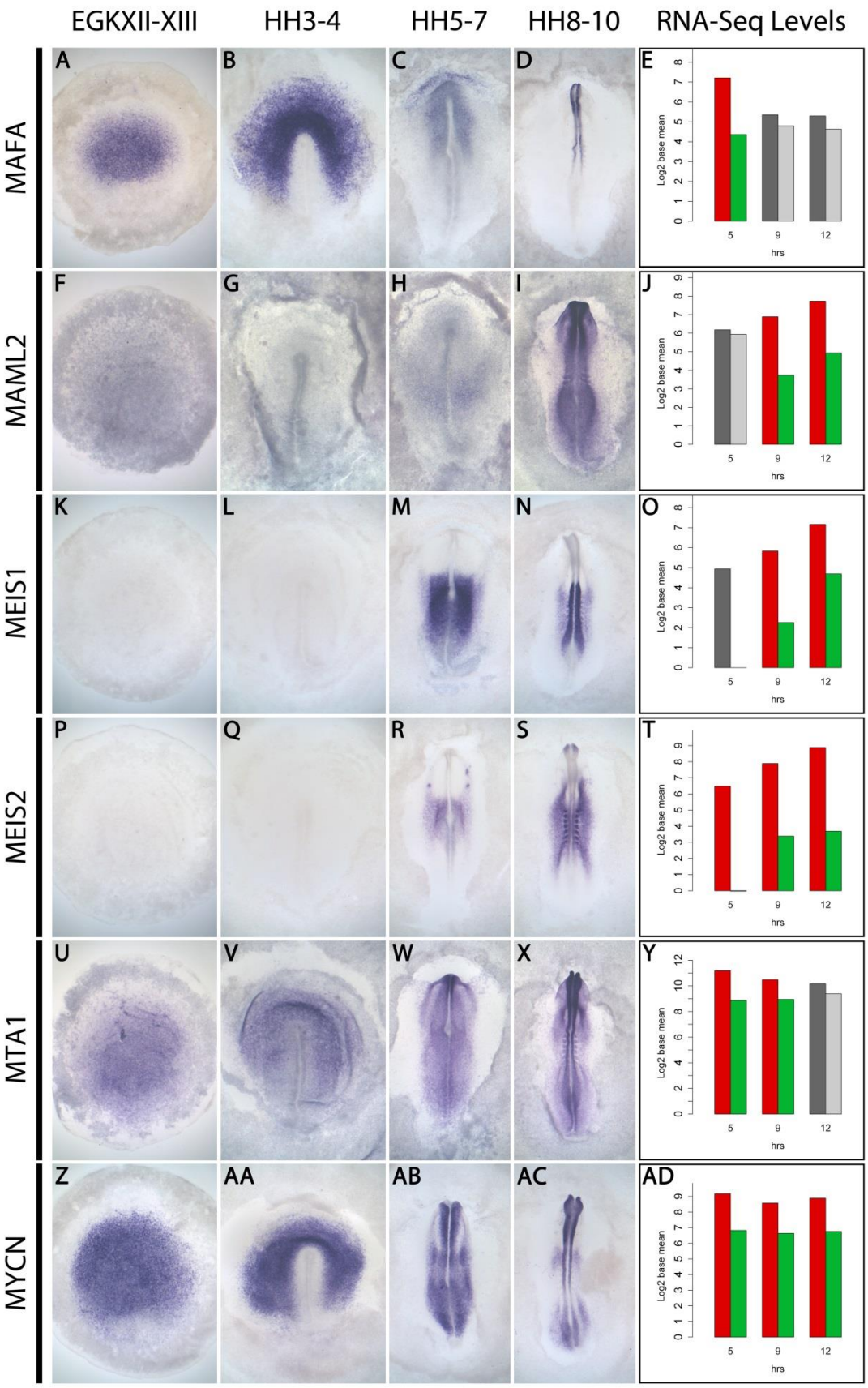

Figure 4.12: Expression of MAFA, MAML2, MEIS1, MEIS2, MTA1 and MYCN.

For details, see Fig. 4.6.

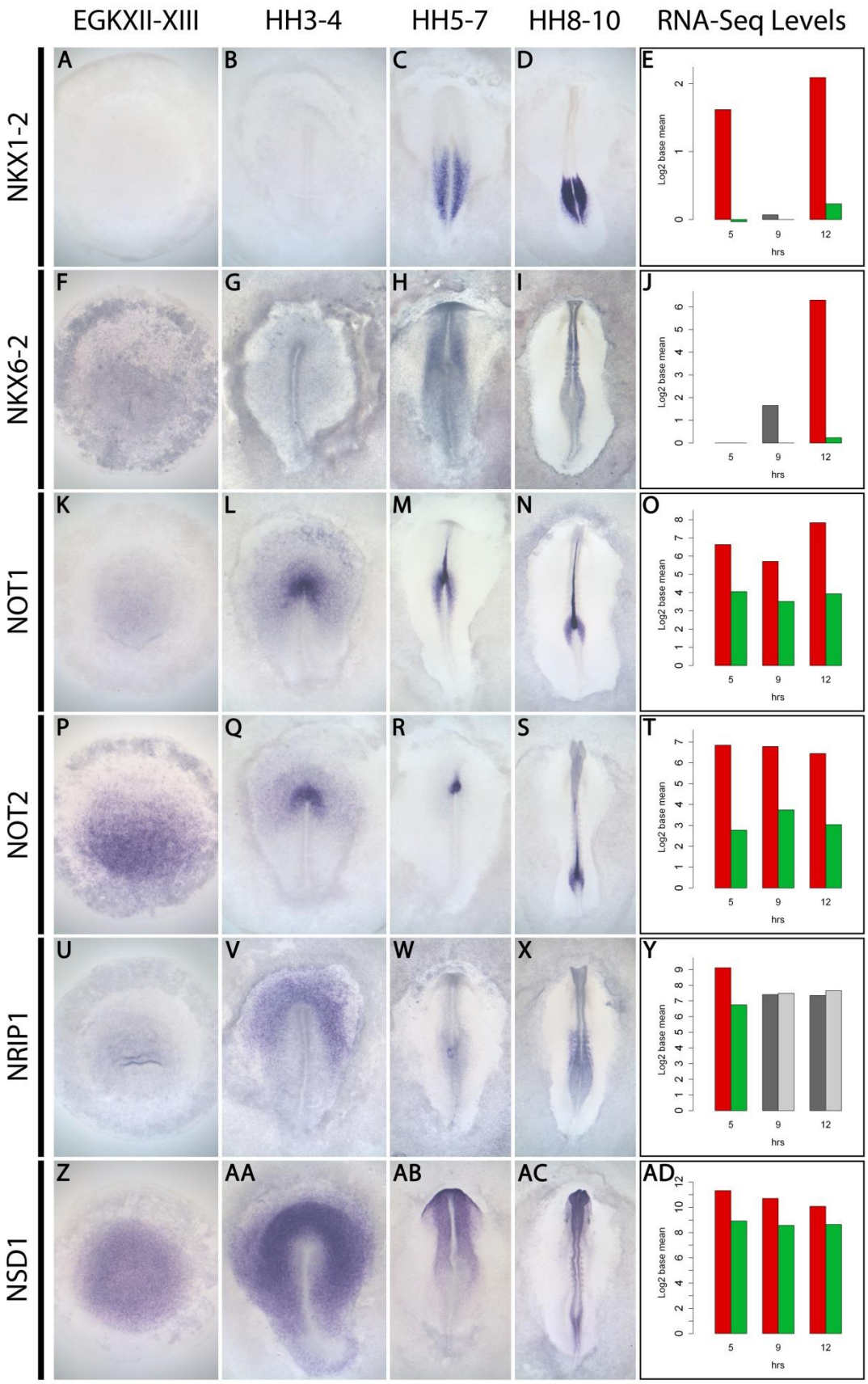

Figure 4.13: Expression of NKX1-2, NKX6-2, NOT1, NOT2, NRIP1 and NSD1.

For details, see Fig. 4.6.

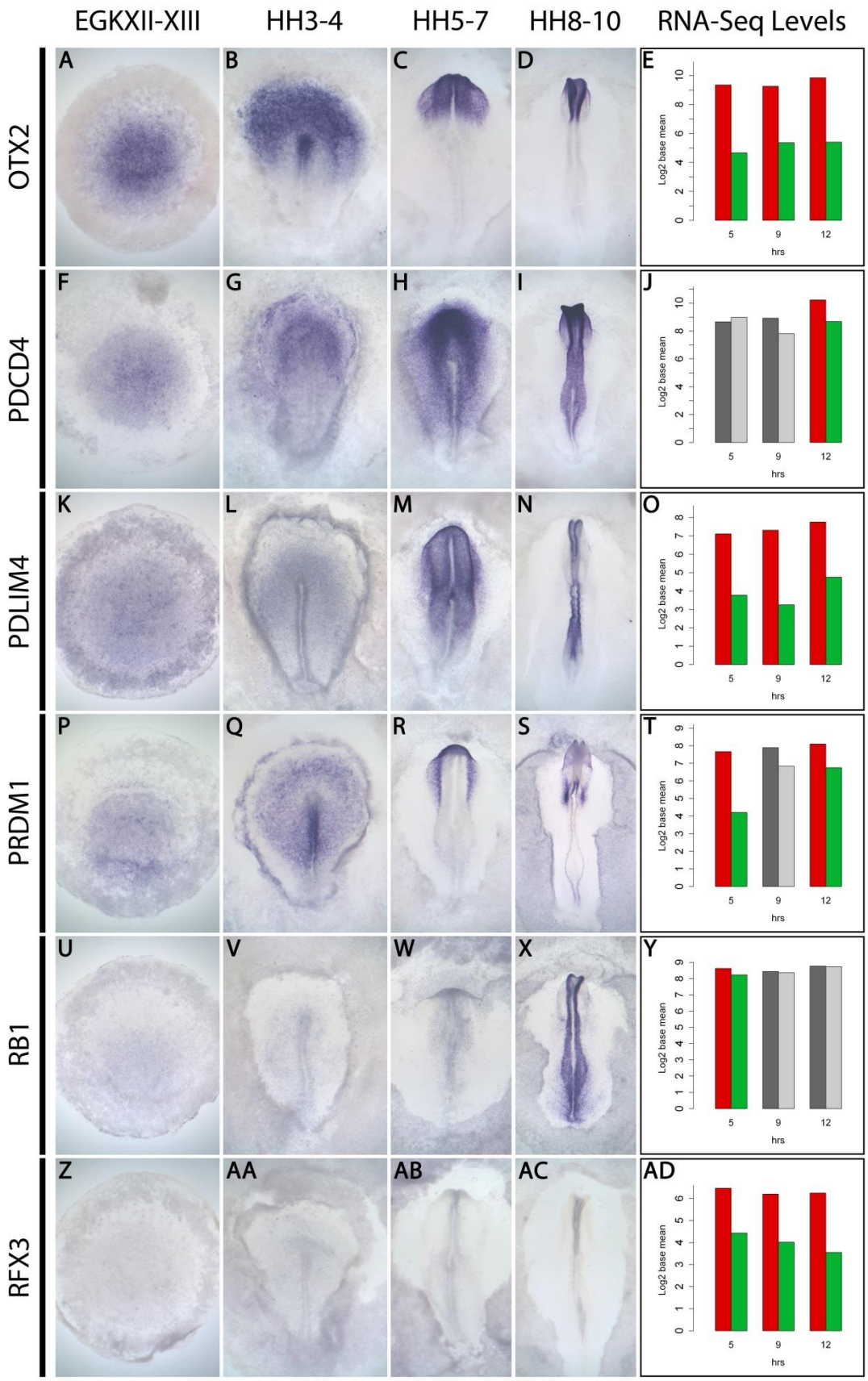

Figure 4.14: Expression of OTX2, PDCD4, PDLIM4, PRDM1, RB1 and RFX3.

For details, see Fig. 4.6.

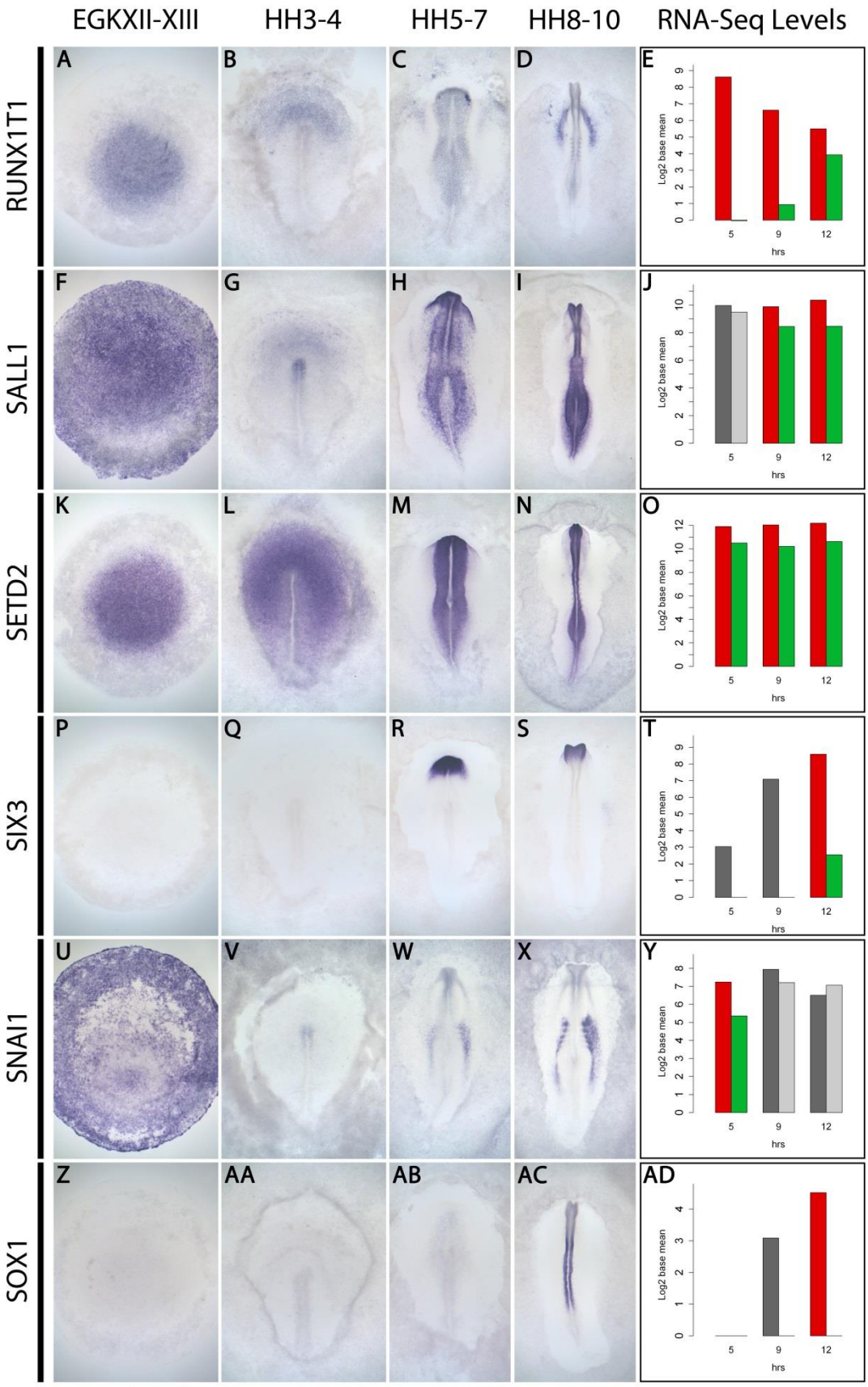

Figure 4.15: Expression of RUNX1T1, SALL1, SETD2, SIX3, SNAI1 and SOX1.

For details, see Fig. 4.6.

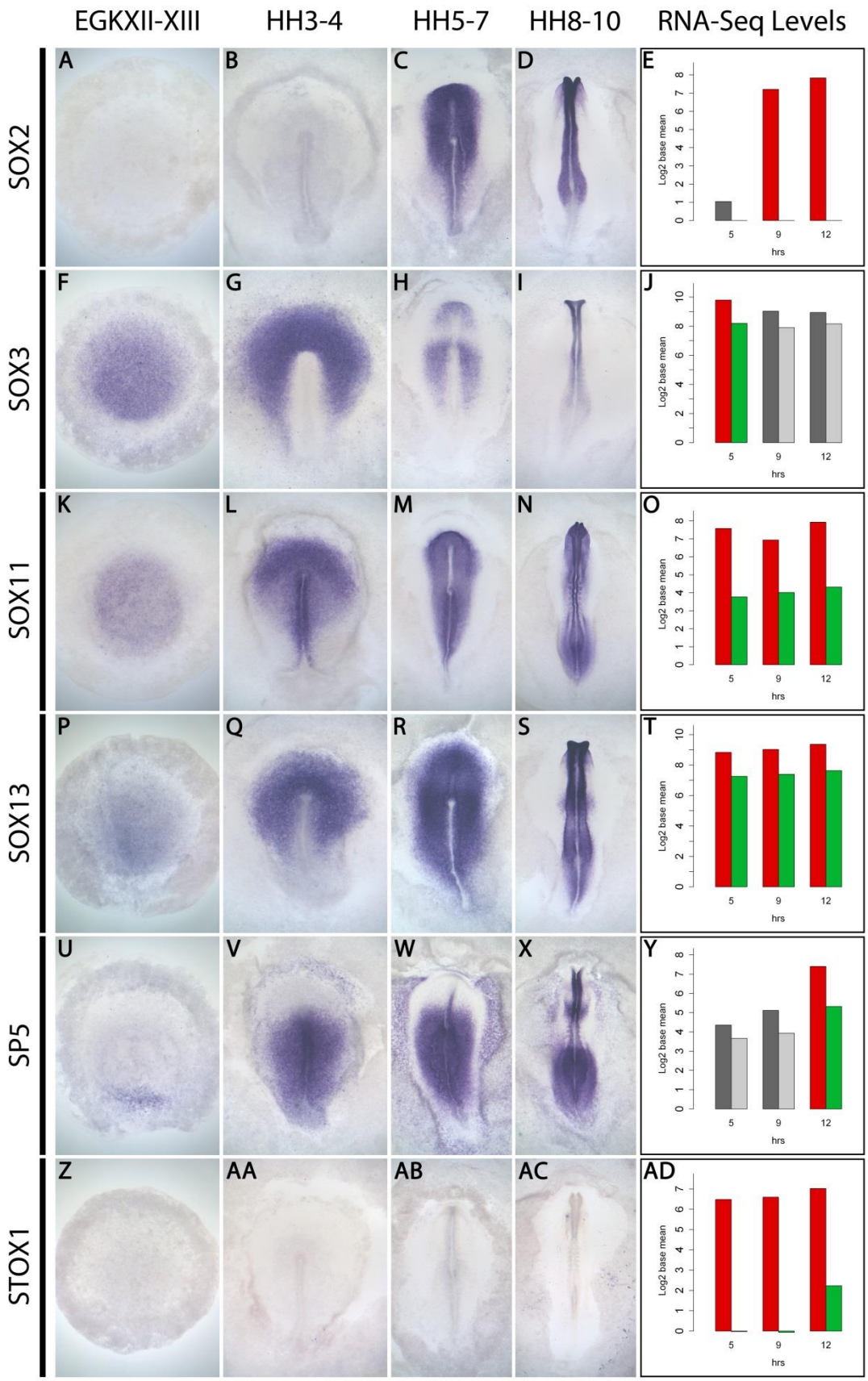

Figure 4.16: Expression of SOX2, SOX3, SOX11, SOX13, SP5 and STOX1.

For details, see Fig. 4.6.

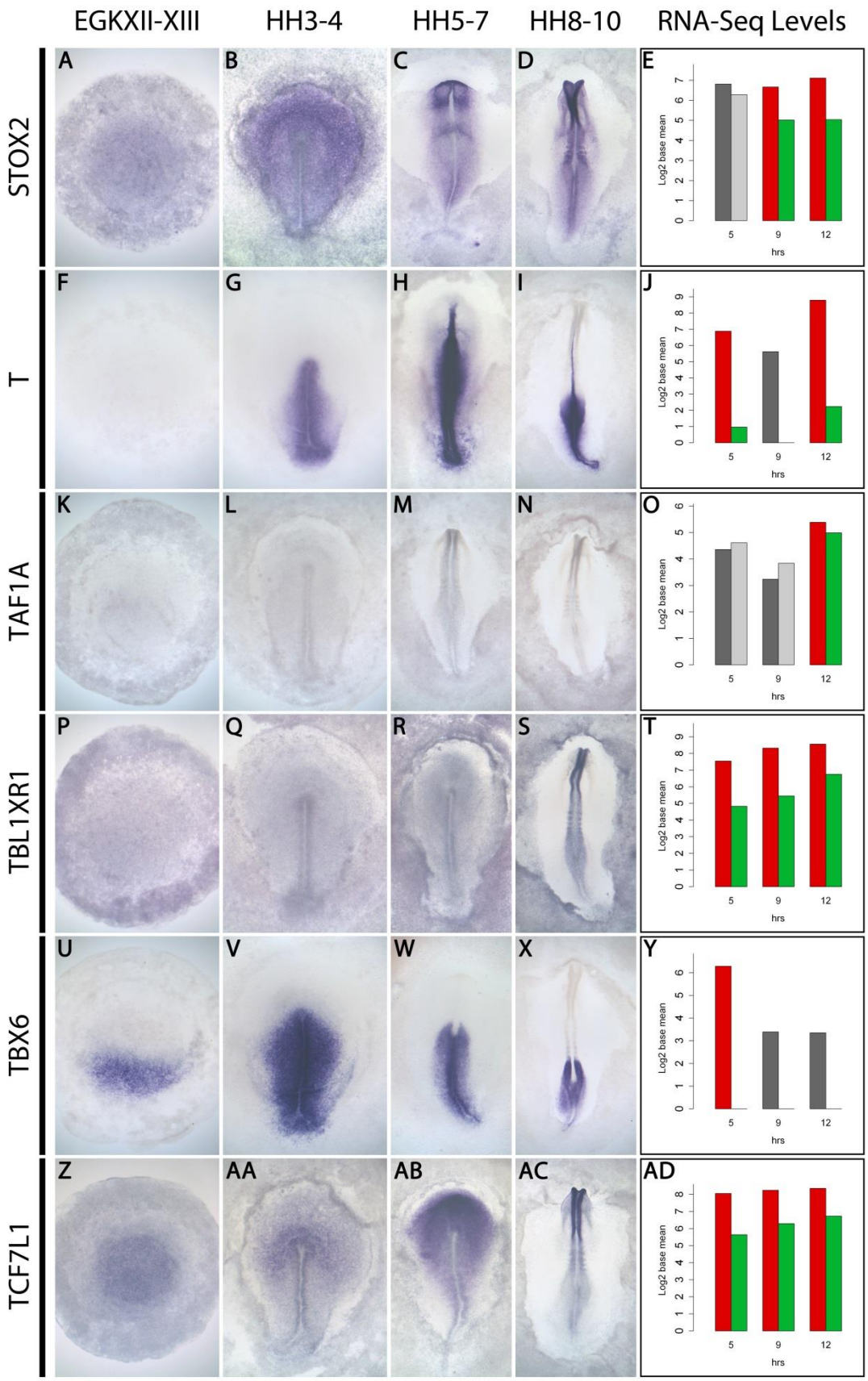

Figure 4.17: Expression of STOX2, T, TAF1A, TBL1XR1, TBX6 and TCF7L1.

For details, see Fig. 4.6.

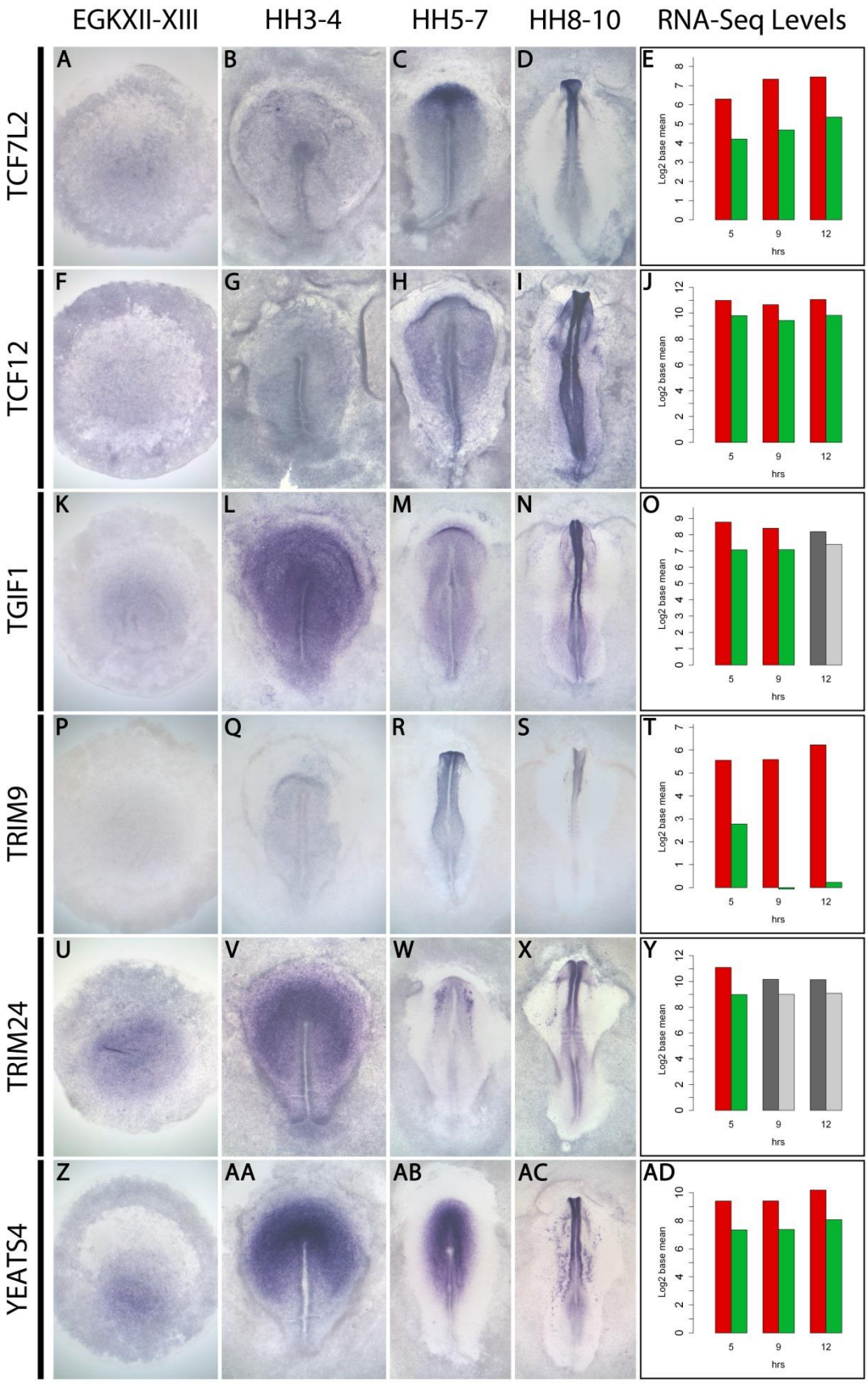

Figure 4.18: Expression of TCF7L2, TCF12, TGIF1, TRIM9, TRIM24 and YEATS4.

For details, see Fig. 4.6.

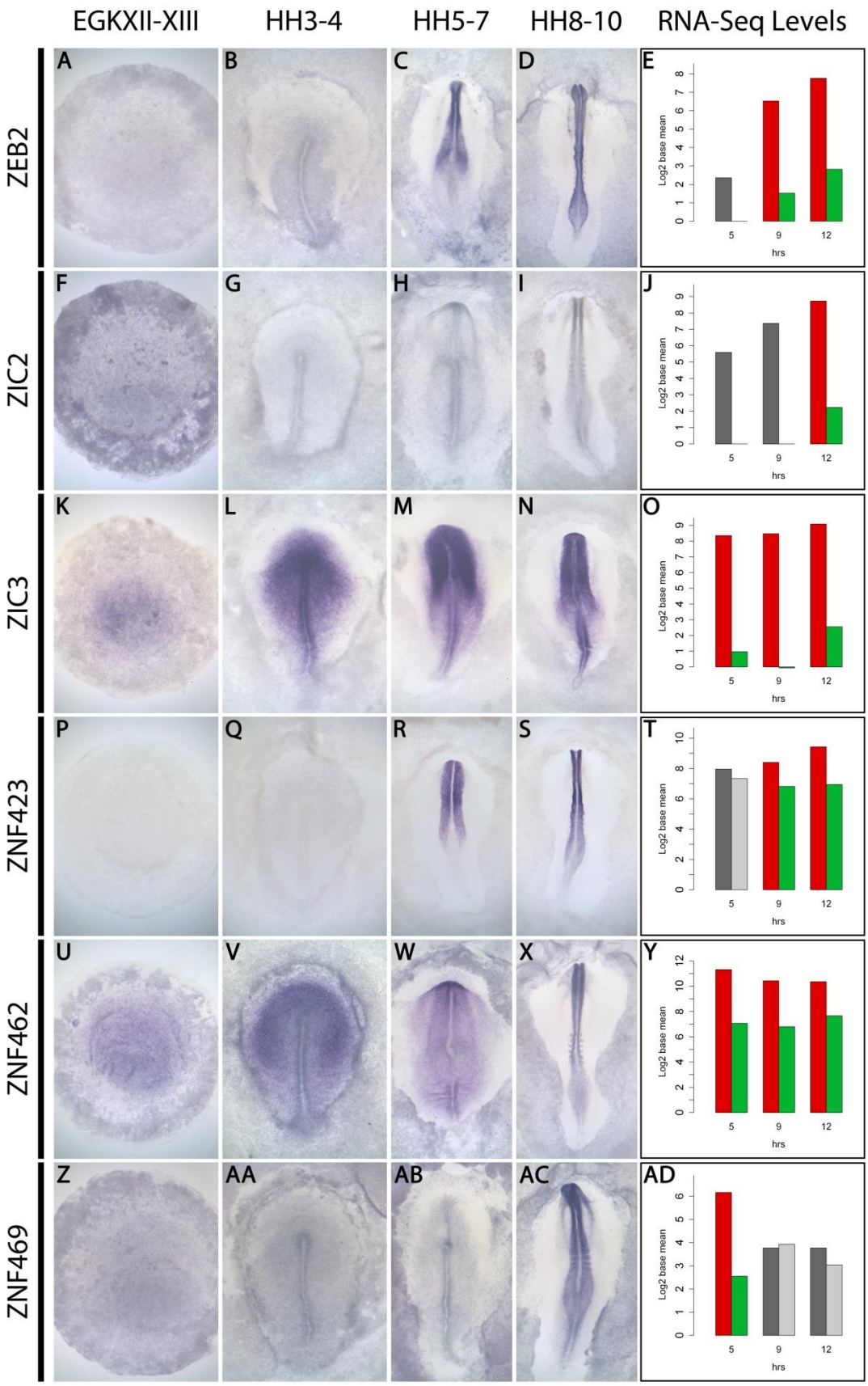

Figure 4.19: Expression of ZEB2, ZIC2, ZIC3, ZNF423, ZNF462 and ZNF469.

For details, see Fig. 4.6.

4.3.4.2 Downregulated transcriptional regulators

Also verified by in situ hybridisation, were the expression of 83 transcriptional regulators which are downregulated by grafts of Hensen's node, including 49 not previously studied in chick. Such responses have not been previously detected by screens for neural induction (Streit *et al.*, 2000). Although the expression of these factors may not contribute to neural identity, these responses could have important functions to repress neural fates, or they may provide evidence of alternative cell state or cell fate decisions that accompany neural induction.

AHR encodes a ligand-activated transcription factor, whose ligands included a variety of aromatic hydrocarbons (Allan and Sherr, 2005). In the screen AHR is downregulated but specific expression is not detected at EGKXII-XIII, HH4 or HH5. Only very faint expression can be detected in the neural tube at HH8 (Fig. 4.20A-E).

ARID5B encodes a DNA binding protein which forms a histone H3K9 demethylase complex with PHF2 (Baba *et al.*, 2011). The screen detects ARID5B transcripts as downregulated after 9 and 12h. Consistent with this, ARID5B is expressed only in the area opaca at HH5 and HH8+. Expression was not observed in embryonic tissues, or earlier at EGKXIII and HH4 (Fig. 4.20F-J).

ATF3 is a member of the mammalian activation transcription factor/cAMP responsive element-binding (CREB) protein family. It exists as two isoforms. The longer isoform represses transcription via ATF binding elements. The shorter isoform lacks a basic leucine zipper motif and does not bind to DNA. Instead it appears to stimulate transcription by sequestering inhibitory co-factors (Chen *et al.*, 1994). In the screen, ATF3 is upregulated after 5h, but downregulated after 9 and 12h. Despite using a probe which targets all ATF3 isoforms, expression was not detected at EGKXIII or HH4. At HH5, it is strongly expressed in lateral plate mesoderm directly adjacent to the anterior neural plate. By HH9, ATF3 is weakly expressed in the lumen of the anterior neural tube (Fig. 4.20K-O).

BACH1 functions to repress transcription from MAF recognition elements (Warnatz *et al.*, 2011). It was identified as being consistently downregulated. By in situ hybridisation, BACH1 appears to be expressed ubiquitously at low levels at HH4-, HH6 and HH8. No specific expression is detected at EGKXII (Fig. 4.20P-T).

BACH2 is similar in structure and function to BACH1, and also represses transcription from MAF elements (Yoshida *et al.*, 2007). It was downregulated at each time point in the

screen. BACH2 appears to be weakly expressed in the neural plate at HH4- and HH5 and this expression strengthens in the neural tube at HH9-. However it is also expressed at a similar level in extra-embryonic tissue at these stages (Fig. 4.20U-Y).

BHLHE40 encodes a basic helix-loop-helix transcription factor which has been implicated in circadian regulation (Sato *et al.*, 2004). In the screen BHLHE40 is downregulated at each time point but no specific expression is detected at EGKXIII, HH4 or HH7. It is only expressed at HH9 in multiple regions including the notochord, heart field and hindbrain (Fig. 4.20Z-AD).

CDX2 (Fig. 4.21A-E) is consistently absent from prospective neural tissues and is expressed strongly in the area opaca at all stages assessed. At HH3-4 it is also expressed posteriorly in the early mesoderm, and later at HH5-7 and HH8-10 in the lateral plate mesoderm (Marom *et al.*, 1997).

CDX4 (Fig. 4.21F-J) expression is not detected at EGKXII-XIII or HH3-4. By HH5-7 it is expressed caudally in the lateral plate mesoderm. This continues at HH8-10, when it is also expressed in the caudal neural tube adjacent to Hensen's node (Alev *et al.*, 2010).

CEBPB encodes a transcription factor which can regulate chromatin conformation (Burk *et al.*, 1993, Plachetka *et al.*, 2008). CEBPB is downregulated at 9 and 12h in the screen, but there is no observable expression at any of the stages assessed (Fig. 4.21K-O).

CREB3L1 is a transcription factor which activates transcription via B-box elements (Omori *et al.*, 2002). It is downregulated at the 12h time point in the screen. No specific expression is observed at EGKXIII and HH4. CREB3L1 is absent from the neural plate and tube at HH6 and HH9-. Instead, strong expression is detected in the heart field, lateral plate mesoderm and in the extra-embryonic blood islands (Fig. 4.21P-T).

CREG1 antagonises transcriptional activation by the adenovirus E1A protein, which normally functions to promote proliferation and inhibit differentiation (Veal *et al.*, 1998). CREG1 is downregulated at the 5h time point but no specific CREG1 expression was detected at any stage (Fig. 4.21U-Y).

CSRP2 belongs to the CSRP family of genes with putative zinc finger binding activity (Weiskirchen *et al.*, 1995). In the screen, CSRP2 is downregulated at each time point and it is absent from neural tissue at all stages. It is expressed strongly in the hypoblast at EGKXIII and in the germinal crescent at HH4. Later at HH6 and HH8+ it is expressed in lateral plate mesoderm, non-neural ectoderm and germinal crescent (Fig. 4.21Z-AD).

DLX3 (Fig. 4.22A-E) is expressed broadly at very low levels at EGKXII-XIII and HH3-4. By HH5-7 it is expressed in the neural plate but also in the lateral plate mesoderm and anterior non-neural ectoderm. This continues at HH8-10 (Pera and Kessel, 1999).

DLX5 (Fig. 4.22F-J) expression is not detected at EGKXII-XIII or HH3-4. By HH5-7 it is strongly expressed in the neural plate border, pre-placodal region and non-neural ectoderm. This continues at HH8-10 in the neural plate border and neural folds (Ferrari *et al.*, 1995).

ELF1 encodes an E26 transformation-specific related transcription factor (Leiden *et al.*, 1992). In the screen, it is detected as downregulated at each time point. Specific ELF1 expression was not observed at EGKXIII or HH4. It is very weakly expressed in the neural plate and neural tube at HH7+ and HH9 (Fig. 4.22K-O).

ELF3 is an epithelial specific ETS-related transcription factor (Oettgen *et al.*, 1997, Brembeck *et al.*, 2000). It is downregulated at each time point. There is no specific ELF3 expression at EGKXIII or HH4. It is expressed in the lateral plate mesoderm adjacent to the posterior neural plate at HH7 and by HH8 very faint expression is detected in the neural tube (Fig. 4.22P-T).

EPAS1 (Fig. 4.22U-Y) is broadly expressed at low levels at EGKXII-XIII and very weakly in the early mesoderm at HH3-4. Later it is absent from the neural plate but is expressed strongly in the extra-embryonic and embryonic non-neural ectoderm as well as the germinal crescent (Ota *et al.*, 2007).

ESRRG encodes an oestrogen receptor-related receptor (Hentschke *et al.*, 2009). It was identified as downregulated at the 5h time point but at EGKXIII and HH4 no specific expression is detected. By HH6, it is ubiquitously expressed throughout the embryo and area opaca and is strongest in the head fold. By HH8 it is expressed in the neural plate border and head fold as well as the area opaca (Fig. 4.22Z-AD).

ETS2 (Fig. 4.23A-E) is expressed strongly in the area opaca at EGKXII-XIII, but no expression was detected by HH3-4. Later, at HH5-7 it is expressed weakly in mesoderm of the lateral plate and head fold. By HH8-10 it is expressed mainly in the embryonic mesoderm and blood islands (Mey *et al.*, 2012).

FKHR belongs to the forkhead family of transcription factors and is a key target of insulin signalling (Biggs *et al.*, 2001, Zhang *et al.*, 2002, Nakae *et al.*, 2012). It is downregulated

after 9 and 12h by the screen. No specific expression is observed at any stage assessed (Fig. 4.23F-J).

FOXO3 also belongs to the forkhead family of transcription factors (Biggs *et al.*, 2001, Bakker *et al.*, 2004). It was identified as being consistently downregulated. Expression is not observed at EGKXIII, HH4- or HH8+. However at HH5 it appears to be expressed just anterior to the head fold and in patches of extra-embryonic tissue (Fig. 4.23K-O).

FRY has also been demonstrated to function as a transcriptional activator by repressing microRNA gene silencing in *Xenopus* (Goto *et al.*, 2010). It is downregulated in the screen at each time point. In the embryo, FRY is expressed ubiquitously at low levels in the stages assessed (Fig. 4.23P-T).

GATA2 (Fig. 4.23U-Y) is consistently absent from neural tissue. At EGKXII-XIII it is expressed in the area opaca and anteriorly in a domain fated to form non-neural ectoderm. By HH3-4 it is expressed in the posterior primitive streak. Later at HH5-7 and HH8-10 it is expressed strongly in the embryonic and extra-embryonic ectoderm, lateral plate mesoderm and blood islands (Sheng and Stern, 1999, Sheng *et al.*, 2003).

GATA4 (Fig. 4.23Z-AD) is expressed in Koller's sickle at EGKXII-XIII and then strongly in the primitive streak and area opaca at HH3-4. No specific expression is detected at HH5-7, but by HH8-10 it is strongly expressed in the lateral plate and pre-cardiac mesoderm (Chapman *et al.*, 2002, Jean *et al.*, 2015).

GATA5 (Fig. 4.24A-E) and **GATA6** (Fig. 4.24F-J) display similar expression patterns. No specific expression was detected at EGKXII-XIII, but they are expressed in the germinal crescent and early endoderm at HH3-4. Later they are expressed weakly in the lateral plate mesoderm and anteriorly in the endoderm of the head fold. By HH8-10 they are detected more strongly in the lateral plate and pre-cardiac mesoderm as well as the anterior intestinal portal (Jean *et al.*, 2015).

GRHL1 encodes a member of the grainyhead family of transcription factors (Wilanowski *et al.*, 2002, Ting *et al.*, 2003) which is downregulated at each time point in the screen. At EGKXIII, there is weak expression in the area opaca and Koller's sickle. Later at HH4, HH5 and HH8 expression is ubiquitous at low levels (Fig. 4.24K-O).

GRHL2 also belongs to the grainyhead family of transcription factors (Wilanowski *et al.*, 2002, Ting *et al.*, 2003). In the screen it is downregulated at 9 and 12h. Consistent with this there is no specific expression at EGKXIII and HH3+. Later at HH6, GRHL2 is absent from

the neural plate but upregulated in the bordering pre-placodal region. This expression continues at HH9 in the neural folds, future placodes and head surface ectoderm (Fig. 4.24P-T).

GRHL3 encodes another member of the grainyhead family of transcription factors (Wilanowski *et al.*, 2002, Ting *et al.*, 2003). It is strongly downregulated in each time point and is absent from neural tissue at all stages. At EGKXIII it is expressed weakly anteriorly in cell fated to contribute to non-neural ectoderm. By HH4 expression is restricted to the area opaca. Later, it is expressed strongly in non-neural ectoderm surrounding the neural plate and pre-placodal region at HH5. This continues at HH8 (Fig. 4.24U-Y).

HAND1 (Fig. 4.24Z-AD) is expressed weakly in the hypoblast at EGKXII-XIII and in the early endoderm and mesoderm at HH3-4. This continues at HH5-7 and HH8-10, where it is expressed strongly in embryonic and extra-embryonic lateral plate mesoderm and blood islands (Srivastava *et al.*, 1995).

HIC2 is closely related to HIC1 (Deltour *et al.*, 2001), which encodes a transcriptional repressor (Pinte *et al.*, 2004). In the screen it was downregulated at each time point. In the embryo, it is expressed anteriorly at EGKXIII. By HH4 it is expressed in the area opaca and also in the primitive streak. By HH7 and HH8+ it is expressed in the area opaca and in the embryonic non-neural ectoderm bordering the neural plate and neural tube (Fig. 4.25A-E).

HIPK2 acts as a co-repressor of SMAD1 mediated BMP signalling (Harada *et al.*, 2003). The screen detects it as being downregulated only at the 12h time point. HIPK2 expression is not observed at EGKXIII. By HH4 it is expressed weakly in the zone between the area opaca and the area pellucida. By HH7, HIPK2 is expressed throughout the extra-embryonic ectoderm and lateral plate mesoderm. Expression is restricted to the lateral plate mesoderm and the heart field at HH9 (Fig. 4.25F-J).

HIVEP2 is a member of the human immunodeficiency virus type 1 enhancer-binding protein family (Nomura *et al.*, 1991), which has been implicated in regulating TGFB signalling (Shukla *et al.*, 2009). In the screen, HIVEP2 is downregulated after 9 and 12h. Weak HIVEP2 expression is detected in the primitive groove at HH4 but no specific staining was observed at any other stages (Fig. 4.25K-O).

HNF1B (Fig. 4.25P-T) is weakly expressed in the hypoblast at EGKXII-XIII and in the germ wall at HH3-4. This continues at HH5-7 and HH-10, when it is also expressed in the anterior intestinal portal, caudal hindbrain and future spinal cord (Aragon and Pujades, 2009).

HOXA1 (Fig. 4.25U-Y) is not detected at EGKXII-XIII. By HH3-4 it is expressed posteriorly in the emerging lateral plate mesoderm of the primitive streak. This continues more strongly at HH5-7, when it is also expressed in the non-neural ectoderm surrounding the anterior neural plate. By HH8-10, it is absent anteriorly but is expressed in the caudal neural tube and lateral plate mesoderm (McClintock *et al.*, 2003).

HOXA2 (Fig. 4.25Z-AD) expression is similar to HOXA1. No expression is detected at EGKXII-XIII and only very weak expression is observed in the posterior primitive streak at HH3-4. It is robustly expressed in the lateral plate and pre-somitic mesoderm at HH5-7 and this continues at HH8-10 in the somites, lateral plate mesoderm and caudal hindbrain (Prince and Lumsden, 1994).

ID2 (Fig. 4.26A-E) is mainly expressed in the area opaca and Koller's sickle at EGKXII-XIII. Then, at HH3-4 its expression is restricted to the germ wall. Later at HH5-7 it is expressed weakly in the area opaca but also in the forming anterior intestinal portal, lateral plate mesoderm, pre-cardiac mesoderm and sub-regions of the neural plate. This continues at HH8-10 (Martinsen *et al.*, 2004).

ID3 (Fig. 4.26F-J) is expressed in the hypoblast at EGKXII-XIII and in embryonic and extra-embryonic ectoderm, germinal crescent and early mesoderm at HH3-4. By HH5-7, it is mainly expressed in the lateral plate and pre-cardiac mesoderm of the forming anterior intestinal portal. This continues at HH8-10, when it is also expressed in the forming somites and anterior neural tube (Kee and Bronner-Fraser, 2001).

IRF7 encodes a member of the interferon regulatory transcription factor (IRF) family (Caillaud *et al.*, 2002, Bentz *et al.*, 2010). IRF7 transcripts are detected as downregulated in the screen after 9 and 12h and in the embryo IRF7 is generally absent from neural tissue. At EGKXIII it is expressed in cells at the outer edge of the area opaca, and weakly in the marginal zone at HH4. By HH7 and HH8+ it is expressed very weakly in the neural plate and anterior neural tube respectively, but more strongly in the area opaca (Fig. 4.26K-O).

ISX encodes a member of the RAXLX homeobox gene family and regulates vitamin A metabolism (Seino *et al.*, 2008, Lobo *et al.*, 2013) which is only downregulated at the 12h time point. There is no specific expression at EGKXIII but at HH4, HH6 and HH8, ISX is expressed in the marginal zone and area opaca, but never in embryonic tissue (Fig. 4.26P-T).

JMJD4 belongs to the jumonji family of transcription factors (Zhang *et al.*, 2005, Liu *et al.*, 2013). It is downregulated after 5 and 9h, but only by the Galgal3 analysis. Expression of JMJD4 was not detected at EGKXIII or HH4. By HH6, it is expressed strongly in patches of the area opaca and at HH9- it is weakly expressed in the neural tube (Fig. 4.26U-Y).

KLF2 (Fig. 4.27A-E) is expressed broadly at low levels throughout the embryo at EGKXII-XIII, HH3-4 and HH5-7. At HH8-10 it is upregulated in the forming somites (Antin *et al.*, 2010).

KLF4 (Fig. 4.27F-J) demonstrates a similar expression pattern to KLF2. It is weakly but ubiquitously expressed at all stages assessed (Antin *et al.*, 2010).

KLF5 (Fig. 4.27K-O) is expressed at low levels throughout the embryo at EGKXII-XIII and HH3-4. Then at HH5-7 it is expressed in the embryonic non-neural ectoderm surrounding the neural plate. This continues at HH8-10 when it is also observed in the head surface ectoderm (Antin *et al.*, 2010).

KLF6 (Fig. 4.27P-T) expression is not detected at EGKXII-XIII, HH3-4 or HH5-7. It is strongly expressed in the head mesenchyme and surface ectoderm at HH8-10 (Antin *et al.*, 2010).

LMO7 encodes a protein implicated in the expression of genes required for myogenesis (Holaska *et al.*, 2006, Dedeic *et al.*, 2011). It is downregulated in the neural induction screen at each time point. LMO7 expression is not observed at EGKXIII, and at HH4 it is expressed only in cells at the outer edge of the area opaca (not shown). By HH7, faint expression is observed along the notochord. This continues at HH9+, when LMO7 is also expressed in the lateral plate mesoderm and the anterior intestinal portal (Fig. 4.27U-Y).

MBNL2 is a member of the muscleblind family. It encodes a protein which modulates alternative splicing of pre-mRNAs (Ho *et al.*, 2004, Huang *et al.*, 2008). MBNL2 was identified as being downregulated at every time point in the screen, but specific expression was not detected at any stage assessed (Fig. 4.27Z-AD).

MEF2D is a member of the myocyte-specific enhancer factor 2 (MEF2) family of transcription factors (Breitbart *et al.*, 1993). In the screen, it was identified as downregulated after 5, 9 and 12h. In the embryo expression is not observed at EGKXIII or HH4. By HH7 it is strongly expressed in pre-cardiac mesoderm and this continues at HH8+ (Fig. 4.28A-E).

MSX1 (Fig. 4.28F-J) is expressed in the area opaca at EGKXII-XIII. Then at HH3-4 it is expressed posteriorly in the early lateral plate mesoderm. This continues at HH5-7 and HH8-10, when it is also expressed in the neural plate border and neural folds (Suzuki *et al.*, 1991).

MSX2 (Fig. 4.28K-O) expression is not detected at EGKXII-XIII and at HH3-4 it is detected only weakly at the posterior end of the streak. Robust expression is observed at HH5-7, where MSX2 is expressed in the embryonic and extra-embryonic lateral plate mesoderm, blood islands and anterior non-neural ectoderm. By HH8-10 it is also expressed throughout the neural folds (Brown *et al.*, 1997).

MYC, or C-MYC (Fig. 4.28P-T) is weakly at expressed in the area opaca at EGKXII-XIII. By HH3-4 it is also expressed in the lateral plate mesoderm emerging from the posterior primitive streak. This expression continues at HH5-7, when it is also present in the extra-embryonic blood islands. Expression persists in the caudal lateral plate mesoderm at HH8-10 when it is also observed in the anterior neural folds (Khudyakov and Bronner-Fraser, 2009).

NANOG (Fig. 4.28U-Y) is strongly expressed in the epiblast at EGKXII-XIII and embryonic and extra-embryonic ectoderm at HH3-4. At later stages NANOG expression cannot be detected at HH5-7 or HH8-10 (Lavial *et al.*, 2007).

NCOA2 encodes a nuclear receptor co-activator (Voegel *et al.*, 1996). In the screen it was identified as downregulated but only after 12h. In the embryo, it is expressed in the hypoblast at EGKXIII, but is more ubiquitously expressed by HH4. At HH6 and HH8, expression appears in the neural plate and neural tube, but also throughout the area opaca (Fig. 4.28Z-AD).

NFKBIZ is a transcriptional co-activator required for the expression of NFκB target genes (Totzke *et al.*, 2006, Hildebrand *et al.*, 2013). It is downregulated at each time point in the screen, but specific expression was not detected at any of the stages assessed (Fig. 4.29A-E).

OVOL2 is zinc finger transcription factor which functions downstream of BMP signalling during mesendoderm development (Zhang *et al.*, 2013). It was identified as downregulated at the 9 and 12h time points of the screen. However, only low level ubiquitous expression is detected at HH4, HH5 or HH8+. It appears to be weakly expressed in Koller's sickle at EGKXIII (Fig. 4.29F-J).

PDLIM1 functions as a co-activator of LIM homeodomain transcription factors, but inhibits transcriptional activation mediated by oestrogen receptor alpha (Johnsen *et al.*, 2009). It was identified as being downregulated after 9 and 12h by the screen. Specific expression was not observed at EGKXIII, HH4 or HH5. By HH8+ PDLIM1 is strongly expressed in the neural folds, neural plate border and lateral plate mesoderm but is absent from the neural plate itself (Fig. 4.29K-O).

PDLIM5 is a member of the PDZ-LIM family, which can sequester nuclear factors to control transcription (Krcmery *et al.*, 2010). The screen identified it as a downregulated candidate at each time point. Specific expression is not observed in the embryo at EGKXIII, HH4, or HH8+. However at HH5, PDLIM5 is expressed in patches of extra-embryonic cells (Fig. 4.29P-T).

PITX2 (Fig. 4.29U-Y) is expressed strongly in the posterior marginal zone and adjacent area opaca at EGKXII-XIII. By HH3-4 it is absent from the prospective neural plate and expressed strongly in the area opaca and germ wall. At later stages it continues to be expressed extra-embryonically. However it is also expressed in the pre-cardiac mesoderm at HH5-7 and in the head mesenchyme and lateral plate mesoderm on the left side of the embryo at HH8-10 (Zhu *et al.*, 1999).

PITX3 encodes a bicoid class homeodomain transcription factor (Semina *et al.*, 1998). It was downregulated only after 5h in the screen. PITX3 expression was not observed at EGKXIII. Instead at HH4, HH7 and HH9- it is expressed in the area opaca and is completely absent from embryonic tissue (Fig. 4.29Z-AD).

PPARGC1A functions as a transcriptional co-activator (Knutti *et al.*, 2000, Puigserver and Spiegelman, 2003, Ueda *et al.*, 2005). It was identified as being downregulated at each time point in the screen, but PPARGC1A expression could not be detected at any of the stages assessed (Fig. 4.30A-E).

PTRF encodes a protein that enables the dissociation of paused ternary polymerase I transcription complexes (Jansa *et al.*, 1998). It was identified as downregulated at each time point by the screen. PTRF is strongly expressed at the outer edge of the embryo at EGKXIII and HH4. Specific expression is not observed at HH5 or HH8+ (Fig. 4.30F-J).

RARB (Fig. 4.30K-O) expression is not detected at EGKXII-XIII or HH3-4. At later stages it is expressed weakly in the area opaca, but also in the caudal neural plate and neural tube at HH5-7 and HH8-10 (Mercader *et al.*, 2000).

RASSF7 modulates transcription by negatively regulating JNK signalling (Takahashi *et al.*, 2011). It was identified as a downregulated candidate at each time point in the screen. Expression of RASSF7 is first detected in the hypoblast at EGKII and in the germinal crescent and endoderm overlying the node at HH4. By HH7 it appears to be expressed in the anterior neural plate but by HH9- it is only weakly expressed in the neural tube (Fig. 4.30P-T).

RREB1 encodes a zinc finger transcription factor (Miyake *et al.*, 1997). It is consistently downregulated in the screen and is appropriately absent from neural tissue. RREB1 is weakly expressed in Koller's sickle at EGKXIII and the marginal zone at HH4. By HH5 it is strongly expressed in the germinal crescent, lateral plate mesoderm and area opaca. At HH8 it is mainly expressed in the lateral plate mesoderm (Fig. 4.30U-Y).

SCML2 contributes to a polycomb complex involved in transcriptional repression (Bonasio *et al.*, 2014). In the screen it was identified as downregulated, but specific expression was not observed at any stage assessed (Fig. 4.30Z-AD).

SERTAD2 acts at E2F-responsive promoters to integrate PHD or bromodomain-containing transcription factors (Hsu *et al.*, 2001). It was identified as downregulated by a node graft after 9 and 12h, but SERTAD2 transcripts were not detected at the stages assessed (Fig. 4.31A-E).

SMAD6 (Fig. 4.31F-J) is weakly expressed in the anterior edge of the hypoblast at EGKXII-XIII. By HH3-4 it remains in the germinal crescent but is also expressed in the germ wall and early mesoderm. Later it is expressed strongly in the lateral plate mesoderm and extra-embryonic blood islands at HH5-7 and HH8-10 (Vargesson and Laufer, 2001).

SMAD7 (Fig. 4.31K-O) is detected in the area opaca at EGKXII-XIII. At HH3-4 and HH5-7 it is expressed weakly in the germ wall and lateral plate mesoderm. This continues at HH8-10, when it is also expressed in pre-cardiac mesoderm (Vargesson and Laufer, 2001).

SMAD9 (Fig. 4.31P-T) expression is not detected at EGKXII-XIII. By HH3-4 expression is observed in the lateral plate mesoderm and germinal crescent and this continues at HH5-7. By HH8-10, SMAD9 is expressed in the posterior lateral plate and weakly in the neural tube (Zuzarte-Luis *et al.*, 2004).

SMARCA2 is a member of the SWI/SNF family of chromatin modifiers and is highly similar to the brahma protein in *Drosophila* (Goodwin, 1997, Papanayotou *et al.*, 2008). In the

screen it was identified as a downregulated candidate at each time point but expression was not detected at any of the stages assessed (Fig. 4.31U-Y).

TBX3 (Fig. 4.31Z-AD) is expressed strongly in the hypoblast at EGKXII-XIII and the germ wall at HH3-4. Later it is expressed strongly in the area opaca and embryonic lateral plate mesoderm at HH5-7 and HH8-10, but remains absent from neural territories (Isaac *et al.*, 1998).

TFAP2A (Fig. 4.32A-E) is strongly expressed at all stages assessed. At EGKXII-XIII and HH3-4 it is only expressed in the area opaca. Later, expression shifts to non-neural ectoderm as well as the neural plate border and pre-placodal region at HH5-7 and the neural folds at HH8-10 (Khudyakov and Bronner-Fraser, 2009).

TFAP2C (Fig. 4.32F-J) is expressed in the epiblast and prospective neural plate at EGKXII-XIII and HH3-4 respectively. Then, its expression shifts to the non-neural ectoderm, neural plate border and neural folds at HH5-7 and HH8-10 (Qiao *et al.*, 2012).

TFAP2E also belongs to the AP2 family of transcription factors (Tummala *et al.*, 2003). It is identified in the screen as downregulated at each time point. Expression of TFAP2E is not observed at EGKXIII or HH4. By HH5 it is expressed at a low level throughout the embryo but more strongly in the lateral plate mesoderm. This continues at HH8 when it is also expressed in the dorsal neural folds (Fig. 4.32K-O).

TFCP2L1 contains a region coding for a CP2 domain and is related to the grainyhead family of transcription factors (Rodda *et al.*, 2001). It was identified as downregulated at each time point in the screen. Specific expression could not be detected at EGKXIII, but by HH4 it is weakly expressed in the neural plate. At HH6 and HH8+ expression is completely absent from the embryo itself and is expressed only in the area opaca (Fig. 4.32P-T).

TRIM3 is a member of the tripartite motif (TRIM) family which has three zinc-binding domains (El-Husseini and Vincent, 1999). In the screen it is consistently downregulated. Expression could not be detected at EGKXIII by in situ hybridisation. However, it is upregulated in the prospective neural plate at HH4, the neural plate at HH6 and neural tube HH8+ but is also ubiquitously expressed at low levels in other tissues (Fig. 4.32U-Y).

VGLL1 binds TEA domain family of transcription factors through a vestigial homology domain to function as a TEF co-activator (Vaudin *et al.*, 1999). VGLL1 was identified in the

screen as downregulated at each time point. Specific expression is not detected at EGKXIII or at HH8+. At HH4 and HH5 it is completely absent from embryonic tissue and is expressed only in the area opaca (Fig. 4.32Z-AD).

WWTR1 is a transcriptional co-activator which functions as a downstream regulatory target of the Hippo signalling pathway (Kanai *et al.*, 2000, Di Palma *et al.*, 2009). In the screen it is identified as downregulated at each time point, however specific expression could not be detected at any of the stages assessed (Fig. 4.33A-E).

ZBTB46 is a zinc finger transcription factor (Meredith *et al.*, 2012). It was identified as downregulated after 9 and 12h in the screen. Non-specific expression was observed at EGKXIII and only weak expression in the prospective neural plate at HH4. This continues in the neural plate at HH6 and by HH8 it is expressed weakly throughout the neural tube but also in the extra-embryonic mesoderm and blood islands (Fig. 4.33F-J).

ZFHX3 encodes a transcription factor with multiple homeodomains and zinc finger motifs (Berry *et al.*, 2001, Mori *et al.*, 2007). It was identified as consistently downregulated in the screen. In the embryo, expression is only observed at HH8+ when it is ubiquitously expressed but is more strongly expressed in the lateral plate mesoderm (Fig. 4.33K-O).

ZFPM1 protein can either activate or repress transcription by functioning as a cofactor for GATA proteins (Freson *et al.*, 2003). It was identified as a downregulated candidate at each time point of the screen. Specific expression could not be observed at EGKXIII. At HH4 and HH6 it is expressed in the germinal crescent and lateral plate mesoderm and is specifically absent from neural territories. By HH9 it is also detected in the blood islands (Fig. 4.33P-T).

ZMYND11 encodes a protein with a PHD finger and bromodomain, which functions as a transcriptional repressor (Masselink and Bernards, 2000, Velasco *et al.*, 2006). It was identified as a downregulated candidate at each time point in the screen however expression was not observed at any of the stages evaluated (Fig. 4.33U-Y).

ZNF185 encodes a LIM-domain zinc finger protein (Heiss *et al.*, 1997). It was found to be downregulated at each time point in the screen and in situ hybridisation reveals broad expression throughout the embryo at all stages assessed (Fig. 4.33Z-AD).

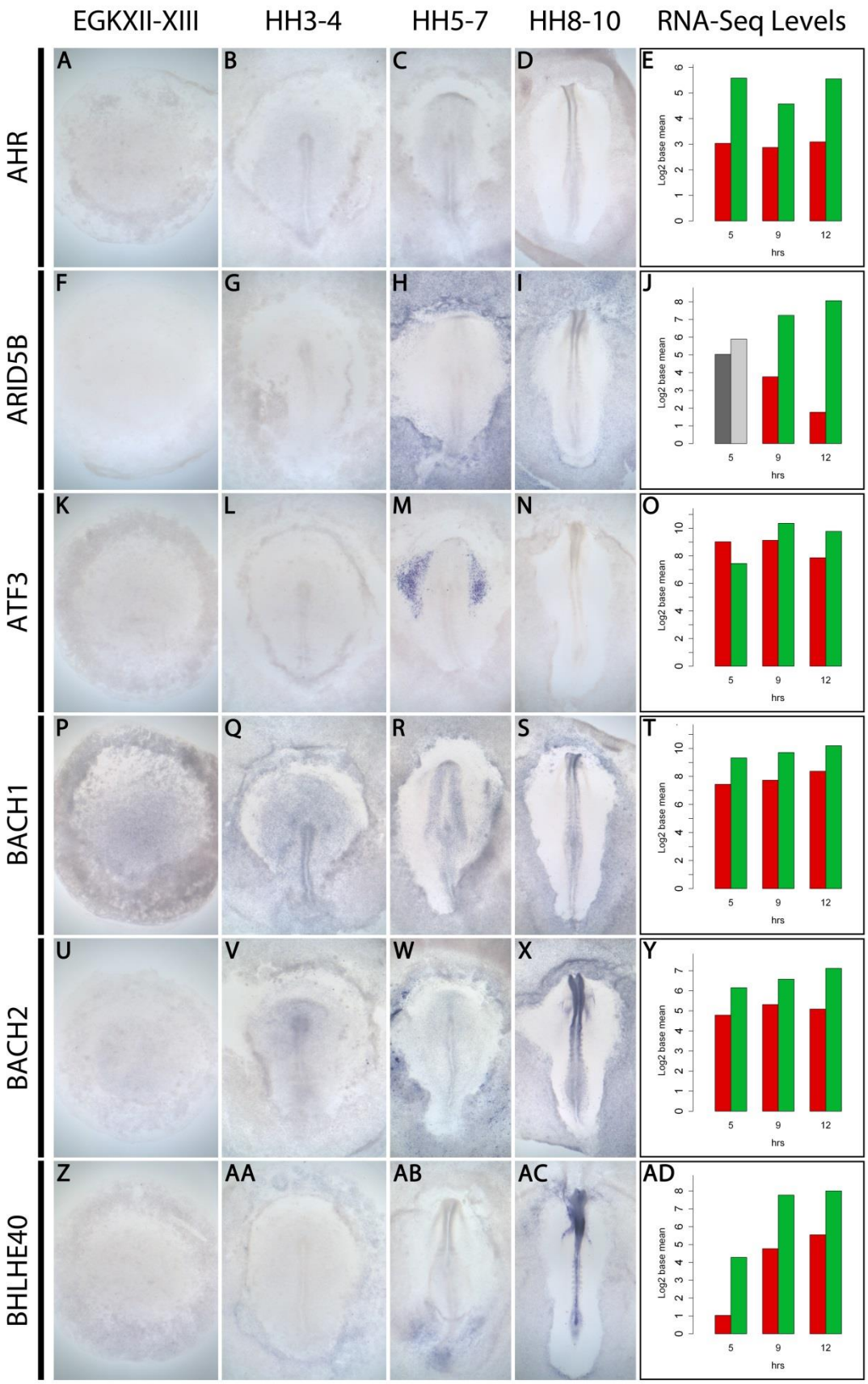

Figure 4.20: Expression of AHR, ARID5B, ATF3, BACH1, BACH2 and BHLHE40.

The expression of downregulated markers was assessed by in situ hybridisation at four key stages: pre-streak at EGKXII-XIII (A, F, K, P, U, Z), during gastrulation at HH3-4 (B, G, L, Q, V, AA), at neural plate stages HH5-7 (C, H, M, R, W, AB) and neural tube stages HH8-10 (D, I, N, S, X, AC). Expression patterns are compared to the absolute transcript counts as quantified by the RNA-Seq screen (E, J, O, T, Y, AD). Expression levels at each time point are plotted as bar graphs of $\log_2$ of the base mean for induced (red or dark grey) and uninduced (green or light grey) tissues at each time point. Where columns are coloured red and green, induced and uninduced values differ by at least $\log_2$ 1.2 and markers are differentially expressed. Columns coloured dark and light grey distinguish when markers are not differentially expressed.

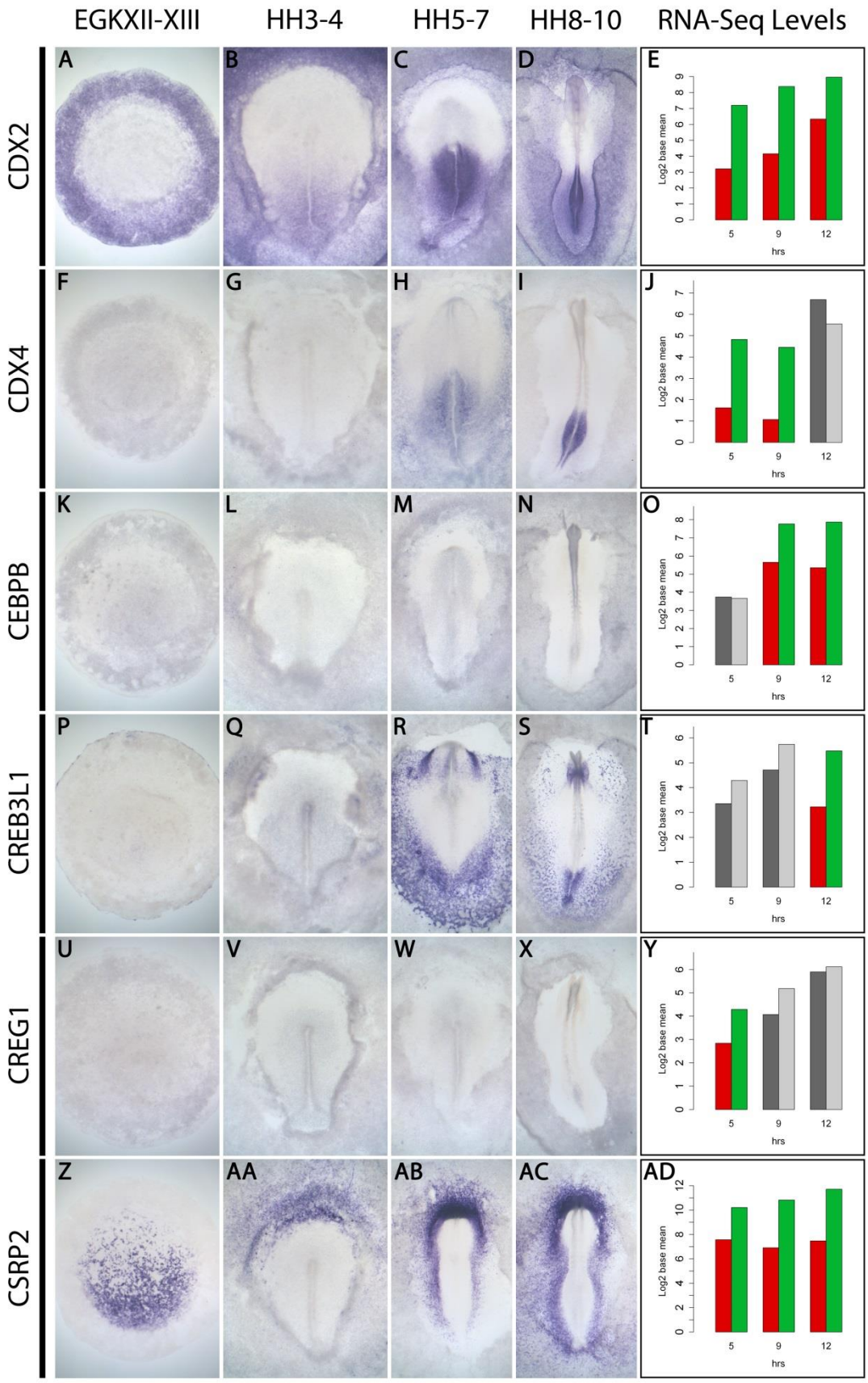

Figure 4.21: Expression of CDX2, CDX4, CEBPB, CREB3L1, CREG1 and CSRP2.

For details, see Fig. 4.20.

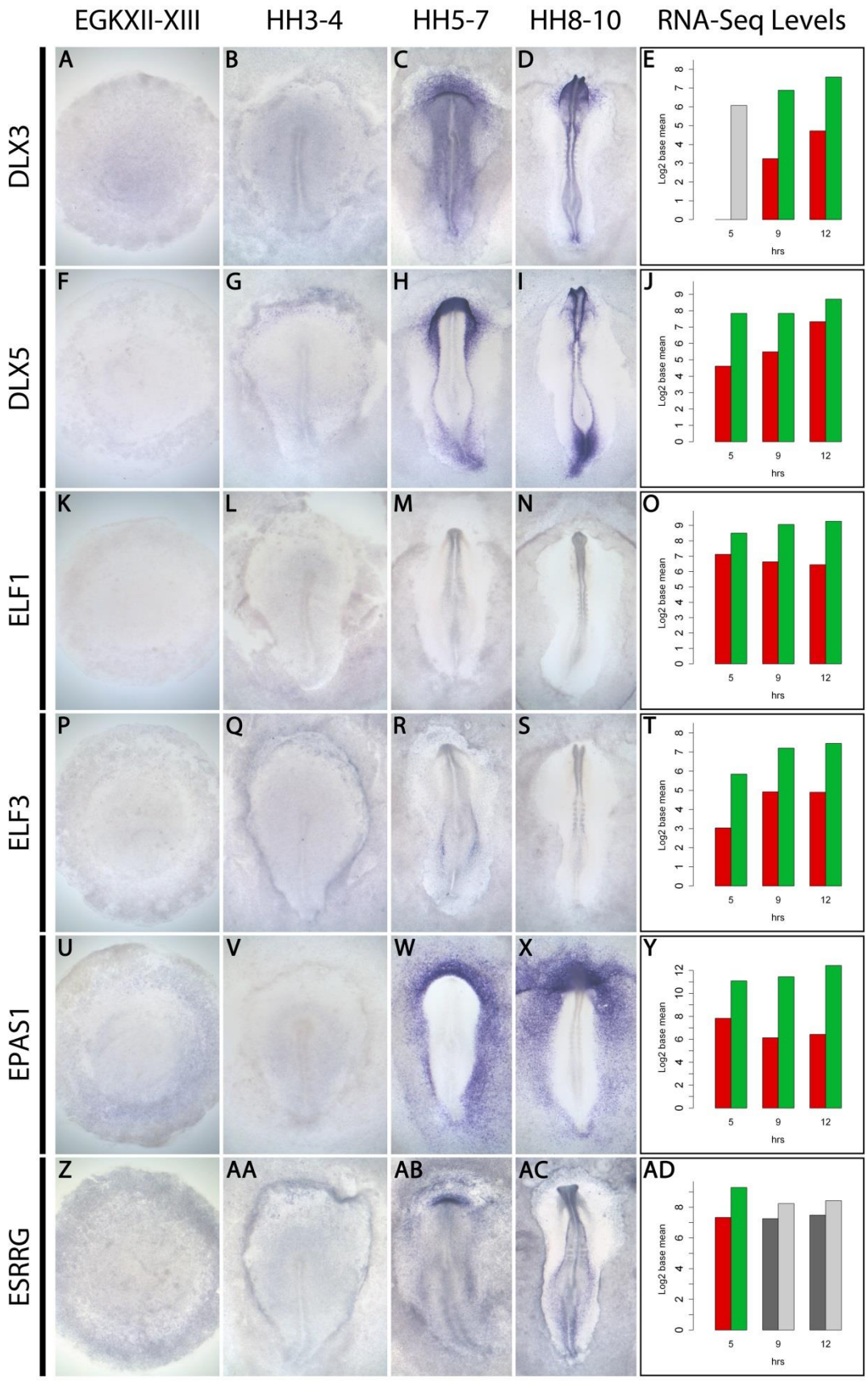

Figure 4.22: Expression of DLX3, DLX5, ELF1, ELF3, EPAS1 and ESRRG.

For details, see Fig. 4.20.

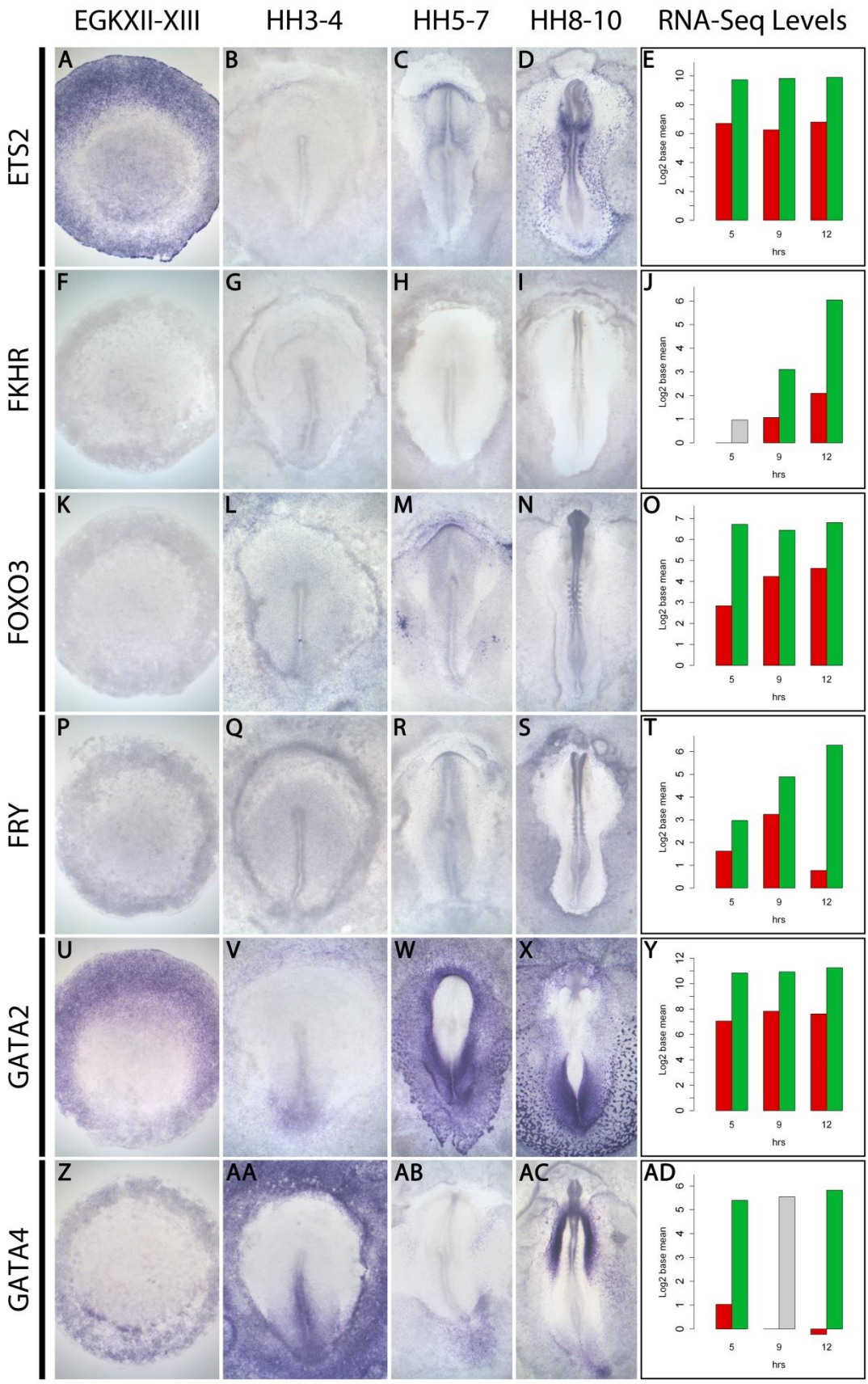

Figure 4.23: Expression of ETS2, FKHR, FOXO3, FRY, GATA2 and GATA4.

For details, see Fig. 4.20.

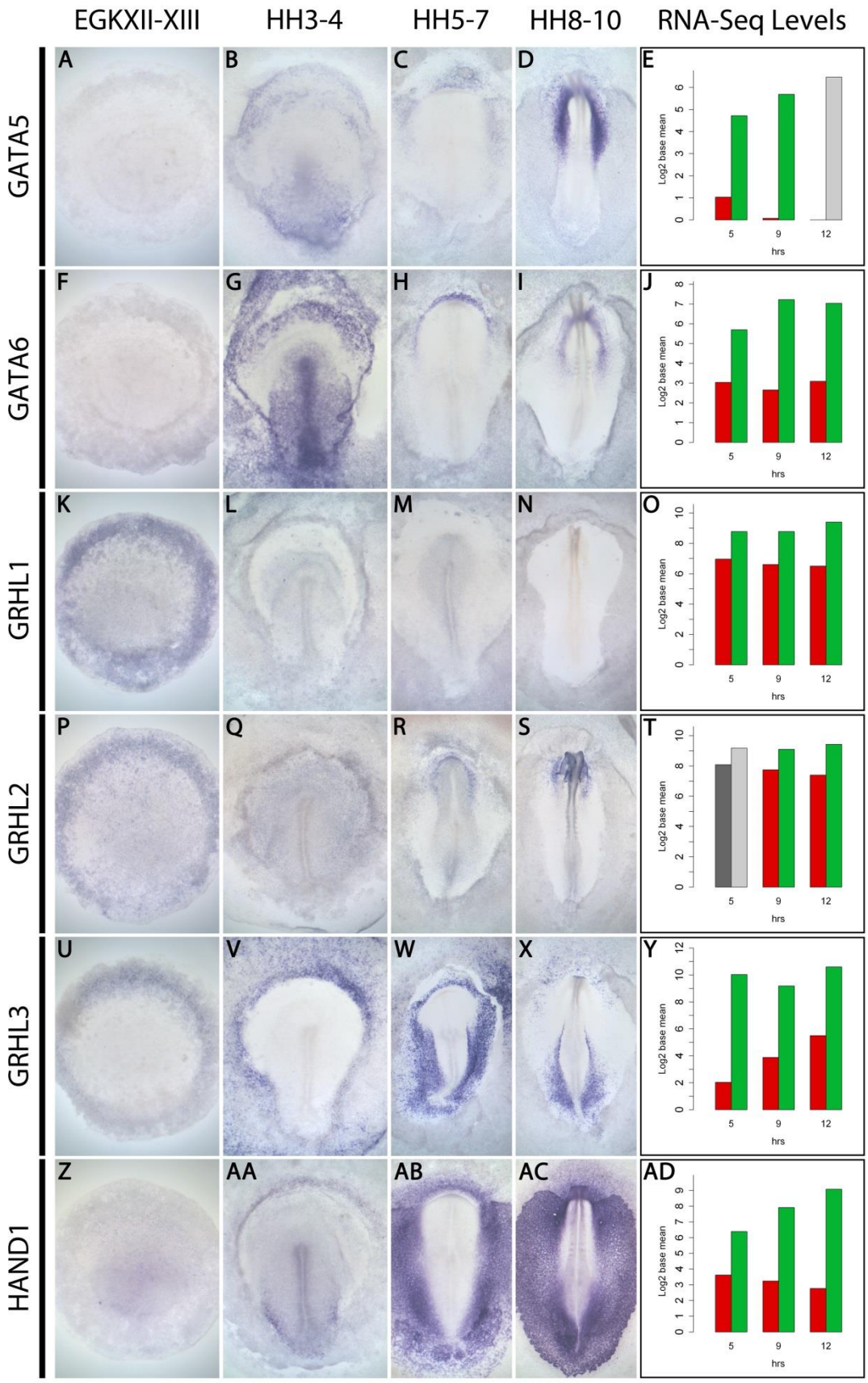

Figure 4.24: Expression of GATA5, GATA6, GRHL1, GRHL2, GRHL3 and HAND1.

For details, see Fig. 4.20.

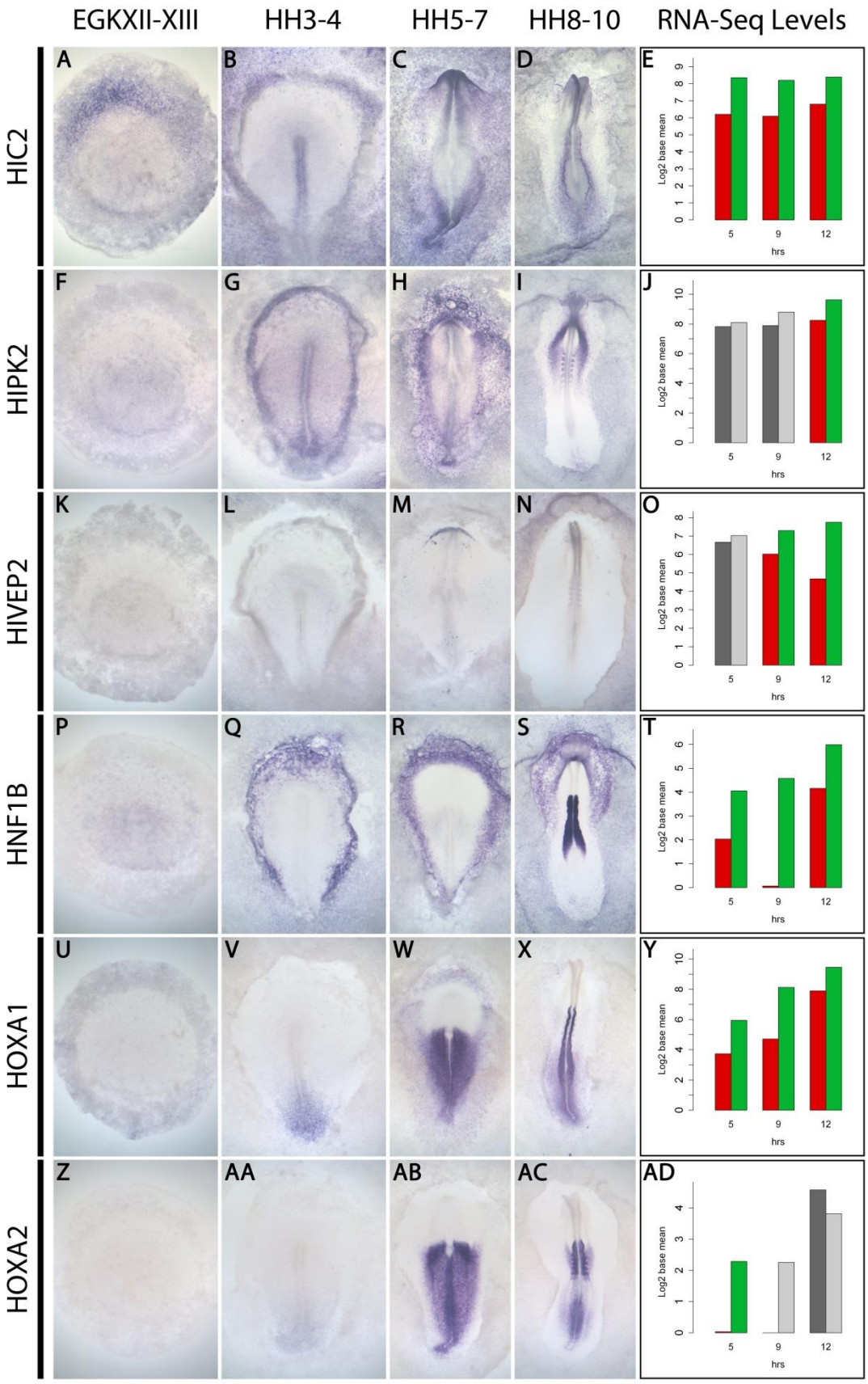

Figure 4.25: Expression of HIC2, HIPK2, HIVEP2, HNF1B, HOXA1 and HOXA2.

For details, see Fig. 4.20.

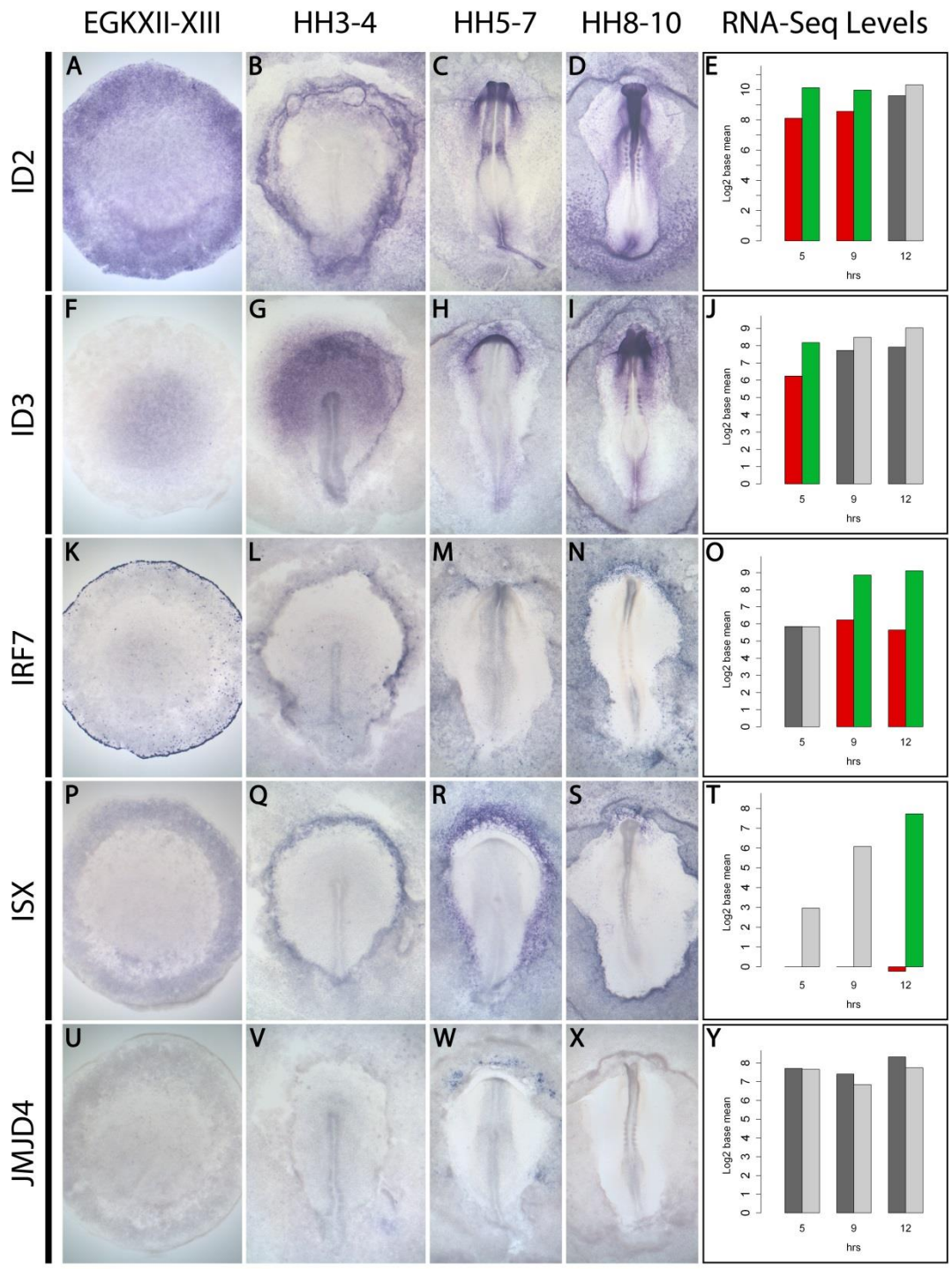

Figure 4.26: Expression of ID2, ID3, IRF7, ISX and JMJD4.

For details, see Fig. 4.20.

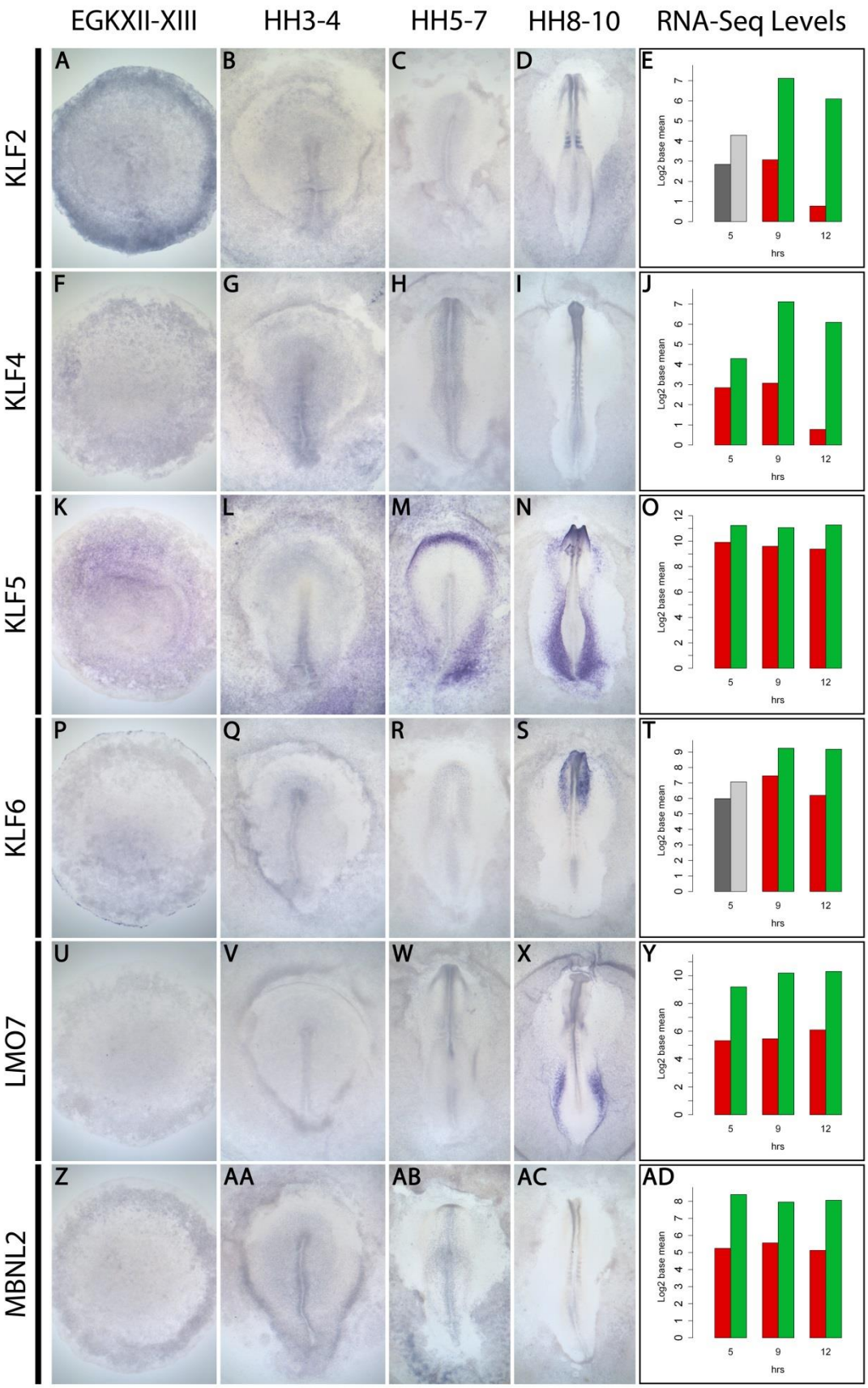

Figure 4.27: Expression of KLF2, KLF4, KLF5, KLF6, LMO7 and MBNL2.

For details, see Fig. 4.20.

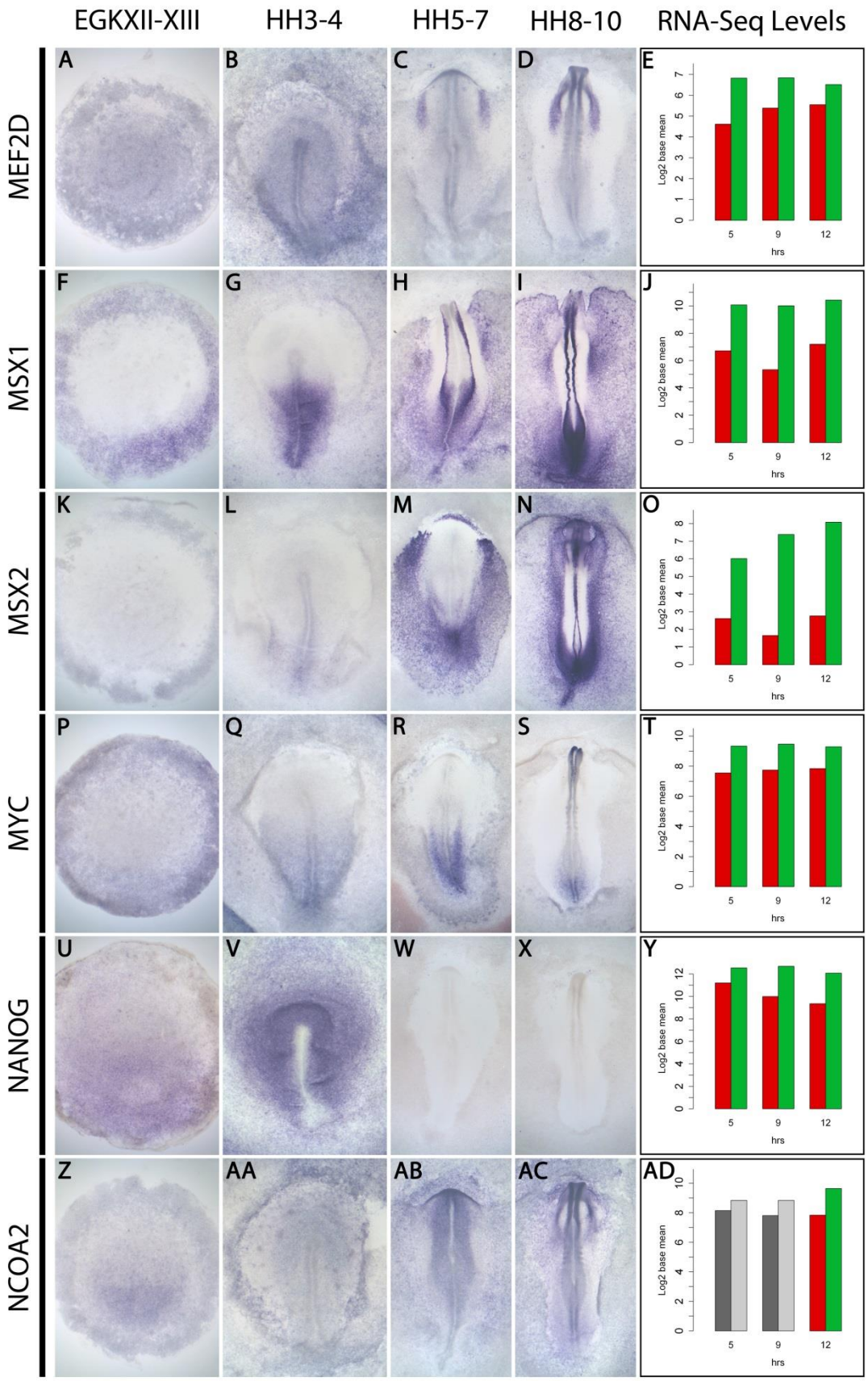

Figure 4.28: Expression of MEF2D, MSX1, MSX2, MYC, NANOG and NCOA2.

For details, see Fig. 4.20.

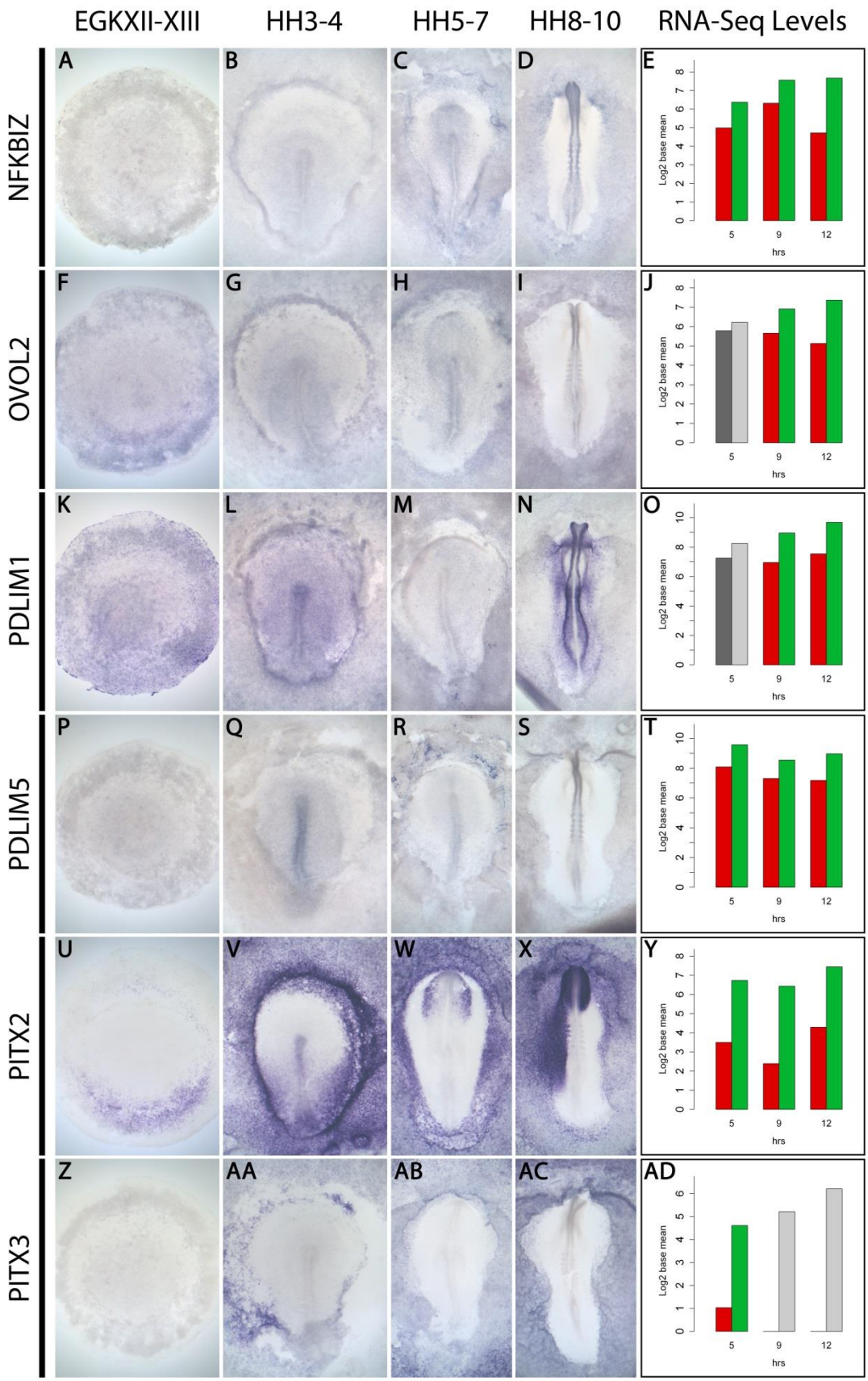

Figure 4.29: Expression of NFKBIZ, OVOL2, PDLIM1, PDLIM5, PITX2 and PITX3.

For details, see Fig. 4.20.

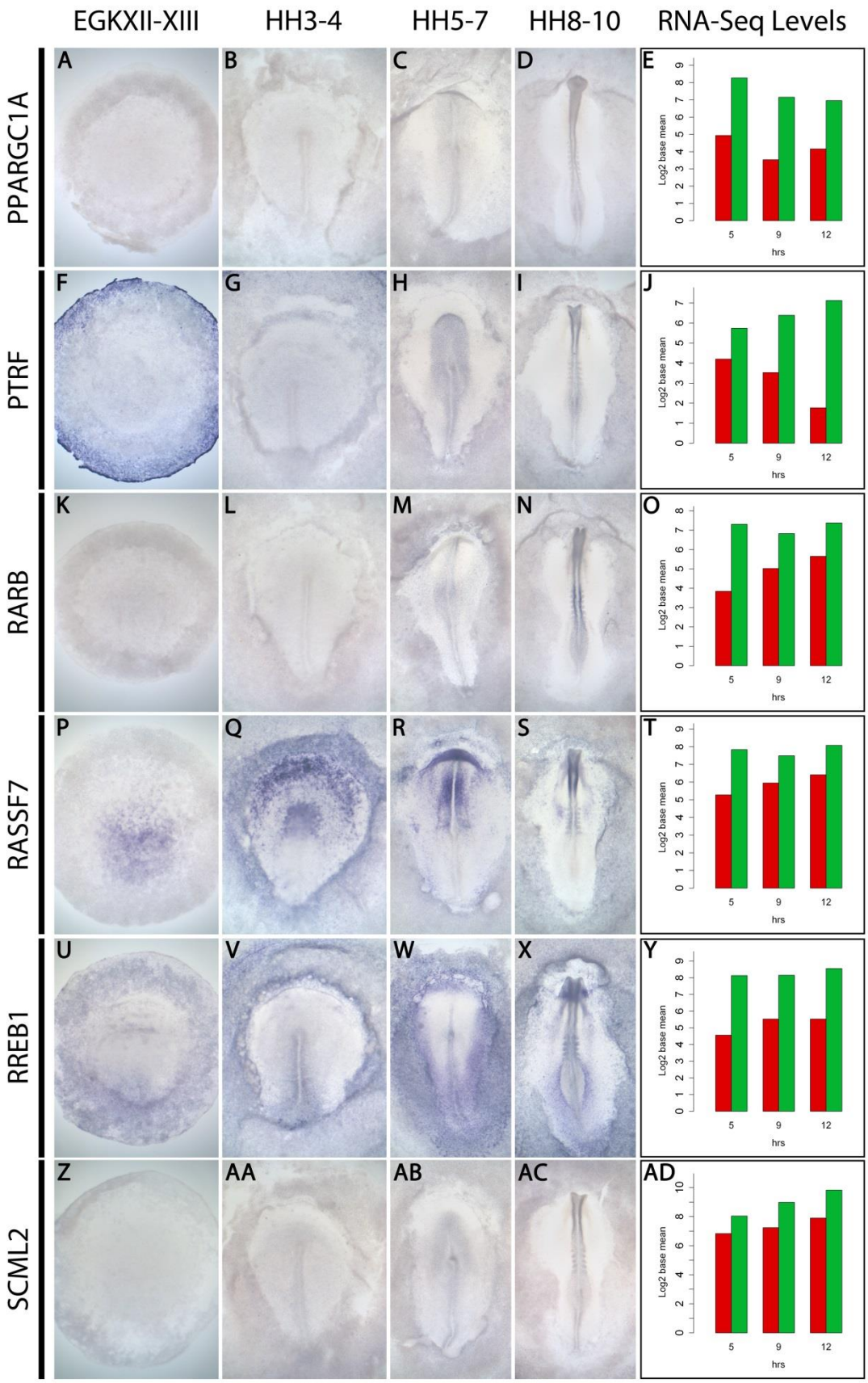

Figure 4.30: Expression of PPARGC1A, PTRF, RARB, RASSF7, RREB1 and SCML2.

For details, see Fig. 4.20.

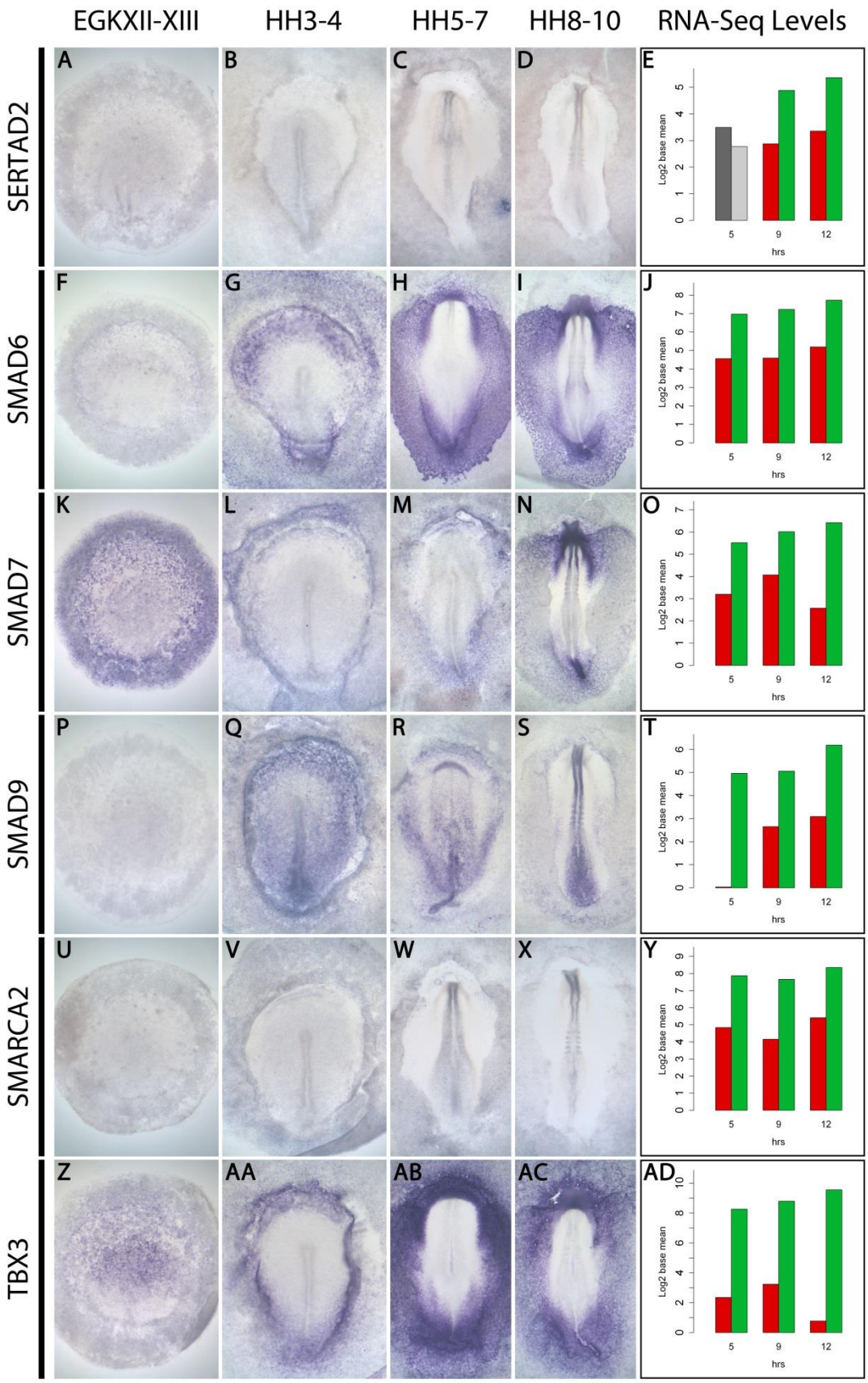

Figure 4.31: Expression of SERTAD2, SMAD6, SMAD7, SMAD9, SMARCA2 and TBX3.

For details, see Fig. 4.20.

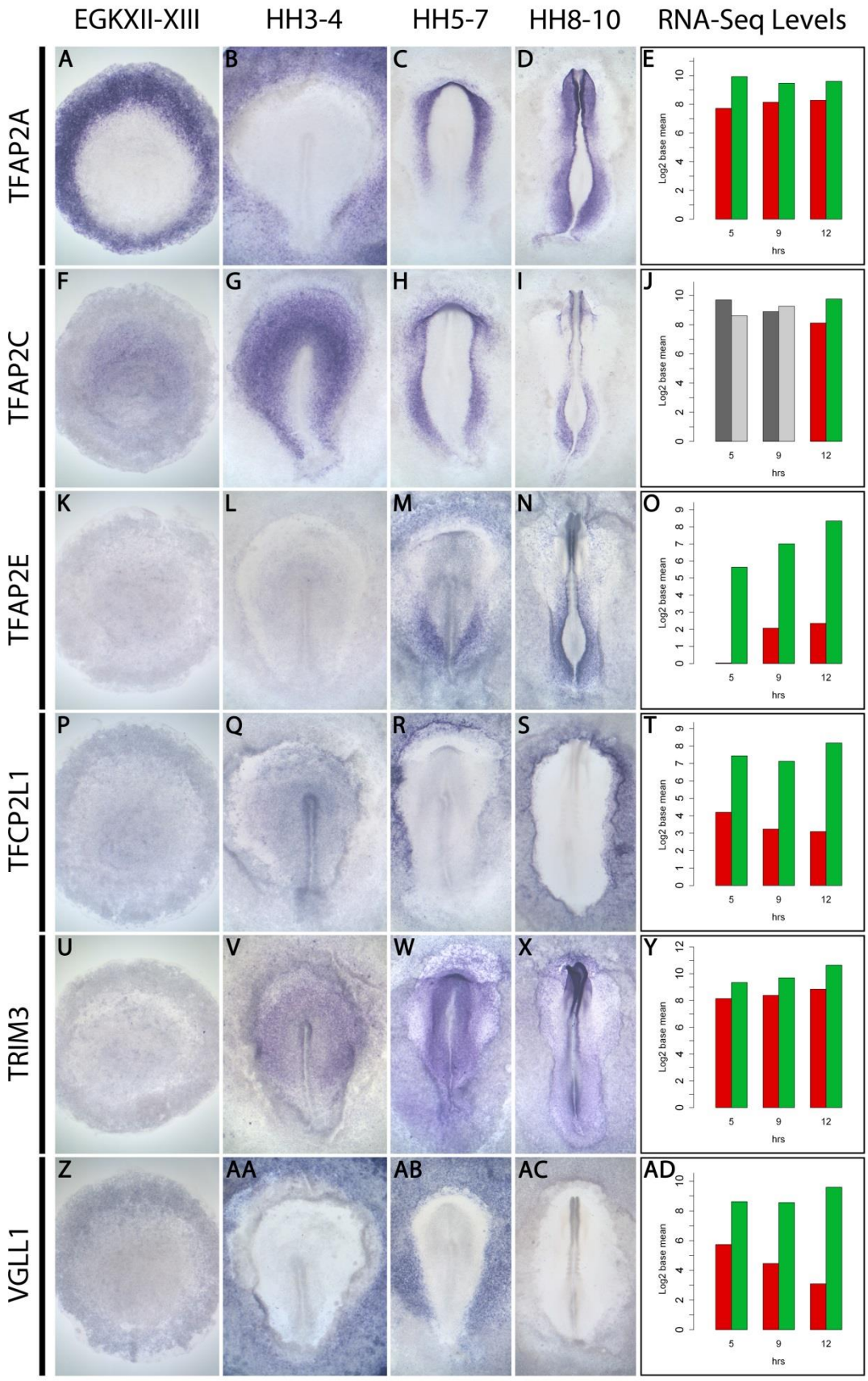

Figure 4.32: Expression of TFAP2A, TFAP2C, TFAP2E, TFCP2L1, TRIM3 and VGLL1.

For details, see Fig. 4.20.

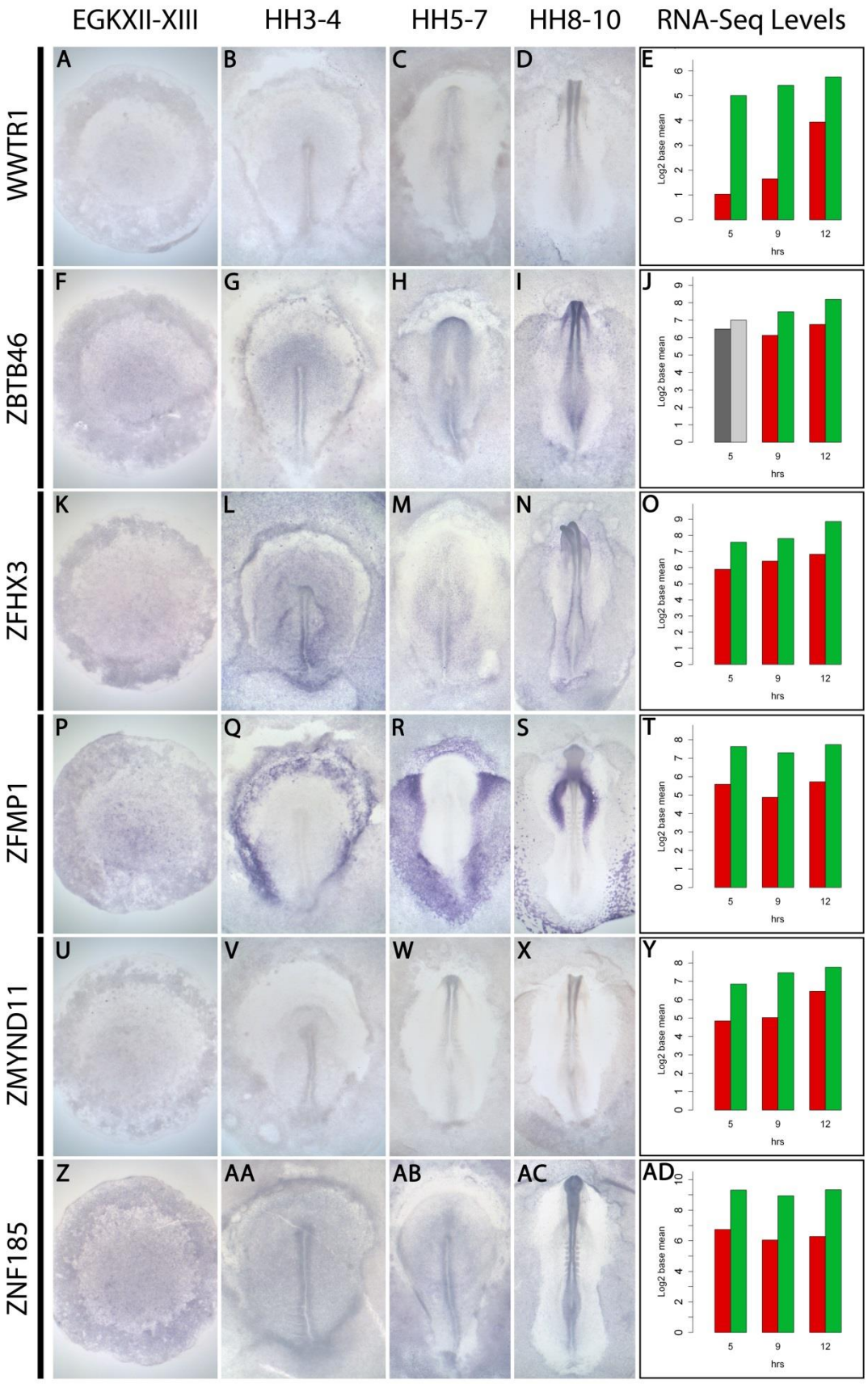

Figure 4.33: Expression of WWTR1, ZBTB46, ZFHX3, ZFPM1, ZMYND11 and ZNF185.

For details, see Fig. 4.20.

4.3.4.3 Summarising the normal expression of differentially expressed transcriptional regulators

Generally, the screen has identified markers with the types of expression patterns we would expect as responses to neural induction. Upregulated genes are expressed in prospective neural tissue at some stage during early neural development in the embryo. Some, like SOX11 (Fig. 4.16K-O) and SOX13 (Fig. 4.16P-T) are expressed at all stages, while others such as ZNF423 (Fig. 4.19P-T) or LHX5 (Fig. 4.11F-J) are absent from the epiblast and prospective neural plate at EGKXIII and HH4 but are expressed later in the neural plate proper.

In contrast, the expression of downregulated genes tends to be more varied. Often these are expressed in various non-neural tissues. Examples include ZFPM1 (Fig. 4.33P-T) which is expressed strongly in the lateral plate mesoderm and extra-embryonic blood islands. GRHL3 (Fig. 4.24U-Y) is absent from the neural plate, neural plate border and pre-placodal region but is expressed strongly in the surrounding embryonic ectoderm. ISX is consistently downregulated in the screen and its expression is detected only in the area opaca (Fig. 4.26P-T). Despite these differences, a common theme among downregulated candidates, is that they tend to be relatively absent from neural tissue as compared to neighbouring regions.

Moreover, candidate expression is generally detected at stages corresponding to the time points predicted by the screen. Markers upregulated across each time point such as NSD1 (Fig. 4.13Z-AD), SETD2 (Fig. 4.15K-O) and ZIC3 (Fig. 4.19K-O) are first expressed prior to gastrulation in the epiblast at EGKXIII, and their expression persists later in the prospective neural plate, neural plate proper and neural tube. These contrast with genes such as ERNI (Fig. 4.8A-E), CITED4 (Fig. 4.6U-Y), PRDM1 (Fig. 4.14P-T) and MAFA (Fig. 4.12A-E), which are upregulated only after 5h and are expressed stronger in the epiblast and prospective neural plate than in the neural plate from HH6 onwards. Alternatively, LHX5 (Fig. 4.11F-J) and ZNF423 (Fig. 4.19P-T) are only upregulated at later time points and are absent from the early embryo, but expressed in the neural plate at later stages. Therefore candidates tend to be normally expressed in the appropriate space and time, based on their predicted responses to neural induction by a grafted node.

However not all candidates demonstrate such clear expression patterns. Some, such as HIVEP3 (Fig. 4.10A-E), KAT2B (Fig. 4.10Z-AD), NFKBIZ (Fig. 4.29A-E) and WWTR1 (Fig. 4.33A-E) appear to be more ubiquitously expressed while others; RFX3 (Fig. 4.14Z-AD), STOX1 (Fig. 4.16Z-AD), AHR (Fig. 4.20A-E) and CREG1 (Fig. 4.21U-Y) are barely detected, if at all. The RNA-Seq screen predicts that these candidates are expressed at absolute levels lower than base mean 128, or 7 $\log_2$. So although they are differentially expressed, it seems that these changes are occurring at

levels which cannot be detected by in situ hybridisation. This is especially clear when compared to robustly expressed candidates such as DNMT3A (Fig. 4.7K-O), SETD2 (Fig. 4.15K-O), CSRP2 (Fig. 4.21Z-AD) and GATA2 (Fig. 4.23U-Y) which were detected by the RNA-Seq at absolute levels higher than 1024 (10 $\log_2$). These observations may also explain some differences between the stage of expression in the embryo and timing of induction in the screen. For example MEIS2 (Fig. 4.12P-T) and GLI2 (Fig. 4.9F-J) are identified as upregulated candidates at each time point, but their expression is not detected early at EGKXIII or HH4 when the RNA-Seq predicts base mean levels less than 64 (6 $\log_2$). Instead transcripts are detected later between HH5-7 and HH8-10 when the absolute expression values increase above 250 (8 $\log_2$) at the 9 or 12h time points.

As a general rule, expression by in situ hybridisation was never detected at base mean levels less than 64 (6 $\log_2$) and was only weakly or rarely detected at base mean levels less than 128 or (7 $\log_2$). Expression was almost always observed when base mean levels were detected above 250-500 (8-9 $\log_2$).

4.4 Discussion

Presented here are the results of an RNA-Seq screen conducted to identify a time-course of responses to neural induction. The most up-to-date Galgal4 analysis revealed 8673 differentially expressed transcriptional responses to neural induction over 5, 9 and 12h. These correspond to 4145 unique genes: 1903 upregulated, 2002 downregulated and 240 that are up and downregulated at different times.

4.4.1 Neural induction is a highly dynamic process

Heat maps representing expression intensity demonstrate that responses to neural induction are highly dynamic in terms of absolute levels (Fig. 4.2, Fig. 4.3 and Fig. 4.4). The RNA-Seq detected transcripts across a wide range of expression levels; ERNI is one of the highest expressed transcripts in the screen and is detected at a base mean induced value of over 15000, compared to the lowest differentially expressed gene MIR1538 which was detected at an induced level of 0.849479697. Therefore the RNA-Seq approach detects expression across a wide dynamic range. Heat maps and Venn diagrams comparing differential expression across the three time points also reveal the dynamic temporal nature of expression (Fig. 4.5). Gene expression varies widely over this time-course; genes can be up- or down-regulated at each time point while others are differentially expressed at some time points but not others. One

particular example is ATF3 (Fig. 4.20K-O) which is upregulated after 5h yet downregulated by 9 and 12h. Therefore the screen reveals more dynamic transcriptional activity during neural induction than was previously appreciated.

4.4.2 The screen predicts spatial expression levels in the normal embryo

To define the progressive specification changes that cells undergo during neural induction, we have focused on 482 differentially expressed transcriptional regulators (Fig. 4.5). The original plan was to confirm the expression of all transcriptional regulators by in situ hybridisation, but the screen detected so many differentially expressed markers that this was not feasible. Therefore, we instead chose to verify a proportion -those calculated as statistically significant.

By picking candidates based on P-value, genes were selected from a wide range of expression levels. At some stage, upregulated candidates are expressed in neural territories while downregulated candidates are relatively absent. Often, where clear in situ expression patterns were not detected, those candidates were predicted to be expressed at lower absolute levels by the screen compared to markers that are more robustly expressed. The clearest in situ expression patterns are those with the highest absolute expression values or greatest differential expression between tissues. The ubiquitous low level in situ staining observed for some markers probably reflects low level transcript expression. The robustness with which we can predict embryonic expression of markers based on their absolute values and the identification of known and anticipated responses to a node graft, suggests that the screen predicts the transcriptional dynamics that accompany early stages of neural development in the embryo. The present findings suggest that the other highly expressed but as yet unverified markers are also likely to be expressed in the embryo.

4.4.3 The screen predicts appropriate temporal expression in the embryo

Many upregulated markers are expressed in neural territories at all stages. However, other markers are expressed with a more dynamic temporal time-course. This was initially confirmed by the detection of SOX3 (Fig. 4.16F-J), SOX2 (Fig. 4.16A-E) and SOX1 (Fig. 4.15Z-AD) as distinct markers of the 5, 9 and 12h time points respectively. By verifying the expression of a broad cohort of markers we demonstrate that this is a more general feature of the screen.

Some markers such as CITED4 (Fig. 4.6U-Y), ERNI (Fig. 4.8A-E), ING5 (Fig. 4.10K-O), and MAFA (Fig. 4.12A-E) are more associated with the earlier stages of neural induction. They are expressed robustly in the epiblast prior to gastrulation and the prospective neural plate, but

later their expression decreases. This characteristic is reflected by the screen which predicts that they are highly expressed initially and lower later. Transcript levels in the pre-gastrula embryo are normally very low and increase as the embryo develops, so this type of expression pattern is highly unusual. In contrast, DMBX1 (Fig. 4.7F-J), HOXB1 (Fig. 4.10F-J), LHX5 (Fig. 4.11F-J), SIX3 (Fig. 4.15P-T) are examples of markers which were only predicted to be expressed at high levels after 9 and 12h -corresponding well with their expression which is only observed later between HH5-10.

This temporal trend is less obvious in downregulated candidates, which have more varied expression patterns and are more consistently differentially expressed across the 3 time points. HOXA2 (Fig. 4.25Z-AD) expression cannot be detected at EGKXII-XIII or HH3-4 when it is predicted to be downregulated. Instead it is expressed in the caudal neural tube, coinciding with it being detected at higher levels in induced tissue after 12h. Conversely, NANOG (Fig. 4.28U-Y) and TFAP2C (Fig. 4.32F-J) expression is absent from the neural plate and neural tube between HH5-10 when they are predicted to be downregulated. Both are expressed in the epiblast and prospective neural plate at EGKXII-XIII and HH3-4 when the RNA-Seq registers high expression values in the 5h induced condition. Therefore the screen not only accurately predicts the spatial expression of differentially expressed markers, but also their expression over time.

4.4.4 Distinct classes of expression pattern imply functional significance

Within our data, up- and downregulated candidates have different functional significance. In neural territories, upregulated candidates probably contribute to progressive neural specification. Downregulated genes tend to be relatively absent from the neural plate as they are often markers of alternative (non-neural) fates. However, they may function normally to repress neural induction. Although we do not investigate the specific function of these markers, it is possible to infer putative functions to groups of markers based on the timing and location of their expression.

The neural induction cascade is defined by the expression of three SOXB1 subgroup transcription factors; SOX3, SOX2 and SOX1 (Uwanogho *et al.*, 1995, Rex *et al.*, 1997, Uchikawa *et al.*, 1999). Each has a distinct temporal expression pattern: SOX3 is induced within 3h, SOX2 after 9h and SOX1 after 12h. As such, they are associated with different phases of neural induction: SOX3 marks a pre-neural state, SOX2 marks definitive neural specification, while SOX1 expression coincides with commitment to the neural fate (Pinho *et al.*, 2011). The screen successfully identifies these markers at the appropriate times as well as two previously

unappreciated members the SOXC and SOXD subgroups; SOX11 (Fig. 4.16K-O) and SOX13 (Fig. 4.16P-T) respectively. They are induced at each time point and are expressed strongly throughout neural induction. SOX11 has been implicated in nervous system development via its expression in older embryos (Uwanogho *et al.*, 1995). Furthermore, SOX11 homozygous knock-out mice display neonatal lethality and abnormal nervous system development (Bhattaram *et al.*, 2010, Wang *et al.*, 2013). Though neither SOX11 nor SOX13 has been studied directly in relation to neural induction, their expression at all relevant stages, suggests that they may have important roles in the process.

Also expressed strongly at all stages are many chromatin remodelling factors including DNMT3A (Fig. 4.7K-O), DNMT3B (Fig. 4.7P-T), SETD2 (Fig. 4.15K-O), NSD1 (Fig. 4.13Z-AD), BMI1 (Fig. 4.6A-E), KDM4A (Fig. 4.11A-E) and MTA1 (Fig. 4.12U-Y). They are upregulated after 5h and are already strongly expressed in the pre-streak epiblast, suggesting that they may be among some of the earliest induced genes. Since chromatin modifiers exert global control over chromatin structure and activity, and since some (such as Brahma) have been implicated in the regulation of the timing of SOX2 expression, together with ERNI and Geminin (Papanayotou *et al.*, 2008), it is reassuring that they are expressed early, when they may control the initial transition from non-neural to neural specification. Such genes and the signals that induce them will be critical in launching the neural induction programme. Given their similarity to ERNI and SOX3 in terms of timing and location of expression (Streit *et al.*, 2000), it is possible that they also function together with Brahma/Geminin/ERNI, and may also be co-regulated by FGF signals.

ERNI-like genes represent another class of markers. Although ERNI and SOX3 are expressed in the epiblast at EGKXII-XIII and prospective neural plate at HH3-4, later their expression diverges. SOX3 remains in the neural plate while ERNI is downregulated and expression shifts to the neural plate border and pre-placodal region by HH6 (Streit *et al.*, 2000). Since ERNI and SOX3 are co-expressed in the epiblast at EGKXIII (Streit *et al.*, 2000), it has been suggested that the neural plate and its border might derive from a common pre-neural state (Streit, 2008). Within the screen, CITED4 (Fig. 4.6U-Y) (Andrews *et al.*, 2000) and PRDM1 (Fig. 4.14P-T) (Riddle *et al.*, 1995) respond in the same way to a node graft as ERNI and are also upregulated only after 5h. Although TFAP2C (Fig. 4.32F-J) (Qiao *et al.*, 2012), was identified only as a downregulated candidate after 9 and 12h, it too is mildly upregulated after 5h in induced tissue. The ERNI-like expression patterns of these genes further reinforces the idea that a state common to the neural plate and its border already exists is the early embryo (Linker *et al.*, 2009) and that induction of this state might be one of the first responses to neural inducing signals.

Other markers display more SOX2-like expression patterns, where they are absent at EGKXIII and HH3-4, but are expressed in the neural plate from around HH5 onwards. Examples include the hedgehog pathway targets GLI2 (Fig. 4.9F-J) and GLI3 (Fig. 4.9K-O) (Marigo *et al.*, 1996, Schweitzer *et al.*, 2000) and the SMAD interacting proteins ZEB2 (Fig. 4.19A-E) (Postigo *et al.*, 2003, van Grunsven *et al.*, 2007) and ZNF423 (Fig. 4.19P-T) (Hata *et al.*, 2000).

Other distinct markers induced after 9h are LMO1, TRIM9 and LHX5. At HH6, LHX5 (Fig. 4.11F-J) is expressed in the anterior neural plate and extends broadly to encompass the PPR. At this stage its expression is highly reminiscent of OTX2 (Bally-Cuif *et al.*, 1995) and SIX3 (Bovolenta *et al.*, 1998), which are also upregulated at the 9h time point. As such, these markers are appropriately expressed to be involved in conferring anterior neural and PPR identity. Conversely, LMO1 (Fig. 4.11U-Y) is expressed exclusively in the neural plate and is markedly absent from the anterior border/PPR domain. Similarly, TRIM9 is absent from the neural plate's anterior lateral edges (Fig. 4.18P-T). Many neural markers including SOX2 (Fig. 4.16A-E) (Rex *et al.*, 1997) and OTX2 (Fig. 4.14A-E) (Bally-Cuif *et al.*, 1995) are commonly expressed in the neural plate as well as the neural border and PPR. Therefore, LMO1/TRIM9-like and ERNI-like markers could be important specifiers separating neural plate from border derived fates.

The diverse range of expression patterns for downregulated genes and their absence from the neural plate makes it more difficult to speculate on the roles of these candidates. Some, such as VGLL1 (Fig. 4.32Z-AD), PITX3 (Fig. 4.29Z-AD) and ARID5B (Fig. 4.20F-J) are only expressed in the area opaca. Others including EPAS1 (Fig. 4.22U-Y) (Ota *et al.*, 2007) and RREB1 (Fig. 4.30U-Y) are strongly expressed in embryonic non-neural ectoderm. Another new marker of this state is GRHL3 (Fig. 4.24U-Y), whose expression perfectly borders all neural territories at HH5 and HH8.

These differ from other downregulated markers such as DLX5 (Fig. 4.22F-J) (McLarren *et al.*, 2003), GRHL2 (Fig. 4.24P-T), GATA2 (Fig. 4.23U-Y) (Sheng *et al.*, 2003), MSX1 (Fig. 4.28F-J) (Suzuki *et al.*, 1991), MSX2 (Fig. 4.28K-O) (Brown *et al.*, 1997), TFAP2A (Fig. 4.32A-E) (Khudyakov and Bronner-Fraser, 2009) and HIC2 (Fig. 4.25A-E), which are expressed in the neural plate border or its derivatives the PPR, neural folds and neural crest. Given that so many markers are common to the neural plate and neural plate border, the downregulation of border and non-neural ectoderm specific markers in the neural plate could be the major mechanism separating neural border from neural plate fates (Streit, 2004).

4.4.5 Which signals might be responsible for inducing these responses?

This time-course of new responses now provides the opportunity to identify the signals that regulate them. The specific contribution of signalling pathways has not been assessed here. However it has been possible to extract transcriptional readouts of pathways known to be required for neural induction, and some not previously considered.

FGF signalling has previously been implicated in the onset of neural induction by inducing the earliest neural markers ERNI and SOX3 (Streit *et al.*, 2000). We now find that these are not the only FGF responses identified within the first 5h of a node graft. The FGF signalling targets SPRY1 and SPRY2 (Minowada *et al.*, 1999) are consistently upregulated. Furthermore the transcriptional regulators ETV4 and ETV5 are also regulated by FGF signalling (Lunn *et al.*, 2007) and are similarly upregulated over 5, 9 and 12h. Therefore, the screen provides further evidence of the prominence of FGF signalling throughout neural induction.

BMP inhibition has long been championed as the neural inducing signal by the "default model" (Lamb *et al.*, 1993, Hemmati-Brivanlou *et al.*, 1994, Sasai *et al.*, 1995, Hemmati-Brivanlou and Melton, 1997). We confirm that targets of BMP signalling; GATA2 (Sheng *et al.*, 2003), MSX1 (Suzuki *et al.*, 1991), SMAD6 and SMAD7 (Vargesson and Laufer, 2001) are consistently downregulated. Previous work suggests that chick ectodermal cells are insensitive to BMP signalling until they have received 5h of signals from an organizer graft (Streit *et al.*, 1998) and that BMP inhibition does not induce the earliest neural responses ERNI and SOX3 (Streit *et al.*, 2000). BMP inhibition appears to be important to downregulate border and non-neural ectoderm markers including DLX5 (McLarren *et al.*, 2003), GATA2 (Sheng and Stern, 1999), MSX1 (Suzuki *et al.*, 1991) and MSX2 (Brown *et al.*, 1997). It remains to be tested whether it induces *de novo* transcription of neural markers and if so, at what time.

WNT inhibition has also been implicated in neural induction by allowing the ectoderm to respond to FGF signals, a response suggested to be under negative regulation by WNTs (Wilson and Edlund, 2001). This implies that WNT signalling has an important early role in the process. Accordingly, the WNT antagonists SFRP1 and FRZB (Ladher *et al.*, 2000) are consistently upregulated while the endogenous WNT reporter AXIN2 (Quinlan *et al.*, 2009) is downregulated. This suggests overall dampening of the WNT pathway throughout neural induction.

Retinoic acid has also been associated with the induction of early neural responses. NOT1 and NOT2 are regulated by retinoic acid signalling from the hypoblast (Knezevic *et al.*, 1995, Knezevic and Mackem, 2001) while CYP26A1 which can be induced by retinoic acid, is expressed in the prospective neural plate (Swindell *et al.*, 1999, Albazerchi and Stern, 2007).

Appropriately then, NOT1 and NOT2 are upregulated in the screen at each time point, while CYP26A1 and RAI1, are induced but only after 9 and 12h. This might suggest that retinoic acid makes a greater contribution to neural induction at later stages when its levels are higher. However, CYP26A1 can also be induced by FGF signalling (Wahl *et al.*, 2007), WNT or FGF inhibition (Kudoh *et al.*, 2002) and Notch (Echeverri and Oates, 2007) so its expression may not necessarily reflect the presence of retinoic acid. RARB (Cui *et al.*, 2003), a more specific retinoic acid target (Olivera-Martinez and Storey, 2007) is consistently downregulated perhaps indicating that retinoic acid signalling is restricted. This is quite possible as it could be antagonised by persistent FGF signalling (Diez del Corral and Storey, 2004, Olivera-Martinez and Storey, 2007) throughout the time-course.

Notch signalling is known to contribute to neural crest development (Kintner, 1992, Cornell and Eisen, 2002, Endo *et al.*, 2002, Glavic *et al.*, 2004) and the observation that homeogenetic signals travel between BMP-inhibited cells has previously implicated Notch signalling in neural induction (Linker *et al.*, 2009). Furthermore, ES cells do not differentiate into neurons when Notch signalling is blocked, suggesting that Notch promotes either neural specification or differentiation (Lowell *et al.*, 2006). Consistent with this, upregulation of the Notch pathway modifier LFNG is detected at each time point.

Calcium signalling has also been implicated in neural induction. Calcineurin integrates FGF and BMP signalling (Cho *et al.*, 2014), while the calcium channel modulator Calfacilitin increases intracellular calcium levels and is required for SOX2 and Geminin expression (Papanayotou *et al.*, 2013). Furthermore, Calreticulin, a calcium binding protein, has been identified from a screen for secreted factors from the Hensen's node (Marta de Almeida, 2012). Here we find that the transcription factor ATF3, a direct target of the calcium activated cAMP response element binding protein (Zhang *et al.*, 2011, Ahlgren *et al.*, 2014), is upregulated after 5h but downregulated later. These various observations do not clarify the precise role of Calcium in neural induction, but it seems possible that it is involved in multiple events, at different times.

Despite the role of Sonic hedgehog (SHH) in patterning the neural tube (Chiang *et al.*, 1996, Patten and Placzek, 2000, Dessaud *et al.*, 2007, Dessaud *et al.*, 2008), to date, the hedgehog pathway has been given little consideration in terms of neural induction. The receptors PTCH2 and PTCH1 are direct targets of hedgehog signalling (Pearse *et al.*, 2001) and are upregulated at each time point in the screen. Furthermore, the transcription factors and hedgehog targets GLI2 (Schweitzer *et al.*, 2000) and GLI3 (Marigo *et al.*, 1996) are similarly upregulated. Their expression is detected by in situ hybridisation at HH5, which positions them closer to the 9h time point. Furthermore, SHH is first expressed in Hensen's node around HH4 (Levin *et al.*,

1995), coinciding with the onset of SOX2 expression around Hensen's node in the definitive neural plate (Rex *et al.*, 1997). Therefore ligands, receptors and transcriptional targets of the hedgehog pathway are appropriately expressed in the embryo or are induced in our screen, consistent with a role in the relatively late steps of neural induction.

Although a more thorough and functional analysis of signalling readouts in the screen is necessary, it has already been possible to extract basic signalling trends from the RNA-Seq data. Our observations confirm that neural induction is accompanied by early FGF signalling as well as general BMP and WNT inhibition. We also obtained evidence of calcium and retinoic acid modulation and directly associate hedgehog signalling with neural induction. How these pathways function during neural induction remains to be determined, but it will now be possible to test their contributions to the transcriptional responses identified here.

4.4.6 Comparing RNA-Seq to the original 5h neural induction screen

The original 5h screen revealed 10 markers induced by a node graft (Streit *et al.*, 2000, Sheng *et al.*, 2003, Gibson *et al.*, 2011, Pinho *et al.*, 2011, Papanayotou *et al.*, 2013), but results in Chapter 3 demonstrated that these were not the only responses to neural induction. The increased sensitivity of next generation sequencing provided a new opportunity to reassess the effects of grafting a node graft for 5h. RNA-Seq now reveals 1987 genes as differentially expressed at this time point, of which 129 are upregulated and 122 are downregulated transcriptional regulators. We successfully identified ERNI and SOX3 from the original screen (Streit *et al.*, 2000), as well as NOT1, NOT2 (Knezevic *et al.*, 1995, Knezevic and Mackem, 2001) and OTX2 (Bally-Cuif *et al.*, 1995) which were predicted and verified in Chapter 3. Therefore we have identified many new transcriptional regulators at this time point, and for the first time identify responses that are specifically downregulated by a node graft.

Somewhat unexpectedly, ERNI and SOX3 are the only candidates from the original screen common to this new analysis. However other genes from the 5h screen are expressed much weaker than ERNI and SOX3. For example, FTH1 is expressed so weakly that it has not been possible to assess its induction by a node graft (Gibson *et al.*, 2011). Therefore, it seems plausible that the other genes which were not detected (Churchill (Sheng *et al.*, 2003), Calfacilitin (Papanayotou *et al.*, 2013), Dad1, UBII (Gibson *et al.*, 2011), Asterix, Obelix and TRKC (Pinho *et al.*, 2011)) may not be differentially expressed above the stringent threshold fold change used here. Lowering this below 1.2 $\log_2$ causes a substantial increase in the number of transcripts identified as well as the false discovery rate. To focus on the best

markers, we chose to maintain a high threshold cut-off to limit the selection of potential false positives. As a consequence, subtler responses to neural induction have not been selected.

4.4.7 Limitations of the RNA-Seq differential screen

The RNA-Seq screen has identified hundreds of new, relevant responses to neural induction. These are accompanied by appropriate signalling dynamics, suggesting that ectopic induction by a node accurately represents the endogenous process. One benefit of this assay is that the time of grafting represents the beginning of the process, allowing the entire period of neural induction to be studied. By comparing ectopic induction to contralateral uninduced tissue, we have been able to extract differentially expressed markers specific for the process. However this approach has a number of important limitations that should also be considered.

An RNA-Seq protocol was chosen because it has certain advantages compared to microarray analysis. It provides base level resolution and deeper transcriptome coverage and is able to identify specific alleles, splice variants, SNPs and non-coding RNAs (Wang *et al.*, 2009). Also, RNA-Seq is quantitative and measures transcriptome dynamics more accurately, making it ideal for our screen. However it does suffer from biases introduced via RNA fragmentation and amplification, which can preferentially identify shorter transcripts over longer ones (Wang *et al.*, 2009). In addition, by using oligo-dT to extract mRNAs, most microRNAs (which might have regulatory contributions) would not be detected. Despite this, a number of microRNAs did appear in our data, though their expression has not been studied here. Another complication arises from the dependence of RNA-Seq on a reference genome to identify transcripts, as annotation of the chicken genome is currently very incomplete. Although reanalysis of our data with the Galgal4 build identified many more transcripts than Galgal3, some remain unannotated. Fortunately, these data can be reanalysed against future releases of the genome to complete the data set.

Any screen based around differential expression deliberately ignores ubiquitously expressed genes that may function in concert with differentially expressed ones. Despite this, we have identified many new factors that have not been previously associated with neural induction. Lowering the fold change threshold would further increase the number of responses and make it harder to study the overall process. We do not discount that more ubiquitous markers might function during neural induction, but we have chosen to focus on some of the best markers to describe the progression of the neural induction cascade.

An additional caveat of the screen design is created by conducting the differential screen in the area opaca. Although uninduced tissue was used to subtract the effects of culture and identify specific responses to neural induction, the area opaca is not a naïve tissue, and might differ from the embryonic ectoderm where the normal decision to make the neural plate takes place. For example WNTs are expressed throughout the area opaca (Skromne and Stern, 2001). Therefore some markers may be downregulated as re-specification responses, rather than as direct targets of neural induction. These re-specification events are likely to occur soon after a node is grafted and therefore be identified as early as the 5h time point. Conversely, some genes already expressed in the area opaca could be required for neural induction but these will not be identified as being induced.

Other issues arise when comparing the differential expression of markers in the area opaca to their actual expression level in the neural plate. Differentially expressed genes in the screen may function at only marginally upregulated levels in the neural plate while some downregulated genes may still be required but only at slightly lower levels. Therefore some up- and downregulated genes may not be expressed strongly or completely absent from the neural plate. Furthermore, we find that markers present in induced tissue are actually expressed at far higher levels in the embryonic neural plate. This has greater implications for downregulated genes, which were identified because they are expressed at higher levels in the area opaca than in induced tissue. Their normal expression will contradict the screen's predictions if expression in the neural plate proper exceeds that of the area opaca, as appears to be the case with TRIM3 (Fig. 4.32U-Y) and possibly also DLX3 (Fig. 4.22A-E) and ID3 (Fig. 4.26F-J). This problem is more likely with downregulated markers expressed at low levels in the area opaca, where the impact of fold change means that the absolute difference between induced and uninduced values is smaller than between more highly expressed genes.

It is also worth considering that some genes expressed in the neural plate and neural tube may be induced by combinations of signals from surrounding tissues, which a graft of Hensen's node may not be able reproduce. These types of response will not be identified by our screen, but they are more likely to include markers of neural plate patterning since grafts can induce markers of the entire neural plate such as SOX2 and SOX1.

4.5 Conclusions

Presented here is a RNA-Seq analysis of a time-course of responses to neural induction, which identified 4145 differentially expressed genes including 482 transcriptional regulators. Of these we have confirmed the expression of 83 upregulated and 83 downregulated transcriptional regulators and demonstrate that the screen accurately predicts the location and timing of their normal expression. Upregulated genes tend to be expressed in the neural plate at some stage, while downregulated genes are relatively absent. Despite conducting the analysis ectopically, the pattern of markers and signalling readouts closely resembles the spatio-temporal events that occur in the neural plate. Therefore we consider the screen to be an accurate representation of the transcriptional responses that occur during endogenous neural induction. Among these responses are many that have not previously been implicated in neural induction and 80 that are previously undescribed in chick.

Although we have not yet tested the function of these during neural induction, we can speculate on the putative roles of distinct classes of markers based on the timing and location of their expression. Different combinations of upregulated genes mark the neural plate at stages before the expression of SOX1, thereby revealing the dynamic and complex nature of neural induction. These events overlap with varying combinations of downregulated genes which may act normally to repress the process.

It has also been possible to extract accompanying signalling trends; some previously associated with neural induction such as FGFs, BMP inhibition and WNT inhibition as well as others less appreciated including responses to hedgehog signals. How these contribute to neural induction remains to be determined, but it is now possible to evaluate their relative contributions to the expression of the neural markers found here.

Chapter 5: FGFs regulate most early responses to neural induction

5.1 Introduction

In Chapter 4, a screen conducted to identify responses to neural inducing signals revealed a large set of differentially expressed transcription factors -key regulators of neural induction. Analysis of their expression patterns reveals that they can be separated into distinct classes based on the timing and location of their expression in the normal embryo.

To date, the earliest known responses to neural induction were ERNI and SOX3 (Streit *et al.*, 2000). We have now identified new ERNI-like markers such as CITED4 (Fig. 4.6U-Y), ETV4 (Fig. 4.8K-O), MAFA (Fig. 4.12A-E), PRDM1 (Fig. 4.14P-T) and TFAP2C (Fig. 4.32F-J), which are normally expressed in the pre-streak epiblast at EGKXIII and prospective neural plate at HH3-4. Later, they are downregulated in the neural plate but are expressed in the neural plate border and pre-placodal region from HH5 and then in the future placodes after HH9. These differ from SOX3-like genes, such as MTA1 (Fig. 4.12U-Y), SOX13 (Fig. 4.16P-T), STOX2 (Fig. 4.17A-E) and TCF7L1 (Fig. 4.17Z-AD), which are also expressed in the pre-streak epiblast and prospective neural plate, but persist in the neural plate and neural tube after HH4, as ERNI-like genes are downregulated. Later neural markers are not expressed in the early embryo, but are present in the neural plate after HH4. For example, SOX2-like genes including GLI2 (Fig. 4.9F-J), GLI3 (Fig. 4.9K-O), ZEB2 (Fig. 4.19A-E), ZNF423 (Fig. 4.19P-T) and LHX5 (Fig. 4.11F-J) are expressed in the neural plate and PPR between HH5-7 while LMO1 (Fig. 4.11U-Y) is expressed in the neural plate but is specifically absent from the PPR. SOX1 (Fig. 4.15Z-AD), is expressed later still as it can first be detected in the neural tube at HH8-9. This panel of markers, which are expressed at different stages of neural induction, serve as useful indicators of a hierarchical progression through distinct, definable states along the pathway towards acquisition of neural fate.

The RNA-Seq screen also identified markers that are downregulated upon exposure to Hensen's node. Although these are more varied in their expression patterns, several classes could be distinguished. Markers that are excluded from the embryo and only expressed in the area opaca include ISX1 (Fig. 4.26P-T) and VGLL1 (Fig. 4.32Z-AD), while HIC2 (Fig. 4.25A-E) and GRHL3 (Fig. 4.24U-Y) are examples of markers normally expressed in embryonic non-neural ectoderm. Other downregulated genes include those that that mark the neural plate border from HH6 such as DLX5 (Fig. 4.22F-J) (Streit, 2002) and MSX1 (Fig. 4.28F-J) (Suzuki *et al.*, 1991), as well as GRHL2 (Fig. 4.24K-O) and TFAP2A (Fig. 4.32A-E) (Khudyakov and Bronner-Fraser,

2009), which are expressed early in the EGKXIII area opaca and later the neural plate border. Therefore it is now possible to define the time-course of neural induction by the loss of non-neural and neural border markers as well as the acquisition of neural markers.

Considerable evidence already implicates FGFs as an important early signal during neural induction. They are sufficient and necessary to induce ERNI and SOX3 within 1-3h of neural induction (Streit *et al.*, 1998, Streit *et al.*, 2000), and are required or sufficient for the expression of OTX2 (Albazerchi and Stern, 2007), Churchill (Sheng *et al.*, 2003), Asterix, Obelix (Pinho *et al.*, 2011) and SOX2 (Linker and Stern, 2004, Delaune *et al.*, 2005). The RNA-Seq screen further reiterates the important contribution of FGFs, as transcriptional targets of the FGF pathway including ERNI, SOX3 (Streit *et al.*, 2000), SPRY1, SPRY2 (Minowada *et al.*, 1999), SPRED1 (Sivak *et al.*, 2005) and ETV5 (Lunn *et al.*, 2007), are upregulated within the first 5h. However, many of these continue to be upregulated over 5-12h of a node graft suggesting that FGF signals may also function later during the cascade. Changes in the expression of AXIN2 (Quinlan *et al.*, 2009), RARB (Cui *et al.*, 2003), GATA2 (Sheng and Stern, 1999) and PTCH2 (Pearse *et al.*, 2001), targets of the WNT, retinoic acid, BMP and hedgehog pathways, predict that neural induction is accompanied by hedgehog pathway activity and inhibition of BMP, WNT and retinoid signals. Therefore transcriptional reporters of signalling pathways provide clues as to which signals cells are exposed and respond to throughout neural induction.

The induction by Hensen's node of ERNI and SOX3 are, to date, the earliest confirmed responses to neural induction. Their expression, in the epiblast at EGKXIII or after 3h of a node graft by FGFs (Streit *et al.*, 2000), has been predicted to define a pre-neural state similar in specification to the neural plate border (NPB) (Stern, 2004). Like the border, epiblast can be neuralised by BMP antagonists (Streit and Stern, 1999, Wilson *et al.*, 2000, Wilson *et al.*, 2001) and can be induced to form ectopic lens after prolonged culture in the absence of further signals (Bailey *et al.*, 2006, Stower, 2012). This suggests that the pre-streak epiblast shares a common specification with the neural plate border, and that neural induction might begin with the induction of such a state by FGF signals (Stern, 2004).

To establish the precise timing and signals responsible for inducing distinct specification states during neural induction, a selected panel of key markers were used to study responses in more detail. A first set of ERNI-like, SOX3-like, and SOX2-like markers as well as markers which are downregulated by neural induction, were selected to more precisely define the progression of the neural induction cascade by assessing the timing of their responses over a refined time-course. Then, the relative contribution of FGF signalling to their expression was assessed by FGF gain- and loss-of-function experiments.

The time-course screen also provides the opportunity to determine whether the pre-streak epiblast is more generally specified as “border-like”. If this is the case, then markers expressed in the PPR and induced as early responses to neural induction should also be expressed as ERNI and SOX3; in the pre-streak epiblast and prospective neural plate. These would confirm whether neural induction begins with the specification of a “border-like” state and we can then test FGF signals are responsible for its induction.

5.2 Results

5.2.1 A detailed analysis of neural induction and the contribution of FGFs

The identification of many new transcriptional regulators that are differentially expressed during neural induction provides the opportunity to assess the timing and regulation of key responses in greater detail. A custom NanoString probe set targeting specific transcripts, was used to quantify gene expression in control and experimental conditions. Specific markers were used to describe important states that accompany neural induction. ERNI-like (ERNI, CITED4, ETV4, MAFA, PRDM1, TFAP2C), SOX3-like (SOX3, MTA1, SOX13, STOX2, TCF7L1), SOX2-like (SOX2, GLI2, GLI3, ZEB2, ZNF423), other later neural markers (LHX5, LMO1, SOX1, TRKC) and PPR markers (EYA1, SIX1, SIX3), were used to define the phases of pre-neural and neural specification and finally neural commitment (Fig. 3.11). The simultaneous downregulation of area opaca (ISX, VGLL1), non-neural ectoderm (HIC2, GRHL3, KRT19) and neural plate border markers (DLX5, PAX7, GRHL2, TFAP2A) was also assessed. Signalling changes were monitored using SPRY2, RARB, AXIN2, PTCH2, GATA2 and MSX1; readouts of FGF, retinoic acid, WNT, hedgehog and BMP pathways. Brachyury (BRA) and TBX6 were included as markers of mesoderm, while potential contamination by grafted tissue was monitored using Goosecoid (GSC) to mark Hensen’s node itself, and Noggin (NOG) to mark grafted node tissue later when it self-differentiates into notochord.

5.2.1.1 A refined time-course of responses to neural induction over 1-12h

To establish the earliest responses to neural induction and to refine the time-course, epiblast exposed to a node graft and an equivalent piece of uninduced contralateral area opaca epiblast were isolated after 1, 3, 5, 7, 9, and 12h of culture. The expression level of markers was quantified using NanoString (in triplicate). Genes were considered to be differentially expressed in induced tissue when they were upregulated by at least 1.2-fold or downregulated

by at least 0.75-fold. (Fig. 5.1-5.6 are also provided as a slideshow on the accompanying CD; see Appendix 10.)

Transcriptional changes can already be detected in induced tissue after just 1h (Fig. 5.1). ERNI is already upregulated, as is the ERNI-like marker PRDM1. No obvious trends are detected for other neural markers, which record only low level fluctuations. Some non-neural and area opaca markers including GRHL3, KRT19, HIC2 and VGLL1 are downregulated, as are the neural plate border markers DLX5 and TFAP2A.

Greater transcriptional divergence is observed after 3h of a node graft (Fig. 5.2). All ERNI-like markers (CITED4, ETV4, MAFA, PRDM1 and TFAP2C) are now upregulated, while weak upregulation of SOX3 and the SOX3-like markers (MTA1, STOX2 and TCF7L1), is now observed. Downregulation of all non-neural and area-opaca markers is detected, as well as the neural plate border markers DLX5, GRHL2 and TFAP2A.

No new responses are detected after 5h of signals from Hensen's node. Instead the induction of ERNI- and SOX3-like markers is maintained and reinforced (Fig. 5.3). Little expression is yet detected for SOX2-like and other neural markers, which are only detected at very low levels, if at all. Non-neural, area opaca and neural plate border markers continue to be strongly downregulated.

Responses after 7h of a grafted node (Fig. 5.4) are similar to those observed over the first 5h, except that later neural markers including SOX2, GLI2, GLI3, ZEB2, ZNF423, LHX5, LMO1 and TRKC are now upregulated, though only at very low levels. Non-neural, area opaca, neural plate border and PPR markers are generally downregulated, although the PPR marker and forebrain marker SIX3 is mildly upregulated.

It is only after 9h (Fig. 5.5) that later neural markers including SOX2, GLI2, GLI3, ZEB2, ZNF423, LHX5, LMO1, TRKC and SIX3, are robustly upregulated. Even so, SOX1 can still only be detected at very low levels. ERNI- and SOX3-like markers continue to be upregulated but, compared to the earlier time points, their induced relative expression levels are slightly decreased. All non-neural, area opaca and border markers are downregulated apart from SIX3 and EYA2, the latter being only very weakly induced.

After 12h of signals from Hensen's node, all neural markers are robustly expressed (Fig. 5.6). SOX2-like and later neural markers including SOX2, GLI2, GLI3, ZEB2, ZNF423, LHX5, LMO1, TRKC and SOX1 are expressed at much higher levels than they were after 9h. There is also general upregulation of the PPR markers SIX1, SIX3 and EYA2, although neural plate border markers including DLX5, GRHL2 and TFAP2A remain downregulated, alongside area opaca and

non-neural markers. Although ERNI-like and SOX3-like genes are still upregulated, their induced expression levels have further decreased.

Transcriptional readouts of signalling pathways provide clues as to the types of signals cells receive over the 1-12h period of a node graft. Robust downregulation of AXIN2, GATA2 and MSX1 is observed after just 1h of organizer signals (Fig. 5.1). At this time point, PTCH2 is upregulated, while SPRY2 is also weakly induced (Fig. 5.1). The retinoid receptor RARB is also downregulated from 3h (Fig. 5.2), before these transcriptional responses are enhanced and maintained over the following time points (Fig. 5.3 – 5.6).

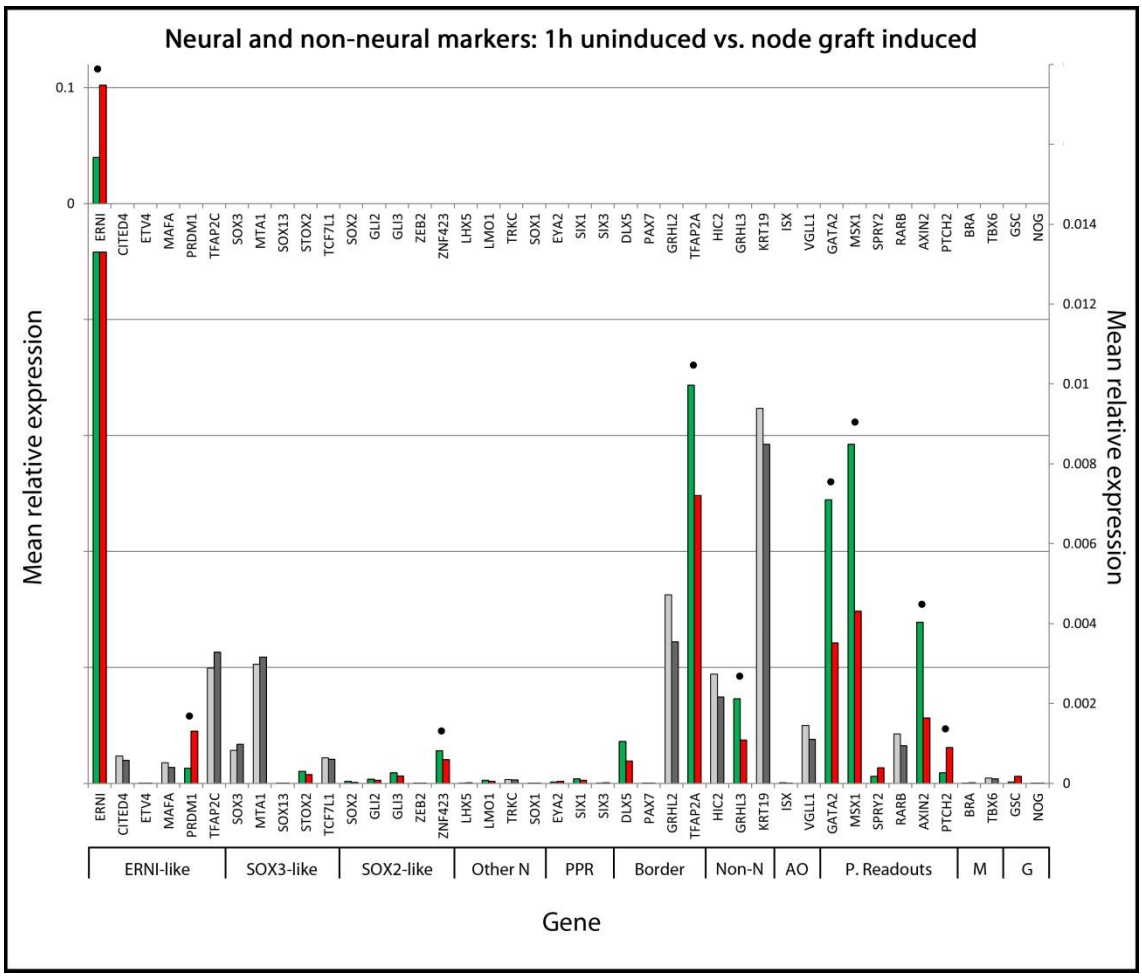

Figure 5.1: The induction of neural and non-neural markers after 1h of a grafted node.

Gene expression, as a proportion of the mRNA count, plotted as a bar graph comparing uninduced (green or light grey) and induced (red or dark grey) conditions after 1h. Differentially expressed genes (fold change >1.2 or <0.75) are shown in colour. Black dots mark statistically significant differences. High level expression changes are plotted on the primary axis (0-0.12), while lower level changes are shown on the secondary axis (0-0.014). Genes include ERNI-like, SOX3-like, SOX2-like, other neural (Other N), PPR, border, non-neural (Non-N), area opaca, signalling pathway readouts (P. readouts), mesoderm (M) and graft (G) markers.

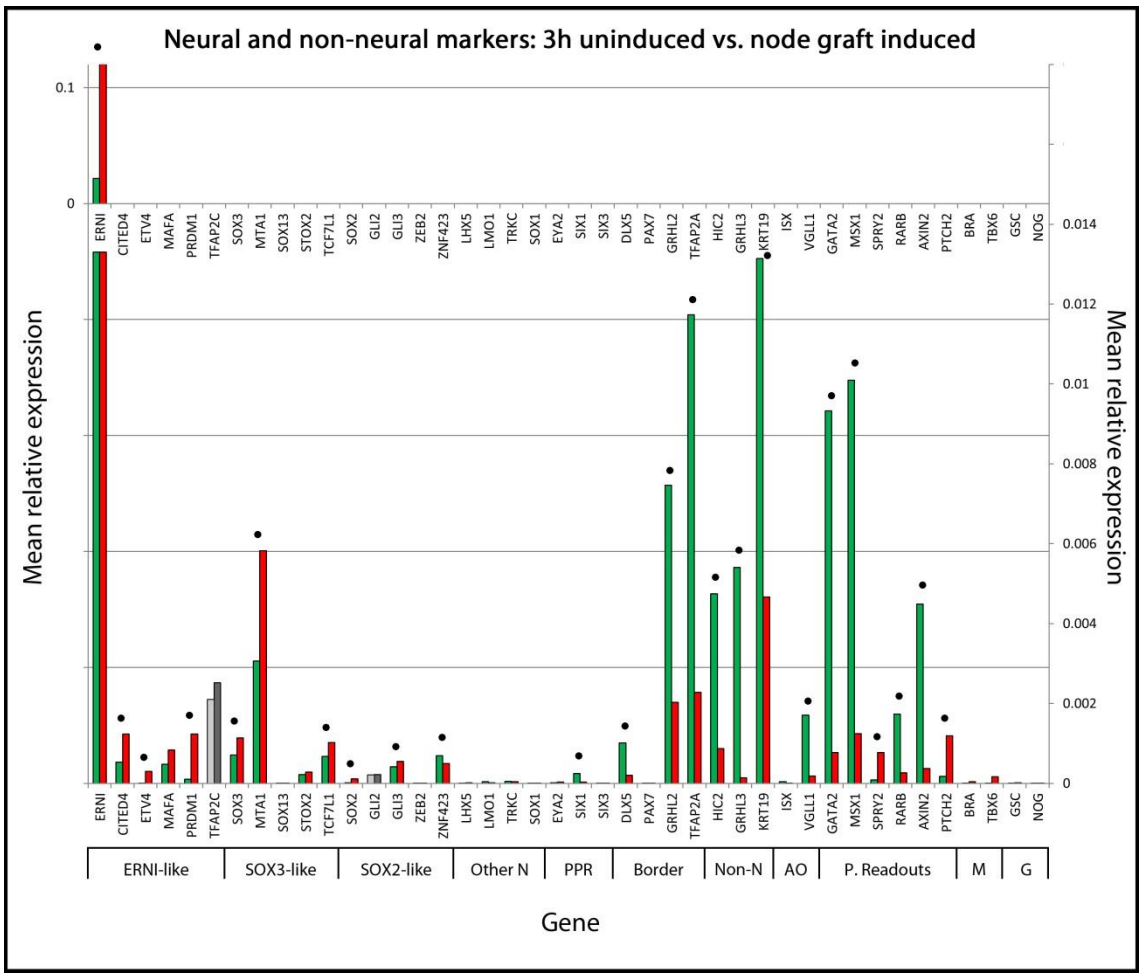

Figure 5.2: The induction of neural and non-neural markers after 3h of a grafted node.

Gene expression, as a proportion of the mRNA count, plotted as a bar graph comparing uninduced and induced conditions after 3h. For details, see Fig. 5.1.

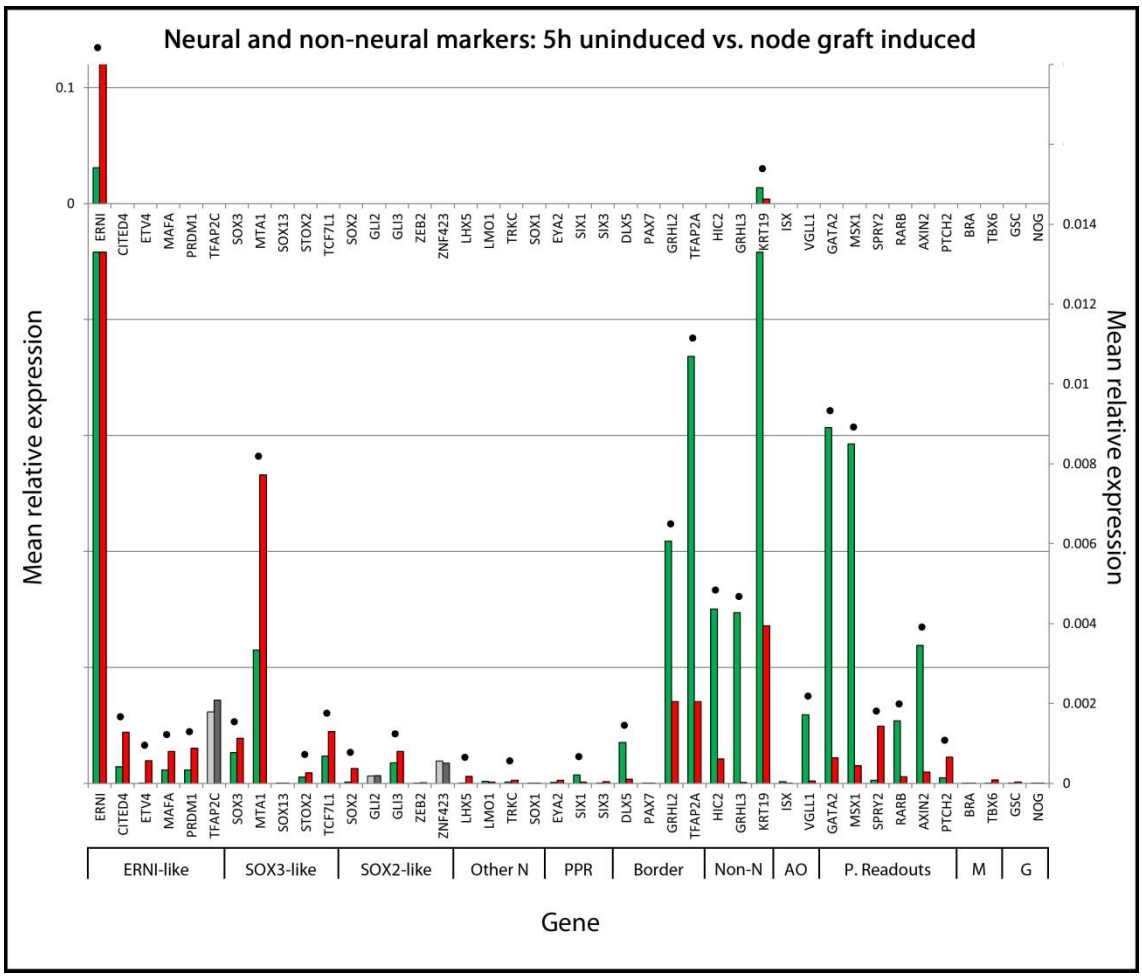

Figure 5.3: The induction of neural and non-neural markers after 5h of a grafted node.

Gene expression, as a proportion of the mRNA count, plotted as a bar graph comparing uninduced and induced conditions after 5h. For details, see Fig. 5.1.

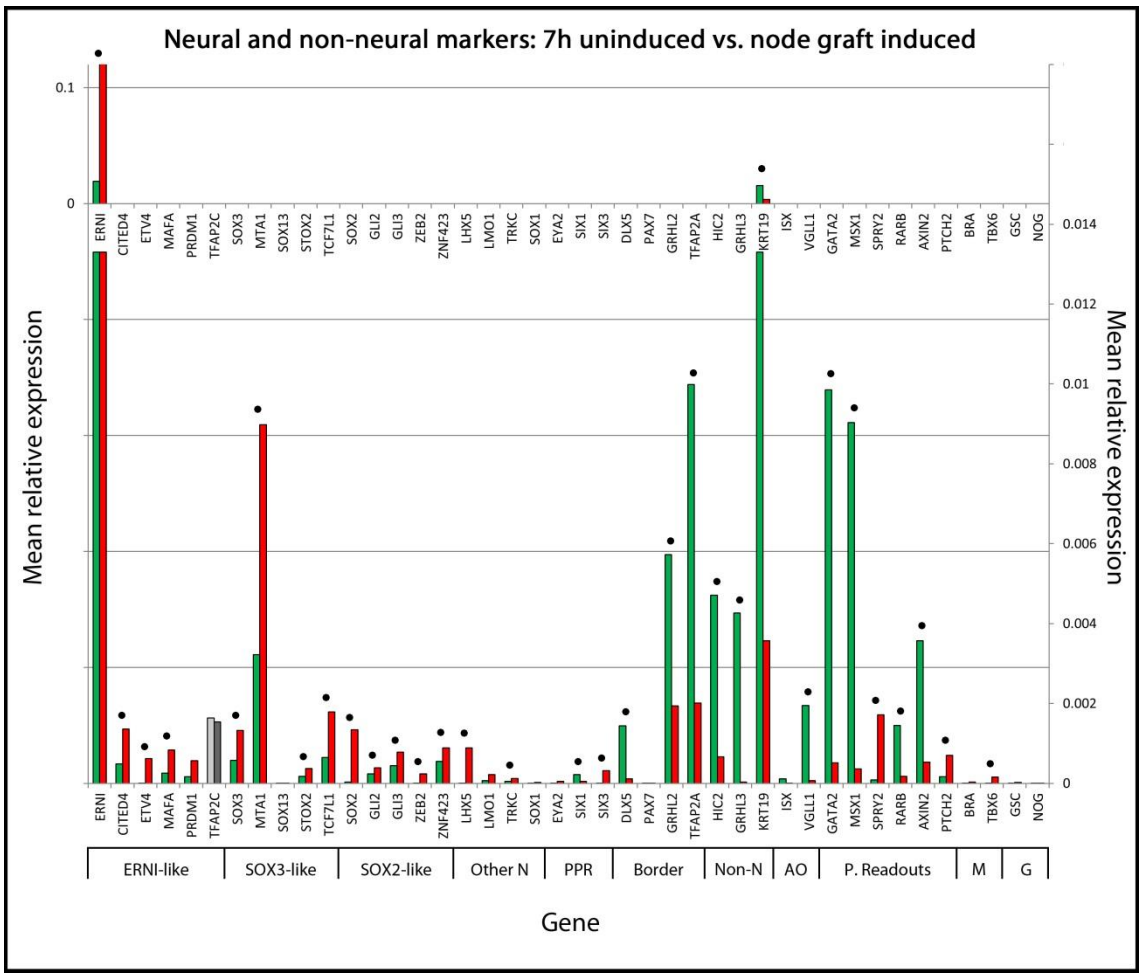

Figure 5.4: The induction of neural and non-neural markers after 7h of a grafted node.

Gene expression, as a proportion of the mRNA count, plotted as a bar graph comparing uninduced and induced conditions after 7h. For details, see Fig. 5.1.

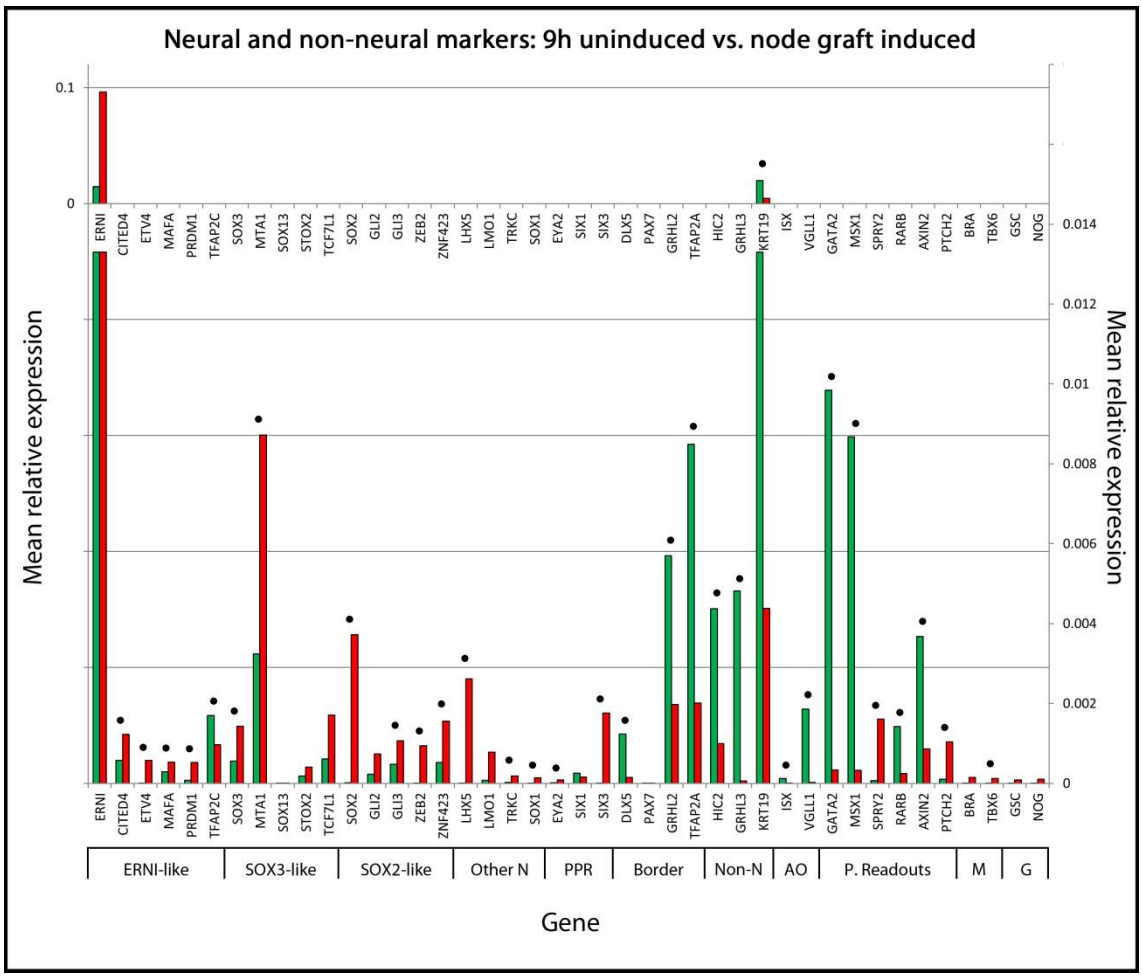

Figure 5.5: The induction of neural and non-neural markers after 9h of a grafted node.

Gene expression, as a proportion of the mRNA count, plotted as a bar graph comparing uninduced and induced conditions after 9h. For details, see Fig. 5.1.

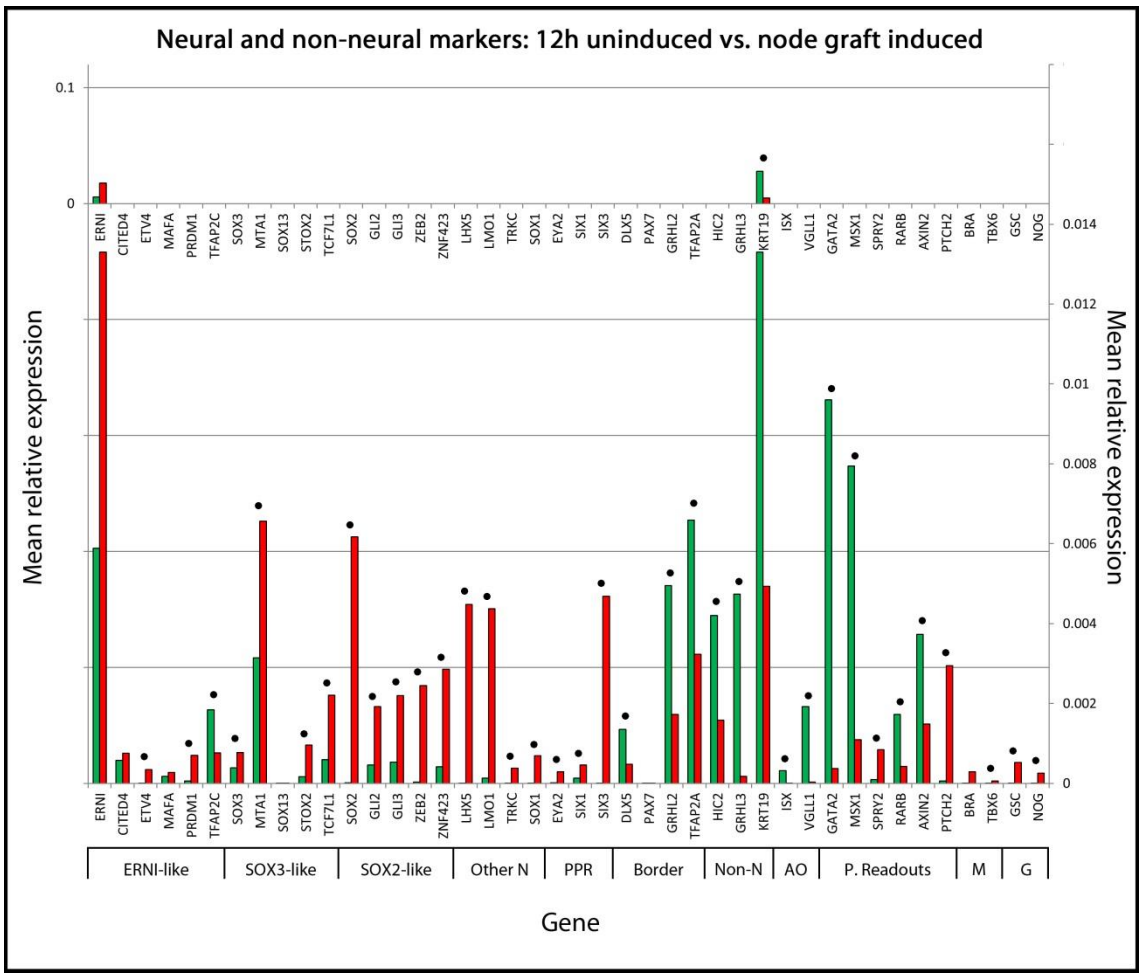

Figure 5.6: The induction of neural and non-neural markers after 12h of a grafted node.

Gene expression, as a proportion of the mRNA count, plotted as a bar graph comparing uninduced and induced conditions after 12h. For details, see Fig. 5.1.

To summarise, all neural markers are upregulated at some stage during neural induction. The earliest responses are upregulated after 1h and include ERNI and PRDM1 (an ERNI-like gene), perhaps representing an early transition towards a neural fate (Fig. 5.1). A more robust neural response is observed after 3h when all ERNI- and SOX3-like markers are upregulated, characterising a pre-neural state. This state is then maintained and reinforced over 3-5h (Fig. 5.2-5.3). As we would predict, SOX2-like markers are only induced after 7-9h of a node graft (Fig. 5.4 and 5.5), when they define neural specification. Then, once cells are committed to a neural fate after 12h (Gallera and Ivanov, 1964, Gallera, 1965, Gallera, 1971), all neural markers including SOX1 are robustly upregulated, or have been upregulated at some point during the time course (Fig. 5.6).

Although ERNI-like markers are still upregulated after 9 and 12h, closer examination of their expression levels over time, reveals that their induction peaks after 7h (Fig. 5.4) before decreasing mildly over 9-12h (Fig. 5.5, 5.6). In particular, TFAP2C is weakly upregulated between 1-5h (Fig. 5.1-5.3) and robustly downregulated from 7h (Fig. 5.4-5.6). This is consistent with the idea that ERNI-like genes are expressed in the prospective neural plate, but downregulated in the neural plate proper from HH5. SOX3-like marker expression similarly peaks over 7-9h (Fig. 5.4, 5.5). Therefore pre-neural markers are less dominant, as the expression of later neural markers takes over during neural specification and commitment after 9-12h (Fig. 5.6). The transcriptional changes we describe occur over substantial levels or as general trends over time. They are not accompanied, at any time point, by substantial expression of either Goosecoid or Noggin. This indicates that induced tissue is not significantly contaminated with grafted tissue. It is likely that the probe designed for SOX13 failed to hybridise to its target transcripts as, despite being strongly expressed in the embryo, NanoString was unable to detect SOX13 expression at any time point.

Unlike neural-associated markers which are induced in 4 distinct waves between 1-12h, markers of non-neural ectoderm and the area opaca are downregulated early (within 1-3h) and remain strongly inhibited by node grafts throughout the remaining time-course. Neural plate border and PPR markers including DLX5, GRHL2, and TFAP2A are also downregulated early but some PPR and anterior neural plate markers (EYA2, SIX3 and SIX1) are upregulated between 9-12h (Fig. 5.6), which, correlates well with PPR formation between HH6-7.

Accompanying these responses, is evidence of early FGF signalling, as demonstrated by upregulation of FGF responses such as ERNI, SOX3, ETV4 and SPRY2 over 1-3h (Fig. 5.1, 5.2). Simultaneously, the BMP and WNT pathways also seem to be inhibited within 1h, as target genes GATA2 and MSX1 are downregulated alongside AXIN2 (Fig. 5.1). Inhibition of retinoid signalling may also occur after 3h as RARB is downregulated. Grafts of Hensen's node are sufficient to induce the hedgehog pathway receptor and target PTCH2 after 1h, but other targets of the hedgehog pathway; GLI2 and GLI3, are not robustly upregulated until 9h (Fig. 5.5).

5.2.1.2 FGFs regulate most early responses to neural induction after 5h

The FGF targets ERNI and SOX3 are known to be upregulated within 1-3h of a node graft (Streit *et al.*, 2000, Pinho *et al.*, 2011). Therefore, other early responses also induced within this time period might also be regulated by FGFs (Fig. 5.1 and 5.2). To evaluate the contribution of FGF signalling to the regulation of these markers, we assessed their expression by gain- and loss-

of-function experiments. Genes were considered to be differentially expressed in response to FGF perturbation when they were upregulated by at least 1.2-fold or downregulated by at least 0.75, compared to the uninduced control. (Fig. 5.7-5.8 are also provided as a slideshow on the accompanying CD; see Appendix 10.)

To test whether FGF signals are sufficient for early neural responses, the expression of markers in uninduced tissue was compared to 5h of signals from a bead soaked in FGF8b (Fig. 5.7). FGFs are sufficient to induce ERNI itself and the ERNI-like markers ETV4, MAFA and PRDM1, but not CITED4. SOX3 and SOX3-like genes including MTA1, STOX2 and TCF7L1 are also upregulated. The SOX2-like marker ZNF423 is also upregulated, but FGFs have little or no effect on other later neural markers, though these are not normally expressed after 5h. FGF signals also dramatically downregulate HIC2, GRHL3, KRT19 and VGLL1 -markers of non-neural ectoderm and the area opaca. The neural plate border markers GRHL2 and TFAP2A are also downregulated, though DLX5 is upregulated. As expected, FGF signals induce SPRY2, but they also upregulate PTCH2 and robustly downregulate AXIN2, RARB, GATA2 and MSX1. Despite prior verification by in situ hybridisation that 25µg/ml FGF8b does not induce mesoderm after 5h (Appendix 9), NanoString is sensitive to detect upregulation of Brachyury and TBX6. Therefore these results should be interpreted with caution as the induction of pre-neural markers could be indirect.

To test whether FGF signals are required to regulate these early responses, their expression after 5h of a node graft was compared to their induction when FGF signalling from a grafted node is inhibited by SU5402 (Fig. 5.8). FGF inhibition downregulates ERNI and ERNI-like markers such as CITED4, ETV4 and MAFA, but paradoxically upregulates PRDM1. FGF signals are also necessary for the expression of SOX3 and MTA1, but not for the SOX3-like markers STOX2 or TCF7L1. Upregulation of non-neural and neural plate border markers including KRT19, GATA2, GRHL2 and TFAP2A is observed upon FGF inhibition, although HIC2 is downregulated and DLX5 is unaffected. Loss of FGF signalling causes mild downregulation of SPRY2 and PTCH2, but has little or no effect on RARB or AXIN2.

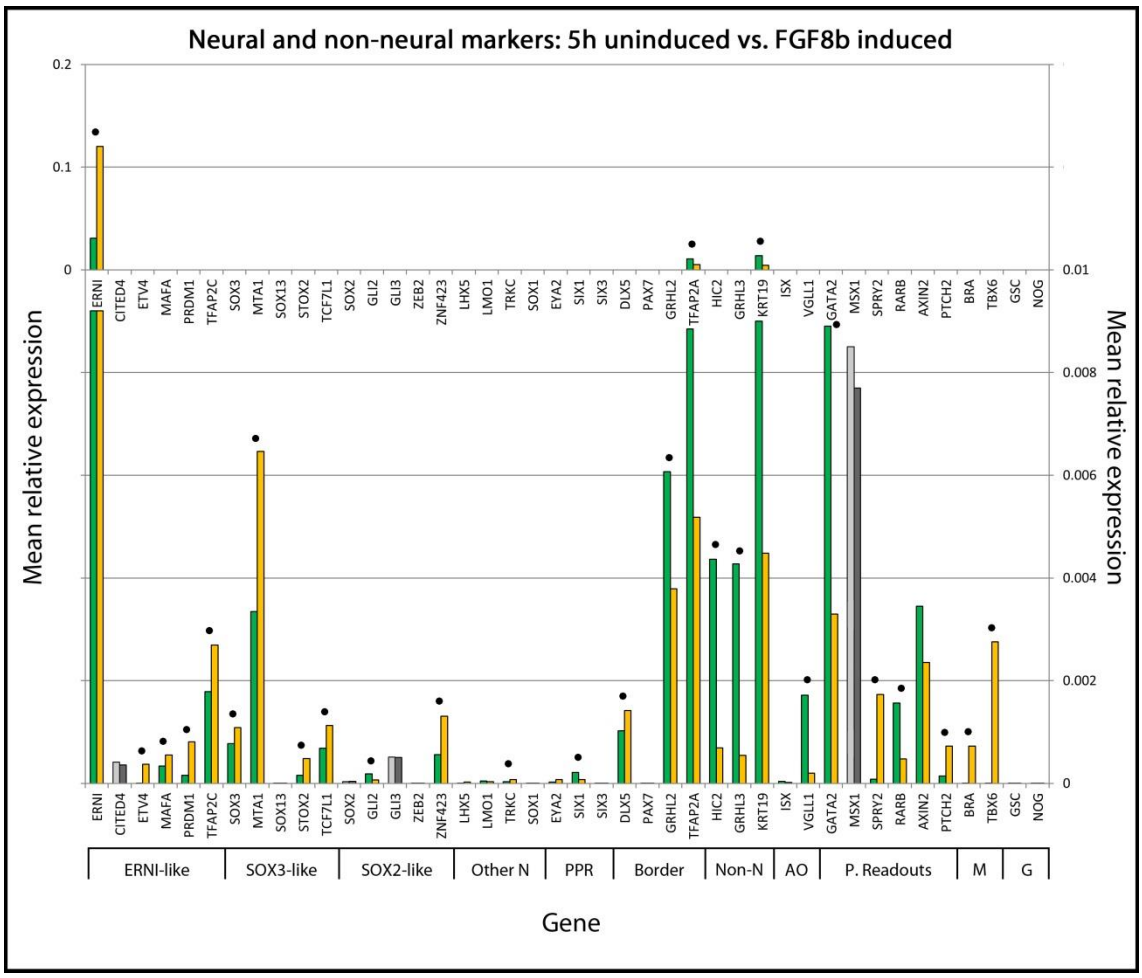

Figure 5.7: The induction of neural and non-neural markers after 5h of FGF signalling.

Gene expression, as a proportion of the mRNA count, plotted as a bar graph comparing uninduced epiblast (green or light grey) and FGF exposure (orange or dark grey) after 5h. Differentially expressed genes (fold change >1.2 or <0.75) are shown in colour. Black dots mark statistically significant differences. High level expression changes are plotted on the primary axis (0-0.2), while lower level changes are shown on the secondary axis (0-0.01). Genes include ERNI-like, SOX3-like, SOX2-like, other neural (Other N), PPR, border, non-neural (Non-N), area opaca, signalling pathway readouts (P. readouts), mesoderm (M) and graft (G) markers.

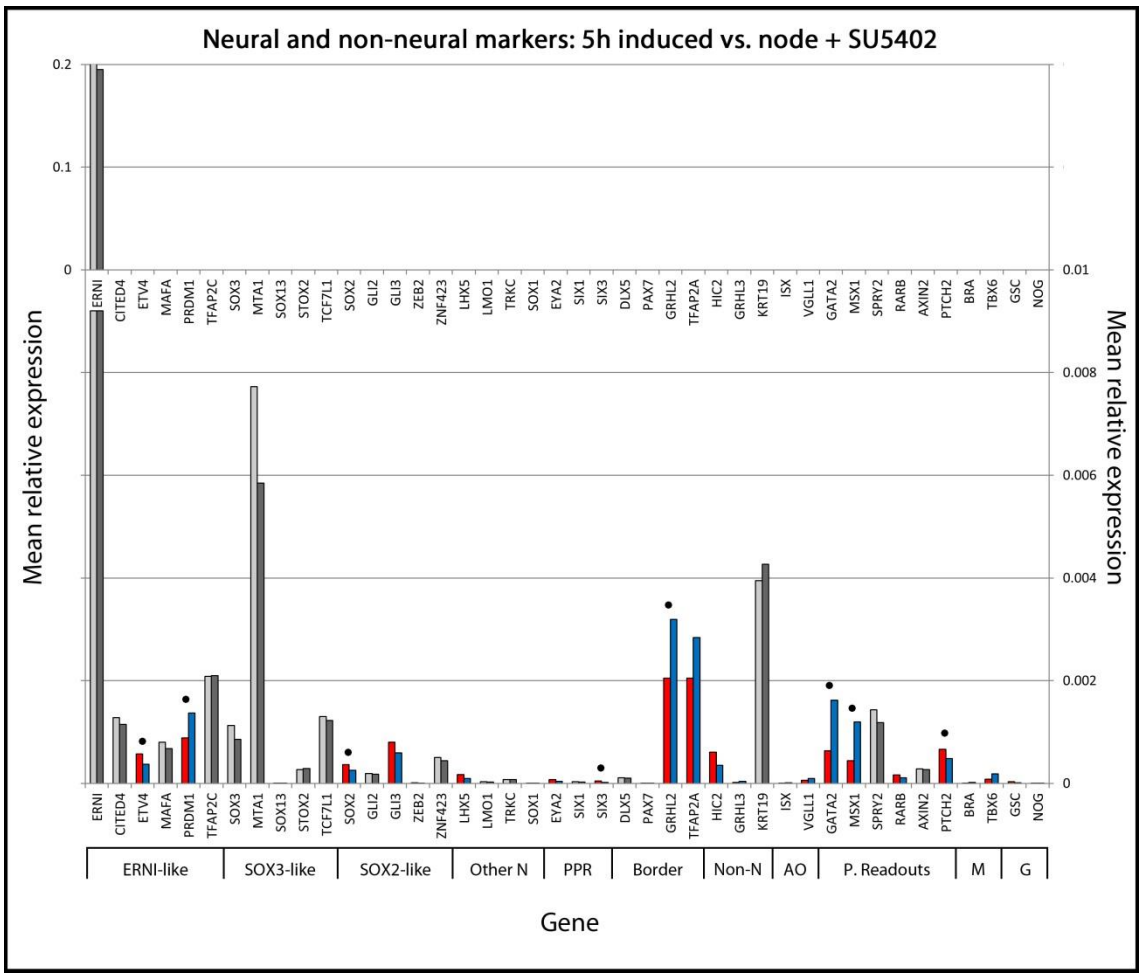

Figure 5.8: The induction of neural and non-neural markers after 5h of FGF inhibition.

Gene expression, as a proportion of the mRNA count, plotted as a bar graph comparing induced tissue (red or light grey) after 5h to neural induction when FGFs are inhibited (blue or dark grey). For details, see Fig. 5.7.

In summary (Fig. 5.9) FGFs regulate early neural responses to varying degrees. They are sufficient and necessary to induce ERNI, ETV4, MAFA, SOX3, MTA1 and TCF7L1 expression. CITED4 requires FGF signalling, but this is not sufficient for its expression. Conversely, FGFs are sufficient but not necessary for the expression of TFAP2C and STOX2. Simultaneously, FGF signals are sufficient and necessary to downregulate GRHL2, TFAP2A, GRHL3, VGLL1 and GATA2. They are sufficient but not necessary to downregulate HIC2, but necessary and sufficient for MSX1. Although PRDM1 is upregulated in response to FGF signalling, it is also upregulated by FGF inhibition. Furthermore, DLX5, which is normally downregulated in response to a node graft, is actually upregulated by FGF alone, although FGFs are not required for its expression. Therefore, other signals must contribute to CITED4, MSX1, STOX2, TFAP2C

and HIC2 expression, and modulate the responses of PRDM1 and DLX5 to FGF signalling during neural induction.

As expected, FGFs are sufficient and necessary to upregulate the FGF target SPRY2, but the results also suggest that they can regulate markers normally associated with other signalling pathways. FGFs are sufficient and necessary to dramatically downregulate GATA2 and MSX1, and sufficient to repress RARB and AXIN2. They are sufficient and necessary for PTCH2 expression. This suggests that FGFs can facilitate hedgehog signalling and may even antagonise BMP, WNT and retinoic acid pathways during neural induction.

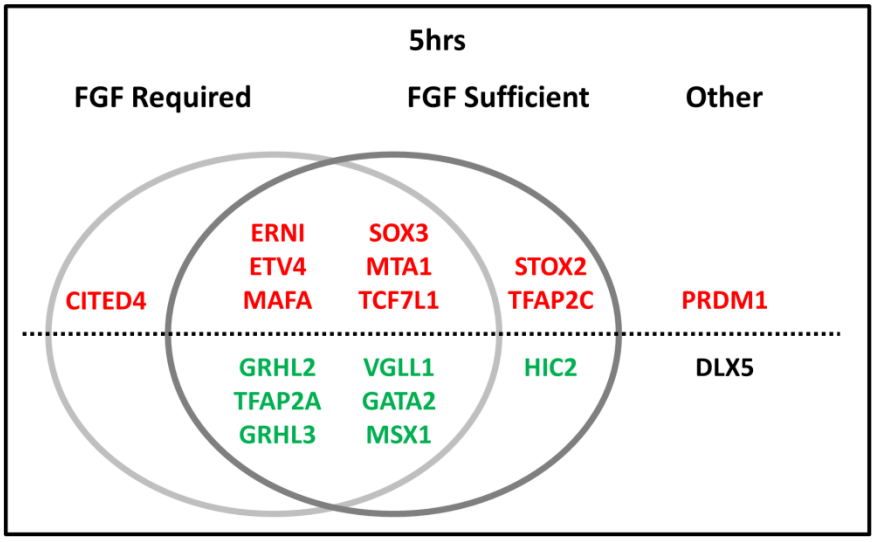

Figure 5.9: The contribution of FGFs to neural induction after 5h.

A Venn diagram summarising upregulated (red) and downregulated (green) genes that require FGFs, those for which FGF signalling is sufficient for their responses, and those that respond differently to FGFs.

5.2.1.3 FGFs maintain early responses and are required for the expression of later markers after 9h

After 5h, it is only possible to assess the effects of FGF perturbation on the earliest neural responses, as later neural markers are not induced until at least 7-9h of signals from a node graft. Therefore, to evaluate the contribution of FGF signalling to the regulation of later markers and the continuing expression of early responses, we assessed their expression after 9h of FGF perturbation. (Fig. 5.10-5.11 are also provided as a slideshow on the accompanying CD; see Appendix 10.)

To test the sufficiency of FGFs for responses after 9h, the expression of markers in uninduced tissue was compared to their response after 9h of signals from a bead soaked in FGF8b. FGFs are still sufficient to induce ERNI, SOX3, ETV4, MAFA, PRDM1, TFAP2C, MTA1, STOX2, and TCF7L1 after this period (Fig. 5.10), although they now downregulate the ERNI-like marker CITED4. FGFs remain sufficient to upregulate ZNF423, but even after 9h, they are unable to fully upregulate SOX2, GLI2, GLI3, ZEB2, LHX5, LMO1 or TRKC, which are normally expressed at much higher levels following a node graft. FGFs continue to downregulate non-neural markers including HIC2, GRHL3, KRT19 and VGLL1. The neural border markers SIX1 and GRHL2 are also slightly downregulated in response, although TFAP2A and MSX1, which were mildly downregulated after 5h, are now weakly upregulated. FGF signals still downregulate AXIN2, RARB and GATA2 and induce SPRY2 and PTCH2. As observed after 5h (Fig. 5.7), expression of Brachyury and TBX6 can also be detected at 9h.

In response to FGF inhibition for 9h (Fig. 5.11), the ERNI-like genes ETV4 and CITED4 are downregulated, while ERNI and TFAP2C are mildly upregulated and MAFA and PRDM1 are relatively unaffected. SOX3 and MTA1 are downregulated, though other SOX3-like genes (STOX2 and TCF7L1) are mildly upregulated. Later neural markers such as GLI3, ZEB2, ZNF423, LHX5 and LMO1 are weakly downregulated, although SOX2 and GLI2 are relatively unaffected. The expression of GRHL2 and TFAP2A increases slightly upon FGF inhibition, but other neural plate border markers are not generally affected. The non-neural markers KRT19, HIC2 and GRHL3 are even further downregulated after 9h than after 5h. In terms of signalling readouts, the BMP targets GATA2 and MSX1 are mildly upregulated. SPRY2 and PTCH2 which were downregulated after 5h are now weakly upregulated, while AXIN2 and RARB are downregulated.

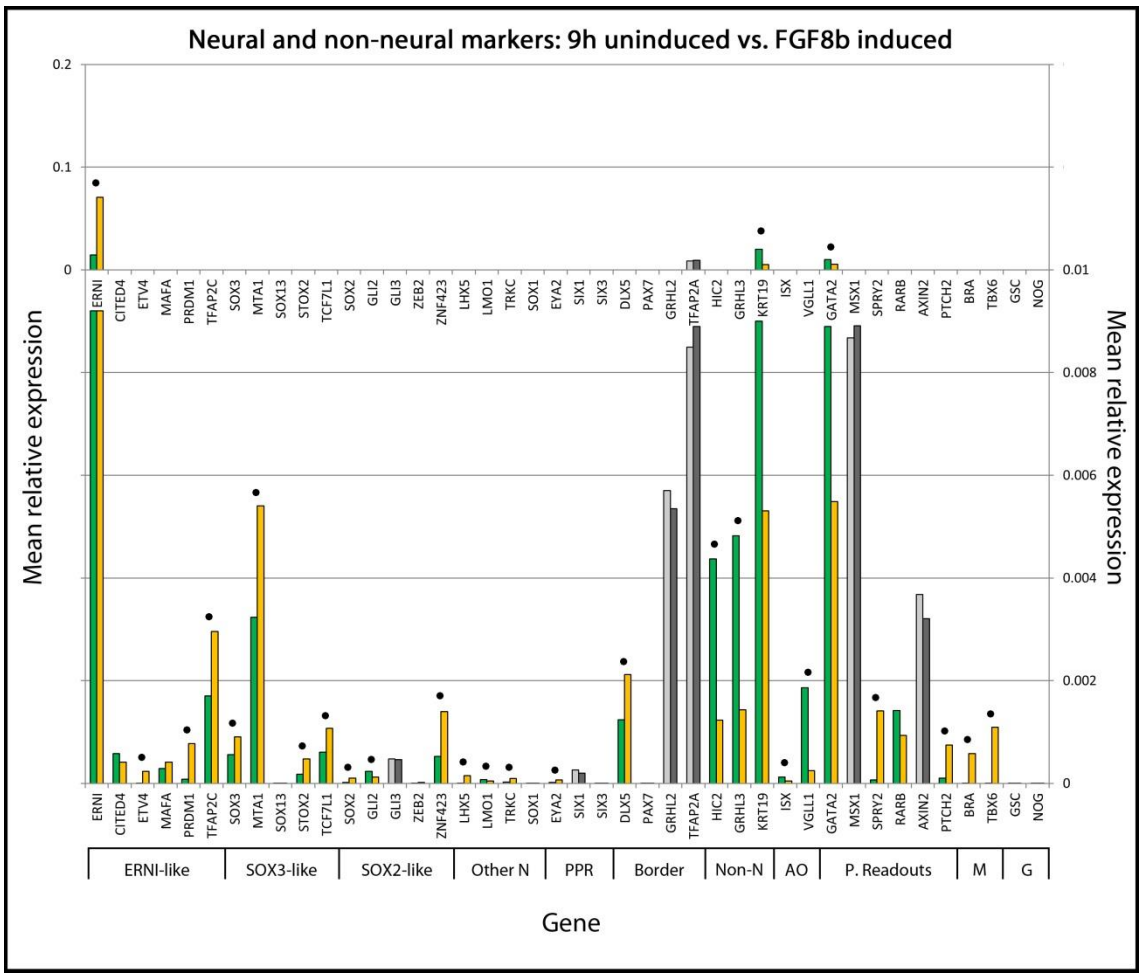

Figure 5.10: The induction of neural and non-neural markers after 9h of FGF signalling.

Gene expression, as a proportion of the mRNA count, plotted as a bar graph comparing uninduced (green or light grey) and FGF induced (orange or dark grey) conditions after 9h. Differentially expressed genes (fold change >1.2 or <0.75) are shown in colour. Black dots mark statistically significant differences. High level expression changes are plotted on the primary axis (0-0.2), while lower level changes are shown on the secondary axis (0-0.01). Genes include ERNI-like, SOX3-like, SOX2-like, other neural (Other N), PPR, border, non-neural (Non-N), area opaca, signalling pathway readouts (P. readouts), mesoderm (M) and graft (G) markers.

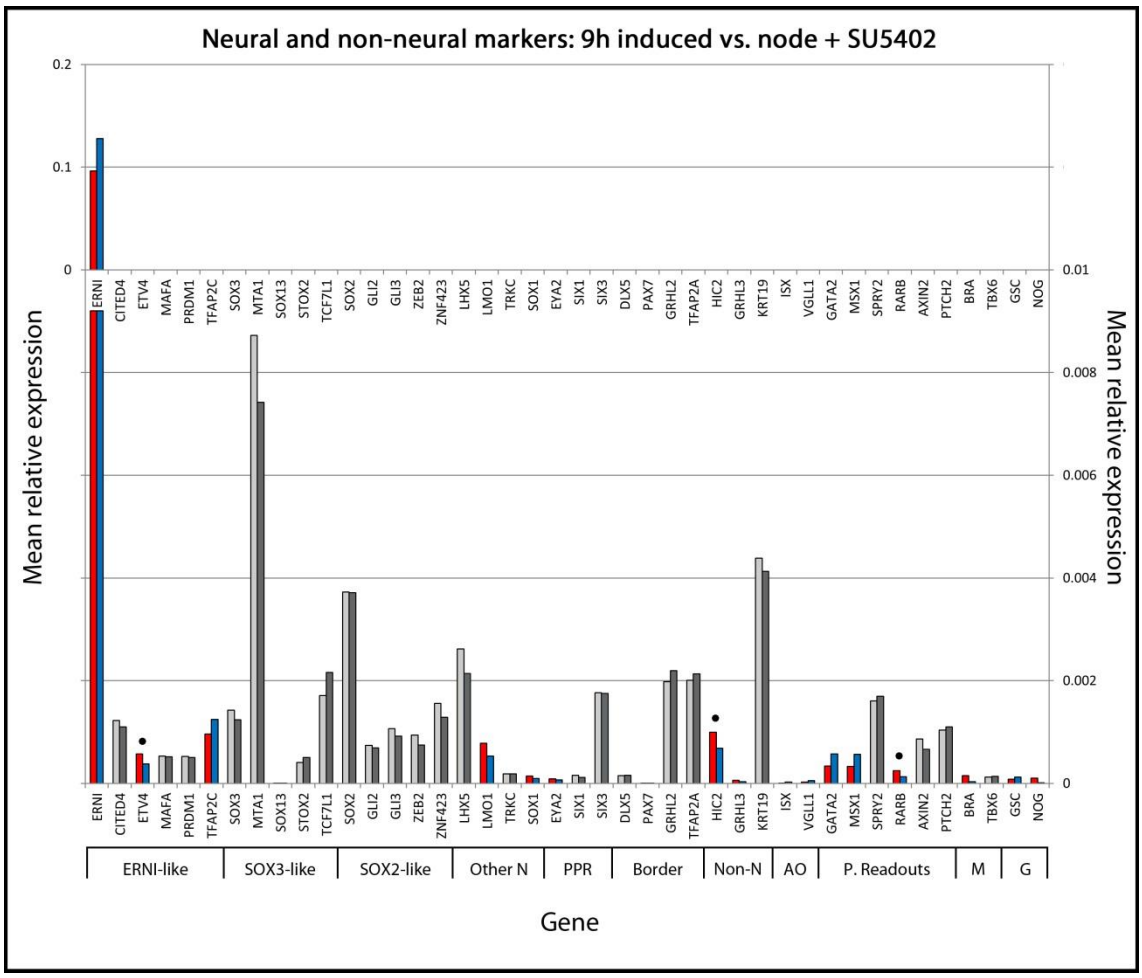

Figure 5.11: The induction of neural and non-neural markers after 9h of FGF inhibition.

Gene expression, as a proportion of the mRNA count, plotted as a bar graph comparing induced tissue (red or light grey) after 9h to neural induction when FGFs are inhibited (blue or dark grey). For details, see Fig. 5.10.

The responses that occur after 9h of FGF perturbation can be summarised as follows (Fig. 5.12). FGFs are still necessary and sufficient to induce ETV4, SOX3 and MTA1, but also ZNF423. Where FGFs were sufficient and necessary after 5h, they are sufficient but no longer required for ERNI, MAFA, STOX2 and TCF7L1 expression after 9h. Expression of later neural markers such as GLI2, GLI3, ZEB2, LHX5 and LMO1 requires FGF signalling, but it is not sufficient for their expression. FGFs remain sufficient and required to downregulate GRHL2, TFAP2A, VGLL1 and GATA2, but only required for MSX1 inhibition. They are sufficient, but no longer necessary to downregulate HIC2 and GRHL3 after 9h. FGF signalling continues to upregulate DLX5, despite node grafts normally repressing its expression. TRKC, SIX3 and surprisingly also SOX2, do not appear to respond to FGF activity or antagonism, suggesting that their expression might be relatively FGF independent. CITED4 is now downregulated by both FGF activity and

inhibition, while TFAP2C, which is normally downregulated after 9h of neural induction, is upregulated by both FGF gain- and loss-of-function. It could be that CITED4 and TFAP2C are normally regulated by signals which compete with MAPK signalling, such as IGFs, EGFs or HGFs.

After 9h, FGF signals still downregulate the BMP target GATA2, although FGF activity upregulates MSX1. They are also sufficient but not necessary to downregulate RARB and AXIN2 after 9h suggesting that other factors normally inhibit their expression. Although ETV4 and SOX3 are downregulated by FGF inhibition after 9h, SPRY2 expression is unaffected. This observation raises the possibility that FGF signals may not be effectively inhibited after 9h and if so, the requirement of FGF signalling may not be accurately assessed. Alternatively, it is possible that SPRY2 expression may now be FGF-independent.

Generally, FGFs remain an important regulator of some early neural markers after 9h, but other signals now seem to maintain the responses of STOX2, TCF7L1, HIC2 and GRHL3. Although FGFs are sufficient to induce ZNF423, they are only required for the expression of other neural markers after 9h. This supports the idea that additional signals are required after 5h for the expression of later neural markers. Furthermore, the effects of FGF signalling on targets of BMP, WNT and retinoid signalling after 5h, will have downstream consequences at later time points.

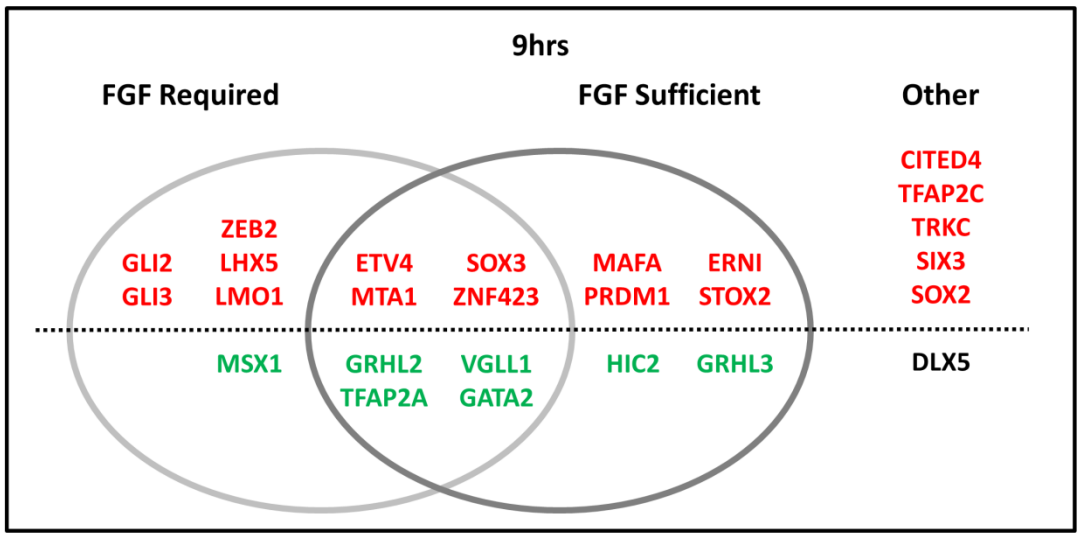

Figure 5.12: The contribution of FGFs to neural induction after 9h.

Venn diagram summarising which upregulated (red) and downregulated (green) genes require FGFs, those for which FGF signalling is sufficient for their responses, and those that respond differently to FGFs.

5.2.2 A detailed analysis of pre-neural markers and their regulation by FGFs

Until now, ERNI and SOX3 were the two earliest genes known to be expressed during neural induction (Streit *et al.*, 2000). Both are induced within 3h of a node graft and in response to FGF signalling. In the embryo, their expression in the epiblast at EGKXII-XIII first suggested that neural induction starts before gastrulation (Streit *et al.*, 2000). Later, they are commonly expressed in the prospective neural plate at HH3-4, but their expression diverges from HH5 when SOX3 expression persists in the neural plate and neural tube, whereas ERNI expression shifts to the neural plate border (NPB) and pre-placodal region (PPR) (Streit *et al.*, 2000). The PPR is a domain which derives from the anterior NPB and later gives rise to the sensory placodes (Papalopulu, 1995, Baker and Bronner-Fraser, 2001, Bailey and Streit, 2005, Streit, 2008). Based on experiments using ERNI and SOX3 as markers, it has been suggested that the neural plate and PPR might derive from a common "border-like" pre-neural territory (Stern, 2004, Streit, 2008).

To determine whether the pre-streak epiblast can be more generally characterised as "border-like", the expression of other neural plate and PPR markers was assessed. Transcriptional regulators commonly identified by two separate screens were selected for analysis; markers upregulated after 5h in the neural induction RNA-Seq screen (above a base mean induced level of 45), and upregulated in a microarray screen of PPR tissue conducted by Andrea Streit's group at King's College London. From this, 20 markers of the neural plate and pre-placodal region were selected, including ERNI and SOX3. To test whether these markers are also expressed in the early embryo their normal expression was assessed by in situ hybridisation at EGKXII-XIII and HH3-4 (Fig. 5.13). The expression of these was already shown in Chapter 4, but is repeated here for clarity.

Of the 20 transcriptional regulators assessed, 16 are robustly expressed in the epiblast at EGKXII-XIII and in the prospective neural plate at HH3-4 (Fig. 5.13). These include the transcription factors ETV5 (Fig. 5.13E, M), MYCN (Fig. 5.13G, O), OTX2 (Fig. 5.13Q, Y), SOX11 (Fig. 5.13T, AB) and ZIC3 (Fig. 5.13W, AE). Also expressed are genes coding for verified or putative chromatin modifiers including BMI1 (Fig. 5.13A, I), DNMT3A (Fig. 5.13B, J), DMNT3B (Fig. 5.13C, K), ING5 (Fig. 5.13F, N), NSD1 (Fig. 5.13H, P), SETD2 (Fig. 5.13R, Z), TRIM24 (Fig. 5.13U, AC), YEATS4 (Fig. 5.13V, AD), and ZNF462 (Fig. 5.13X, AF). Despite subtle differences in expression pattern (for example, OTX2 is expressed in Hensen's node), the similarity of expression of these genes to ERNI (Fig. 5.13D, L) and SOX3 (Fig. 5.13S, AA) is striking. This confirms that other NPB/PPR markers are expressed in the EGKXII-XIII epiblast and HH3-4 prospective neural plate. Therefore the pre-neural state can be more generally described as being "border-like".

Non-specific expression was observed for four other markers at these stages; BCL11A, HEY1, TBL1XR1 and ZHX2 (see Appendix 11), but these were all predicted to be expressed at much lower levels by the RNA-Seq analysis.

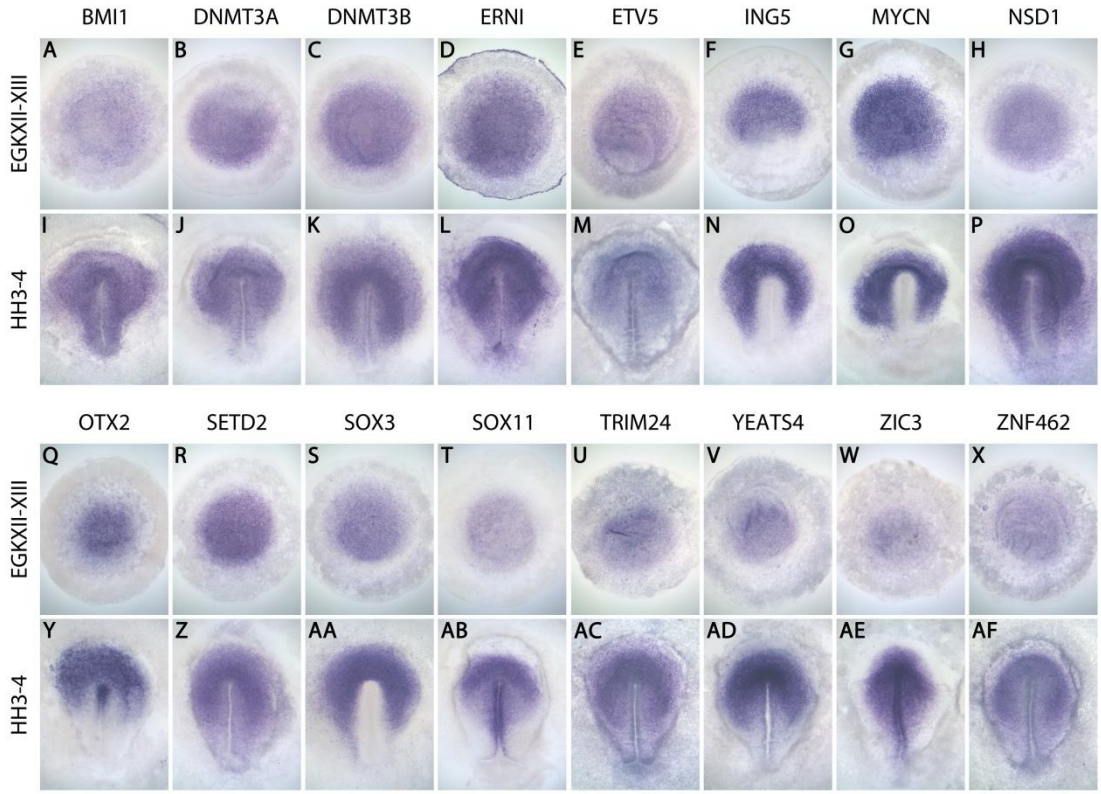

Figure 5.13: Transcriptional regulators common to early neural induction and the PPR.

The expression of 20 markers, common to a microarray screen of PPR tissue and an RNA-Seq screen for responses to 5h of neural inducing signals, was assessed at two stages: before gastrulation at EGKXII-XIII (A-H, Q-X), and during gastrulation at HH3-4 (I-P, Y-AF). Of these, 16 are robustly expressed in the epiblast at EGKXII-XIII and the prospective neural plate at HH3-4, including BMI1 (A, I), DNMT3A (B, J), DMNT3B (C, K), ERNI (D, L), ETV5 (E, M), ING5 (F, N), MYCN (G, O), NSD1 (H, P), OTX2 (Q, Y), SETD2 (R, Z), SOX3 (S, AA), SOX11 (T, AB), TRIM24 (U, AC), YEATS4 (V, AD), ZIC3 (W, AE) and ZNF462 (X, AF).

5.2.2.1 A refined time-course of pre-neural markers over 1-5h

Although these pre-neural markers were selected because they are upregulated within the first 5h of signals from a grafted node, ERNI and SOX3 are known to respond even faster. SOX3 requires 3h of neuralising signals to be induced, while ERNI expression is dramatically upregulated after just 1h (Streit *et al.*, 2000). Therefore some of these pre-neural "border-like" markers could also be induced even earlier than 5h.

To determine the earliest induction of these markers and to refine the time-course of neural induction, their expression was assessed in response to node grafts after 1, 3 and 5h. At each time point, expression was measured in uninduced and node induced tissue using NanoString technology (in triplicate). The relative expression of markers is plotted as bar graphs comparing uninduced and node induced conditions. (Fig. 5.14, 5.15 and 5.16 are also provided as a slideshow on the accompanying CD; see Appendix 12.)

Transcriptional changes can already be detected in cells that have received 1h of signals from Hensen's node (Fig. 5.14). As previously observed (Streit *et al.*, 2000), ERNI is upregulated at high levels in induced tissue after 1h. Also induced, but at lower levels are MYCN, OTX2, TRIM24, ZIC3 and ZNF462. The chromatin modifier BMI1 is weakly downregulated, while SPRY2 and SPRED1; targets of FGF signalling, are subtly upregulated.

After 3h of signals from Hensen's node, ERNI, MYCN, OTX2, TRIM24, ZIC3 and ZNF462 continue to be upregulated but at higher levels than after 1h (Fig. 5.15). Newly induced after 3h, are ETV5, ING5 and YEATS4, as well as SOX3 -in agreement with previous observations (Streit *et al.*, 1998, Streit *et al.*, 2000).

After 5h, all pre-neural markers are upregulated except DNMT3A, NSD1 and SOX11, which can be barely detected (Fig. 5.16). DNMT3B and SETD2 are newly upregulated after 5h, while the expression of ERNI, ETV5, ING5, MYCN, OTX2, SOX3, TRIM24, YEATS4, ZIC3 and ZNF462 as well as SPRY2 and SPRED1, is maintained or reinforced, compared to 3h of induction.

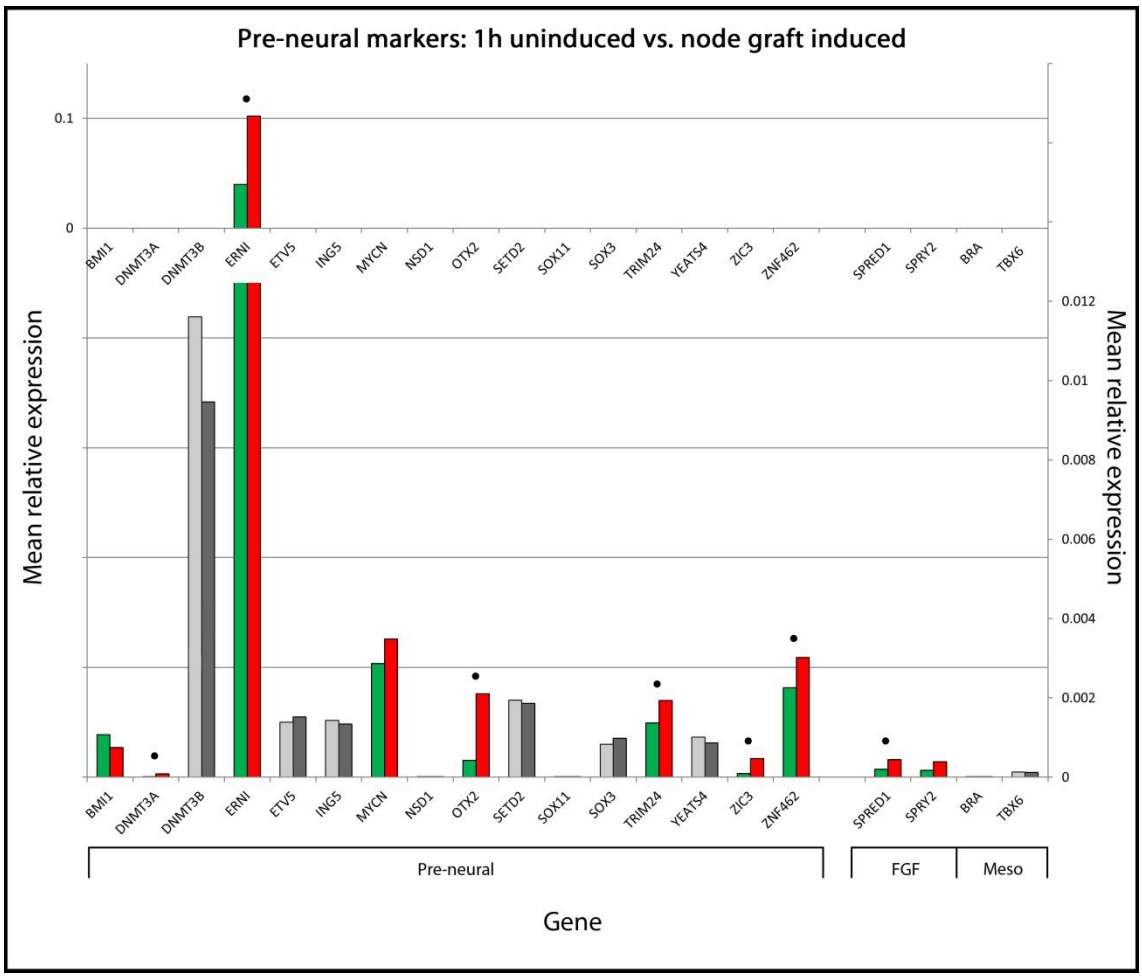

Figure 5.14: The induction of pre-neural markers after 1h of a grafted node.

Gene expression, as a proportion of the mRNA count, plotted as a bar graph comparing uninduced (green or light grey) and induced (red or dark grey) conditions after 1h. Differentially expressed genes (fold change >1.2 or <0.75) are shown in colour. Black dots mark statistically significant differences. High level expression changes are plotted on the primary axis (0-0.15), while lower level changes are shown on the secondary axis (0-0.012). Genes include pre-neural and mesodermal markers, but also FGF targets.

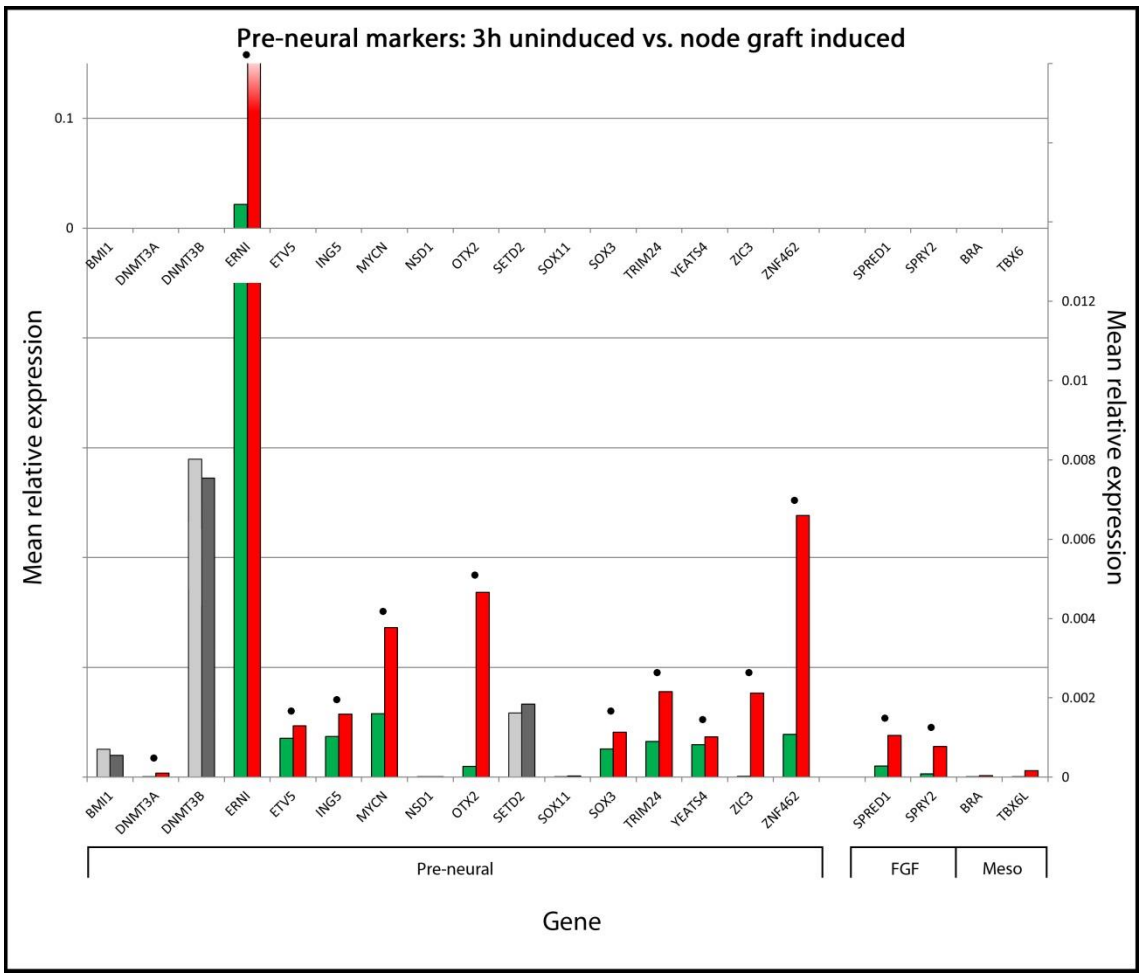

Figure 5.15: The induction of pre-neural markers after 3h of a grafted node.

Gene expression, as a proportion of the mRNA count, plotted as a bar graph comparing uninduced (green or light grey) and induced (red or dark grey) conditions after 3h. For details, see Fig. 5.14.

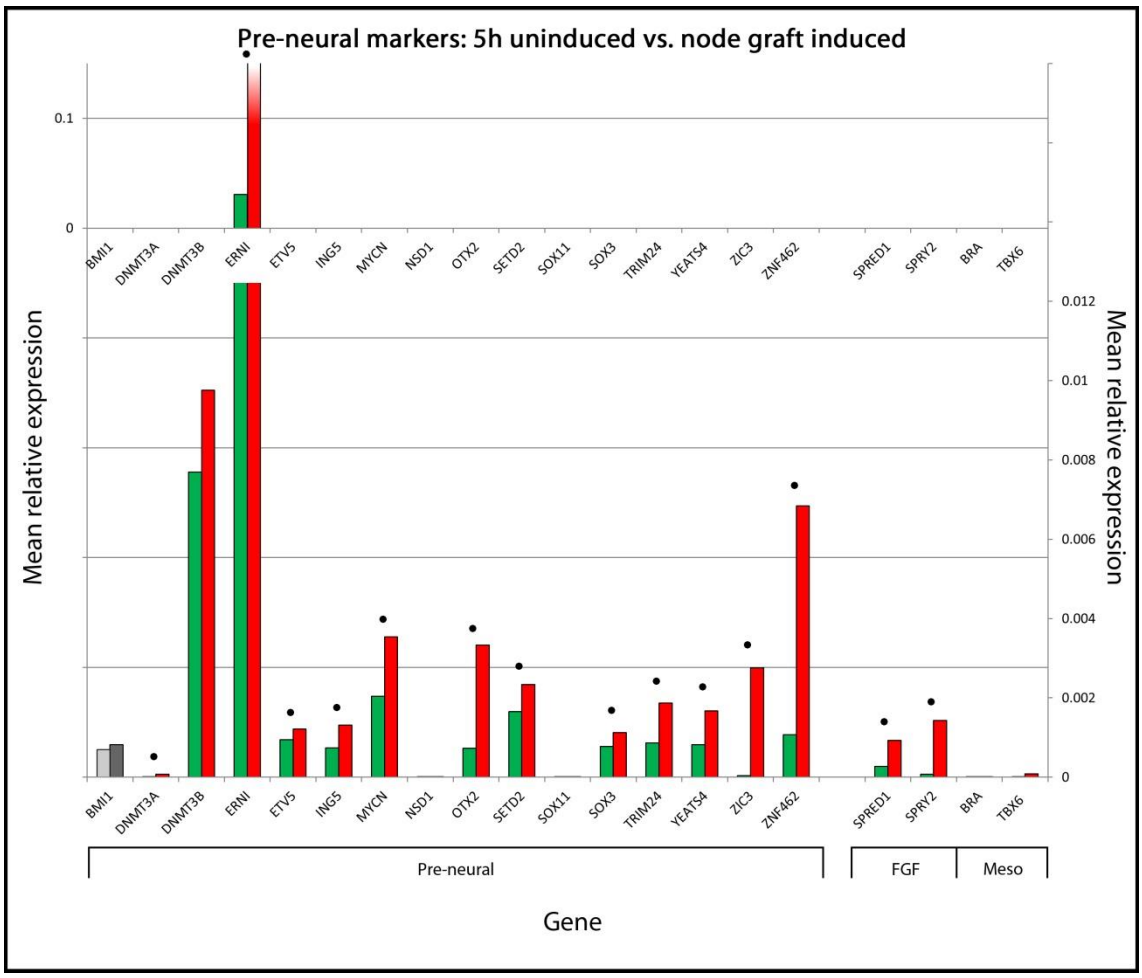

Figure 5.16: The induction of pre-neural markers after 5h of a grafted node.

Gene expression, as a proportion of the mRNA count, plotted as a bar graph comparing uninduced (green or light grey) and induced (red or dark grey) conditions after 5h. For details, see Fig. 5.14.

To summarise, these pre-neural markers are upregulated alongside ERNI and SOX3, and therefore are among the earliest responses to neural induction. ERNI, MYCN, OTX2, TRIM24, ZIC3 and ZNF462 are all induced after 1h and continue to be upregulated over 3h and 5h, when additional pre-neural markers are progressively acquired. All pre-neural markers are induced by 5h, except BMI1 which is only weakly induced by a grafted node. Therefore an early event during neural induction includes the upregulation of transcription factors and chromatin modifiers which confer pre-neural “border-like” character to the ectoderm progressively over 1-5h.

To verify whether similar transcriptional changes can also be detected by in situ hybridisation, a time-course of TRIM24 induction by a node graft was assessed over the same period. TRIM24

encodes a protein which interacts with the AF2 domain of nuclear receptors (Tsai *et al.*, 2010) and we chose to verify its induction because it was predicted by NanoString to be among the earliest responses. TRIM24 transcripts were not detected by in situ hybridisation after 1h of signals from a grafted node (Fig. 5.17A, A'), but could be observed in all cases after 3h (Fig. 5.17B, B') and 5h (Fig. 5.17C). Therefore NanoString analysis comparing induced and uninduced tissue predicts appropriate transcriptional changes during neural induction, but is more sensitive to detect responses earlier, at levels which cannot be observed by in situ hybridisation.

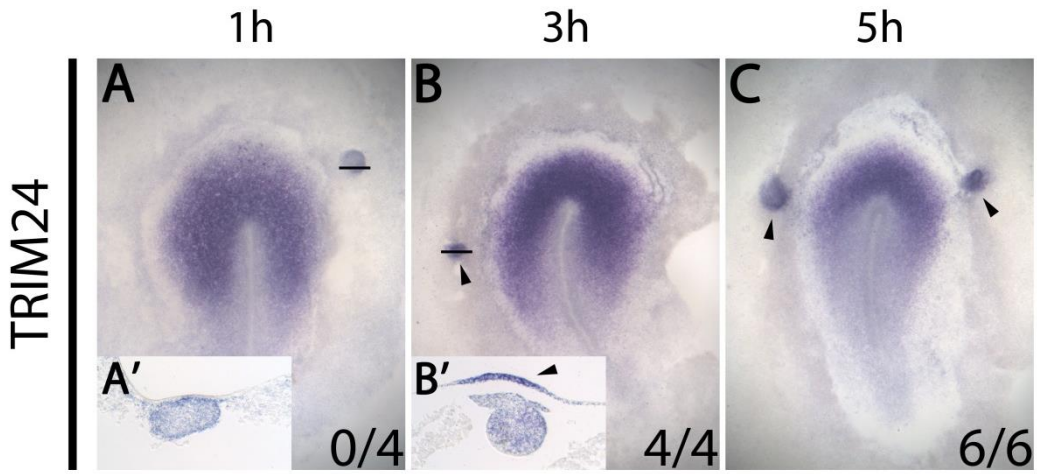

Figure 5.17: A time-course of TRIM24 induction by grafts of Hensen's node.

The induction of TRIM24 by a Hensen's node was examined after 1, 3 and 5h of exposure to a node graft. No induction was observed after 1h (A, A'; 0/4) by in situ hybridisation, staining at this time point is observed only in the grafted node itself. Instead, transcripts are detected in induced epiblast tissue after 3h (B, B'; 4/4) and 5h (C; 6/6). Lines in A and B mark the level at which sections A' and B' were taken.

5.2.2.2 FGFs induce pre-neural markers within 5h

The similarity of these pre-neural markers to ERNI and SOX3, in terms of the timing and location of their expression, raises the possibility that they are co-regulated. Since ERNI and SOX3 are already known to be induced by FGF8 (Streit *et al.*, 2000), we tested whether other pre-neural markers are also regulated by FGF signals. (Fig. 5.18-5.19 are also provided as a slideshow on the accompanying CD; see Appendix 12.)

Beads soaked in FGF8b were grafted for 5h to a competent region of the area opaca that normally responds to signals from a grafted node. The relative expression of markers in FGF induced tissue was compared to their expression in uninduced tissue after 5h of culture (Fig. 5.18). As previously demonstrated (Streit *et al.*, 1998, Streit *et al.*, 2000), ERNI and SOX3 are upregulated after 5h of FGF signals (Fig. 5.18). In addition, FGFs are also sufficient to induce BMI1, DNMT3B, ETV5, ING5, MYCN, SETD2, TRIM24, YEATS4, ZIC3 and ZNF462. FGFs are insufficient to induce OTX2, as previously reported (Albazerchi and Stern, 2007). These responses are accompanied by the upregulation of FGF signalling targets SPRY2 and SPRED1, but also Brachyury and TBX6.

The expression of these markers after a node graft was also assessed when FGF signals are inhibited by SU5402 (Fig. 5.19). The expression of almost all pre-neural markers is repressed by FGF inhibition. ING5, OTX2, YEATS4 and ZIC3 are robustly downregulated, while BMI1, DNMT3B, ETV5, MYCN, SETD2, SOX3 and ZNF462 are downregulated weakly. ERNI and TRIM24 barely respond to loss of FGF signalling, suggesting that it is not required for their expression. This contrasts with observations that FGFs are necessary and sufficient for ERNI expression (Streit *et al.*, 2000). Although the FGF targets SPRY2 and SPRED1 are mildly downregulated, it is possible that the concentration of SU5402 used here may not effectively inhibit all targets of the FGF pathway.

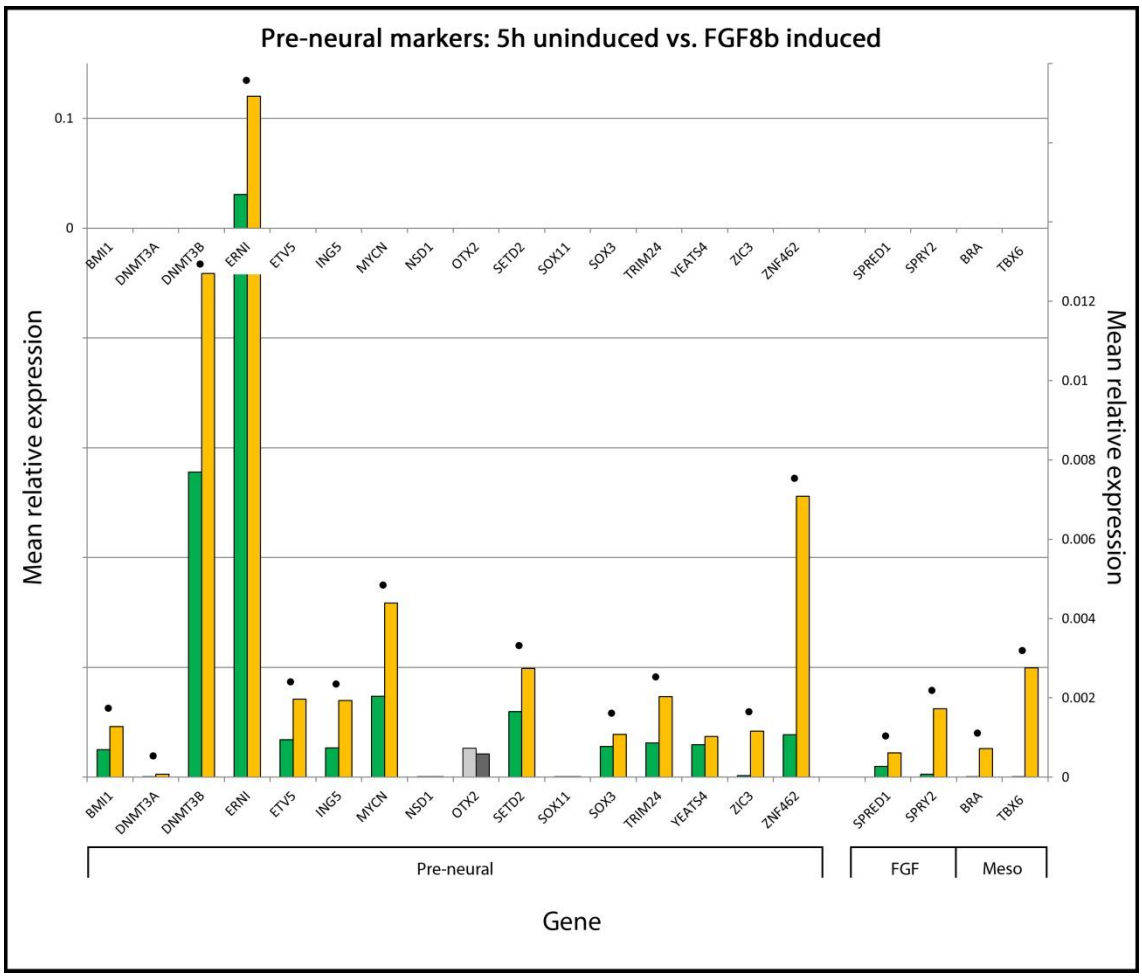

Figure 5.18: The induction of pre-neural markers after 5h of FGF signals.

Gene expression, as a proportion of the mRNA count, plotted as a bar graph comparing uninduced (green or light grey) and FGF8 induced (orange or dark grey) conditions after 5h. Differentially expressed genes (fold change >1.2 or <0.75) are shown in colour. Black dots mark statistically significant differences. High level expression changes are plotted on the primary axis (0-0.15), while lower level changes are shown on the secondary axis (0-0.012). Genes include pre-neural and mesodermal markers, but also FGF targets.

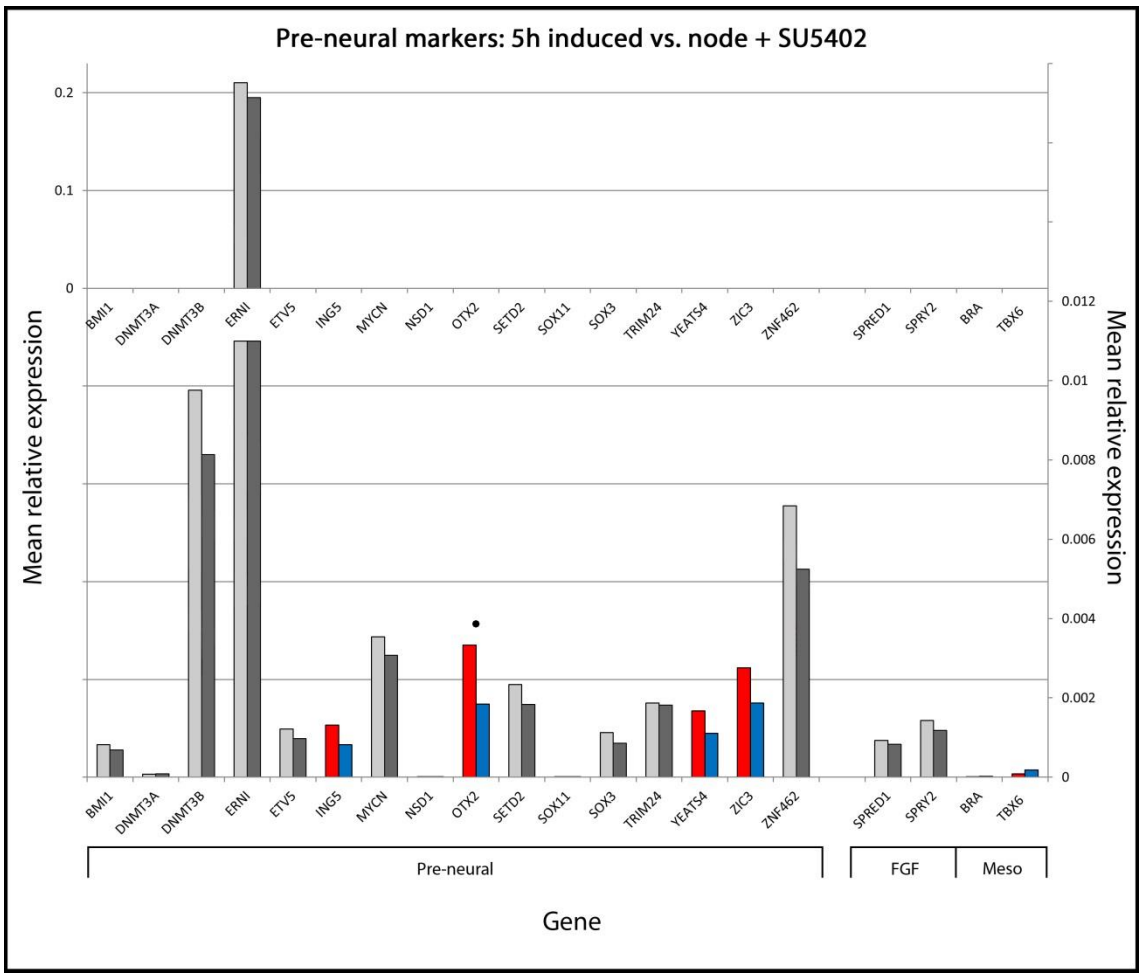

Figure 5.19: The induction of pre-neural markers after 5h of FGF inhibition.

Gene expression, as a proportion of the mRNA count, plotted as a bar graph comparing induced tissue (red or light grey) after 5h to neural induction when FGFs are inhibited (blue or dark grey). For details, see Fig. 5.18.

The changes of these pre-neural markers over time after a node graft and their response to FGF signals can be summarised as follows (Fig. 5.20). Markers are acquired progressively over 1, 3 and 5h of a node graft (Fig. 5.20A). Almost all “border-like” markers respond to some extent to perturbation of FGF signalling (Fig. 5.20B). FGFs are necessary and sufficient to induce ING5, YEATS4 and ZIC3, and necessary but insufficient for OTX2. FGF signalling may also be necessary and sufficient for BMI1, DNMT3B, ETV5, MYCN, SETD2, SOX3 and ZNF462 expression, as they are weakly downregulated upon exposure to node signals in the presence of FGF inhibition. The induction of ERNI and TRIM24 is barely affected by SU5402, suggesting that FGF signalling is sufficient, but may not be necessary for their expression. However, it is also possible that FGF signals were not inhibited enough to markedly alter their expression. Despite being upregulated to high levels in the RNA-Seq screen, NSD1, SOX11 and DNMT3A are

scarcely detected in any NanoString experiment. It is possible that the probes designed to target these transcripts do not hybridise appropriately, so their responses cannot be considered accurately.

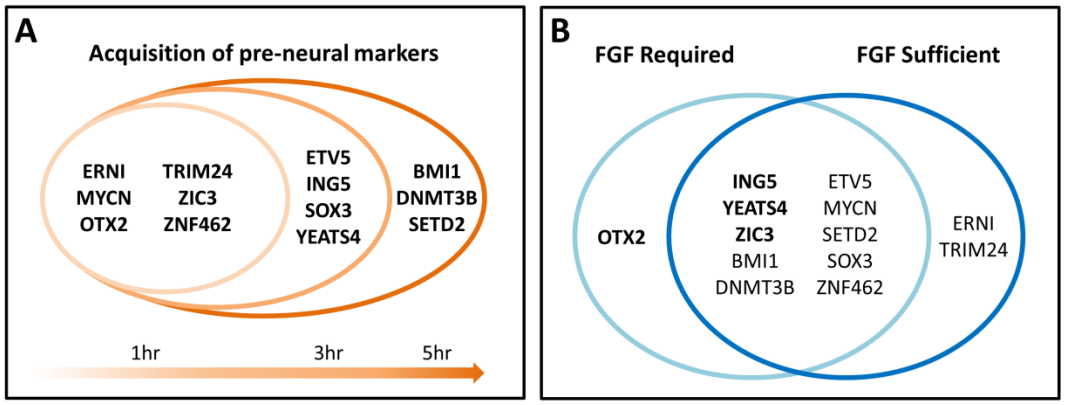

Figure 5.20: Summary of the responses of pre-neural markers to neural induction and FGFs.

Pre-neural markers are progressively induced within 1-5h of a Hensen's node graft (A). FGF signalling makes a major contribution to the regulation of pre-neural markers after 5h, but the extent of their responses differs (B).

5.3 Discussion

The identification of additional responses to neural inducing signals by the RNA-Seq screen provides new opportunities to assess more precisely the timing and signals responsible for their induction. We have successfully used NanoString technology to quantify multiple transcripts simultaneously in induced and uninduced ectoderm. Presented here are the findings for this analysis, using two panels of markers for distinct specification states.

5.3.1 A refined time-course of transcriptional responses to neural induction

To perform a more refined analysis of the neural induction time-course and the transitions through different specification states that accompany it, a panel of markers was selected. Neural markers were picked based on the similarity of their expression to known markers of distinct specification states during the neural induction cascade. ERNI- and SOX3-like genes are expressed early in the epiblast at EGKXIII and prospective neural plate at HH3-4 (Streit *et al.*, 2000). Their expression is considered to represent a pre-neural state which is induced as the earliest response to neuralising signals (Pinho *et al.*, 2011). Although similar in their early

expression, ERNI and SOX3-like markers later differ; SOX3-like markers persist in the neural plate while ERNI-like markers are downregulated and instead mark the neural plate border and pre-placodal region (Streit *et al.*, 2000). SOX2-like genes are not expressed in the early embryo (Jean *et al.*, 2015), but are first expressed in the neural plate proper around HH5-7 (Rex *et al.*, 1997) and persist in the neural tube at HH8-10 when cells are committed to a neural fate and also express SOX1 (Pevny *et al.*, 1998). Therefore the markers selected provide a useful readout of the progress through distinct specification states that accompanies neural induction (Pinho *et al.*, 2011). To define neural induction by not only the markers acquired, but also those that are lost, key downregulated responses were also included for analysis. These were separated into distinct groups: markers of the area opaca and embryonic non-neural ectoderm but also the neural plate border and pre-placodal region which are either up- or downregulated at different stages of the process.

By studying their differential expression over time in some detail after a node graft, this panel of markers was used to describe the transition from area opaca to neural fate. As expected, all ERNI-like and SOX3-like markers are induced over the first 1-3h of a grafted node. Simultaneously there is rapid and large scale downregulation of area opaca, non-neural ectoderm and neural plate border markers including TFAP2A, GATA2, MSX1, DLX5, GRHL2, GHRL3 and KRT19. Therefore even within a very short time frame, potent signals from Hensen's node induce major transcriptional changes in ectodermal tissue.

Very little change is observed in the ectoderm between 3-5h. The initial responses observed over the first 1-3h are maintained and reinforced, but no new markers are induced. Subtle changes are next observed after 7h, when later neural markers including SOX2, GLI2, GLI3, ZEB2, ZNF423 and LHX5 start to be upregulated, though only at very low levels. It is not until 9h that these are robustly upregulated, while SOX1 can only be detected after 12h. Over this period, markers of non-neural ectoderm, the area opaca and neural plate border are consistently downregulated, but PPR markers including EYA2, SIX1 and SIX3, which are expressed in the anterior neural tube, start to be induced. Although ERNI-like markers CITED4, ETV4, MAFA and PRDM1 are upregulated throughout the time-course, their expression progressively decreases in induced tissue over 7-12h, correlating well with their general clearance from the neural plate after HH4-5 (Streit *et al.*, 2000). Another ERNI-like gene, TFAP2C follows the same expression dynamic but at different levels as it is only weakly upregulated over 1-5h, before being completely downregulated later.

Overall, markers for specific states and stages in the embryo are differentially expressed at the time points we would predict; pre-neural markers between 1-5h, early neural markers

between 7-9h and later neural markers between 9-12h. Non-neural markers are downregulated quickly in response to Hensen's node and not expressed again later.

5.3.2 A refined time-course of signalling responses during neural induction

Transcriptional readouts of selected signalling pathways also respond quickly to neural inducing signals. AXIN2, an endogenous reporter of the WNT pathway, is robustly downregulated after 1h, as are GATA2 and MSX1, BMP signalling targets. These findings suggest that node grafts quickly inhibit signalling via the BMP and WNT pathways. The retinoic acid receptor RARB is also downregulated within 3h, indicating that retinoid signalling, at least via this receptor, may be repressed. Known FGF targets including ERNI, SOX3 (Streit *et al.*, 2000), ETV4 (Lunn *et al.*, 2007) and SPRY2 (Sivak *et al.*, 2005) are upregulated within 1-3h, reiterating the prominence of early FGF signals during neural induction. In addition, upregulation of the receptor PTCH2 (Pearse *et al.*, 2001) within 1-3h suggests that cells responding to neural induction also integrate signals from the hedgehog pathway. These responses occur quickly after exposure to a grafted node and are then maintained over the remaining time-course. Although signalling by other pathways may also be altered, these selected markers provide possible clues about the signals to which cells are exposed. Responding cells seem to be integrating a mixture of FGF and hedgehog signals at the same time that signalling by BMPs, WNTs and retinoic acid appears to be inhibited.

5.3.3 FGFs are a major contributor to the induction of early responses

FGFs are already known to be among the earliest signals during neural induction. They are necessary and sufficient to induce expression of the earliest neural markers ERNI and SOX3 (Streit *et al.*, 2000), and are required for SOX2 expression (Linker and Stern, 2004, Delaune *et al.*, 2005). To evaluate the contribution of FGFs to neural induction, the response of markers already studied in time-course was assessed after FGF perturbation. FGFs are sufficient and necessary for almost all early responses to neural induction after 5h. We also demonstrate for the first time, that FGFs are sufficient and necessary to downregulate non-neural markers including GRHL2, TFAP2A, GRLH3, VGLL1, MSX1 and GATA2 rapidly. Therefore FGFs contribute instructively to the onset of neural induction by regulating rapid and striking transcriptional changes over the first 5h.

However, there is evidence to suggest they are not the only signals acting at these stages. FGFs are required but not sufficient to induce expression of CITED4. Conversely, they are sufficient

but not required to regulate STOX2, TFAP2C and HIC2. Furthermore, DLX5 (a downregulated marker) is dramatically upregulated by FGF activity (McLarren *et al.*, 2003, Litsiou *et al.*, 2005), suggesting that other signals normally prevent DLX5 from responding to Hensen's node as a source of FGFs. FGFs are also potent inducers of ZNF423 after 5h, a marker which is normally only upregulated after 7-9h of signalling from a node graft. It is possible that other signals normally prevent ZNF423 from responding to FGFs until later. In addition, PRDM1 is upregulated both by node signals when FGF is inhibited and in response to FGF alone, raising the possibility that it is normally regulated by signals that compete with FGF ligands. This implicates IGFs, EGFs and HGFs, which also activate the MAPK pathway and have been previously been suggested to play a role in neural induction (Streit *et al.*, 1995, Kretzschmar *et al.*, 1997, Streit *et al.*, 1997, Kretzschmar *et al.*, 1999, Pera *et al.*, 2003, Aubin *et al.*, 2004, Kuroda *et al.*, 2005). So, although FGFs are dominant in regulating the early responses to neural induction, they are not the only signals present and active within the first 5h.

5.3.4 FGFs continue to be required for later responses to neural induction

While FGFs make a significant early contribution to neural induction, our analysis also reveals that FGFs continue to regulate responses after 9h. They are still sufficient and required to induce expression of ETV4, SOX3 and MTA1 and inhibit GRHL2, GATA2, TFAP2A and VGLL1. However, they are sufficient but no longer required to regulate ERNI, MAFA and GRHL3, suggesting that other signals are now involved in maintaining these responses. FGFs are sufficient for ZNF423 expression but are only required for the expression of other later neural markers including GLI2, GLI3, ZEB2, LHX5 and LMO1. As shown previously (see Chapter 3.2.3), TRKC is relatively FGF independent but so is SOX2. This is unexpected as SOX2 expression has hitherto been shown to require FGFs (Linker and Stern, 2004, Delaune *et al.*, 2005). It is possible that SU5402 treatment is no longer sufficient to reduce SOX2 and SPRY2 expression effectively after 9h, especially if these genes integrate signals from many other pathways. However, the continued inhibition of ETV4 and SOX3 expression would argue against this. To clarify whether SOX2 requires FGF signals it will be important to repeat this experiment using a higher concentration of SU5402 to inhibit FGFs effectively even after longer culture periods. To confirm these results, it will also be necessary to assess FGF inhibition using another inhibitor such as PD173074, as SU5402 is not specific for FGFR1 and can also inhibit signalling via VEGFR2, PDGFRβ and EGFR. Clearly though, FGF signals are required for the expression of later neural markers but are insufficient to induce new responses after 9h. So it seems that FGFs make a more minor contribution to neural induction after 9h. In the future, it will also be

important to use inhibitors which selectively target the MAPK, PI3K and PLCγ pathways downstream of FGFRs, to determine which intracellular cascades regulate specific markers.

Although we suggest that FGF signalling is sufficient to regulate neural responses, the FGF gain-of function experiments must also be considered with some caution. Despite prior verification by in situ hybridisation that the concentration of FGF8b does not induce Brachyury expression (Appendix 9), NanoString is more sensitive in detecting an increase in Brachyury and TBX6 expression. If FGFs induce mesoderm, then the responses observed may not be direct. However, TBX6 is also normally expressed in the posterior epiblast of the pre-streak embryo at EGKXII-XIII (Fig. 4.17F); before mesoderm is induced. Therefore it is expressed transiently in epiblast cells fated to contribute to neural tissue, as well as cells that later form mesoderm (Hatada and Stern, 1994). Since TBX6 is at least transiently expressed during neural induction, it is possible that its upregulation after 5h actually reflects a normal ectodermal response to FGF signals and not necessarily the formation of mesoderm. In support of this, mesodermal cells which can be induced by high FGF concentrations (Streit and Stern, 1999, Linker and Stern, 2004) were never observed around the grafted beads. Even so, we cannot exclude the possibility that mesoderm is induced. To resolve this issue it is necessary to repeat FGF gain-of function experiments with lower FGF8b concentrations and also to assess expression of other definitive mesodermal markers such as MIXL1 (Peale *et al.*, 1998, Stein *et al.*, 1998) and Paraxis (Burgess *et al.*, 1995).

5.3.5 FGF signalling may cross-talk with other pathways

Within 3h of signals from a node graft, dramatic changes are also observed in the expression of reporters of other signalling pathways. FGF signalling contributes to these as 5h of FGF activity is sufficient and necessary to upregulate PTCH2 but downregulate GATA2 and MSX1. In addition, it is sufficient but not required to downregulate RARB and AXIN2. After 9h it continues to be important for these responses, though it is now only sufficient for SPRY2 and PTCH2 expression and AXIN2 and RARB repression. Therefore at early and later stages of neural induction, FGFs significantly influences the expression of BMP, WNT, retinoic acid and hedgehog pathway targets.

From these experiments, we cannot distinguish whether these effects are a result of FGF cross-talk with other signalling pathways, or their direct regulation of these targets. However, the ability of FGFs to inhibit BMP signalling has previously been demonstrated and integrated into the default model (Pera *et al.*, 2001, Pera *et al.*, 2003) through the convergence of FGF signalling on SMAD1 (Kretzschmar *et al.*, 1997, Kretzschmar *et al.*, 1999). The proposed model

suggests that MAPK activation leads to phosphorylation of the SMAD1 linker region by ERK, thus preventing its translocation to the nucleus and therefore BMP signalling. Our observations that FGFs can effectively acts as BMP inhibitors do agree with these suggestions, but we cannot determine the mechanism of action. Given the rapid and robust contribution of FGF signals to BMP inhibition, it is difficult to argue for the proposed sufficiency of endogenous BMP antagonists during neural induction (Smith and Harland, 1992, Lamb *et al.*, 1993, Hemmati-Brivanlou *et al.*, 1994, Hemmati-Brivanlou and Melton, 1994, Sasai *et al.*, 1994, Sasai *et al.*, 1995, Piccolo *et al.*, 1996), as originally suggested by the "default" model (Hemmati-Brivanlou and Melton, 1997). Future experiments perturbing the BMP pathway using endogenous antagonists are necessary to determine their relative impact on the expression of these markers, and therefore the overall process.

We also demonstrate that FGFs are sufficient, but not necessary to downregulate RARB over 5 and 9h. FGFs are already known to downregulate RARB as one of the mechanisms by which they antagonise retinoid signalling (Mercader *et al.*, 2000, Olivera-Martinez and Storey, 2007). However we cannot distinguish whether retinoid signalling is inhibited globally, just via RARB or whether there is a requirement for only low retinoid levels. The retinoic acid synthesising enzymes ALDH1A1 and ALDH1A2 (also known as RALDH1 and RALDH2 respectively) (Blentic *et al.*, 2003, Cui *et al.*, 2003, Reijntjes *et al.*, 2005) are not expressed in the prospective neural plate, while ALDH1A1, ALDH1A3, ALDH3B1 and ALDH6 were generally downregulated in the RNA-Seq screen (Appendix 8). These findings perhaps point towards a general reduction in retinoid signalling over 5-12h. This seemingly contradicts suggestions that retinoic acid is required for neural development (Chen *et al.*, 1992, Chen and Solursh, 1992, Albazerchi and Stern, 2007, Stavridis *et al.*, 2010), though as its contribution has been predicted be very early, it may be necessary to assess the contribution of retinoic acid much earlier than 5h. FGFs are also sufficient but not required for AXIN2 downregulation, so other factors must normally inhibit the WNT pathway. Certainly the organizer is a potent source of WNT antagonists including DKK1 (Foley *et al.*, 2000) and Cerberus (Zhu *et al.*, 1999), which probably contribute to this. As with BMP antagonists, further experiments are required to evaluate the contributions of endogenous WNT antagonists and retinoid signalling and/or inhibition to neural induction.

It is possible that later neural markers are simply induced as a result of accumulating step-wise responses to preceding signals. However, increasing evidence implicates the hedgehog pathway later during neural induction. FGFs are sufficient and necessary to upregulate the hedgehog pathway receptor PTCH2 (Pearse *et al.*, 2001) after 5h and sufficient but no longer necessary for its maintenance after 9h. This suggests that FGFs initially facilitate hedgehog

signalling by inducing PTCH2, before its expression is later maintained by sonic hedgehog from Hensen's node and notochord (Levin *et al.*, 1995). This observation resembles recent findings that FGFs behave as competence factors for SHH-mediated induction of floor plate markers in the neural tube (Sasai *et al.*, 2014). It also positions hedgehog signals as possible regulators of later markers and particularly the transition from pre-neural to neural specification, especially as FGFs are required, but insufficient for expression of hedgehog effectors and SOX2-like markers GLI2 and GLI3 after 9h. Therefore it will be particularly interesting to assess the specific contributions of hedgehog signalling to neural induction.

Although these readouts illustrate only a handful of the signalling events that accompany neural induction, they provide evidence that FGF signals could be responsible for the inhibition of BMP, WNT and retinoid targets observed after a Hensen's node graft. Many of the changes described occur quickly (within 1-3h of a grafted node) and persist until 12h. Therefore modulation of BMP, WNT and retinoid signalling by FGFs may have ongoing consequences for downstream events in the neural induction cascade. Given the possible contribution of FGF signals to these changes, a thorough analysis of the contributions of endogenous BMP (Smith and Harland, 1992, Lamb *et al.*, 1993, Hemmati-Brivanlou *et al.*, 1994, Sasai *et al.*, 1994, Sasai *et al.*, 1995, Piccolo *et al.*, 1996, Fainsod *et al.*, 1997) and WNT antagonists (Zhu *et al.*, 1999, Foley *et al.*, 2000, Wilson *et al.*, 2001) is necessary as these have often been considered key regulators of neural induction. The possible contributions or effects on calcium (Leclerc *et al.*, 2011, Papanayotou *et al.*, 2013) and Notch (Linker *et al.*, 2009) signalling have also not been considered here. In the future it will also be necessary to test the effects of combinations of signals, but at the time of thesis submission, experiments have been conducted to test the contribution of BMP and WNT inhibition to neural induction and are waiting NanoString processing.

5.3.6 Neural induction begins with a "pre-neural/pre-border" state

To monitor the changes in specification that accompany the onset of neural induction, we decided to focus on the earliest responses to neuralising signals. In particular, evidence from the neural plate marker SOX3 and NPB/PPR marker ERNI (Streit *et al.*, 2000), suggested that the neural plate and PPR might derive from a common "border-like" domain (Streit, 2008), which exists before gastrulation (Stern, 2004). To determine whether this is a more general characteristic of neural induction, we sought to identify other ERNI and SOX3-like markers within the RNA-Seq screen data. This was done by focusing specifically on early responses to a node graft that were common to a microarray screen of PPR tissue conducted by Andrea

Streit's group at King's College London. Analysis of their expression at EGKXII-XIII and HH3-4 reveals that 80% of the markers selected (including ERNI and SOX3), are expressed strongly in the epiblast at EGKXII-XIII and later in the prospective neural plate at HH3-4. Therefore, all markers are expressed in a striking ERNI/SOX3-like pattern. As so many border markers define this pre-neural state, it suggests that it can be more generally characterised as "border-like".

The 14 new markers common to this pre-neural state include the transcription factors ETV5, SOX11, MYCN, OTX2, and ZIC3 and putative chromatin modifiers BMI1, DNMT3A, DNMT3B, NSD1, SETD2, TRIM24, YEATS4 and ZNF462. NanoString experiments further confirm that these are induced within 5h of signals from a node graft, but even within this brief window, responses can be separated across 1, 3 and 5h. Therefore, neural induction begins with the expression of pre-neural markers which contribute to a "border-like" specification state. This goes some way to explain observations that, like the neural plate border (Streit and Stern, 1999, Bailey *et al.*, 2006), the pre-streak epiblast can respond to BMP signalling (Wilson *et al.*, 2000, Wilson *et al.*, 2001) and differentiates into a lens when placed in culture (Stower, 2012). Considering that the expression of many markers from the 5h time point of the RNA-Seq screen have not yet been confirmed, and the PPR microarray is limited by the probes present on the array chip, it is likely that more markers that define this state are yet to be described.

However, we already know from Chapter 4 that there are many other markers with similar expression patterns. The ERNI-like markers CITED4 (Fig. 4.6U-Y), ETV4 (Fig. 4.8K-O) and MAFA (Fig. 4.12A-E) and PRDM1 (Fig. 4.14P-T) and SOX3-like markers MTA1 (Fig. 4.12U-Y), SOX13 (Fig. 4.16U-Y), STOX2 (Fig. 4.17A-E) and TCF7L2 (Fig. 4.17Z-AD) were already selected to characterise the earliest responses to neural induction and are also regulated by FGFs. Additional markers include CRIP2 (Fig. 4.6Z-AD), DACH1 (Fig. 4.7A-E) and KDM4A (Fig. 4.11A-E), which are expressed in the NPB or PPR at later stages but were only identified in the RNA-Seq screen and not the PPR microarray perhaps because RNA-Seq is more sensitive. The PPR transcriptome is currently being reassessed using RNA-Seq, but a considerable body of evidence already exists from the expression patterns presented here to suggest that the pre-streak epiblast transcriptionally resembles the neural plate border.

However we also show that new border markers DMBX1 (Fig. 4.7F-J), LHX5 (Fig. 4.11F-J) and MEIS2 (Fig. 4.12P-T), and classical border/PPR markers such as SIX3 (Fig. 4.15P-T) or EYA2 (Fig. 4.8U-Y) are not among the earliest responses to neural inducing signals and are not expressed in the pre-streak embryo. These are expressed after HH4 in the embryo or after 9h of signals from a grafted node. So, although the pre-streak epiblast may be "border-like", it does not

express mature PPR or border markers, suggesting that it has a more primitive or "pre-border" specification.

5.3.7 FGFs are sufficient and necessary to induce "pre-neural/pre-border" markers

While we already demonstrate the importance of FGFs for the onset of neural induction (see Chapter 5.2.1.2), we also show that they are necessary and sufficient to induce ING5, YEATS4, ZIC3 and probably also BMI1, DNMT3B, ETV5, MYCN, SETD2 and ZNF462. ETV5 is a known target of FGF signalling (Lunn *et al.*, 2007) and in agreement with previous work (Streit *et al.*, 1998, Streit *et al.*, 2000) we confirm that FGFs are necessary and sufficient to induce SOX3. They are required, but not sufficient for the expression of OTX2, which can only be induced by a combination of FGFs together with BMP and WNT inhibition (Albazerchi and Stern, 2007). Despite this, FGFs seems to be the major signal regulating this early state, as they induce almost all pre-neural markers. However, as mentioned already, the FGF gain-of-function experiments described here should be considered with caution.

Although this study describes neural induction as a set of responses induced by Hensen's node, the hypoblast is the source of signals necessary to initiate neural induction before gastrulation. Hypoblast grafts can transiently induce early markers such as ERNI, SOX3 and OTX2 (Albazerchi and Stern, 2007), and it is a known source of FGF8, retinoic acid and the WNT antagonists Crescent, Cerberus and DKK1 (Foley *et al.*, 2000). To verify whether early pre-neural responses to a Hensen's node graft accurately reflect events during endogenous neural induction, it will be necessary to assess hypoblast function in the context of these new markers. A direct comparison of the responses induced by the hypoblast and by Hensen's node will confirm the earliest responses and separate the contribution of particular signalling pathways to neural induction. It would also clarify a role for the hypoblast, which is able to induce a "pre-neural/pre-forebrain" state (Foley *et al.*, 2000, Albazerchi and Stern, 2007) and confirm whether some of the FGF-regulated responses we detect are a possible consequence of the caudalising effect of potent FGF signalling (Storey *et al.*, 1998), as may be the case with DLX5 (Litsiou *et al.*, 2005) and MSX1 (Streit and Stern, 1999), which are expressed caudally (Fig. 4.22F-J and 4.28F-J) and aberrantly upregulated by FGFs in our gain-of-function experiments.

5.3.8 FGFs may regulate gene expression and chromatin organisation via chromatin modifiers during neural induction

Changes in chromatin structure are predicted to accompany transitions between specification states, so it is satisfying that chromatin modifiers are identified as early responses to neuralising signals. Furthermore, we demonstrate a specific link between cell signalling and chromatin structure and activity, via the induction of specific chromatin modifiers such as TRIM24, ING5, YEATS4, DNMT3B and SETD2. FGF signals are necessary, and probably also sufficient for their induction. This is especially critical in light of recent findings that FGF signals regulate chromatin organisation at neural differentiation loci such as PAX6 and IRX3 (Patel *et al.*, 2013) and that FGFs are necessary and sufficient to induce HDAC1 expression in neural precursors of the spinal cord (Olivera-Martinez *et al.*, 2014). Our findings that FGFs induce a broad range of chromatin modifiers suggest that this may be a general mechanism by which FGF signals indirectly regulate gene expression.

Unfortunately, we were unable to quantify expression of DNMT3A, NSD1 and SOX11 accurately during neural induction or in response to FGF gain- and loss-of-function experiments. These targets were barely detected in any assay. With the knowledge that they are expressed strongly in the pre-streak embryo and are predicted to be highly expressed by the RNA-Seq screen, we must assume that the NanoString probes designed to recognise them do not hybridise appropriately. However, their spatio-temporal expression patterns predict that they too are probably co-regulated by FGFs. The possibility that DNMT3A may also be a target of FGF signalling is of particular interest since it is known to interact at SOX3 and SOX2 loci (Hu *et al.*, 2012), which require FGF signals for their expression (Streit *et al.*, 2000, Linker and Stern, 2004).

5.3.9 "Pre-neural/pre-border" specification; implications for pluripotency

This study ultimately takes advantage of Hensen's node ability to transform ectodermal cells of the area opaca from an extra-embryonic fate towards a neural specification. The earliest steps in this process re-programme cells to adopt a pre-neural state which exists in the embryo at EGKXII-XIII, before gastrulation. The expression territory of pre-neural markers covers a broad domain of epiblast cells fated to form the future nervous system, but also many other cell types (Hatada and Stern, 1994). Therefore, pre-neural markers are common to the initial development of multiple cell lineages that arise later.

This raises the possibility that the combination of pre-border transcription factors and chromatin modifiers described here might actually define a more general pluripotent state

that exists in the early ectoderm, directly implicating them in cellular and epigenetic reprogramming during pluripotency. Many of these factors have already been studied in this context, lending considerable support to this idea. For example PRDM1 and TFAP2C form part of a complex sufficient to reset the epigenome towards a basal state (Magnúsdóttir *et al.*, 2013), while ERNI has been associated with pluripotency (Papanayotou *et al.*, 2008, Jean *et al.*, 2013) and is expressed in chick embryonic stem cells while they self-renew (Acloque *et al.*, 2001, Papanayotou *et al.*, 2008, Intarapat and Stern, 2013). Furthermore, SOX3 expression in chick is more similar to SOX2 in the mouse, another transcription factor of the SOXB1 family (Kamachi *et al.*, 2000), which has also been associated with pluripotency (Takahashi and Yamanaka, 2006) or multipotency (Avilion *et al.*, 2003). Alternatively, some responses may reflect an early exit from a pluripotent state, as DNMT3A and DNMT3B regulate NANOG during the differentiation of pluripotent cells (Li *et al.*, 2007) and OTX2 is critical for exit from ground state pluripotency (Yang *et al.*, 2014). Therefore, future efforts to confirm additional markers and the specific signals from Hensen's node that induce this state are of fundamental importance, not only to neural induction during embryonic development, but possibly for reprogramming and pluripotency.

5.4 Conclusions

Having assessed the precise timing and signals responsible for regulating key responses, we find that FGF signals make a significant contribution to neural induction. Within the first 5h, they induce most pre-neural markers, but are not sufficient or required for all early responses, suggesting that other signals are also important to initiate neural induction. Later, FGFs continue to be required but are insufficient to induce new responses. Therefore they make a major early contribution to the onset of neural induction, but their role becomes more minor as additional signals become involved.

FGFs also have a major early and persisting influence on BMP, WNT and retinoid pathways and they may facilitate later hedgehog signalling by inducing PTCH2. Increasing evidence suggests hedgehog ligands, receptors and target genes are expressed at the appropriate time to influence the induction of later neural markers such as SOX2. Therefore hedgehog signalling might be a crucial missing piece to the neural induction puzzle.

We also demonstrate that the induction of a "pre-neural/pre-border" state is among the earliest events during neural induction. This largely occurs in response to FGF signals which are necessary and sufficient to induce the transcription factors ETV5, ERNI, SOX3, MYCN, and ZIC3

and chromatin modifiers BMI1, DNMT3B, ING5, SETD2, TRIM24, YEATS4 and ZNF462, which define this state.

Although such genes are induced as responses to neuralising signals from Hensen's node, their expression in the early embryo marks cells fated to contribute to other lineages as well as the future nervous system. This raises the possibility that markers of this "pre-neural/pre-border" state actually define a more general pluripotent state that exists during early development. If so, then these early responses to signals from Hensen's node have implications for reprogramming during pluripotency as well as the initiation of neural induction.

Chapter 6: General Discussion

6.1 The timing of neural induction

Until now, it has been difficult to determine precisely how and when neural induction occurs. Since induction of an ectopic nervous system by a graft of Hensen's node appears to follow similar morphological and molecular events to the embryo's own neural plate (Pinho *et al.*, 2011), the node graft assay has proved to be a useful tool to study the process. Our results confirm that the earliest responses to a grafted node occur within the first 1-3h (Pinho *et al.*, 2011), but that 9h of signals are required to induce the definitive neural marker SOX2 robustly and 12h to induce SOX1 and commit cells to a neural fate. This provided the first evidence that cells acquire a neural fate as a consequence of molecular steps that occur within 0-12h of a node graft. All transcriptional responses to neural induction that occur within this period were then identified using RNA-Seq. Thousands of differentially expressed transcriptional responses to neural induction were detected, including 482 transcriptional regulators. A proportion of these were verified by in situ hybridisation, revealing that they are expressed appropriately: upregulated genes are expressed in neural tissue at some stage, while downregulated markers are relatively absent. Furthermore, markers are detected at the appropriate time after a node graft, compared to their endogenous expression. This confirms that the genes identified represent accurate markers for the sequence of events that occur during neural induction in the normal embryo, revealing that neural induction is accompanied by complex transcriptional changes over time.

By assessing a subset of key markers in greater detail, neural induction can now be described as follows. It begins with the induction of ERNI-like and SOX3-like markers within the first 3h of a node graft; markers which are already expressed the epiblast of normal EGKXII-XIII embryos. Their patterns of expression later in development suggest that this set of markers defines a pre-neural state prior to gastrulation that has "neural plate border-like" properties. FGFs, which are probably secreted from the hypoblast, are largely responsible for the induction of these pre-neural markers, but they also act to prevent expression of non-neural ectoderm markers. These early responses are reinforced and maintained between 3-5h of a node graft, as they are in the prospective neural plate of normal embryos at HH3-4. Later neural markers including SOX2 are first induced after 7h but only at very low levels, which correlates closely with the start of neural plate formation around Hensen's node at HH4. Neural plate markers and markers of anterior-posterior patterning such as SIX3 are robustly expressed by HH5-6, or after 9h of a node graft. However cells specified as neural plate are not committed to this fate until they have received at least 12h of signals from a grafted node. This corresponds with the

onset of SOX1 expression, which first occurs in the neural tube at HH8-9. Therefore neural induction begins with the simultaneous induction of pre-neural markers and repression of non-neural markers. These responses are maintained as additional markers are acquired which confer neural specification and patterning, before concluding with neural commitment.

Furthermore, our analyses highlight the significant contribution of FGF signalling in launching this process. Although they are not the only early signal, FGFs induce some of the earliest responses but also contribute to the repression of non-neural markers, including typical BMP target genes. Therefore, consistent with previous observations (Wilson *et al.*, 2000, Pera *et al.*, 2001), FGFs appear to act at least partially as BMP inhibitors, though our experiments do not distinguish the mechanism by which this occurs. Although we are yet to test the specific contribution of endogenous BMP antagonists to the expression of these markers, they are already known as insufficient to induce a number of the earliest responses (Streit *et al.*, 2000, Sheng *et al.*, 2003, Gibson *et al.*, 2011, Pinho *et al.*, 2011, Papanayotou *et al.*, 2013). This confirms the importance of BMP/SMAD1-independent FGF signalling (Launay *et al.*, 1996) (Sasai *et al.*, 1996, Linker and Stern, 2004, Delaune *et al.*, 2005, Stavridis *et al.*, 2007) as an early step in neural induction. However BMP antagonists do seem to be required later (Linker and Stern, 2004), when they maintain SOX3 expression after 5h of a grafted node (Streit *et al.*, 1998). However additional signals must be required, since no combination of BMP antagonists and FGFs is sufficient to induce the neural plate marker SOX2 (Streit and Stern, 1999, Linker and Stern, 2004, Linker *et al.*, 2009).

Of the responses we describe, no individual event in isolation seems to be sufficient for cells to acquire a neural fate. It cannot be just an early but reversible bias towards a neural fate nor the onset of SOX2 expression in the neural plate, or the final commitment to neural specification. Furthermore, each of these developmental events is likely to comprise many layers of transcriptional change. As it is not possible to identify a single “inductive” event, we must consider neural induction to comprise the sum of all molecular steps which ultimately result in cellular commitment to a neural fate. Our findings indicate that neural induction occurs as a cascade of molecular events in response to multiple signals, which begins in the early embryonic ectoderm prior to gastrulation in response to FGF signals, and ends when cells acquire commitment to neural differentiation in the forming neural plate and tube. These changes occur in the embryo between EGKXII-XIII and HH8-9, within the first 30h of incubation after an egg is laid. This contrasts with the “default model” of neural induction (Hemmati-Brivanlou and Melton, 1997) which implies that a single stimulus (BMP antagonism by Chordin, Noggin or Follistatin) is sufficient for neural induction and SOX2 expression.

6.2 Neural induction begins by inducing a "pre-neural/pre-border" state with a pluripotency-related gene signature

The earliest responses to neural induction include neural plate border markers such as ERNI (Fig. 4.8A-E) (Streit *et al.*, 2000), TFAP2C (Fig. 4.32F-J) (Qiao *et al.*, 2012), PRDM1 (Fig. 4.14P-T) (Riddle *et al.*, 1995) and ETV4 (Fig. 4.8K-O) (Lunn *et al.*, 2007). These are upregulated within the first 1-3h of a node graft and their expression in the early embryonic ectoderm suggests that neural induction begins with the induction of a "pre-neural/pre-border"-like state. FGF signals are a major contributor to the induction of these early markers and probably impart "border-like" properties to the early epiblast (Streit *et al.*, 2000, Wilson *et al.*, 2000, Wilson *et al.*, 2001, Bailey *et al.*, 2006, Stower, 2012).

Although pre-neural markers illustrate transcriptional changes during neural induction, a number are also associated with epigenetic reprogramming, stem cell self-renewal or pluripotency. The pluripotency factors NANOG (Fig. 4.28U-Y) and TFAP2C (Fig. 4.32F-J) are expressed in the early embryo and prospective neural plate, though they were actually identified in the RNA-Seq screen by virtue of their later downregulation. MTA1 (Fig. 4.12U-Y) forms a complex with NANOG and OCT4 to regulate repression in stem cells (Liang *et al.*, 2008), while MYCN (N-MYC) (Fig. 4.12Z-AD), a close relative of C-MYC (one of the original "Yamanaka factors" (Takahashi and Yamanaka, 2006)), induces the pluripotency factors KLF2, KLF4 and LIN28B (Cotterman and Knoepfler, 2009). Furthermore, TCF7L1 (Fig. 4.17Z-AD) co-occupies promoter sites throughout the genome with OCT4 and NANOG (Cole *et al.*, 2008), while DNMT3B (Fig. 4.7P-T) is expressed in primordial germ cells (Rengaraj *et al.*, 2011). There is also evidence that BMI1 (Fig. 4.6A-E) (Moon *et al.*, 2011), ERNI (Fig. 4.8A-E) (Acloque *et al.*, 2001, Papanayotou *et al.*, 2008, Intarapat and Stern, 2013), ZNF462 (Fig. 4.19U-Y) (Masse *et al.*, 2011) and ZIC3 (Fig. 4.19K-O) (Lim *et al.*, 2007) also contribute to the regulation of pluripotency.

Many other markers associated with reprogramming and pluripotency which were not studied in greater detail here, are also expressed in the epiblast at EGKXII-XIII. For example the transcriptional repressor SALL1 (Fig. 4.15F-J) which interacts with NANOG to regulate stem cell pluripotency (Karantzali *et al.*, 2011), LIN28A (Fig. 4.11K-O) and LIN28B (Fig. 4.11P-T) (Yu *et al.*, 2007, Cotterman and Knoepfler, 2009, Jean *et al.*, 2015) have also been implicated. Surprisingly though the pluripotency factor OCT3/4 (Takahashi and Yamanaka, 2006, Yu *et al.*, 2007) was not identified, although it is expressed in the area opaca at the time of grafting (Lavial *et al.*, 2007) which might explain why it is not differentially expressed. Therefore the pre-streak epiblast is likely to have properties associated with pluripotency and epigenetic reprogramming.

As overall levels of transcription seem generally to be quite low at pre-streak stages, it is unusual for genes to be as strongly expressed at EGKXII-XIII, as at later stages (ERNI is an exception, as it is expressed extremely strongly before streak formation). Therefore, it is possible that some of these markers are already expressed even earlier, perhaps as early as the transcription factor CP2 in the EGKX blastoderm (Acloque *et al.*, 2004), from which tissue pluripotent stem cells can be derived (Petitte *et al.*, 1990, Pain *et al.*, 1996). Since this pre-neural state covers a broad domain of cells fated to multiple lineages in the early embryonic epiblast, we predict that neural induction begins with the acquisition of a "pre-neural/pre-border state" with pluripotent properties, which is largely induced by FGFs. To confirm if such markers contribute to pluripotency, their expression should be confirmed and functional experiments (gain- and loss-of-function) performed in embryonic stem cells and the embryo at EGKX. Given that we have only verified a proportion of new responses to neural induction by in situ hybridisation, there are likely to be many other factors associated with this state.

Alternatively, after 5h we may be detecting responses that, like OTX2 (Yang *et al.*, 2014), represent an early exit from pluripotency. Indeed, FGF inhibition is considered to promote stem cell self-renewal (Burdon *et al.*, 1999, Ying *et al.*, 2008) and FGF signalling to be an initial step towards differentiation (Chen *et al.*, 2006, Kunath *et al.*, 2007, Stavridis *et al.*, 2007, Stavridis *et al.*, 2010). Even if this is the case, many of the pluripotency associated markers, seem to still be expressed at the early stages of such a shift. Future experiments are necessary to more accurately profile the transcriptome of cells exposed to 1 or 3h of signals from a grafted node, which may provide additional pluripotency markers, but also to consider the specification state of the uninduced area opaca.

Intriguingly, some "pre-neural/pre-border" markers are also expressed later in the lens, including BMI1 (Fraser and Sauka-Spengler, 2004), ETV4 (McCabe *et al.*, 2006) and SOX3 (Matsumata *et al.*, 2005). Furthermore, ASL1 and ASL2 (encoding δ1- and δ2-crystallin), were upregulated in the RNA-Seq screen after 5h, in addition to MAFA which regulates lens differentiation (Benkhelifa *et al.*, 1998, Ogino and Yasuda, 1998, Ring *et al.*, 2000) and δ-crystallin expression (Kanai *et al.*, 2010). In addition, CP2 which is required for αA-crystallin expression in the lens (Murata *et al.*, 1998) is also associated with pluripotency in the embryonic epiblast (Acloque *et al.*, 2004). These observations suggest a surprising level of transcriptional similarity between the pluripotency-associated state of the pre-streak epiblast and neural plate border, to the specification of lens fate. Such markers probably contribute to the ability of the pre-streak epiblast (Stower, 2012), HH6 neural plate border (Bailey *et al.*, 2006) and human embryonic stem cells (Yang *et al.*, 2010) to form lentoid bodies.

6.3 Neural induction involves multiple cell fate decisions

Although acquisition of the "pre-neural/pre-border" state is integral to neural development, these early events also occur in epiblast cells which later migrate through the primitive streak between HH3-4. Therefore this "border-like" state is probably also common to early mesoderm and endoderm development. This observation further reinforces the idea that neural development does not just depend on decisions between epidermal and neural cell fates (at the neural plate border (Linker *et al.*, 2009)), but also on events that regulate the choice between neural and mesendodermal cell fates at the anterior primitive streak (Sheng *et al.*, 2003). As many downregulated responses to neural induction are markers of alternative fates, e.g. HAND1 (Fig. 4.24Z-AD) (Srivastava *et al.*, 1995) and APOA1 (Bertocchini and Stern, 2008), these and other responses may provide clues to some of the key decisions that occur in the divergence of mesodermal and endodermal lineages. Therefore, the node graft assay could turn out to be a useful tool to study embryonic pluripotency, as well as the early divergence of alternative lineages during neural induction.

Since FGFs induce a "border-like" state, a crucial function of additional signals will be to mediate its transformation to a neural plate fate. To date, LMO1 (Fig. 4.11U-Y) may be a key specifier of the neural plate as it is the only neural marker that is absent from the neural plate border. However, since many markers are common to the neural plate and its border, the downregulation of specific border markers in the neural plate could also be central to this process. Although FGFs appear to significantly inhibit BMP signalling, we confirm that they induce the border markers MSX1 (Streit and Stern, 1999) and DLX5 (Litsiou *et al.*, 2005), which are also BMP targets. As MSX1 and DLX5 are normally downregulated by a node graft, it will be particularly interesting to determine whether BMP antagonists counteract FGFs to downregulate these border markers. BMPs are known to position the neural plate border so BMP inhibition is likely to be important to define the domain that gives rise to the neural plate, especially as DLX5 misexpression in the neural plate represses SOX3 and SOX2 (McLarren *et al.*, 2003). This would fit with a permissive, rather than instructive role for BMP antagonists during neural induction, which are able to maintain SOX3 expression (Streit *et al.*, 1998), though not induce neural markers *de novo* (Streit and Stern, 1999, Linker and Stern, 2004).

6.4 Regulating the transition from pre-neural to neural specification

A key step in the divergence of neural fates from this "border-like" state occurs at HH4 when the neural plate proper arises around Hensen's node and expresses markers of neural specification such as SOX2. Indeed the onset of SOX2 expression has generally been considered the neural "inductive event" in *Xenopus* and although it is a key step in the transition to a neural fate, it alone cannot account for the entire process of neural induction. However it is currently unclear how this transition occurs.

Evidence from *Xenopus* originally suggested that BMP antagonists secreted by the organizer are sufficient to neuralise ectoderm (Smith and Harland, 1992, Lamb *et al.*, 1993, Hemmati-Brivanlou *et al.*, 1994, Sasai *et al.*, 1995, Hemmati-Brivanlou and Melton, 1997). However we now know that many experiments in the whole embryo, actually target cells that contribute to the neural plate or neural plate border. Therefore they represent an expansion of the prospective neural plate territory, and that this is not exactly equivalent to *de novo* SOX2 induction in ectodermal cells remote from the neural plate (Linker and Stern, 2004, Linker *et al.*, 2009). Furthermore, BMP antagonism is insufficient to induce neural markers in animal caps when FGF signalling is inhibited, suggesting that FGF activity is required upstream of BMP inhibition to neuralise these explants (Launay *et al.*, 1996, Sasai *et al.*, 1996, Linker and Stern, 2004, Delaune *et al.*, 2005). Therefore, animal caps are not a naïve ectoderm. Our finding that FGFs are critical to induce the pre-neural state, is consistent with evidence from *Xenopus* that FGFs function upstream of BMP inhibition during neural induction, though they too are insufficient to induce definitive neural markers even in combination with BMP antagonists (Launay *et al.*, 1996, Sasai *et al.*, 1996, Linker and Stern, 2004, Delaune *et al.*, 2005). This suggests that other signals are also necessary to mediate the transition from a "pre-neural/pre-border" state with pluripotent properties to neural specification.

To date our analyses have been unable to reveal precisely which factors might be responsible for this. No new transcriptional responses are detected between 3-5h of a node graft, just prior to the onset of SOX2 expression. Instead, pre-neural ERNI-like and SOX3-like markers are maintained. However, only a fraction of the responses to neural induction have so far been analysed in this refined time course and only after all 400 markers on the NanoString probe set have been assessed, will we be able to confirm if this is a general characteristic.

One mechanism that could contribute to SOX2 expression and neural specification after 7-9h is the simultaneous downregulation of pre-neural markers which are later absent from the neural plate. Downregulation of ERNI has already been implicated in relieving transcriptional repression at the SOX2 locus to allow expression (Papanayotou *et al.*, 2008). Particularly

interesting evidence also comes from a recent study of the transcriptional repressor PRDM1 (BLIMP1), suggesting that it normally suppresses SOX2 expression to promote germ cell fate (Lin *et al.*, 2014). We observe that PRDM1 is expressed in the EGKXII-XIII epiblast and HH3-4 prospective neural plate (Fig. 4.14P-T) but appears to clear from around the node at HH4, at precisely the time when SOX2 is upregulated. Later, when SOX2 is strongly expressed at HH6, PRDM1 is completely absent from the neural plate. Therefore PRDM1 might also serve as a molecular switch regulating the onset of SOX2 expression and neural specification during embryonic development.

Since other pre-neural genes including TFAP2C seem to be downregulated later, this may represent a general mechanism regulating the transition from a pluripotent neural precursor state to neural specification and differentiation. In fact, although FGFs seem to be required as an early neural signal in embryonic stem cells and in the embryo (Streit *et al.*, 2000, Kunath *et al.*, 2007, Stavridis *et al.*, 2007), they actually function to repress neural differentiation later (Stavridis *et al.*, 2010). Furthermore, FGF signalling can influence chromatin architecture and activity around neural differentiation loci such as PAX6 and IRX3, to repress their transcription (Patel *et al.*, 2013). Therefore the induction of early chromatin modifiers and transcriptional regulators that we observe in response to FGFs, may have the dual role of contributing to a "pre-neural/pre-border" precursor state, while simultaneously repressing the transition to neural differentiation during neural induction. Multiple layers of repression by FGF-induced pre-neural markers could build a tightly regulated switch controlling the onset of neural specification, a key step in neural development.

This raises further questions about how such FGF-mediated repression could be relieved to permit neural specification and differentiation. Retinoid signalling, which generally antagonises the FGF pathway could play a key role in this process. Retinoic acid is required to promote SOX1 expression and neural differentiation by limiting FGF signalling (Stavridis *et al.*, 2010). It may achieve this by relieving FGF-mediated chromatin compaction and transcriptional repression at neural differentiation loci (Patel *et al.*, 2013). If retinoids were required in our assays, it would reveal striking similarities between neural induction in the early embryo and neural differentiation during body axis extension. There, FGFs promote cells in the caudal stem zone to form neural precursors, but also function to prevent their differentiation (Diez del Corral *et al.*, 2003, Olivera-Martinez and Storey, 2007). FGF signals eventually induce expression of WNT8C which promotes retinoic acid mediated neural differentiation via RALDH2 (Olivera-Martinez and Storey, 2007).

However our assays suggest that neural induction is accompanied by downregulation of RARB at all stages, but we cannot determine whether this represents a general inhibition of retinoid signalling, inhibition just via the receptor RARB, or perhaps even a requirement for only low levels of retinoid signalling. This contrasts with CYP26A1 which can be induced by retinoic acid (White *et al.*, 1996, Loudig *et al.*, 2000) and is upregulated only after the 9 and 12h time points of the screen. The later timing of its induction perhaps suggests that retinoic acid signalling is more likely to play an active role at later stages, when it might be important to promote neural specification and a move towards differentiation by limiting FGFs.

Furthermore, although our assays suggest that FGFs generally induce early responses, they are also sufficient to induce ZNF423, one later neural marker. ZNF423 can integrate BMP-SMAD signalling (Hata *et al.*, 2000) but has also been implicated in mediating retinoic acid induced neural differentiation by interacting with the RAR-RXR nuclear complex (Huang *et al.*, 2009). Therefore ZNF423 could provide an important link between the FGF-mediated onset of neural induction, with the later integration of BMP and retinoic acid signals during neural specification. Like Churchill (Sheng *et al.*, 2003), it may also contribute to the acquisition of BMP signalling sensitivity that occurs in the epiblast after 5h of signals from a grafted node or source of FGFs (Streit *et al.*, 1998).

We do observe that the hedgehog pathway targets GLI2 and GLI3 are induced concurrently with SOX2 after 7h. In fact the hedgehog pathway may have a previously unappreciated role in the transition to neural specification as many components of the hedgehog pathway are expressed in the appropriate spatio-temporal manner. Furthermore our assays suggest that SHH is expressed in Hensen's node (Levin *et al.*, 1995) after the hedgehog pathway receptor PTCH2 is mildly upregulated by FGFs. Therefore early FGF signals may also function to facilitate competence to later hedgehog signals, as has been observed in the floor plate (Sasai *et al.*, 2014). The relative contribution of hedgehog signalling remains to be tested but the presence of a GLI2 binding site in a SOX2 enhancer and the loss of SOX2 expression in GLI2 deficient mice (Takanaga *et al.*, 2009) further implicates this pathway in neural induction.

In light of these observations, it will be important to evaluate the contribution of retinoid and hedgehog signalling in addition to BMP and WNT antagonism during neural induction. These pathways could be critical determinants of neural specification and SOX2 induction by functioning in combination with FGFs to repress the early induction of pre-neural genes or to directly regulate SOX2 transcription. Other signals not yet considered, such as calcium and Notch may also make important contributions to this process.

6.5 Towards a gene regulatory network for neural induction

Having defined a time-course of regulatory states through which neural induction proceeds, we are now performing gain- and loss-of function experiments to evaluate the relative contribution of key signalling pathways to this process. So far, perturbation of the FGF pathway provides significant evidence that FGFs contribute to the onset of neural induction by inducing expression of markers which confer a “pre-neural/pre-border” state to the early ectoderm. Perturbation of other pathways will provide important information about the precise timing and signals responsible for regulating individual markers. This will enable transcriptional responses to grouped based not only on the spatio-temporal similarity of their expression, but also by the signals that regulate them. In this way, a rudimentary network can be constructed, describing neural induction as groups of distinct responses.

However, additional information is required before a more complete network can be constructed. Targeted overexpression or knockdown of genes by electroporation of expression constructs or morpholinos will start to reveal their specific contributions and epistatic relationships (Streit *et al.*, 2013). However they are unable to establish whether putative network interactions occur directly or indirectly. This requires the identification of cis-regulatory elements such as enhancers and promoters that integrate upstream inputs on their transcriptional targets (Streit *et al.*, 2013). New molecular and computational tools now enable such analysis on a systems level. Active and inactive cis-regulatory elements can be identified for responses to neural induction, based on their epigenetic signatures using ChIP-Seq (Rada-Iglesias *et al.*, 2011). Bioinformatics tools such as DREiVe are then able to identify conserved the transcription factor binding sites that comprise putative enhancers (Khan *et al.*, 2013). Finally, the activity of putative enhancers can be tested *in vivo* by electroporating them as reporter constructs into the embryo (Streit *et al.*, 2013).

In this way, a network describing neural induction can be constructed by linking transcriptional responses to neuralising signals by their upstream regulatory elements and downstream targets, as has been done elegantly in the sea urchin by Eric Davidson (Davidson, 2010).

6.6 The conservation of neural induction

Despite the finding that inter-species organizer grafts can also induce secondary axes (Waddington, 1934, Oppenheimer, 1936, Kintner and Dodd, 1991, Blum *et al.*, 1992, Hatta and Takahashi, 1996), there has been some debate about whether the molecular basis of neural induction differs between vertebrates. This was due to apparent differences in the requirement of BMP inhibition in chick and *Xenopus*. In chick, BMP inhibition alone cannot induce neural plate markers in ectoderm (Streit *et al.*, 1998, Streit and Stern, 1999, Linker and Stern, 2004), compared to *Xenopus* animal caps which are readily neuralised (reviewed in (Harland, 2000, Munoz-Sanjuan and Brivanlou, 2002, De Robertis and Kuroda, 2004)). These differences were reconciled by the finding that *Xenopus* animal caps contribute cells to the neural plate and even the smallest animal caps contribute to the neural plate border (Linker *et al.*, 2009). In chick, the neural plate border is the only region sensitive to BMP inhibition, which causes expansion of neural markers (Streit and Stern, 1999, Linker *et al.*, 2009). Since animal caps contain cells normally fated to contribute to the neural plate border, this raises the possibility that the only cells which respond to BMP inhibition may be those that would have done so anyway in the intact embryo. In addition, results in whole embryos suggest that, as in the chick, BMP inhibition can only travel between adjacent "border-like" cells (Linker *et al.*, 2009), so it can only expand the neural plate, but never to induce it in a more distant region. Indeed, BMP inhibition is not sufficient to induce neural markers in cells normally fated to form ventral epidermis or extra-embryonic tissue respectively in *Xenopus* or chick (Linker and Stern, 2004, Delaune *et al.*, 2005, Linker *et al.*, 2009). Subsequently it was determined that FGFs are required for neural induction before gastrulation in both organisms, but that they too are insufficient to induce definitive neural markers (Streit *et al.*, 1998, Streit *et al.*, 2000, Linker and Stern, 2004, Delaune *et al.*, 2005, Linker *et al.*, 2009).

These similarities suggest that neural induction may rely on the same signals and responses in chick and *Xenopus*. Indeed, the entire process of neural induction can now be reassessed in *Xenopus*, in the context of these newly identified responses to neural induction. If homologues of the novel markers described here are expressed in similar spatio-temporal patterns in *Xenopus* as in chick, this would point towards conservation of neural induction as a cascade of signals and responses. The conserved requirement for FGFs (Launay *et al.*, 1996, Sasai *et al.*, 1996, Linker and Stern, 2004, Delaune *et al.*, 2005) raises the possibility that they contribute to a similar "pre-neural/pre-border" state in the early *Xenopus* embryo. However some divergence could arise from the inheritance of maternal transcripts which might influence the earliest stages of neural induction, and perhaps explain reports that weak FGF plus BMP

inhibition is sufficient to induce the neural marker SOX2 in *Xenopus* (Delaune *et al.*, 2005), but not in chick (Linker and Stern, 2004, Linker *et al.*, 2009).

6.7 Conclusions

Although we cannot yet provide a detailed explanation for how neural induction occurs, the identification of all transcriptional responses during this process now offers new opportunities to assess the contribution of individual signalling pathways and interrogate the key molecular events. However, we can conclude that neural induction is a highly dynamic and complex process. It is accompanied by thousands of transcriptional responses including the differential expression of over 400 transcriptional regulators. These contribute to the induction of key states and regulate the progression from a non-neural state to pre-neural and neural specification, and finally the acquisition of neural commitment. It seems likely that key steps are tightly regulated by multiple layers of transcriptional repression and activation. Therefore, neural induction is not a single step process. Instead, our evidence predicts that neural induction proceeds as a cascade of molecular events, including responses to multiple signals at different time points – in this last respect, our findings suggest a different view of the process to the "default model", which postulates a single important signalling event: inhibition of BMP signalling.

FGF signalling makes a major contribution to the onset of neural induction, by inducing pre-neural markers and downregulating non-neural and neural plate border markers. In particular, FGFs probably induce expression of transcription factors and chromatin modifiers in the pre-streak epiblast, providing further evidence that neural induction begins before gastrulation. As this pre-neural state is transcriptionally similar to the neural plate border, it goes some way to explain how these tissues share functional similarities. Furthermore, many of these transcription factors and chromatin modifiers are associated with epigenetic reprogramming and pluripotency suggesting that a major consequence of FGF signalling might be the induction of neural precursor state with multipotent properties. However, FGFs are not sufficient for all early responses, suggesting that other signals are required even for the acquisition of this pre-neural state. Furthermore, FGFs are required but insufficient to induce later neural markers, highlighting the need to confirm which additional signals instruct or permit neural specification and commitment.

6.8 Future perspectives

Although this body of work provides new perspectives on neural induction, it also raises many new possibilities. Further insight will be gained from our experiments conducted to date, once all 400 markers on the NanoString probe set have been analysed in detail. However before the complexity of the entire process can be fully appreciated, future work *in vivo* is necessary to address the following questions:

1. What other signals contribute to the induction of pre-neural markers?
2. Given that FGFs impose BMP and WNT inhibition, what are the relative contributions of endogenous BMP and WNT antagonists to neural induction?
3. Which signals trigger the transition from pre-neural to neural specification?
4. Is there a role for hedgehog signalling in neural induction?
5. Do these signals induce definitive neural markers directly, or by relieving repression which might be imposed on neural differentiation by the pre-neural state?
6. Does PRDM1 regulate SOX2 expression during neural induction?
7. What mechanisms regulate the choice between neural plate and neural plate border from the common “pre-neural/pre-border” state?
8. Do pre-neural markers generally confer pluripotency to the early embryonic ectoderm and neural precursors?
9. Since the neural crest is often described as a multipotent cell population, could the same “pre-neural/pre-border” markers confer multipotency to the neural plate border at later stages?
10. Does SOX1 expression confer commitment to a neural fate after 12h?

Chapter 7: Supplementary Data

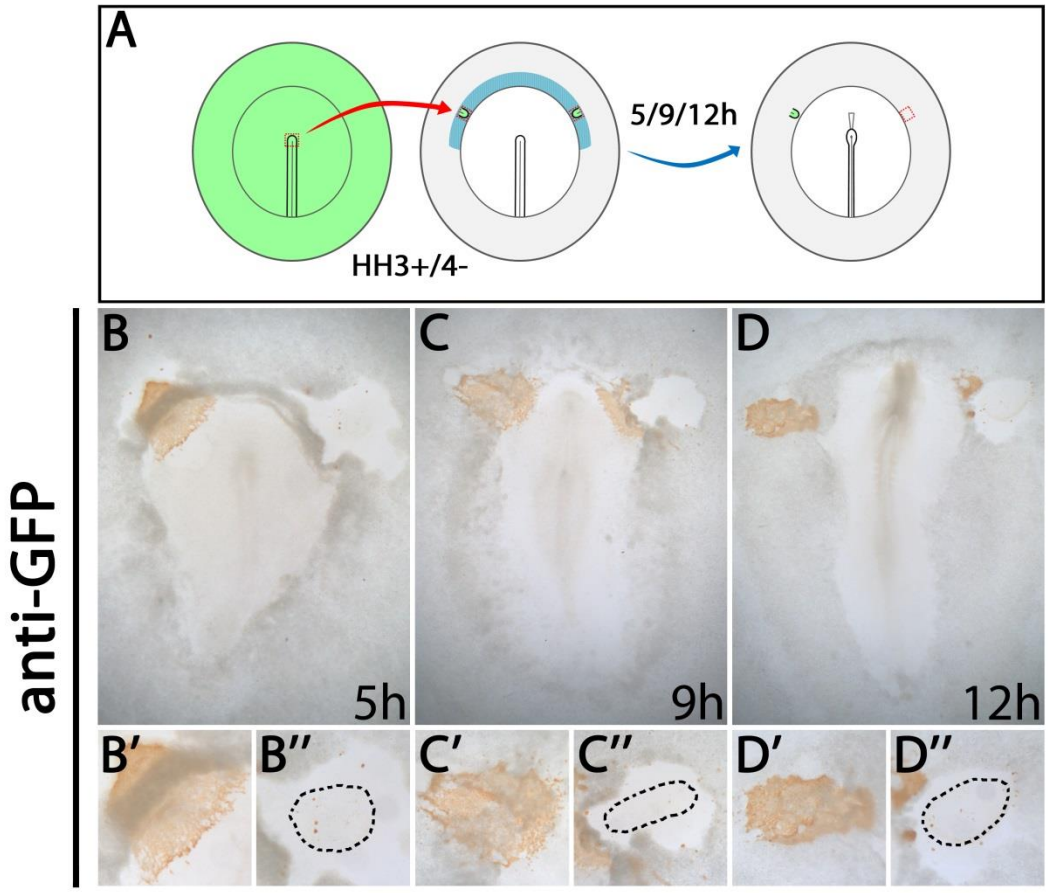

Appendix 1: Hensen's node graft removal proof-of-principle.

To demonstrate that induced tissue could be dissected cleanly, grafts of Hensen's node were cultured and later removed, to check that excess graft cells did not remain. Nodes from transgenic cytoplasmic GFP chickens were grafted into the left and right sides of normal chick hosts at HH3+/4- (A). Embryos were cultured for 5, 9 or 12h and one of the grafts removed. Embryos were fixed and processed for anti-GFP staining to reveal where grafted cells remained. Grafted tissue spreads out during culture but the majority can be removed at each time point; 5h (B) 9h (C) and 12h (D). High magnification images of remaining grafts (B', C', D') and graft removals (B'', C'', D'') reveals that very few graft cells remain after node graft removal, which will not significantly contaminate induced tissue samples. Circled areas indicate the region of induced tissue which would have been dissected from underneath the graft (B'', C'', D'').

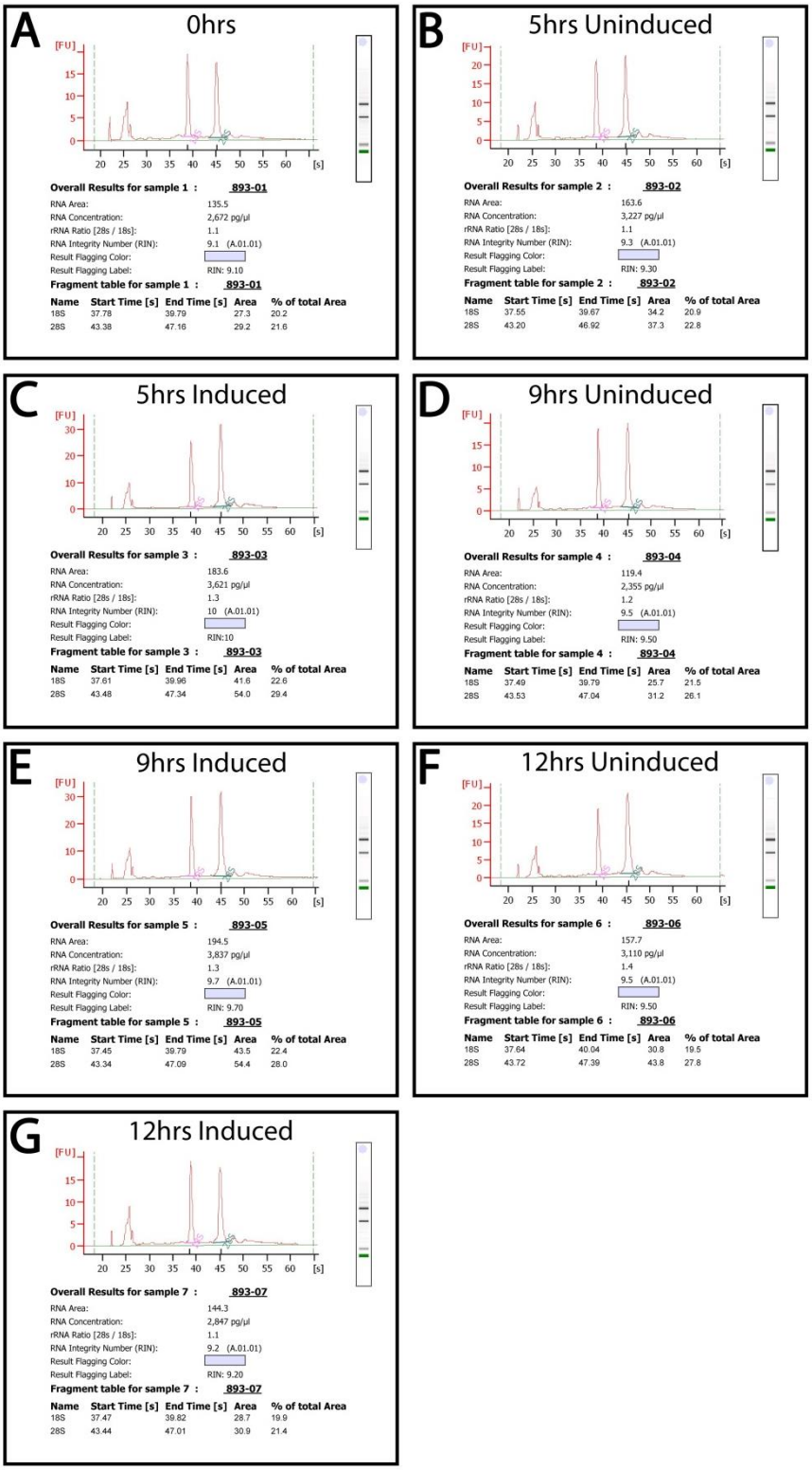

Appendix 2: RNA quality reports for RNA-Seq library preparation.

The quality of extracted total RNA for each sample for RNA-Seq analysis was assessed using the Agilent Bioanalyzer 2100 (A-G). The concentration, rRNA ratio and RNA Integrity Number (RIN) were calculated. All samples achieved a RIN value between 9.0-10.0; greater than the 7.0 value necessary for library preparation.

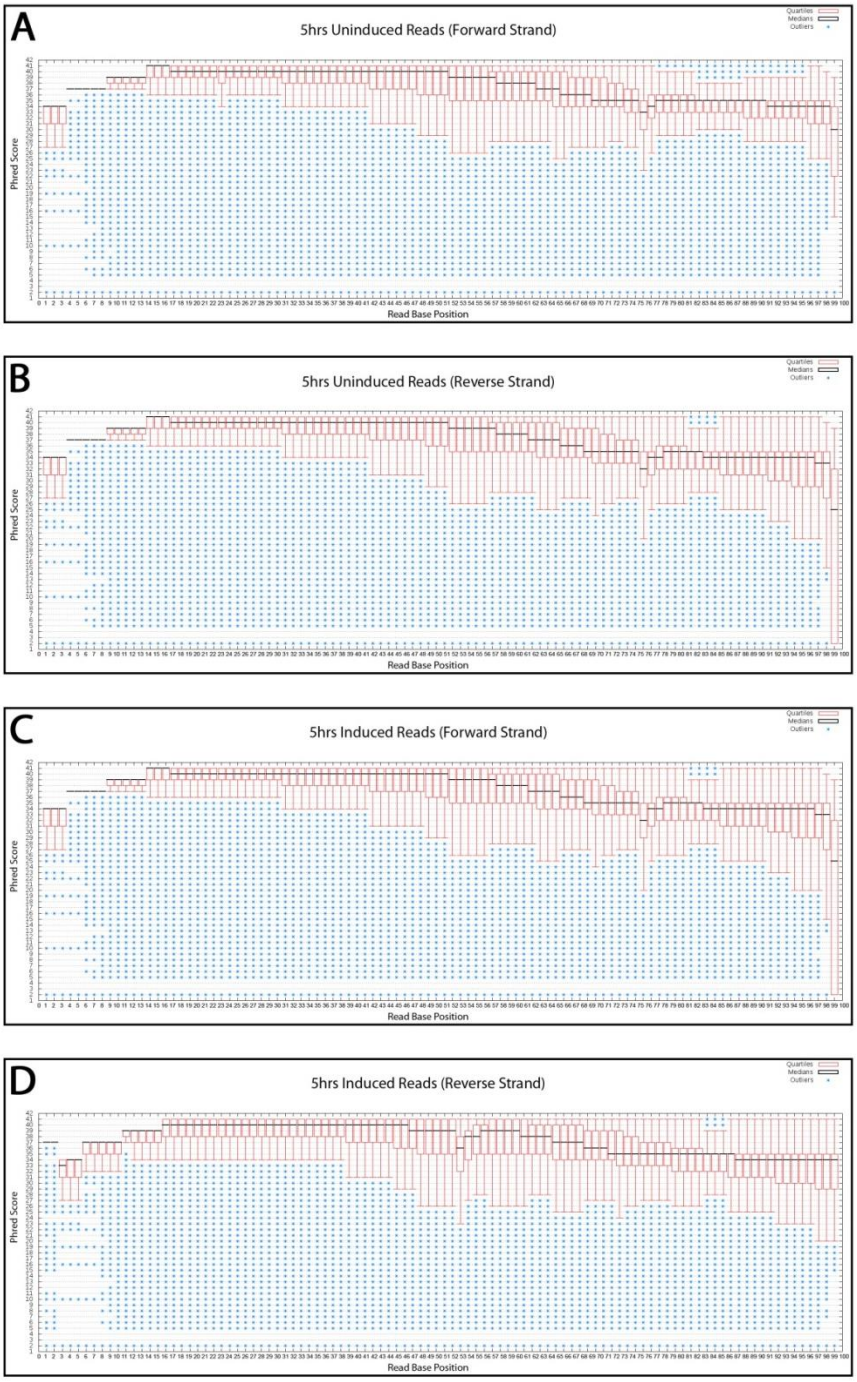

Appendix 3: Quality control box plots for 5h induced and uninduced RNA-Seq libraries.

Quality Control (QC) box plots for reads sequenced from the 5h uninduced (A, B) and 5h induced (C, D) samples. QC was performed for reads in forward (A, C) and reverse (B, D) orientations in paired-end samples. For each plot, the X axis represents the read base position (from 1 to 100) and the Y axis measures the phred read quality at each base position. The median phred score is displayed as a horizontal black bar, with the upper and lower quartiles shown in red. Outliers are shown in blue. These plots were used to only select reads with phred values above 20 and then trim the last 10 bases at the 3' end where quality scores drop.

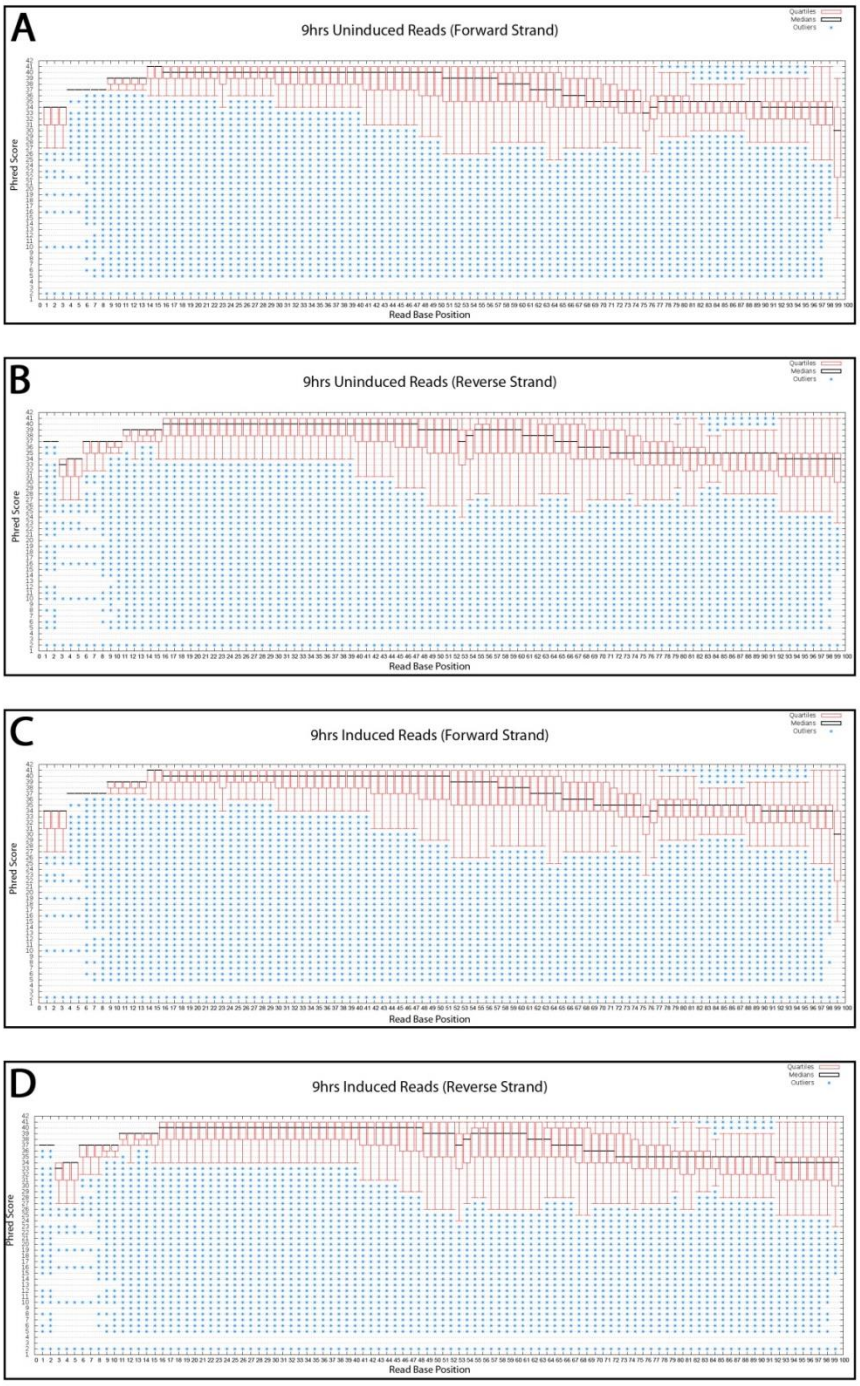

Appendix 4: Quality control box plots for 9h induced and uninduced RNA-Seq libraries.

Quality Control (QC) box plots for reads sequenced from the 9h uninduced (A, B) and 5h induced (C, D) samples. For details, see Appendix 3.

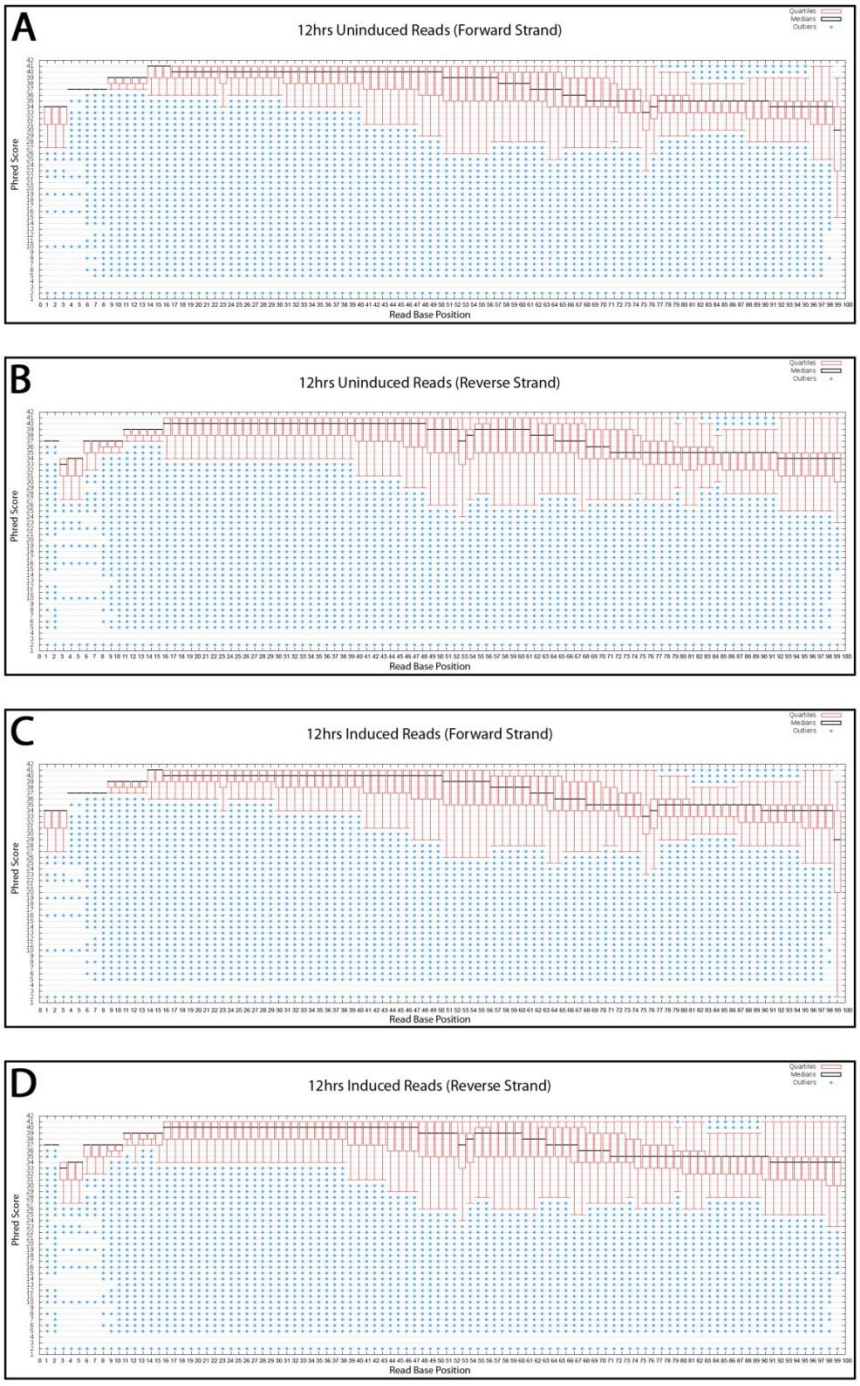

Appendix 5: Quality control box plots for 12h induced and uninduced RNA-Seq libraries.

Quality Control (QC) box plots for reads sequenced from the 12h uninduced (A, B) and 5h induced (C, D) samples. For details, see Appendix 3.

Appendix 6: Differentially expressed transcripts from Galgal3 RNA-Seq analysis.

Reads that passed QC analysis were aligned to the Galgal3 chicken genome using "Tophat", and annotated using the Ensembl Galgal3 GTF. Differential expression analysis was used to compare counts for each transcript between uninduced and induced conditions at each time point (5, 9 and 12h) using two separate methods; "Cuffdiff" and DE-Seq. Transcripts that were differentially expressed with a $\log_2$ fold change of at least 1.2 were extracted from each analysis. Each data set was combined in one spreadsheet and transcripts categorised as follows; transcripts commonly identified as statistically significant (using a P-value threshold of 0.05) by both methods were displayed as red, transcripts identified as statistically significant by either method were displayed as orange and those identified as statistically insignificant by both methods were displayed as yellow. These analyses identified 7745 differentially expressed transcripts across 3 time points. Gene annotations could be assigned to 4508 of these, corresponding to 2333 unique genes. Due to the incomplete nature of the Galgal3 chicken genome, 3237 transcripts were left unannotated. See spreadsheet on accompanying CD.

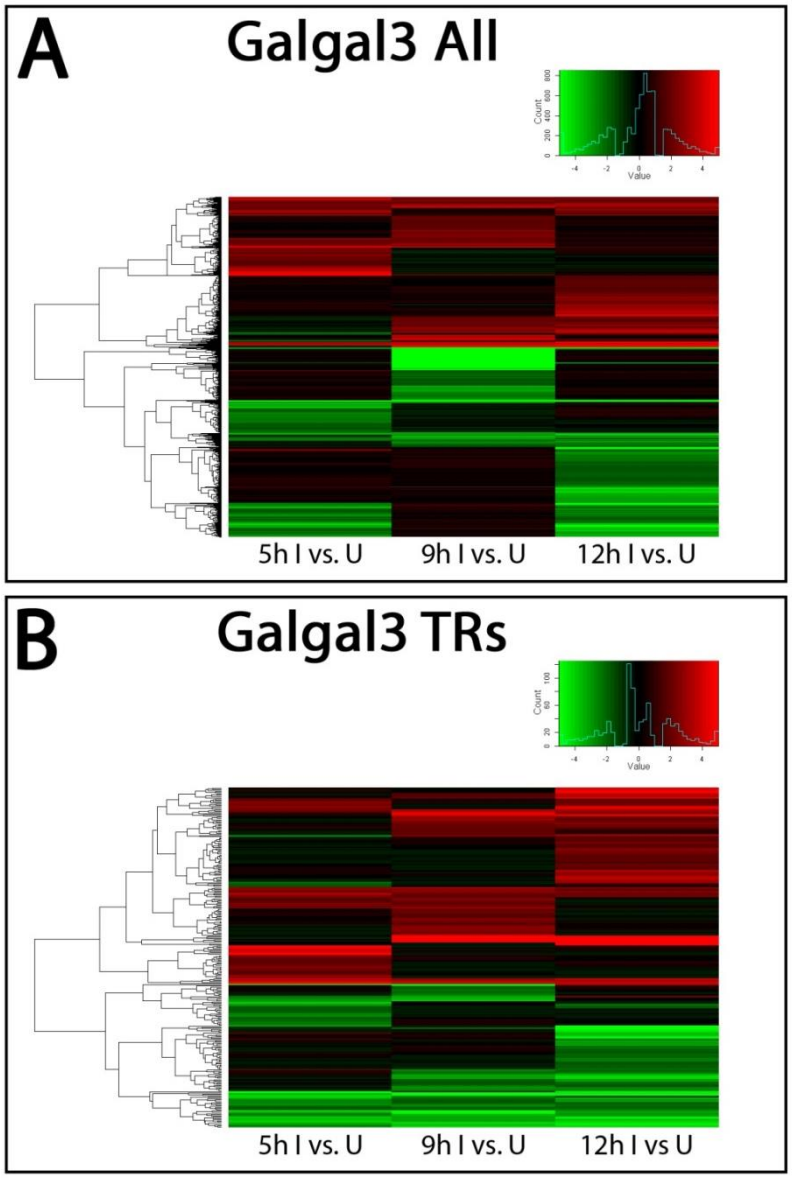

Appendix 7: Differential analysis of RNA-Seq Galgal3 data across 5, 9 and 12h.

DE-Seq analysis was used to compare transcripts from uninduced and induced conditions at each time point, using the Galgal3 version of the chicken genome and a $\log_2$ fold change threshold of 1.2. Heat map representing the hierarchical clustering of all 7745 upregulated (red) and downregulated (green) transcripts across the following comparisons: 5h induced vs. 5h uninduced, 9h induced vs. 9h uninduced and 12h induced vs. 12h uninduced (A). These correspond to 2333 unique annotated genes. Of these, 540 transcripts were extracted, coding for 284 unique transcriptional regulators (B).

Appendix 8: Differentially expressed transcripts from Galgal4 RNA-Seq analysis.

Reads that passed QC analysis were aligned to the Galgal4 chicken genome using "Tophat", and differential expression analysis was used to compare counts for each transcript between uninduced and induced conditions at each time point (5, 9 and 12h) using DE-Seq. Transcripts that were differentially expressed with a $\log_2$ fold change of at least 1.2 were extracted and annotations were added using the Ensembl Galgal4 GTF, Ensembl Biomart data, UCSC Galgal4 GTF and annotation data from the UCSC table browser. Statistically significant (using a P-value threshold of 0.05) transcripts were colour-coded blue, while statistically insignificant transcripts were displayed as white. This reanalysis identified 8673 differentially expressed transcripts across all 3 time points. Gene annotations could be assigned to 7184 of these, corresponding to 4145 unique genes. Due to the incomplete nature of the chicken genome only 989 transcripts remain unannotated. See spreadsheet on accompanying CD.

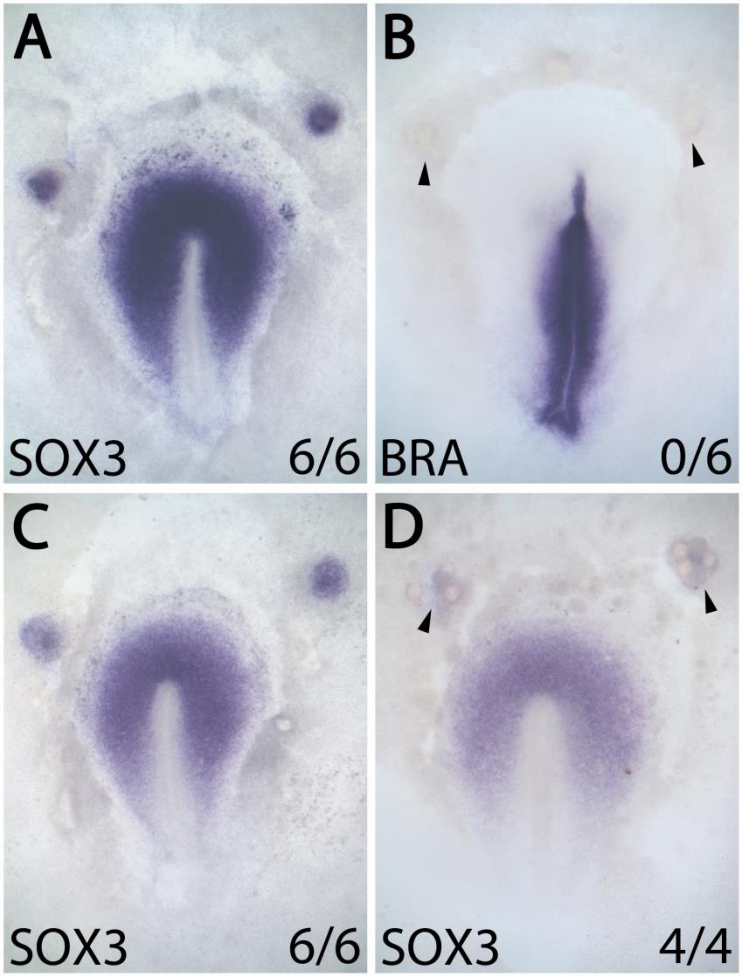

Appendix 9: FGF pathway perturbation experiment validation.

Appropriate concentrations of FGF8 and SU5402 were used for FGF gain- and loss-of-function experiments. Heparin beads soaked in 25µg/ml FGF8 were able to induce SOX3 (A; 6/6), without inducing Brachyury (B; 0/6), when grafted into the area opaca at HH4 and incubated for 5h. AG1X2 beads soaked in 25µM SU5402, reduced induction of SOX3 by a node graft after 5h (D; 4/4) compared to normal induction of SOX3 after 5h, which is much stronger (C; 6/6). For each comparison, embryos were processed simultaneously.

Appendix 10: The induction of neural and non-neural markers in a refined time-course and after FGF perturbation.

Graphs showing the expression of neural and non-neural markers after 1, 3, 5, 7, 9 and 12h of a grafted node (Fig 5.1-5.6), and the responses of these markers to FGF signalling and FGF inhibition after 5h (Fig. 5.7, 5.8) and 9h (Fig. 5.10, 5.11) are also provided a slideshow. This allows a more interactive view of the subtle changes in expression that occur across time points and between conditions. See Powerpoint document on accompanying CD.

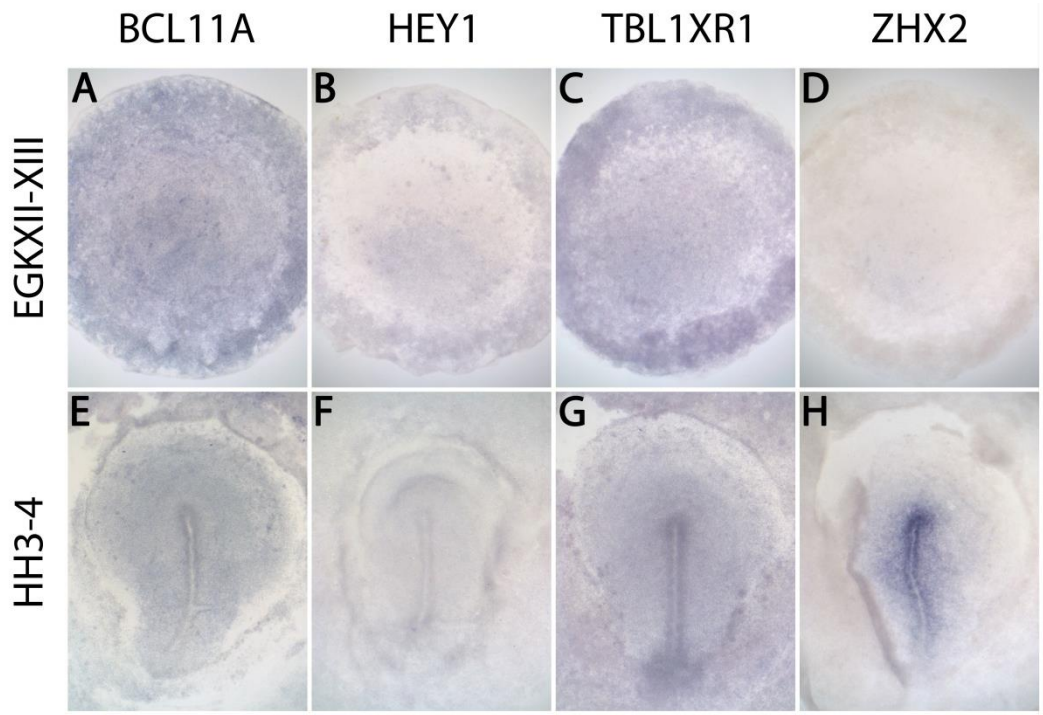

Appendix 11: The early expression of BCL11A, HEY1, TBL1XR1 and ZHX2.

The expression of 20 markers, common to a microarray screen of PPR tissue and an RNA-Seq screen for responses to 5h of neural inducing signals, was assessed. Expression patterns were confirmed at two stages; prior to gastrulation at EGKXII-XIII (A-D), and during gastrulation at HH3-4 (E-H). Of these, 16 are robustly expressed in the epiblast at EGKXII-XIII and in the prospective neural plate at HH3-4 as predicted. Specific expression of four markers was not observed at these stages, including BCL11A (A E), HEY1 (B, F), TBL1XR1 (C, G) and ZHX2 (D, H).

Appendix 12: The induction of pre-neural markers in a refined time course and after FGF perturbation.

Graphs showing the expression of pre-neural markers after 1, 3, 5, 7, 9 and 12h of a grafted node (Fig 5.14-5.16), and the responses of these markers after 5h of FGF signalling (Fig. 5.18) and FGF inhibition (Fig. 5.19) are also provided also a slideshow. This allows a more interactive view of the subtle changes in expression that occur across time points and between conditions. See Powerpoint document on accompanying CD.

Bibliography

ABE, T., FURUE, M., KONDOW, A., MATSUZAKI, K. & ASASHIMA, M. (2005). Notch signaling modulates the nuclear localization of carboxy-terminal-phosphorylated smad2 and controls the competence of ectodermal cells for activin A. *Mech Dev,* **122**, 671-80.

ABU, A., FRYDMAN, M., MAREK, D., PRAS, E., NIR, U., REZNIK-WOLF, H. & PRAS, E. (2008). Deleterious mutations in the Zinc-Finger 469 gene cause brittle cornea syndrome. *Am J Hum Genet,* **82**, 1217-22.

ACLOQUE, H., MEY, A., BIROT, A. M., GRUFFAT, H., PAIN, B. & SAMARUT, J. (2004). Transcription factor cCP2 controls gene expression in chicken embryonic stem cells. *Nucleic Acids Res,* **32**, 2259-71.

ACLOQUE, H., OCAÑA, OSCAR H., MATHEU, A., RIZZOTI, K., WISE, C., LOVELL-BADGE, R. & NIETO, M. A. (2011). Reciprocal Repression between Sox3 and Snail Transcription Factors Defines Embryonic Territories at Gastrulation. *Developmental Cell,* **21**, 546-558.

ACLOQUE, H., RISSON, V., BIROT, A. M., KUNITA, R., PAIN, B. & SAMARUT, J. (2001). Identification of a new gene family specifically expressed in chicken embryonic stem cells and early embryo. *Mech Dev,* **103**, 79-91.

AHLGREN, H., BAS-ORTH, C., FREITAG, H. E., HELLWIG, A., OTTERSEN, O. P. & BADING, H. (2014). The nuclear calcium signaling target, activating transcription factor 3 (ATF3), protects against dendrotoxicity and facilitates the recovery of synaptic transmission after an excitotoxic insult. *J Biol Chem,* **289**, 9970-82.

AKAI, J., HALLEY, P. A. & STOREY, K. G. (2005). FGF-dependent Notch signaling maintains the spinal cord stem zone. *Genes Dev,* **19**, 2877-87.

AKIYAMA-ODA, Y. & ODA, H. (2006). Axis specification in the spider embryo: dpp is required for radial-to-axial symmetry transformation and sog for ventral patterning. *Development,* **133**, 2347-57.

ALBANO, R. M., ARKELL, R., BEDDINGTON, R. S. & SMITH, J. C. (1994). Expression of inhibin subunits and follistatin during postimplantation mouse development: decidual expression of activin and expression of follistatin in primitive streak, somites and hindbrain. *Development,* **120**, 803-13.

ALBAZERCHI, A. & STERN, C. D. (2007). A role for the hypoblast (AVE) in the initiation of neural induction, independent of its ability to position the primitive streak. *Developmental Biology,* **301**, 489-503.

ALEV, C., WU, Y., KASUKAWA, T., JAKT, L. M., UEDA, H. R. & SHENG, G. (2010). Transcriptomic landscape of the primitive streak. *Development,* **137**, 2863-74.

ALLAN, L. L. & SHERR, D. H. (2005). Constitutive activation and environmental chemical induction of the aryl hydrocarbon receptor/transcription factor in activated human B lymphocytes. *Mol Pharmacol,* **67**, 1740-50.

ALVAREZ, I. S., ARAUJO, M. & NIETO, M. A. (1998). Neural induction in whole chick embryo cultures by FGF. *Dev Biol,* **199**, 42-54.

AMAYA, E., MUSCI, T. J. & KIRSCHNER, M. W. (1991). Expression of a dominant negative mutant of the FGF receptor disrupts mesoderm formation in Xenopus embryos. *Cell,* **66**, 257-70.

ANDERS, S. & HUBER, W. (2010). Differential expression analysis for sequence count data. *Genome Biol,* **11**, R106.

ANDREWS, J. E., O'NEILL, M. J., BINDER, M., SHIODA, T. & SINCLAIR, A. H. (2000). Isolation and expression of a novel member of the CITED family. *Mech Dev,* **95**, 305-8.

ANTIN, P. B., PIER, M., SESEPASARA, T., YATSKIEVYCH, T. A. & DARNELL, D. K. (2010). Embryonic expression of the chicken Kruppel-like (KLF) transcription factor gene family. *Dev Dyn,* **239**, 1879-87.

ARAGON, F. & PUJADES, C. (2009). FGF signaling controls caudal hindbrain specification through Ras-ERK1/2 pathway. *BMC Dev Biol,* **9**, 61.

ARENDT, D. & NUBLER-JUNG, K. (1999). Rearranging gastrulation in the name of yolk: evolution of gastrulation in yolk-rich amniote eggs. *Mech Dev,* **81**, 3-22.

ARÉVALO, J. C. & WU, S. H. (2006). Neurotrophin signaling: many exciting surprises! *Cellular and Molecular Life Sciences: CMLS,* **63**, 1523-1537.

ASHE, H. L. & LEVINE, M. (1999). Local inhibition and long-range enhancement of Dpp signal transduction by Sog. *Nature,* **398**, 427-31.

AUBERT, J., DUNSTAN, H., CHAMBERS, I. & SMITH, A. (2002). Functional gene screening in embryonic stem cells implicates Wnt antagonism in neural differentiation. *Nat Biotechnol,* **20**, 1240-5.

AUBIN, J., DAVY, A. & SORIANO, P. (2004). In vivo convergence of BMP and MAPK signaling pathways: impact of differential Smad1 phosphorylation on development and homeostasis. *Genes Dev,* **18**, 1482-94.

AVILION, A. A., NICOLIS, S. K., PEVNY, L. H., PEREZ, L., VIVIAN, N. & LOVELL-BADGE, R. (2003). Multipotent cell lineages in early mouse development depend on SOX2 function. *Genes Dev,* **17**, 126-40.

BABA, A., OHTAKE, F., OKUNO, Y., YOKOTA, K., OKADA, M., IMAI, Y., NI, M., MEYER, C. A., IGARASHI, K., KANNO, J., BROWN, M. & KATO, S. (2011). PKA-dependent regulation of the histone lysine demethylase complex PHF2-ARID5B. *Nat Cell Biol,* **13**, 668-75.

BACHILLER, D., KLINGENSMITH, J., KEMP, C., BELO, J. A., ANDERSON, R. M., MAY, S. R., MCMAHON, J. A., MCMAHON, A. P., HARLAND, R. M., ROSSANT, J. & DE ROBERTIS, E. M. (2000). The organizer factors Chordin and Noggin are required for mouse forebrain development. *Nature,* **403**, 658-61.

BACHVAROVA, R. F., SKROMNE, I. & STERN, C. D. (1998). Induction of primitive streak and Hensen's node by the posterior marginal zone in the early chick embryo. *Development,* **125**, 3521-34.

BAIG, M. A. & KHAN, M. A. (1996). The induction of neurotrophin and TRK receptor mRNA expression during early avian embryogenesis. *International Journal of Developmental Neuroscience: The Official Journal of the International Society for Developmental Neuroscience,* **14**, 55-60.

BAILEY, A. P., BHATTACHARYYA, S., BRONNER-FRASER, M. & STREIT, A. (2006). Lens Specification Is the Ground State of All Sensory Placodes, from which FGF Promotes Olfactory Identity. *Developmental Cell,* **11**, 505-517.

BAKER, C. V. H. & BRONNER-FRASER, M. (2001). Vertebrate cranial placodes I. Embryonic induction. *Developmental Biology,* **232**, 1-61.

BAKER, J. C., BEDDINGTON, R. S. & HARLAND, R. M. (1999). Wnt signaling in Xenopus embryos inhibits bmp4 expression and activates neural development. *Genes Dev,* **13**, 3149-59.

BAKKER, W. J., BLAZQUEZ-DOMINGO, M., KOLBUS, A., BESOOYEN, J., STEINLEIN, P., BEUG, H., COFFER, P. J., LOWENBERG, B., VON LINDERN, M. & VAN DIJK, T. B. (2004). FoxO3a regulates erythroid differentiation and induces BTG1, an activator of protein arginine methyl transferase 1. *J Cell Biol,* **164**, 175-84.

BALKAN, W., COLBERT, M., BOCK, C. & LINNEY, E. (1992). Transgenic indicator mice for studying activated retinoic acid receptors during development. *Proc Natl Acad Sci U S A,* **89**, 3347-51.

BALLY-CUIF, L., GULISANO, M., BROCCOLI, V. & BONCINELLI, E. (1995). c-otx2 is expressed in two different phases of gastrulation and is sensitive to retinoic acid treatment in chick embryo. *Mechanisms of development,* **49**, 49-63.

BANCROFT, M. & BELLAIRS, R. (1974). The onset of differentiation in the epiblast of the chick blastoderm (SEM and TEM). *Cell Tissue Res,* **155**, 399-418.

BANCROFT, M. & BELLAIRS, R. (1975). Differentiation of the neural plate and neural tube in the young chick embryo. A study by scanning and transmission electron microscopy. *Anat Embryol (Berl),* **147**, 309-35.

BARNETT, M. W., OLD, R. W. & JONES, E. A. (1998). Neural induction and patterning by fibroblast growth factor, notochord and somite tissue in Xenopus. *Dev Growth Differ,* **40**, 47-57.

BARTH, L. G. (1941). Neural differentiation without organizer. *J. Exp. Zool.,* **87**, 371–384.

BARTH, L. G. & BARTH, L. J. (1964). Sequential induction of the presumptive epidermis of the Rana pipiens gastrula. *Biol. Bull.,* **127**, 413–427.

BATUT, J., VANDEL, L., LECLERC, C., DAGUZAN, C., MOREAU, M. & NEANT, I. (2005). The Ca2+-induced methyltransferase xPRMT1b controls neural fate in amphibian embryo. *Proc Natl Acad Sci U S A,* **102**, 15128-33.

BAUER, H., MEIER, A., HILD, M., STACHEL, S., ECONOMIDES, A., HAZELETT, D., HARLAND, R. M. & HAMMERSCHMIDT, M. (1998). Follistatin and noggin are excluded from the zebrafish organizer. *Dev Biol,* **204**, 488-507.

BEDDINGTON, R. S. (1994). Induction of a second neural axis by the mouse node. *Development,* **120**, 613-20.

BELLAIRS, R. (1953a). Studies on the Development of the Foregut in the Chick Blastoderm: 1. The Presumptive Foregut Area. *Journal of Embryology and Experimental Morphology,* **1**, 115-124.

BELLAIRS, R. (1953b). Studies on the Development of the Foregut in the Chick Blastoderm: 2. The Morphogenetic Movements. *Journal of Embryology and Experimental Morphology,* **1**, 369-385.

BELLAIRS, R. (1957). Studies on the Development of the Foregut in the Chick Embryo: IV. Mesodermal Induction and Mitosis. *Journal of Embryology and Experimental Morphology,* **5**, 340-350.

BELLAIRS, R., BREATHNACH, A. S. & GROSS, M. (1975). Freeze-fracture replication of junctionsl complexes in unincubated and incubated chick embryos. *Cell Tissue Res,* **162**, 235-52.

BELO, J. A., BACHILLER, D., AGIUS, E., KEMP, C., BORGES, A. C., MARQUES, S., PICCOLO, S. & DE ROBERTIS, E. M. (2000). Cerberus-like is a secreted BMP and nodal antagonist not essential for mouse development. *Genesis,* **26**, 265-70.

BELO, J. A., BOUWMEESTER, T., LEYNS, L., KERTESZ, N., GALLO, M., FOLLETTIE, M. & DE ROBERTIS, E. M. (1997). Cerberus-like is a secreted factor with neutralizing activity expressed in the anterior primitive endoderm of the mouse gastrula. *Mech Dev,* **68**, 45-57.

BENKHELIFA, S., PROVOT, S., LECOQ, O., POUPONNOT, C., CALOTHY, G. & FELDER-SCHMITTBUHL, M. P. (1998). mafA, a novel member of the maf proto-oncogene family, displays developmental regulation and mitogenic capacity in avian neuroretina cells. *Oncogene,* **17**, 247-54.

BENTZ, G. L., LIU, R., HAHN, A. M., SHACKELFORD, J. & PAGANO, J. S. (2010). Epstein-Barr virus BRLF1 inhibits transcription of IRF3 and IRF7 and suppresses induction of interferon-beta. *Virology,* **402**, 121-8.

BERND, P. & LI, R. (1999). Differential expression of trkC mRNA in the chicken embryo from gastrulation to development of secondary brain vesicles. *Brain Research. Developmental Brain Research,* **116**, 205-209.

BERRY, F. B., MIURA, Y., MIHARA, K., KASPAR, P., SAKATA, N., HASHIMOTO-TAMAOKI, T. & TAMAOKI, T. (2001). Positive and negative regulation of myogenic differentiation of C2C12 cells by isoforms of the multiple homeodomain zinc finger transcription factor ATBF1. *J Biol Chem,* **276**, 25057-65.

BERTOCCHINI, F. & STERN, C. D. (2002). The hypoblast of the chick embryo positions the primitive streak by antagonizing nodal signaling. *Dev Cell,* **3**, 735-44.

BERTOCCHINI, F. & STERN, C. D. (2008). A differential screen for genes expressed in the extraembryonic endodermal layer of pre-primitive streak stage chick embryos reveals expression of Apolipoprotein A1 in hypoblast, endoblast and endoderm. *Gene Expr Patterns,* **8**, 477-80.

BERTRAND, N., MEDEVIELLE, F. & PITUELLO, F. (2000). FGF signalling controls the timing of Pax6 activation in the neural tube. *Development,* **127**, 4837-43.

BERTRAND, V., HUDSON, C., CAILLOL, D., POPOVICI, C. & LEMAIRE, P. (2003). Neural tissue in ascidian embryos is induced by FGF9/16/20, acting via a combination of maternal GATA and Ets transcription factors. *Cell,* **115**, 615-27.

BHATTARAM, P., PENZO-MENDEZ, A., SOCK, E., COLMENARES, C., KANEKO, K. J., VASSILEV, A., DEPAMPHILIS, M. L., WEGNER, M. & LEFEBVRE, V. (2010). Organogenesis relies on SoxC transcription factors for the survival of neural and mesenchymal progenitors. *Nat Commun,* **1**, 9.

BIEHS, B., FRANCOIS, V. & BIER, E. (1996). The Drosophila short gastrulation gene prevents Dpp from autoactivating and suppressing neurogenesis in the neuroectoderm. *Genes Dev,* **10**, 2922-34.

BIGGS, W. H., 3RD, CAVENEE, W. K. & ARDEN, K. C. (2001). Identification and characterization of members of the FKHR (FOX O) subclass of winged-helix transcription factors in the mouse. *Mamm Genome,* **12**, 416-25.

BLANKENBERG, D., GORDON, A., VON KUSTER, G., CORAOR, N., TAYLOR, J. & NEKRUTENKO, A. (2010). Manipulation of FASTQ data with Galaxy. *Bioinformatics,* **26**, 1783-5.

BLENTIC, A., GALE, E. & MADEN, M. (2003). Retinoic acid signalling centres in the avian embryo identified by sites of expression of synthesising and catabolising enzymes. *Developmental Dynamics,* **227**, 114-127.

BLOKZIJL, A., DAHLQVIST, C., REISSMANN, E., FALK, A., MOLINER, A., LENDAHL, U. & IBANEZ, C. F. (2003). Cross-talk between the Notch and TGF-beta signaling pathways mediated by interaction of the Notch intracellular domain with Smad3. *J Cell Biol,* **163**, 723-8.

BLUM, M., GAUNT, S. J., CHO, K. W., STEINBEISSER, H., BLUMBERG, B., BITTNER, D. & DE ROBERTIS, E. M. (1992). Gastrulation in the mouse: the role of the homeobox gene goosecoid. *Cell,* **69**, 1097-106.

BOARDMAN, P. E., SANZ-EZQUERRO, J., OVERTON, I. M., BURT, D. W., BOSCH, E., FONG, W. T., TICKLE, C., BROWN, W. R., WILSON, S. A. & HUBBARD, S. J. (2002). A comprehensive collection of chicken cDNAs. *Curr Biol,* **12**, 1965-9.

BOBBS, A. S., SAARELA, A. V., YATSKIEVYCH, T. A. & ANTIN, P. B. (2012). Fibroblast growth factor (FGF) signaling during gastrulation negatively modulates the abundance of microRNAs that regulate proteins required for cell migration and embryo patterning. *J Biol Chem,* **287**, 38505-14.

BONASIO, R., LECONA, E., NARENDRA, V., VOIGT, P., PARISI, F., KLUGER, Y. & REINBERG, D. (2014). Interactions with RNA direct the Polycomb group protein SCML2 to chromatin where it represses target genes. *Elife,* **3**, e02637.

BORN, J., JANECZEK, J., SCHWARZ, W., TIEDEMANN, H. & TIEDEMANN, H. (1989). Activation of masked neural determinants in amphibian eggs and embryos and their release from the inducing tissue. *Cell Differ Dev,* **27**, 1-7.

BOUWMEESTER, T., KIM, S., SASAI, Y., LU, B. & DE ROBERTIS, E. M. (1996). Cerberus is a head-inducing secreted factor expressed in the anterior endoderm of Spemann's organizer. *Nature,* **382**, 595-601.

BOVOLENTA, P., MALLAMACI, A., PUELLES, L. & BONCINELLI, E. (1998). Expression pattern of cSix3, a member of the Six/sine oculis family of transcription factors. *Mech Dev,* **70**, 201-3.

BREITBART, R. E., LIANG, C. S., SMOOT, L. B., LAHERU, D. A., MAHDAVI, V. & NADAL-GINARD, B. (1993). A fourth human MEF2 transcription factor, hMEF2D, is an early marker of the myogenic lineage. *Development,* **118**, 1095-106.

BREMBECK, F. H., OPITZ, O. G., LIBERMANN, T. A. & RUSTGI, A. K. (2000). Dual function of the epithelial specific ets transcription factor, ELF3, in modulating differentiation. *Oncogene,* **19**, 1941-9.

BRONDANI, V., KLIMKAIT, T., EGLY, J. M. & HAMY, F. (2002). Promoter of FGF8 reveals a unique regulation by unliganded RARalpha. *J Mol Biol,* **319**, 715-28.

BROWN, J. M., ROBERTSON, K. E., WEDDEN, S. E. & TICKLE, C. (1997). Alterations in Msx 1 and Msx 2 expression correlate with inhibition of outgrowth of chick facial primordia induced by retinoic acid. *Anat Embryol (Berl),* **195**, 203-7.

BRUNET, L. J., MCMAHON, J. A., MCMAHON, A. P. & HARLAND, R. M. (1998). Noggin, cartilage morphogenesis, and joint formation in the mammalian skeleton. *Science,* **280**, 1455-7.

BURDON, T., STRACEY, C., CHAMBERS, I., NICHOLS, J. & SMITH, A. (1999). Suppression of SHP-2 and ERK signalling promotes self-renewal of mouse embryonic stem cells. *Dev Biol,* **210**, 30-43.

BURGESS, R., CSERJESI, P., LIGON, K. L. & OLSON, E. N. (1995). Paraxis: a basic helix-loop-helix protein expressed in paraxial mesoderm and developing somites. *Dev Biol,* **168**, 296-306.

BURK, O., MINK, S., RINGWALD, M. & KLEMPNAUER, K. H. (1993). Synergistic activation of the chicken mim-1 gene by v-myb and C/EBP transcription factors. *Embo j,* **12**, 2027-38.

CAILLAUD, A., PRAKASH, A., SMITH, E., MASUMI, A., HOVANESSIAN, A. G., LEVY, D. E. & MARIE, I. (2002). Acetylation of interferon regulatory factor-7 by p300/CREB-binding protein (CBP)-associated factor (PCAF) impairs its DNA binding. *J Biol Chem,* **277**, 49417-21.

CALLEBAUT, M. & VAN NUETEN, E. (1994). Rauber's (Koller's) sickle: the early gastrulation organizer of the avian blastoderm. *Eur J Morphol,* **32**, 35-48.

CHAPMAN, D. L. & PAPAIOANNOU, V. E. (1998). Three neural tubes in mouse embryos with mutations in the T-box gene Tbx6. *Nature,* **391**, 695-7.

CHAPMAN, S. C., MATSUMOTO, K., CAI, Q. & SCHOENWOLF, G. C. (2007). Specification of germ layer identity in the chick gastrula. *BMC Dev Biol,* **7**, 91.

CHAPMAN, S. C., SCHUBERT, F. R., SCHOENWOLF, G. C. & LUMSDEN, A. (2002). Analysis of spatial and temporal gene expression patterns in blastula and gastrula stage chick embryos. *Developmental biology,* **245**, 187-199.

CHEN, B. P., LIANG, G., WHELAN, J. & HAI, T. (1994a). ATF3 and ATF3 delta Zip. Transcriptional repression versus activation by alternatively spliced isoforms. *J Biol Chem,* **269**, 15819-26.

CHEN, S., DO, J. T., ZHANG, Q., YAO, S., YAN, F., PETERS, E. C., SCHOLER, H. R., SCHULTZ, P. G. & DING, S. (2006). Self-renewal of embryonic stem cells by a small molecule. *Proc Natl Acad Sci U S A,* **103**, 17266-71.

CHEN, Y., HUANG, L., RUSSO, A. F. & SOLURSH, M. (1992). Retinoic acid is enriched in Hensen's node and is developmentally regulated in the early chicken embryo. *Proceedings of the National Academy of Sciences of the United States of America,* **89**, 10056-10059.

CHEN, Y., HUANG, L. & SOLURSH, M. (1994b). A concentration gradient of retinoids in the early Xenopus laevis embryo. *Dev Biol,* **161**, 70-6.

CHEN, Y. & SOLURSH, M. (1992). Comparison of Hensen's node and retinoic acid in secondary axis induction in the early chick embryo. *Developmental Dynamics: An Official Publication of the American Association of Anatomists,* **195**, 142-151.

CHIANG, C., LITINGTUNG, Y., LEE, E., YOUNG, K. E., CORDEN, J. L., WESTPHAL, H. & BEACHY, P. A. (1996). Cyclopia and defective axial patterning in mice lacking Sonic hedgehog gene function. *Nature,* **383**, 407-413.

CHO, A., TANG, Y., DAVILA, J., DENG, S., CHEN, L., MILLER, E., WERNIG, M. & GRAEF, I. A. (2014). Calcineurin signaling regulates neural induction through antagonizing the BMP pathway. *Neuron,* **82**, 109-24.

CHUNG, C. T. & MILLER, R. H. (1988). A rapid and convenient method for the preparation and storage of competent bacterial cells. *Nucleic Acids Res,* **16**, 3580.

CHUONG, C. M. & EDELMAN, G. M. (1985). Expression of cell-adhesion molecules in embryonic induction. I. Morphogenesis of nestling feathers. *J Cell Biol,* **101**, 1009-26.

COFFMAN, C., HARRIS, W. & KINTNER, C. (1990). Xotch, the Xenopus homolog of Drosophila notch. *Science,* **249**, 1438-41.

COFFMAN, C. R., SKOGLUND, P., HARRIS, W. A. & KINTNER, C. R. (1993). Expression of an extracellular deletion of Xotch diverts cell fate in Xenopus embryos. *Cell,* **73**, 659-71.

COLE, M. F., JOHNSTONE, S. E., NEWMAN, J. J., KAGEY, M. H. & YOUNG, R. A. (2008). Tcf3 is an integral component of the core regulatory circuitry of embryonic stem cells. *Genes Dev,* **22**, 746-55.

CONNOLLY, D. J., PATEL, K., SELEIRO, E. A., WILKINSON, D. G. & COOKE, J. (1995). Cloning, sequencing, and expressional analysis of the chick homologue of follistatin. *Dev Genet,* **17**, 65-77.

COOPER, M. K., PORTER, J. A., YOUNG, K. E. & BEACHY, P. A. (1998). Teratogen-mediated inhibition of target tissue response to Shh signaling. *Science,* **280**, 1603-7.

CORNELL, R. A. & EISEN, J. S. (2002). Delta/Notch signaling promotes formation of zebrafish neural crest by repressing Neurogenin 1 function. *Development,* **129**, 2639-48.

COTTERMAN, R. & KNOEPFLER, P. S. (2009). N-Myc regulates expression of pluripotency genes in neuroblastoma including lif, klf2, klf4, and lin28b. *PLoS One,* **4**, e5799.

COX, W. G. & HEMMATI-BRIVANLOU, A. (1995). Caudalization of neural fate by tissue recombination and bFGF. *Development,* **121**, 4349-58.

CUI, J., MICHAILLE, J. J., JIANG, W. & ZILE, M. H. (2003). Retinoid receptors and vitamin A deficiency: differential patterns of transcription during early avian development and the rapid induction of RARs by retinoic acid. *Dev Biol,* **260**, 496-511.

DAHLQVIST, C., BLOKZIJL, A., CHAPMAN, G., FALK, A., DANNAEUS, K., IBANEZ, C. F. & LENDAHL, U. (2003). Functional Notch signaling is required for BMP4-induced inhibition of myogenic differentiation. *Development,* **130**, 6089-99.

DAL-PRA, S., FURTHAUER, M., VAN-CELST, J., THISSE, B. & THISSE, C. (2006). Noggin1 and Follistatin-like2 function redundantly to Chordin to antagonize BMP activity. *Dev Biol,* **298**, 514-26.

DALE, L., HOWES, G., PRICE, B. M. & SMITH, J. C. (1992). Bone morphogenetic protein 4: a ventralizing factor in early Xenopus development. *Development,* **115**, 573-85.

DARRAS, S. & NISHIDA, H. (2001). The BMP/CHORDIN antagonism controls sensory pigment cell specification and differentiation in the ascidian embryo. *Dev Biol,* **236**, 271-88.

DAVIDSON, E. H. (2010). Emerging properties of animal gene regulatory networks. *Nature,* **468**, 911-920.

DE ROBERTIS, E. M. & KURODA, H. (2004). Dorsal-ventral patterning and neural induction in Xenopus embryos. *Annu Rev Cell Dev Biol,* **20**, 285-308.

DE ROBERTIS, E. M. & SASAI, Y. (1996). A common plan for dorsoventral patterning in Bilateria. *Nature,* **380**, 37-40.

DEDEIC, Z., CETERA, M., COHEN, T. V. & HOLASKA, J. M. (2011). Emerin inhibits Lmo7 binding to the Pax3 and MyoD promoters and expression of myoblast proliferation genes. *J Cell Sci,* **124**, 1691-702.

DELARUE, M., SAEZ, F. J., JOHNSON, K. E. & BOUCAUT, J. C. (1997). Fates of the blastomeres of the 32-cell stage Pleurodeles waltl embryo. *Dev Dyn,* **210**, 236-48.

DELAUNE, E., LEMAIRE, P. & KODJABACHIAN, L. (2005). Neural induction in Xenopus requires early FGF signalling in addition to BMP inhibition. *Development,* **132**, 299-310.

DELHOMME, N., PADIOLEAU, I., FURLONG, E. E. & STEINMETZ, L. M. (2012). easyRNASeq: a bioconductor package for processing RNA-Seq data. *Bioinformatics,* **28**, 2532-3.

DELTOUR, S., PINTE, S., GUERARDEL, C. & LEPRINCE, D. (2001). Characterization of HRG22, a human homologue of the putative tumor suppressor gene HIC1. *Biochem Biophys Res Commun,* **287**, 427-34.

DESSAUD, E., MCMAHON, A. P. & BRISCOE, J. (2008). Pattern formation in the vertebrate neural tube: a sonic hedgehog morphogen-regulated transcriptional network. *Development,* **135**, 2489-503.

DESSAUD, E., YANG, L. L., HILL, K., COX, B., ULLOA, F., RIBEIRO, A., MYNETT, A., NOVITCH, B. G. & BRISCOE, J. (2007). Interpretation of the sonic hedgehog morphogen gradient by a temporal adaptation mechanism. *Nature,* **450**, 717-20.

DI PALMA, T., D'ANDREA, B., LIGUORI, G. L., LIGUORO, A., DE CRISTOFARO, T., DEL PRETE, D., PAPPALARDO, A., MASCIA, A. & ZANNINI, M. (2009). TAZ is a coactivator for Pax8 and TTF-1, two transcription factors involved in thyroid differentiation. *Exp Cell Res,* **315**, 162-75.

DIAS, M. S. & SCHOENWOLF, G. C. (1990). Formation of ectopic neurepithelium in chick blastoderms: age-related capacities for induction and self-differentiation following transplantation of quail Hensen's nodes. *Anat Rec,* **228**, 437-48.

DIEZ DEL CORRAL, R., OLIVERA-MARTINEZ, I., GORIELY, A., GALE, E., MADEN, M. & STOREY, K. (2003). Opposing FGF and retinoid pathways control ventral neural pattern, neuronal differentiation, and segmentation during body axis extension. *Neuron,* **40**, 65-79.

DIEZ DEL CORRAL, R. & STOREY, K. G. (2004). Opposing FGF and retinoid pathways: a signalling switch that controls differentiation and patterning onset in the extending vertebrate body axis. *Bioessays,* **26**, 857-69.

DOYON, Y., CAYROU, C., ULLAH, M., LANDRY, A. J., COTE, V., SELLECK, W., LANE, W. S., TAN, S., YANG, X. J. & COTE, J. (2006). ING tumor suppressor proteins are critical regulators of chromatin acetylation required for genome expression and perpetuation. *Mol Cell,* **21**, 51-64.

DREAN, G., LECLERC, C., DUPRAT, A. M. & MOREAU, M. (1995). Expression of L-type Ca2+ channel during early embryogenesis in Xenopus laevis. *Int J Dev Biol,* **39**, 1027-32.

DUDLEY, A. T., LYONS, K. M. & ROBERTSON, E. J. (1995). A requirement for bone morphogenetic protein-7 during development of the mammalian kidney and eye. *Genes Dev,* **9**, 2795-807.

DUNHAM, E. E., STEVENS, E. A., GLOVER, E. & BRADFIELD, C. A. (2006). The aryl hydrocarbon receptor signaling pathway is modified through interactions with a Kelch protein. *Mol Pharmacol,* **70**, 8-15.

DURSTON, A. J., TIMMERMANS, J. P., HAGE, W. J., HENDRIKS, H. F., DE VRIES, N. J., HEIDEVELD, M. & NIEUWKOOP, P. D. (1989). Retinoic acid causes an anteroposterior transformation in the developing central nervous system. *Nature,* **340**, 140-4.

ECHEVERRI, K. & OATES, A. C. (2007). Coordination of symmetric cyclic gene expression during somitogenesis by Suppressor of Hairless involves regulation of retinoic acid catabolism. *Dev Biol,* **301**, 388-403.

EKKER, S. C., MCGREW, L. L., LAI, C. J., LEE, J. J., VON KESSLER, D. P., MOON, R. T. & BEACHY, P. A. (1995). Distinct expression and shared activities of members of the hedgehog gene family of Xenopus laevis. *Development,* **121**, 2337-47.

EL-HUSSEINI, A. E. & VINCENT, S. R. (1999). Cloning and characterization of a novel RING finger protein that interacts with class V myosins. *J Biol Chem,* **274**, 19771-7.

ENDO, Y., OSUMI, N. & WAKAMATSU, Y. (2002). Bimodal functions of Notch-mediated signaling are involved in neural crest formation during avian ectoderm development. *Development,* **129**, 863-73.

ERICSON, J., MUHR, J., JESSELL, T. M. & EDLUND, T. (1995). Sonic hedgehog: a common signal for ventral patterning along the rostrocaudal axis of the neural tube. *Int J Dev Biol,* **39**, 809-16.

ESTEVE, P., MORCILLO, J. & BOVOLENTA, P. (2000). Early and dynamic expression of cSfrp1 during chick embryo development. *Mech Dev,* **97**, 217-21.

EYAL-GILADI, H. (1984). The gradual establishment of cell commitments during the early stages of chick development. *Cell Differ,* **14**, 245-55.

EYAL-GILADI, H. & KOCHAV, S. (1976). From cleavage to primitive streak formation: a complementary normal table and a new look at the first stages of the development of the chick. I. General morphology. *Developmental Biology,* **49**, 321-337.

FABIAN, B. & EYAL-GILADI, H. (1981). A SEM study of cell shedding during the formation of the area pellucida in the chick embryo. *J Embryol Exp Morphol,* **64**, 11-22.

FAINSOD, A., DEISSLER, K., YELIN, R., MAROM, K., EPSTEIN, M., PILLEMER, G., STEINBEISSER, H. & BLUM, M. (1997). The dorsalizing and neural inducing gene follistatin is an antagonist of BMP-4. *Mech Dev,* **63**, 39-50.

FAINSOD, A., STEINBEISSER, H. & DE ROBERTIS, E. M. (1994). On the function of BMP-4 in patterning the marginal zone of the Xenopus embryo. *Embo j,* **13**, 5015-25.

FAURE, S., DE SANTA BARBARA, P., ROBERTS, D. J. & WHITMAN, M. (2002). Endogenous patterns of BMP signaling during early chick development. *Developmental Biology,* **244**, 44-65.

FEINSTEIN, R., BOLTON, W. K., QUINONES, J. N., MOSIALOS, G., SIF, S., HUFF, J. L., CAPOBIANCO, A. J. & GILMORE, T. D. (1994). Characterization of a chicken cDNA encoding the retinoblastoma gene product. *Biochim Biophys Acta,* **1218**, 82-6.

FENSTAD, M. H., JOHNSON, M. P., LOSET, M., MUNDAL, S. B., ROTEN, L. T., EIDE, I. P., BJORGE, L., SANDE, R. K., JOHANSSON, A. K., DYER, T. D., FORSMO, S., BLANGERO, J., MOSES, E. K. & AUSTGULEN, R. (2010). STOX2 but not STOX1 is differentially expressed in decidua from pre-eclamptic women: data from the Second Nord-Trondelag Health Study. *Mol Hum Reprod,* **16**, 960-8.

FERGUSON, E. L. (1996). Conservation of dorsal-ventral patterning in arthropods and chordates. *Curr Opin Genet Dev,* **6**, 424-31.

FERGUSON, E. L. & ANDERSON, K. V. (1992). Decapentaplegic acts as a morphogen to organize dorsal-ventral pattern in the Drosophila embryo. *Cell,* **71**, 451-61.

FERRAN, J. L., SANCHEZ-ARRONES, L., SANDOVAL, J. E. & PUELLES, L. (2007). A model of early molecular regionalization in the chicken embryonic pretectum. *J Comp Neurol,* **505**, 379-403.

FERRARI, D., SUMOY, L., GANNON, J., SUN, H., BROWN, A. M., UPHOLT, W. B. & KOSHER, R. A. (1995). The expression pattern of the Distal-less homeobox-containing gene Dlx-5 in the developing chick limb bud suggests its involvement in apical ectodermal ridge activity, pattern formation, and cartilage differentiation. *Mech Dev,* **52**, 257-64.

FOLEY, A. C., SKROMNE, I. & STERN, C. D. (2000). Reconciling different models of forebrain induction and patterning: a dual role for the hypoblast. *Development (Cambridge, England),* **127**, 3839-3854.

FOLEY, A. C., STOREY, K. G. & STERN, C. D. (1997). The prechordal region lacks neural inducing ability, but can confer anterior character to more posterior neuroepithelium. *Development,* **124**, 2983-96.

FRANCIS, P. H., RICHARDSON, M. K., BRICKELL, P. M. & TICKLE, C. (1994). Bone morphogenetic proteins and a signalling pathway that controls patterning in the developing chick limb. *Development,* **120**, 209-18.

FRANCO, P. G., PAGANELLI, A. R., LOPEZ, S. L. & CARRASCO, A. E. (1999). Functional association of retinoic acid and hedgehog signaling in Xenopus primary neurogenesis. *Development,* **126**, 4257-65.

FRANCOIS, V. & BIER, E. (1995). Xenopus chordin and Drosophila short gastrulation genes encode homologous proteins functioning in dorsal-ventral axis formation. *Cell,* **80**, 19-20.

FRANCOIS, V., SOLLOWAY, M., O'NEILL, J. W., EMERY, J. & BIER, E. (1994). Dorsal-ventral patterning of the Drosophila embryo depends on a putative negative growth factor encoded by the short gastrulation gene. *Genes Dev,* **8**, 2602-16.

FRASER, P. E. & SAUKA-SPENGLER, T. (2004). Expression of the polycomb group gene bmi-1 in the early chick embryo. *Gene Expr Patterns,* **5**, 23-7.

FRESON, K., THYS, C., WITTEWRONGEL, C., VERMYLEN, J., HOYLAERTS, M. F. & VAN GEET, C. (2003). Molecular cloning and characterization of the GATA1 cofactor human FOG1 and assessment of its binding to GATA1 proteins carrying D218 substitutions. *Hum Genet,* **112**, 42-9.

FRIEDRICH, J. K., PANOV, K. I., CABART, P., RUSSELL, J. & ZOMERDIJK, J. C. (2005). TBP-TAF complex SL1 directs RNA polymerase I pre-initiation complex formation and stabilizes upstream binding factor at the rDNA promoter. *J Biol Chem,* **280**, 29551-8.

FURTHAUER, M., THISSE, B. & THISSE, C. (1999). Three different noggin genes antagonize the activity of bone morphogenetic proteins in the zebrafish embryo. *Dev Biol,* **214**, 181-96.

GALLERA, J. (1965). Quelle est la durée nécessaire pour déclencher des inductions neurales chez le Poulet? *Experientia,* **21**, 218-219.

GALLERA, J. (1968). [Neural induction in birds. Time relationship between neurulation of the host ectoderm and appearance of the neural anlage induced by a fragment of the primitive streak]. *Rev Suisse Zool,* **75**, 227-34.

GALLERA, J. (1971). Primary induction in birds. *Adv Morphog,* **9**, 149-80.

GALLERA, J. & NICOLET, G. (1969). Le pouvoir inducteur de l'endoblaste presomptif contenu dans la ligne primitive jeune de poulet. *J. Embryol. Exp. Morph.,* **21**, 105-118.

GALLERA, P. J. & IVANOV, I. (1964). La compétence neurogéne du feuillet externe du blastoderme de Poulet en fonction du facteur 'temps'. *Journal of Embryology and Experimental Morphology,* **12**, 693-711.

GARCIA-CASTRO, M. I., VIELMETTER, E. & BRONNER-FRASER, M. (2000). N-Cadherin, a cell adhesion molecule involved in establishment of embryonic left-right asymmetry. *Science,* **288**, 1047-51.

GEOFFROY SAINT-HILAIRE, É. (1822). *Philosophie anatomique,* Paris, Méquignon-Marvis.

GIBSON, A., ROBINSON, N., STREIT, A., SHENG, G. & STERN, C. D. (2011). Regulation of programmed cell death during neural induction in the chick embryo. *Submitted*.

GILL, R. M., GABOR, T. V., COUZENS, A. L. & SCHEID, M. P. (2013). The MYC-associated protein CDCA7 is phosphorylated by AKT to regulate MYC-dependent apoptosis and transformation. *Mol Cell Biol,* **33**, 498-513.

GIMLICH, R. L. & COOKE, J. (1983). Cell lineage and the induction of second nervous systems in amphibian development. *Nature,* **306**, 471-3.

GLAVIC, A., SILVA, F., AYBAR, M. J., BASTIDAS, F. & MAYOR, R. (2004). Interplay between Notch signaling and the homeoprotein Xiro1 is required for neural crest induction in Xenopus embryos. *Development,* **131**, 347-59.

GLINKA, A., WU, W., DELIUS, H., MONAGHAN, A. P., BLUMENSTOCK, C. & NIEHRS, C. (1998). Dickkopf-1 is a member of a new family of secreted proteins and functions in head induction. *Nature,* **391**, 357-62.

GLINKA, A., WU, W., ONICHTCHOUK, D., BLUMENSTOCK, C. & NIEHRS, C. (1997). Head induction by simultaneous repression of Bmp and Wnt signalling in Xenopus. *Nature,* **389**, 517-9.

GODSAVE, S. F. & DURSTON, A. J. (1997). Neural induction and patterning in embryos deficient in FGF signaling. *Int J Dev Biol,* **41**, 57-65.

GODSAVE, S. F. & SLACK, J. M. (1989). Clonal analysis of mesoderm induction in Xenopus laevis. *Dev Biol,* **134**, 486-90.

GOODWIN, G. H. (1997). Isolation of cDNAs encoding chicken homologues of the yeast SNF2 and Drosophila Brahma proteins. *Gene,* **184**, 27-32.

GOTO, T., FUKUI, A., SHIBUYA, H., KELLER, R. & ASASHIMA, M. (2010). Xenopus furry contributes to release of microRNA gene silencing. *Proceedings of the National Academy of Sciences,* **107**, 19344-19349.

GOTO, Y., HAYASHI, R., MURAMATSU, T., OGAWA, H., EGUCHI, I., OSHIDA, Y., OHTANI, K. & YOSHIDA, K. (2006). JPO1/CDCA7, a novel transcription factor E2F1-induced protein, possesses intrinsic transcriptional regulator activity. *Biochim Biophys Acta,* **1759**, 60-8.

GRAHAM, V., KHUDYAKOV, J., ELLIS, P. & PEVNY, L. (2003). SOX2 functions to maintain neural progenitor identity. *Neuron,* **39**, 749-65.

GRITSMAN, K., ZHANG, J., CHENG, S., HECKSCHER, E., TALBOT, W. S. & SCHIER, A. F. (1999). The EGF-CFC protein one-eyed pinhead is essential for nodal signaling. *Cell,* **97**, 121-32.

GRUNZ, H. (1992). Suramin changes the fate of Spemann's organizer and prevents neural induction in Xenopus laevis. *Mech Dev,* **38**, 133-41.

GRUNZ, H. & TACKE, L. (1989). Neural differentiation of Xenopus laevis ectoderm takes place after disaggregation and delayed reaggregation without inducer. *Cell Differ Dev,* **28**, 211-7.

GURDON, J. B. (1987). Embryonic induction--molecular prospects. *Development,* **99**, 285-306.

HA, A. S. & RIDDLE, R. D. (2003). cBlimp-1 expression in chick limb bud development. *Gene Expr Patterns,* **3**, 297-300.

HAMBURGER, V. & HAMILTON, H. L. (1951). A series of normal stages in the development of the chick embryo. *Journal of Morphology,* **88**, 49-92.

HANSEN, C. S., MARION, C. D., STEELE, K., GEORGE, S. & SMITH, W. C. (1997). Direct neural induction and selective inhibition of mesoderm and epidermis inducers by Xnr3. *Development,* **124**, 483-92.

HARADA, J., KOKURA, K., KANEI-ISHII, C., NOMURA, T., KHAN, M. M., KIM, Y. & ISHII, S. (2003). Requirement of the co-repressor homeodomain-interacting protein kinase 2 for ski-mediated inhibition of bone morphogenetic protein-induced transcriptional activation. *J Biol Chem,* **278**, 38998-9005.

HARDCASTLE, Z., CHALMERS, A. D. & PAPALOPULU, N. (2000). FGF-8 stimulates neuronal differentiation through FGFR-4a and interferes with mesoderm induction in Xenopus embryos. *Curr Biol,* **10**, 1511-4.

HARLAND, R. (2000). Neural induction. *Curr Opin Genet Dev,* **10**, 357-62.

HARTMANN, C. & TABIN, C. J. (2000). Dual roles of Wnt signaling during chondrogenesis in the chicken limb. *Development,* **127**, 3141-59.

HATA, A., SEOANE, J., LAGNA, G., MONTALVO, E., HEMMATI-BRIVANLOU, A. & MASSAGUE, J. (2000). OAZ uses distinct DNA- and protein-binding zinc fingers in separate BMP-Smad and Olf signaling pathways. *Cell,* **100**, 229-40.

HATADA, Y. & STERN, C. D. (1994). A fate map of the epiblast of the early chick embryo. *Development,* **120**, 2879-89.

HATTA, K. & TAKAHASHI, Y. (1996). Secondary axis induction by heterospecific organizers in zebrafish. *Dev Dyn,* **205**, 183-95.

HAWLEY, S. H., WUNNENBERG-STAPLETON, K., HASHIMOTO, C., LAURENT, M. N., WATABE, T., BLUMBERG, B. W. & CHO, K. W. (1995). Disruption of BMP signals in embryonic Xenopus ectoderm leads to direct neural induction. *Genes Dev,* **9**, 2923-35.

HEANUE, T. A., DAVIS, R. J., ROWITCH, D. H., KISPERT, A., MCMAHON, A. P., MARDON, G. & TABIN, C. J. (2002). Dach1, a vertebrate homologue of Drosophila dachshund, is expressed in the developing eye and ear of both chick and mouse and is regulated independently of Pax and Eya genes. *Mech Dev,* **111**, 75-87.

HEEG-TRUESDELL, E. & LABONNE, C. (2006). Neural induction in Xenopus requires inhibition of Wnt-beta-catenin signaling. *Dev Biol,* **298**, 71-86.

HEISS, N. S., GLOECKNER, G., BACHNER, D., KIOSCHIS, P., KLAUCK, S. M., HINZMANN, B., ROSENTHAL, A., HERMAN, G. E. & POUSTKA, A. (1997). Genomic structure of a novel LIM domain gene (ZNF185) in Xq28 and comparisons with the orthologous murine transcript. *Genomics,* **43**, 329-38.

HELLER, S., SHEANE, C. A., JAVED, Z. & HUDSPETH, A. J. (1998). Molecular markers for cell types of the inner ear and candidate genes for hearing disorders. *Proc Natl Acad Sci U S A,* **95**, 11400-5.

HELMS, J. A., KURATANI, S. & MAXWELL, G. D. (1994). Cloning and analysis of a new developmentally regulated member of the basic helix-loop-helix family. *Mech Dev,* **48**, 93-108.

HEMMATI-BRIVANLOU, A., KELLY, O. G. & MELTON, D. A. (1994). Follistatin, an antagonist of activin, is expressed in the Spemann organizer and displays direct neuralizing activity. *Cell,* **77**, 283-95.

HEMMATI-BRIVANLOU, A. & MELTON, D. (1997). Vertebrate embryonic cells will become nerve cells unless told otherwise. *Cell,* **88**, 13-17.

HEMMATI-BRIVANLOU, A. & MELTON, D. A. (1992). A truncated activin receptor inhibits mesoderm induction and formation of axial structures in Xenopus embryos. *Nature,* **359**, 609-14.

HEMMATI-BRIVANLOU, A. & MELTON, D. A. (1994). Inhibition of activin receptor signaling promotes neuralization in Xenopus. *Cell,* **77**, 273-81.

HEMMATI-BRIVANLOU, A., WRIGHT, D. A. & MELTON, D. A. (1992). Embryonic expression and functional analysis of a Xenopus activin receptor. *Dev Dyn,* **194**, 1-11.

HENSEN, V. (1876). Beobachtungen über die Befruchtung und Entwicklung des Kaninchens und Meerschweinchens. *Z. Anat. EntwGesch. ,* **1**, 353-423.

HENTSCHKE, M., SUSENS, U. & BORGMEYER, U. (2009). Transcriptional ERRgamma2-mediated activation is regulated by sentrin-specific proteases. *Biochem J,* **419**, 167-76.

HERMESZ, E., MACKEM, S. & MAHON, K. A. (1996). Rpx: a novel anterior-restricted homeobox gene progressively activated in the prechordal plate, anterior neural plate and Rathke's pouch of the mouse embryo. *Development,* **122**, 41-52.

HICAR, M. D., LIU, Y., ALLEN, C. E. & WU, L. C. (2001). Structure of the human zinc finger protein HIVEP3: molecular cloning, expression, exon-intron structure, and comparison with paralogous genes HIVEP1 and HIVEP2. *Genomics,* **71**, 89-100.

HILDEBRAND, D. G., ALEXANDER, E., HORBER, S., LEHLE, S., OBERMAYER, K., MUNCK, N. A., ROTHFUSS, O., FRICK, J. S., MORIMATSU, M., SCHMITZ, I., ROTH, J., EHRCHEN, J. M., ESSMANN, F. & SCHULZE-OSTHOFF, K. (2013). IkappaBzeta is a transcriptional key regulator of CCL2/MCP-1. *J Immunol,* **190**, 4812-20.

HO, T. H., CHARLET, B. N., POULOS, M. G., SINGH, G., SWANSON, M. S. & COOPER, T. A. (2004). Muscleblind proteins regulate alternative splicing. *Embo j,* **23**, 3103-12.

HOLASKA, J. M., RAIS-BAHRAMI, S. & WILSON, K. L. (2006). Lmo7 is an emerin-binding protein that regulates the transcription of emerin and many other muscle-relevant genes. *Hum Mol Genet,* **15**, 3459-72.

HOLLEY, S. A., JACKSON, P. D., SASAI, Y., LU, B., DE ROBERTIS, E. M., HOFFMANN, F. M. & FERGUSON, E. L. (1995). A conserved system for dorsal-ventral patterning in insects and vertebrates involving sog and chordin. *Nature,* **376**, 249-53.

HOLOWACZ, T. & SOKOL, S. (1999). FGF is required for posterior neural patterning but not for neural induction. *Dev Biol,* **205**, 296-308.

HOLTFRETER, J. (1944). Neural differentiation of ectoderm through exposure to saline solution. *Journal of Experimental Zoology,* **95**, 307-343.

HONGO, I., KENGAKU, M. & OKAMOTO, H. (1999). FGF signaling and the anterior neural induction in Xenopus. *Dev Biol,* **216**, 561-81.

HOPPE, P. E. & GREENSPAN, R. J. (1986). Local function of the Notch gene for embryonic ectodermal pathway choice in Drosophila. *Cell,* **46**, 773-83.

HSU, S. I., YANG, C. M., SIM, K. G., HENTSCHEL, D. M., O'LEARY, E. & BONVENTRE, J. V. (2001). TRIP-Br: a novel family of PHD zinc finger- and bromodomain-interacting proteins that regulate the transcriptional activity of E2F-1/DP-1. *Embo j,* **20**, 2273-85.

HU, N., STROBL-MAZZULLA, P., SAUKA-SPENGLER, T. & BRONNER, M. E. (2012). DNA methyltransferase3A as a molecular switch mediating the neural tube-to-neural crest fate transition. *Genes Dev,* **26**, 2380-5.

HUANG, D. W., SHERMAN, B. T. & LEMPICKI, R. A. (2009a). Bioinformatics enrichment tools: paths toward the comprehensive functional analysis of large gene lists. *Nucleic Acids Res,* **37**, 1-13.

HUANG, D. W., SHERMAN, B. T. & LEMPICKI, R. A. (2009b). Systematic and integrative analysis of large gene lists using DAVID bioinformatics resources. *Nat Protoc,* **4**, 44-57.

HUANG, H., WAHLIN, K. J., MCNALLY, M., IRVING, N. D. & ADLER, R. (2008). Developmental regulation of muscleblind-like (MBNL) gene expression in the chicken embryo retina. *Dev Dyn,* **237**, 286-96.

HUANG, S., LAOUKILI, J., EPPING, M. T., KOSTER, J., HOLZEL, M., WESTERMAN, B. A., NIJKAMP, W., HATA, A., ASGHARZADEH, S., SEEGER, R. C., VERSTEEG, R., BEIJERSBERGEN, R. L. & BERNARDS, R. (2009c). ZNF423 is critically required for retinoic acid-induced differentiation and is a marker of neuroblastoma outcome. *Cancer Cell,* **15**, 328-40.

HUBBARD, S. J., GRAFHAM, D. V., BEATTIE, K. J., OVERTON, I. M., MCLAREN, S. R., CRONING, M. D., BOARDMAN, P. E., BONFIELD, J. K., BURNSIDE, J., DAVIES, R. M., FARRELL, E. R., FRANCIS, M. D., GRIFFITHS-JONES, S., HUMPHRAY, S. J., HYLAND, C., SCOTT, C. E., TANG, H., TAYLOR, R. G., TICKLE, C., BROWN, W. R., BIRNEY, E., ROGERS, J. & WILSON, S. A. (2005). Transcriptome analysis for the chicken based on 19,626 finished cDNA sequences and 485,337 expressed sequence tags. *Genome Res,* **15**, 174-83.

HUDSON, C., DARRAS, S., CAILLOL, D., YASUO, H. & LEMAIRE, P. (2003). A conserved role for the MEK signalling pathway in neural tissue specification and posteriorisation in the invertebrate chordate, the ascidian Ciona intestinalis. *Development,* **130**, 147-59.

HUDSON, C. & LEMAIRE, P. (2001). Induction of anterior neural fates in the ascidian Ciona intestinalis. *Mech Dev,* **100**, 189-203.

INAZAWA, T., OKAMURA, Y. & TAKAHASHI, K. (1998). Basic fibroblast growth factor induction of neuronal ion channel expression in ascidian ectodermal blastomeres. *J Physiol,* **511 (Pt 2)**, 347-59.

INTARAPAT, S. & STERN, C. D. (2013). Sexually dimorphic and sex-independent left-right asymmetries in chicken embryonic gonads. *PLoS One,* **8**, e69893.

ISAAC, A., RODRIGUEZ-ESTEBAN, C., RYAN, A., ALTABEF, M., TSUKUI, T., PATEL, K., TICKLE, C. & IZPISUA-BELMONTE, J. C. (1998). Tbx genes and limb identity in chick embryo development. *Development,* **125**, 1867-75.

ISHIMURA, A., MAEDA, R., TAKEDA, M., KIKKAWA, M., DAAR, I. O. & MAENO, M. (2000). Involvement of BMP-4/msx-1 and FGF pathways in neural induction in the Xenopus embryo. *Dev Growth Differ,* **42**, 307-16.

ITOH, F., ITOH, S., GOUMANS, M. J., VALDIMARSDOTTIR, G., ISO, T., DOTTO, G. P., HAMAMORI, Y., KEDES, L., KATO, M. & DIJKE, P. T. (2004). Synergy and antagonism between Notch and BMP receptor signaling pathways in endothelial cells. **23**, 541-551.

IWAFUCHI-DOI, M., MATSUDA, K., MURAKAMI, K., NIWA, H., TESAR, P. J., ARUGA, J., MATSUO, I. & KONDOH, H. (2012). Transcriptional regulatory networks in epiblast cells and during anterior neural plate development as modeled in epiblast stem cells. *Development*.

IWAFUCHI-DOI, M., YOSHIDA, Y., ONICHTCHOUK, D., LEICHSENRING, M., DRIEVER, W., TAKEMOTO, T., UCHIKAWA, M., KAMACHI, Y. & KONDOH, H. (2011). The Pou5f1/Pou3f-dependent but SoxB-independent regulation of conserved enhancer N2 initiates Sox2 expression during epiblast to neural plate stages in vertebrates. *Dev Biol,* **352**, 354-66.

IZPISUA-BELMONTE, J. C., DE ROBERTIS, E. M., STOREY, K. G. & STERN, C. D. (1993). The homeobox gene goosecoid and the origin of organizer cells in the early chick blastoderm. *Cell,* **74**, 645-59.

JACOBS, K. A., COLLINS-RACIE, L. A., COLBERT, M., DUCKETT, M., GOLDEN-FLEET, M., KELLEHER, K., KRIZ, R., LAVALLIE, E. R., MERBERG, D., SPAULDING, V., STOVER, J., WILLIAMSON, M. J. & MCCOY, J. M. (1997). A genetic selection for isolating cDNAs encoding secreted proteins. *Gene,* **198**, 289-96.

JACOBSON, M. & HIROSE, G. (1981). Clonal organization of the central nervous system of the frog. II. Clones stemming from individual blastomeres of the 32- and 64-cell stages. *J Neurosci,* **1**, 271-84.

JANSA, P., MASON, S. W., HOFFMANN-ROHRER, U. & GRUMMT, I. (1998). Cloning and functional characterization of PTRF, a novel protein which induces dissociation of paused ternary transcription complexes. *Embo j,* **17**, 2855-64.

JEAN, C., AUBEL, P., SOLEIHAVOUP, C., BOUHALLIER, F., VOISIN, S., LAVIAL, F. & PAIN, B. (2013). Pluripotent genes in avian stem cells. *Development, Growth & Differentiation,* **55**, 41-51.

JEAN, C., OLIVEIRA, N. M., INTARAPAT, S., FUET, A., MAZOYER, C., DE ALMEIDA, I., TREVERS, K., BOAST, S., AUBEL, P., BERTOCCHINI, F., STERN, C. D. & PAIN, B. (2015). Transcriptome analysis of chicken ES, blastodermal and germ cells reveals that chick ES cells are equivalent to mouse ES cells rather than EpiSC. *Stem Cell Res,* **14**, 54-67.

JOHNSEN, S. A., GUNGOR, C., PRENZEL, T., RIETHDORF, S., RIETHDORF, L., TANIGUCHI-ISHIGAKI, N., RAU, T., TURSUN, B., FURLOW, J. D., SAUTER, G., SCHEFFNER, M., PANTEL, K., GANNON, F. & BACH, I. (2009). Regulation of estrogen-dependent transcription by the LIM cofactors CLIM and RLIM in breast cancer. *Cancer Res,* **69**, 128-36.

JONES, C. M., LYONS, K. M., LAPAN, P. M., WRIGHT, C. V. & HOGAN, B. L. (1992). DVR-4 (bone morphogenetic protein-4) as a posterior-ventralizing factor in Xenopus mesoderm induction. *Development,* **115**, 639-47.

JOUBIN, K. & STERN, C. D. (1999). Molecular interactions continuously define the organizer during the cell movements of gastrulation. *Cell,* **98**, 559-71.

KAHANE, N. & KALCHEIM, C. (1994). Expression of trkC receptor mRNA during development of the avian nervous system. *Journal of Neurobiology,* **25**, 571-584.

KAMACHI, Y., UCHIKAWA, M., COLLIGNON, J., LOVELL-BADGE, R. & KONDOH, H. (1998). Involvement of Sox1, 2 and 3 in the early and subsequent molecular events of lens induction. *Development,* **125**, 2521-2532.

KAMACHI, Y., UCHIKAWA, M. & KONDOH, H. (2000). Pairing SOX off: with partners in the regulation of embryonic development. *Trends Genet,* **16**, 182-7.

KANAI, F., MARIGNANI, P. A., SARBASSOVA, D., YAGI, R., HALL, R. A., DONOWITZ, M., HISAMINATO, A., FUJIWARA, T., ITO, Y., CANTLEY, L. C. & YAFFE, M. B. (2000). TAZ: a novel transcriptional co-activator regulated by interactions with 14-3-3 and PDZ domain proteins. *Embo j,* **19**, 6778-91.

KANAI, K., REZA, H. M., KAMITANI, A., HAMAZAKI, Y., HAN, S. I., YASUDA, K. & KATAOKA, K. (2010). SUMOylation negatively regulates transcriptional and oncogenic activities of MafA. *Genes Cells,* **15**, 971-82.

KARANTZALI, E., LEKAKIS, V., IOANNOU, M., HADJIMICHAEL, C., PAPAMATHEAKIS, J. & KRETSOVALI, A. (2011). Sall1 regulates embryonic stem cell differentiation in association with nanog. *J Biol Chem,* **286**, 1037-45.

KEE, Y. & BRONNER-FRASER, M. (2001). The transcriptional regulator Id3 is expressed in cranial sensory placodes during early avian embryonic development. *Mech Dev,* **109**, 337-40.

KENGAKU, M. & OKAMOTO, H. (1993). Basic fibroblast growth factor induces differentiation of neural tube and neural crest lineages of cultured ectoderm cells from Xenopus gastrula. *Development,* **119**, 1067-78.

KEYNES, R. J. & STERN, C. D. (1988). Mechanisms of vertebrate segmentation. *Development,* **103**, 413-29.

KHAN, M. A., SOTO-JIMENEZ, L. M., HOWE, T., STREIT, A., SOSINSKY, A. & STERN, C. D. (2013). Computational tools and resources for prediction and analysis of gene regulatory regions in the chick genome. *Genesis,* **51**, 311-24.

KHOKHA, M. K., YEH, J., GRAMMER, T. C. & HARLAND, R. M. (2005). Depletion of three BMP antagonists from Spemann's organizer leads to a catastrophic loss of dorsal structures. *Dev Cell,* **8**, 401-11.

KHUDYAKOV, J. & BRONNER-FRASER, M. (2009). Comprehensive spatiotemporal analysis of early chick neural crest network genes. *Dev Dyn,* **238**, 716-23.

KIM, G. J. & NISHIDA, H. (2001). Role of the FGF and MEK signaling pathway in the ascidian embryo. *Dev Growth Differ,* **43**, 521-33.

KIMURA, W., YASUGI, S., STERN, C. D. & FUKUDA, K. (2006). Fate and plasticity of the endoderm in the early chick embryo. *Developmental Biology,* **289**, 283-295.

KINTNER, C. (1992). Molecular bases of early neural development in Xenopus embryos. *Annu Rev Neurosci,* **15**, 251-84.

KINTNER, C. R. & DODD, J. (1991). Hensen's node induces neural tissue in Xenopus ectoderm. Implications for the action of the organizer in neural induction. *Development,* **113**, 1495-505.

KISHIMOTO, Y., LEE, K. H., ZON, L., HAMMERSCHMIDT, M. & SCHULTE-MERKER, S. (1997). The molecular nature of zebrafish swirl: BMP2 function is essential during early dorsoventral patterning. *Development,* **124**, 4457-66.

KLINGENSMITH, J., ANG, S. L., BACHILLER, D. & ROSSANT, J. (1999). Neural induction and patterning in the mouse in the absence of the node and its derivatives. *Dev Biol,* **216**, 535-49.

KNEZEVIC, V., DE SANTO, R. & MACKEM, S. (1997). Two novel chick T-box genes related to mouse Brachyury are expressed in different, non-overlapping mesodermal domains during gastrulation. *Development,* **124**, 411-9.

KNEZEVIC, V. & MACKEM, S. (2001). Activation of epiblast gene expression by the hypoblast layer in the prestreak chick embryo. *genesis,* **30**, 264-273.

KNEZEVIC, V., RANSON, M. & MACKEM, S. (1995). The organizer-associated chick homeobox gene, Gnot1, is expressed before gastrulation and regulated synergistically by activin and retinoic acid. *Developmental biology,* **171**, 458-470.

KNUTTI, D., KAUL, A. & KRALLI, A. (2000). A tissue-specific coactivator of steroid receptors, identified in a functional genetic screen. *Mol Cell Biol,* **20**, 2411-22.

KOCHAV, S., GINSBURG, M. & EYAL-GILADI, H. (1980). From cleavage to primitive streak formation: a complementary normal table and a new look at the first stages of the development of the chick. II. Microscopic anatomy and cell population dynamics. *Dev Biol,* **79**, 296-308.

KOLLER, C. (1882). Untersuchungen über die Blätterbildung im Hühnerkeim. *Arch. Mikr. Anat* **20**, 174-211.

KORESSAAR, T. & REMM, M. (2007). Enhancements and modifications of primer design program Primer3. *Bioinformatics,* **23**, 1289-91.

KOYANO-NAKAGAWA, N. & KINTNER, C. (2005). The expression and function of MTG/ETO family proteins during neurogenesis. *Dev Biol,* **278**, 22-34.

KRAFT, J. C., SCHUH, T., JUCHAU, M. & KIMELMAN, D. (1994). The retinoid X receptor ligand, 9-cis-retinoic acid, is a potential regulator of early Xenopus development. *Proc Natl Acad Sci U S A,* **91**, 3067-71.

KRCMERY, J., CAMARATA, T., KULISZ, A. & SIMON, H. G. (2010). Nucleocytoplasmic functions of the PDZ-LIM protein family: new insights into organ development. *Bioessays,* **32**, 100-8.

KRETZSCHMAR, M., DOODY, J. & MASSAGUE, J. (1997a). Opposing BMP and EGF signalling pathways converge on the TGF-beta family mediator Smad1. *Nature,* **389**, 618-22.

KRETZSCHMAR, M., DOODY, J., TIMOKHINA, I. & MASSAGUE, J. (1999). A mechanism of repression of TGFbeta/ Smad signaling by oncogenic Ras. *Genes Dev,* **13**, 804-16.

KRETZSCHMAR, M., LIU, F., HATA, A., DOODY, J. & MASSAGUÉ, J. (1997c). The TGF-beta family mediator Smad1 is phosphorylated directly and activated functionally by the BMP receptor kinase. *Genes & Development,* **11**, 984-995.

KROLL, K. L. & AMAYA, E. (1996). Transgenic Xenopus embryos from sperm nuclear transplantations reveal FGF signaling requirements during gastrulation. *Development,* **122**, 3173-83.

KUDOH, T., WILSON, S. W. & DAWID, I. B. (2002). Distinct roles for Fgf, Wnt and retinoic acid in posteriorizing the neural ectoderm. *Development,* **129**, 4335-46.

KUNATH, T., SABA-EL-LEIL, M. K., ALMOUSAILLEAKH, M., WRAY, J., MELOCHE, S. & SMITH, A. (2007). FGF stimulation of the Erk1/2 signalling cascade triggers transition of

pluripotent embryonic stem cells from self-renewal to lineage commitment. *Development,* **134**, 2895-902.

KURAKU, S., USUDA, R. & KURATANI, S. (2005). Comprehensive survey of carapacial ridge-specific genes in turtle implies co-option of some regulatory genes in carapace evolution. *Evol Dev,* **7**, 3-17.

KURIYAMA, S. & MAYOR, R. (2009). A role for Syndecan-4 in neural induction involving ERK- and PKC-dependent pathways. *Development,* **136**, 575-84.

KURODA, H., FUENTEALBA, L., IKEDA, A., REVERSADE, B. & DE ROBERTIS, E. M. (2005). Default neural induction: neuralization of dissociated Xenopus cells is mediated by Ras/MAPK activation. *Genes Dev,* **19**, 1022-7.

LADHER, R. K., CHURCH, V. L., ALLEN, S., ROBSON, L., ABDELFATTAH, A., BROWN, N. A., HATTERSLEY, G., ROSEN, V., LUYTEN, F. P., DALE, L. & FRANCIS-WEST, P. H. (2000). Cloning and expression of the Wnt antagonists Sfrp-2 and Frzb during chick development. *Dev Biol,* **218**, 183-98.

LAI, C. J., EKKER, S. C., BEACHY, P. A. & MOON, R. T. (1995). Patterning of the neural ectoderm of Xenopus laevis by the amino-terminal product of hedgehog autoproteolytic cleavage. *Development,* **121**, 2349-60.

LAMANTIA, A. S., COLBERT, M. C. & LINNEY, E. (1993). Retinoic acid induction and regional differentiation prefigure olfactory pathway formation in the mammalian forebrain. *Neuron,* **10**, 1035-48.

LAMB, T. M. & HARLAND, R. M. (1995). Fibroblast growth factor is a direct neural inducer, which combined with noggin generates anterior-posterior neural pattern. *Development (Cambridge, England),* **121**, 3627-3636.

LAMB, T. M., KNECHT, A. K., SMITH, W. C., STACHEL, S. E., ECONOMIDES, A. N., STAHL, N., YANCOPOLOUS, G. D. & HARLAND, R. M. (1993). Neural induction by the secreted polypeptide noggin. *Science,* **262**, 713-8.

LAUNAY, C., FROMENTOUX, V., SHI, D. L. & BOUCAUT, J. C. (1996). A truncated FGF receptor blocks neural induction by endogenous Xenopus inducers. *Development (Cambridge, England),* **122**, 869-880.

LAVIAL, F., ACLOQUE, H., BERTOCCHINI, F., MACLEOD, D. J., BOAST, S., BACHELARD, E., MONTILLET, G., THENOT, S., SANG, H. M., STERN, C. D., SAMARUT, J. & PAIN, B. (2007). The Oct4 homologue PouV and Nanog regulate pluripotency in chicken embryonic stem cells. *Development,* **134**, 3549-63.

LAWSON, K. A. & PEDERSEN, R. A. (1987). Cell fate, morphogenetic movement and population kinetics of embryonic endoderm at the time of germ layer formation in the mouse. *Development,* **101**, 627-52.

LECLERC, C., DAGUZAN, C., NICOLAS, M. T., CHABRET, C., DUPRAT, A. M. & MOREAU, M. (1997). L-type calcium channel activation controls the in vivo transduction of the neuralizing signal in the amphibian embryos. *Mech Dev,* **64**, 105-10.

LECLERC, C., DUPRAT, A. M. & MOREAU, M. (1995). In vivo labelling of L-type Ca2+ channels by fluorescent dihydropyridine: correlation between ontogenesis of the channels and the acquisition of neural competence in ecotderm cells from Pleurodeles waltl embryos. *Cell Calcium,* **17**, 216-24.

LECLERC, C., NÉANT, I. & MOREAU, M. (2011). Early neural development in vertebrates is also a matter of calcium. *Biochimie*.

LECLERC, C., RIZZO, C., DAGUZAN, C., NEANT, I., BATUT, J., AUGE, B. & MOREAU, M. (2001). [Neural determination in Xenopus laevis embryos: control of early neural gene expression by calcium]. *J Soc Biol,* **195**, 327-37.

LECLERC, C., WEBB, S. E., DAGUZAN, C., MOREAU, M. & MILLER, A. L. (2000). Imaging patterns of calcium transients during neural induction in Xenopus laevis embryos. *J Cell Sci,* **113 Pt 19**, 3519-29.

LEE, K. W., MOREAU, M., NEANT, I., BIBONNE, A. & LECLERC, C. (2009). FGF-activated calcium channels control neural gene expression in Xenopus. *Biochim Biophys Acta,* **1793**, 1033-40.

LEIDEN, J. M., WANG, C. Y., PETRYNIAK, B., MARKOVITZ, D. M., NABEL, G. J. & THOMPSON, C. B. (1992). A novel Ets-related transcription factor, Elf-1, binds to human immunodeficiency virus type 2 regulatory elements that are required for inducible trans activation in T cells. *J Virol,* **66**, 5890-7.

LEIMEISTER, C., DALE, K., FISCHER, A., KLAMT, B., HRABE DE ANGELIS, M., RADTKE, F., MCGREW, M. J., POURQUIÉ, O. & GESSLER, M. (2000). Oscillating Expression of c-Hey2 in the Presomitic Mesoderm Suggests That the Segmentation Clock May Use Combinatorial Signaling through Multiple Interacting bHLH Factors. *Developmental Biology,* **227**, 91-103.

LEVIN, M. (1998). The roles of activin and follistatin signaling in chick gastrulation. *Int J Dev Biol,* **42**, 553-9.

LEVIN, M., JOHNSON, R. L., STERN, C. D., KUEHN, M. & TABIN, C. (1995). A molecular pathway determining left-right asymmetry in chick embryogenesis. *Cell,* **82**, 803-14.

LI, J. Y., PU, M. T., HIRASAWA, R., LI, B. Z., HUANG, Y. N., ZENG, R., JING, N. H., CHEN, T., LI, E., SASAKI, H. & XU, G. L. (2007). Synergistic function of DNA methyltransferases Dnmt3a and Dnmt3b in the methylation of Oct4 and Nanog. *Mol Cell Biol,* **27**, 8748-59.

LI, R. & BERND, P. (1999). Neurotrophin-3 Increases Neurite Outgrowth and Apoptosis in Explants of the Chicken Neural Plate. *Developmental Neuroscience,* **21**, 12-21.

LIANG, J., WAN, M., ZHANG, Y., GU, P., XIN, H., JUNG, S. Y., QIN, J., WONG, J., COONEY, A. J., LIU, D. & SONGYANG, Z. (2008). Nanog and Oct4 associate with unique transcriptional repression complexes in embryonic stem cells. *Nat Cell Biol,* **10**, 731-9.

LIM, L. S., LOH, Y. H., ZHANG, W., LI, Y., CHEN, X., WANG, Y., BAKRE, M., NG, H. H. & STANTON, L. W. (2007). Zic3 is required for maintenance of pluripotency in embryonic stem cells. *Mol Biol Cell,* **18**, 1348-58.

LIN, H. H., BELL, E., UWANOGHO, D., PERFECT, L. W., NORISTANI, H., BATES, T. J., SNETKOV, V., PRICE, J. & SUN, Y. M. (2010). Neuronatin promotes neural lineage in ESCs via Ca(2+) signaling. *Stem Cells,* **28**, 1950-60.

LIN, I. Y., CHIU, F. L., YEANG, C. H., CHEN, H. F., CHUANG, C. Y., YANG, S. Y., HOU, P. S., SINTUPISUT, N., HO, H. N., KUO, H. C. & LIN, K. I. (2014). Suppression of the SOX2 Neural Effector Gene by PRDM1 Promotes Human Germ Cell Fate in Embryonic Stem Cells. *Stem Cell Reports,* **2**, 189-204.

LINKER, C., DE ALMEIDA, I., PAPANAYOTOU, C., STOWER, M., SABADO, V., GHORANI, E., STREIT, A., MAYOR, R. & STERN, C. D. (2009). Cell communication with the neural plate is required for induction of neural markers by BMP inhibition: evidence for homeogenetic induction and implications for Xenopus animal cap and chick explant assays. *Developmental biology,* **327**, 478-486.

LINKER, C. & STERN, C. D. (2004). Neural induction requires BMP inhibition only as a late step, and involves signals other than FGF and Wnt antagonists. *Development,* **131**.

LITSIOU, A., HANSON, S. & STREIT, A. (2005). A balance of FGF, BMP and WNT signalling positions the future placode territory in the head. *Development,* **132**, 4051-4062.

LIU, W., MA, Q., WONG, K., LI, W., OHGI, K., ZHANG, J., AGGARWAL, A. K. & ROSENFELD, M. G. (2013). Brd4 and JMJD6-associated anti-pause enhancers in regulation of transcriptional pause release. *Cell,* **155**, 1581-95.

LLERAS-FORERO, L., TAMBALO, M., CHRISTOPHOROU, N., CHAMBERS, D., HOUART, C. & STREIT, A. (2013). Neuropeptides: developmental signals in placode progenitor formation. *Dev Cell,* **26**, 195-203.

LOBJOIS, V., BENAZERAF, B., BERTRAND, N., MEDEVIELLE, F. & PITUELLO, F. (2004). Specific regulation of cyclins D1 and D2 by FGF and Shh signaling coordinates cell cycle progression, patterning, and differentiation during early steps of spinal cord development. *Dev Biol,* **273**, 195-209.

LOBO, G. P., AMENGUAL, J., BAUS, D., SHIVDASANI, R. A., TAYLOR, D. & VON LINTIG, J. (2013). Genetics and diet regulate vitamin A production via the homeobox transcription factor ISX. *J Biol Chem,* **288**, 9017-27.

LORDA-DIEZ, C. I., MONTERO, J. A., MARTINEZ-CUE, C., GARCIA-PORRERO, J. A. & HURLE, J. M. (2009). Transforming growth factors beta coordinate cartilage and tendon differentiation in the developing limb mesenchyme. *J Biol Chem,* **284**, 29988-96.

LOUDIG, O., BABICHUK, C., WHITE, J., ABU-ABED, S., MUELLER, C. & PETKOVICH, M. (2000). Cytochrome P450RAI(CYP26) promoter: a distinct composite retinoic acid response element underlies the complex regulation of retinoic acid metabolism. *Mol Endocrinol,* **14**, 1483-97.

LOWE, C. J., TERASAKI, M., WU, M., FREEMAN, R. M., JR., RUNFT, L., KWAN, K., HAIGO, S., ARONOWICZ, J., LANDER, E., GRUBER, C., SMITH, M., KIRSCHNER, M. & GERHART, J. (2006). Dorsoventral patterning in hemichordates: insights into early chordate evolution. *PLoS Biol,* **4**, e291.

LOWELL, S., BENCHOUA, A., HEAVEY, B. & SMITH, A. G. (2006). Notch promotes neural lineage entry by pluripotent embryonic stem cells. *PLoS Biol,* **4**, e121.

LUNN, J. S., FISHWICK, K. J., HALLEY, P. A. & STOREY, K. G. (2007). A spatial and temporal map of FGF/Erk1/2 activity and response repertoires in the early chick embryo. *Dev Biol,* **302**, 536-52.

LUTHER, W. H. (1935). Entwicklungsphysiologische Untersuchungen am Forellenkeim: Die Rolle des Organisationszentrums bei der Entstehung der Embryonalanlage. *Biol. Zentralbl. Bd.,* **55**, 114-137.

MADEN, M. (2002). Retinoid signalling in the development of the central nervous system. *Nature Reviews. Neuroscience,* **3**, 843-853.

MADEN, M. (2007). Retinoic acid in the development, regeneration and maintenance of the nervous system. *Nat Rev Neurosci,* **8**, 755-765.

MADEN, M., GALE, E., KOSTETSKII, I. & ZILE, M. (1996). Vitamin A-deficient quail embryos have half a hindbrain and other neural defects. *Curr Biol,* **6**, 417-26.

MADEN, M., SONNEVELD, E., VAN DER SAAG, P. T. & GALE, E. (1998). The distribution of endogenous retinoic acid in the chick embryo: implications for developmental mechanisms. *Development,* **125**, 4133-44.

MAGNÚSDÓTTIR, E., DIETMANN, S., MURAKAMI, K., GÜNESDOGAN, U., TANG, F., BAO, S., DIAMANTI, E., LAO, K., GOTTGENS, B. & AZIM SURANI, M. (2013). A tripartite transcription factor network regulates primordial germ cell specification in mice. *Nat Cell Biol,* **15**, 905-915.

MARIGO, V., JOHNSON, R. L., VORTKAMP, A. & TABIN, C. J. (1996). Sonic hedgehog Differentially Regulates Expression ofGLIandGLI3during Limb Development. *Developmental Biology,* **180**, 273-283.

MAROM, K., SHAPIRA, E. & FAINSOD, A. (1997). The chicken caudal genes establish an anterior-posterior gradient by partially overlapping temporal and spatial patterns of expression. *Mech Dev,* **64**, 41-52.

MARTA DE ALMEIDA, I. (2012). *Searching for novel neural inducing signals.* UCL (University College London).

MARTINSEN, B. J., FRASIER, A. J., BAKER, C. V. & LOHR, J. L. (2004). Cardiac neural crest ablation alters Id2 gene expression in the developing heart. *Dev Biol,* **272**, 176-90.

MASSE, J., PIQUET-PELLORCE, C., VIET, J., GUERRIER, D., PELLERIN, I. & DESCHAMPS, S. (2011). ZFPIP/Zfp462 is involved in P19 cell pluripotency and in their neuronal fate. *Exp Cell Res,* **317**, 1922-34.

MASSELINK, H. & BERNARDS, R. (2000). The adenovirus E1A binding protein BS69 is a corepressor of transcription through recruitment of N-CoR. *Oncogene,* **19**, 1538-46.

MASTON, G. A., EVANS, S. K. & GREEN, M. R. (2006). Transcriptional regulatory elements in the human genome. *Annu Rev Genomics Hum Genet,* **7**, 29-59.

MATSUMATA, M., UCHIKAWA, M., KAMACHI, Y. & KONDOH, H. (2005). Multiple N-cadherin enhancers identified by systematic functional screening indicate its Group B1 SOX-dependent regulation in neural and placodal development. *Dev Biol,* **286**, 601-17.

MATSUMOTO, K., NISHIHARA, S., KAMIMURA, M., SHIRAISHI, T., OTOGURO, T., UEHARA, M., MAEDA, Y., OGURA, K., LUMSDEN, A. & OGURA, T. (2004). The prepattern transcription factor Irx2, a target of the FGF8/MAP kinase cascade, is involved in cerebellum formation. *Nat Neurosci,* **7**, 605-12.

MATZUK, M. M., LU, N., VOGEL, H., SELLHEYER, K., ROOP, D. R. & BRADLEY, A. (1995). Multiple defects and perinatal death in mice deficient in follistatin. *Nature,* **374**, 360-3.

MCCABE, K. L., MCGUIRE, C. & REH, T. A. (2006). Pea3 expression is regulated by FGF signaling in developing retina. *Dev Dyn,* **235**, 327-35.

MCCLINTOCK, J. M., JOZEFOWICZ, C., ASSIMACOPOULOS, S., GROVE, E. A., LOUVI, A. & PRINCE, V. E. (2003). Conserved expression of Hoxa1 in neurons at the ventral forebrain/midbrain boundary of vertebrates. *Dev Genes Evol,* **213**, 399-406.

MCGUIRE, E. A., DAVIS, A. R. & KORSMEYER, S. J. (1991). T-cell translocation gene 1 (Ttg-1) encodes a nuclear protein normally expressed in neural lineage cells. *Blood,* **77**, 599-606.

MCLARREN, K. W., LITSIOU, A. & STREIT, A. (2003). DLX5 positions the neural crest and preplacode region at the border of the neural plate. *Dev Biol,* **259**, 34-47.

MCMAHON, J. A., TAKADA, S., ZIMMERMAN, L. B., FAN, C. M., HARLAND, R. M. & MCMAHON, A. P. (1998). Noggin-mediated antagonism of BMP signaling is required for growth and patterning of the neural tube and somite. *Genes & Development,* **12**, 1438-1452.

MENDELSOHN, C., RUBERTE, E., LEMEUR, M., MORRISS-KAY, G. & CHAMBON, P. (1991). Developmental analysis of the retinoic acid-inducible RAR-beta 2 promoter in transgenic animals. *Development,* **113**, 723-34.

MERCADER, N., LEONARDO, E., AZPIAZU, N., SERRANO, A., MORATA, G., MARTINEZ, C. & TORRES, M. (1999). Conserved regulation of proximodistal limb axis development by Meis1/Hth. *Nature,* **402**, 425-9.

MERCADER, N., LEONARDO, E., PIEDRA, M. E., MARTINEZ, A. C., ROS, M. A. & TORRES, M. (2000). Opposing RA and FGF signals control proximodistal vertebrate limb development through regulation of Meis genes. *Development,* **127**, 3961-70.

MEREDITH, M. M., LIU, K., DARRASSE-JEZE, G., KAMPHORST, A. O., SCHREIBER, H. A., GUERMONPREZ, P., IDOYAGA, J., CHEONG, C., YAO, K. H., NIEC, R. E. & NUSSENZWEIG, M. C. (2012). Expression of the zinc finger transcription factor zDC (Zbtb46, Btbd4) defines the classical dendritic cell lineage. *J Exp Med,* **209**, 1153-65.

MEY, A., ACLOQUE, H., LERAT, E., GOUNEL, S., TRIBOLLET, V., BLANC, S., CURTON, D., BIROT, A. M., NIETO, M. A. & SAMARUT, J. (2012). The endogenous retrovirus ENS-1 provides active binding sites for transcription factors in embryonic stem cells that specify extra embryonic tissue. *Retrovirology,* **9**, 21.

MILLET, S., CAMPBELL, K., EPSTEIN, D. J., LOSOS, K., HARRIS, E. & JOYNER, A. L. (1999). A role for Gbx2 in repression of Otx2 and positioning the mid/hindbrain organizer. *Nature,* **401**, 161-4.

MIN, T. H., KRIEBEL, M., HOU, S. & PERA, E. M. (2011). The dual regulator Sufu integrates Hedgehog and Wnt signals in the early Xenopus embryo. *Dev Biol,* **358**, 262-76.

MINOWADA, G., JARVIS, L. A., CHI, C. L., NEUBUSER, A., SUN, X., HACOHEN, N., KRASNOW, M. A. & MARTIN, G. R. (1999). Vertebrate Sprouty genes are induced by FGF signaling and can cause chondrodysplasia when overexpressed. *Development,* **126**, 4465-75.

MISHIMA, N. & TOMAREV, S. (1998). Chicken Eyes absent 2 gene: isolation and expression pattern during development. *Int J Dev Biol,* **42**, 1109-15.

MIYA, T., MORITA, K., SUZUKI, A., UENO, N. & SATOH, N. (1997). Functional analysis of an ascidian homologue of vertebrate Bmp-2/Bmp-4 suggests its role in the inhibition of neural fate specification. *Development,* **124**, 5149-59.

MIYAKE, J. H., SZETO, D. P. & STUMPH, W. E. (1997). Analysis of the structure and expression of the chicken gene encoding a homolog of the human RREB-1 transcription factor. *Gene,* **202**, 177-86.

MONROE, D. G., JIN, D. F. & SANDERS, M. M. (2000). Estrogen opposes the apoptotic effects of bone morphogenetic protein 7 on tissue remodeling. *Mol Cell Biol,* **20**, 4626-34.

MOODY, S. A. (1987). Fates of the blastomeres of the 32-cell-stage Xenopus embryo. *Dev Biol,* **122**, 300-19.

MOODY, S. A. & KLINE, M. J. (1990). Segregation of fate during cleavage of frog (Xenopus laevis) blastomeres. *Anat Embryol (Berl),* **182**, 347-62.

MOON, J.-H., HEO, J. S., KIM, J. S., JUN, E. K., LEE, J. H., KIM, A., KIM, J., WHANG, K. Y., KANG, Y.-K., YEO, S., LIM, H.-J., HAN, D. W., KIM, D.-W., OH, S., YOON, B. S., SCHOLER, H. R. & YOU, S. (2011). Reprogramming fibroblasts into induced pluripotent stem cells with Bmi1. *Cell Res,* **21**, 1305-1315.

MOREAU, M., LECLERC, C., GUALANDRIS-PARISOT, L. & DUPRAT, A. M. (1994). Increased internal Ca2+ mediates neural induction in the amphibian embryo. *Proc Natl Acad Sci U S A,* **91**, 12639-43.

MORENO, T. A. & KINTNER, C. (2004). Regulation of segmental patterning by retinoic acid signaling during Xenopus somitogenesis. *Dev Cell,* **6**, 205-18.

MORI, Y., KATAOKA, H., MIURA, Y., KAWAGUCHI, M., KUBOTA, E., OGASAWARA, N., OSHIMA, T., TANIDA, S., SASAKI, M., OHARA, H., MIZOSHITA, T., TATEMATSU, M., ASAI, K. & JOH, T. (2007). Subcellular localization of ATBF1 regulates MUC5AC transcription in gastric cancer. *Int J Cancer,* **121**, 241-7.

MOURY, J. D. & JACOBSON, A. G. (1989). Neural fold formation at newly created boundaries between neural plate and epidermis in the axolotl. *Dev Biol,* **133**, 44-57.

MOURY, J. D. & JACOBSON, A. G. (1990). The origins of neural crest cells in the axolotl. *Dev Biol,* **141**, 243-53.

MUKHOPADHYAY, M., SHTROM, S., RODRIGUEZ-ESTEBAN, C., CHEN, L., TSUKUI, T., GOMER, L., DORWARD, D. W., GLINKA, A., GRINBERG, A., HUANG, S. P., NIEHRS, C., IZPISUA BELMONTE, J. C. & WESTPHAL, H. (2001). Dickkopf1 is required for embryonic head induction and limb morphogenesis in the mouse. *Dev Cell,* **1**, 423-34.

MUNOZ-SANJUAN, I. & BRIVANLOU, A. H. (2002). Neural induction, the default model and embryonic stem cells. *Nat Rev Neurosci,* **3**, 271-80.

MURATA, T., NITTA, M. & YASUDA, K. (1998). Transcription factor CP2 is essential for lens-specific expression of the chicken alphaA-crystallin gene. *Genes Cells,* **3**, 443-57.

NAKAE, J., CAO, Y., HAKUNO, F., TAKEMORI, H., KAWANO, Y., SEKIOKA, R., ABE, T., KIYONARI, H., TANAKA, T., SAKAI, J., TAKAHASHI, S. & ITOH, H. (2012). Novel repressor regulates insulin sensitivity through interaction with Foxo1. *Embo j,* **31**, 2275-95.

NAKAMURA, O. & TOIVONEN, S. (1978). *Organizer - a milestone of a half-century from Spemann,* Amsterdam, Elsevier/North-Holland Biomedical Press.

NAKAYAMA, A., MURAKAMI, H., MAEYAMA, N., YAMASHIRO, N., SAKAKIBARA, A., MORI, N. & TAKAHASHI, M. (2003). Role for RFX transcription factors in non-neuronal cell-specific inactivation of the microtubule-associated protein MAP1A promoter. *J Biol Chem,* **278**, 233-40.

NEW, D. A. T. (1955). A new technique for the cultivation of the chick embryo in vitro. *J. Embryol. Exp. Morphol.,* **3**, 326-331.

NICOLET, G. (1967). La chronologie d'invagination chez le Poulet: Etude à l'aide de la thymidine tritiée. *Experientia,* **23**, 576-577.

NOMURA, N., ZHAO, M. J., NAGASE, T., MAEKAWA, T., ISHIZAKI, R., TABATA, S. & ISHII, S. (1991). HIV-EP2, a new member of the gene family encoding the human immunodeficiency virus type 1 enhancer-binding protein. Comparison with HIV-EP1/PRDII-BF1/MBP-1. *J Biol Chem,* **266**, 8590-4.

NORDSTROM, U., JESSELL, T. M. & EDLUND, T. (2002). Progressive induction of caudal neural character by graded Wnt signaling. *Nat Neurosci,* **5**, 525-32.

OETTGEN, P., ALANI, R. M., BARCINSKI, M. A., BROWN, L., AKBARALI, Y., BOLTAX, J., KUNSCH, C., MUNGER, K. & LIBERMANN, T. A. (1997). Isolation and characterization of a novel epithelium-specific transcription factor, ESE-1, a member of the ets family. *Mol Cell Biol,* **17**, 4419-33.

OGINO, H. & YASUDA, K. (1998). Induction of lens differentiation by activation of a bZIP transcription factor, L-Maf. *Science,* **280**, 115-8.

OKAMOTO, R., UCHIKAWA, M. & KONDOH, H. (2015). Sixteen additional enhancers associated with the chicken Sox2 locus outside the central 50-kb region. *Dev Growth Differ,* **57**, 24-39.

OLIVERA-MARTINEZ, I., SCHURCH, N., LI, R. A., SONG, J., HALLEY, P. A., DAS, R. M., BURT, D. W., BARTON, G. J. & STOREY, K. G. (2014). Major transcriptome re-organisation and abrupt changes in signalling, cell cycle and chromatin regulation at neural differentiation in vivo. *Development,* **141**, 3266-76.

OLIVERA-MARTINEZ, I. & STOREY, K. G. (2007). Wnt signals provide a timing mechanism for the FGF-retinoid differentiation switch during vertebrate body axis extension. *Development,* **134**, 2125-35.

OMORI, Y., IMAI, J., SUZUKI, Y., WATANABE, S., TANIGAMI, A. & SUGANO, S. (2002). OASIS is a transcriptional activator of CREB/ATF family with a transmembrane domain. *Biochem Biophys Res Commun,* **293**, 470-7.

OPPENHEIMER, J. M. (1936a). Structures developed in amphibians by implantation of living fish organizer. *Proc. Soc. Exp. Biol. Med.,* **34**, 461-463.

OPPENHEIMER, J. M. (1936c). Transplantation experiments on developing teleosts (Fundulus and Perca). *J. Exp. Zool. ,* **72**, 409-437.

OTA, K., NAGAI, H. & SHENG, G. (2007). Expression and hypoxic regulation of hif1alpha and hif2alpha during early blood and endothelial cell differentiation in chick. *Gene Expr Patterns,* **7**, 761-6.

OTTE, A. P., KOSTER, C. H., SNOEK, G. T. & DURSTON, A. J. (1988). Protein kinase C mediates neural induction in Xenopus laevis. *Nature,* **334**, 618-20.

OTTE, A. P., VAN RUN, P., HEIDEVELD, M., VAN DRIEL, R. & DURSTON, A. J. (1989). Neural induction is mediated by cross-talk between the protein kinase C and cyclic AMP pathways. *Cell,* **58**, 641-8.

OZAIR, M. Z., KINTNER, C. & BRIVANLOU, A. H. (2013). Neural induction and early patterning in vertebrates. *Wiley Interdiscip Rev Dev Biol,* **2**, 479-98.

PADGETT, R. W., WOZNEY, J. M. & GELBART, W. M. (1993). Human BMP sequences can confer normal dorsal-ventral patterning in the Drosophila embryo. *Proc Natl Acad Sci U S A,* **90**, 2905-9.

PAIN, B., CLARK, M. E., SHEN, M., NAKAZAWA, H., SAKURAI, M., SAMARUT, J. & ETCHES, R. J. (1996). Long-term in vitro culture and characterisation of avian embryonic stem cells with multiple morphogenetic potentialities. *Development,* **122**, 2339-48.

PALAMARCHUK, A., EFANOV, A., MAXIMOV, V., AQEILAN, R. I., CROCE, C. M. & PEKARSKY, Y. (2005). Akt phosphorylates and regulates Pdcd4 tumor suppressor protein. *Cancer Res,* **65**, 11282-6.

PANNETT, C. A. & COMPTON, A. (1924). The cultivation of tissue in saline embryonic juice. *The Lancet,* **203**, 381-384.

PAPALOPULU, N. (1995). Regionalization of the forebrain from neural plate to neural tube. *Perspect Dev Neurobiol,* **3**, 39-52.

PAPALOPULU, N. & KINTNER, C. (1996). A posteriorising factor, retinoic acid, reveals that anteroposterior patterning controls the timing of neuronal differentiation in Xenopus neuroectoderm. *Development,* **122**, 3409-18.

PAPANAYOTOU, C., DE ALMEIDA, I., LIAO, P., OLIVEIRA, N. M. M., LU, S.-Q., KOUGIOUMTZIDOU, E., ZHU, L., SHAW, A., SHENG, G., STREIT, A., YU, D., WAH

SOONG, T. & STERN, C. D. (2013). Calfacilitin is a calcium channel modulator essential for initiation of neural plate development. *Nat Commun,* **4**, 1837.

PAPANAYOTOU, C., MEY, A., BIROT, A. M., SAKA, Y., BOAST, S., SMITH, J. C., SAMARUT, J. & STERN, C. D. (2008). A mechanism regulating the onset of Sox2 expression in the embryonic neural plate. *PLoS Biol,* **6**.

PAPPANO, W. N., SCOTT, I. C., CLARK, T. G., EDDY, R. L., SHOWS, T. B. & GREENSPAN, D. S. (1998). Coding sequence and expression patterns of mouse chordin and mapping of the cognate mouse chrd and human CHRD genes. *Genomics,* **52**, 236-9.

PATEL, N. S., RHINN, M., SEMPRICH, C. I., HALLEY, P. A., DOLLE, P., BICKMORE, W. A. & STOREY, K. G. (2013). FGF signalling regulates chromatin organisation during neural differentiation via mechanisms that can be uncoupled from transcription. *PLoS Genet,* **9**, e1003614.

PATTEN, I. & PLACZEK, M. (2000). The role of Sonic hedgehog in neural tube patterning. *Cell Mol Life Sci,* **57**, 1695-708.

PATTYN, A., VALLSTEDT, A., DIAS, J. M., SANDER, M. & ERICSON, J. (2003). Complementary roles for Nkx6 and Nkx2 class proteins in the establishment of motoneuron identity in the hindbrain. *Development,* **130**, 4149-59.

PAXTON, C. N., BLEYL, S. B., CHAPMAN, S. C. & SCHOENWOLF, G. C. (2010). Identification of differentially expressed genes in early inner ear development. *Gene Expr Patterns,* **10**, 31-43.

PEALE, F. V., JR., SUGDEN, L. & BOTHWELL, M. (1998). Characterization of CMIX, a chicken homeobox gene related to the Xenopus gene mix.1. *Mech Dev,* **75**, 167-70.

PEARCE, J. J., PENNY, G. & ROSSANT, J. (1999). A mouse cerberus/Dan-related gene family. *Dev Biol,* **209**, 98-110.

PEARSE, R. V., 2ND, VOGAN, K. J. & TABIN, C. J. (2001). Ptc1 and Ptc2 transcripts provide distinct readouts of Hedgehog signaling activity during chick embryogenesis. *Dev Biol,* **239**, 15-29.

PERA, E. & KESSEL, M. (1999). Expression of DLX3 in chick embryos. *Mech Dev,* **89**, 189-93.

PERA, E. M., IKEDA, A., EIVERS, E. & DE ROBERTIS, E. M. (2003). Integration of IGF, FGF, and anti-BMP signals via Smad1 phosphorylation in neural induction. *Genes Dev,* **17**, 3023-8.

PERA, E. M., WESSELY, O., LI, S. Y. & DE ROBERTIS, E. M. (2001). Neural and head induction by insulin-like growth factor signals. *Dev Cell,* **1**, 655-65.

PEREZ, S. E., REBELO, S. & ANDERSON, D. J. (1999). Early specification of sensory neuron fate revealed by expression and function of neurogenins in the chick embryo. *Development,* **126**, 1715-28.

PERISSI, V., AGGARWAL, A., GLASS, C. K., ROSE, D. W. & ROSENFELD, M. G. (2004). A corepressor/coactivator exchange complex required for transcriptional activation by nuclear receptors and other regulated transcription factors. *Cell,* **116**, 511-26.

PERNAUTE, B., CANON, S., CRESPO, M., FERNANDEZ-TRESGUERRES, B., RAYON, T. & MANZANARES, M. (2010). Comparison of extraembryonic expression of Eomes and Cdx2 in pregastrulation chick and mouse embryo unveils regulatory changes along evolution. *Dev Dyn,* **239**, 620-9.

PETITTE, J. N., CLARK, M. E., LIU, G., VERRINDER GIBBINS, A. M. & ETCHES, R. J. (1990). Production of somatic and germline chimeras in the chicken by transfer of early blastodermal cells. *Development,* **108**, 185-9.

PEVNY, L. H., SOCKANATHAN, S., PLACZEK, M. & LOVELL-BADGE, R. (1998). A role for SOX1 in neural determination. *Development,* **125**, 1967-78.

PFEFFER, P. L., DE ROBERTIS, E. M. & IZPISUA-BELMONTE, J. C. (1997). Crescent, a novel chick gene encoding a Frizzled-like cysteine-rich domain, is expressed in anterior regions during early embryogenesis. *Int J Dev Biol,* **41**, 449-58.

PICCOLO, S., AGIUS, E., LEYNS, L., BHATTACHARYYA, S., GRUNZ, H., BOUWMEESTER, T. & DE ROBERTIS, E. M. (1999). The head inducer Cerberus is a multifunctional antagonist of Nodal, BMP and Wnt signals. *Nature,* **397**, 707-10.

PICCOLO, S., SASAI, Y., LU, B. & DE ROBERTIS, E. M. (1996). Dorsoventral patterning in Xenopus: inhibition of ventral signals by direct binding of chordin to BMP-4. *Cell,* **86**, 589-98.

PINHO, S., SIMONSSON, P. R., TREVERS, K. E., STOWER, M. J., SHERLOCK, W. T., KHAN, M., STREIT, A., SHENG, G. & STERN, C. D. (2011). Distinct steps of neural induction revealed by Asterix, Obelix and TrkC, genes induced by different signals from the organizer. *PloS one,* **6**.

PINTE, S., STANKOVIC-VALENTIN, N., DELTOUR, S., ROOD, B. R., GUERARDEL, C. & LEPRINCE, D. (2004). The tumor suppressor gene HIC1 (hypermethylated in cancer 1) is a sequence-specific transcriptional repressor: definition of its consensus binding sequence and analysis of its DNA binding and repressive properties. *J Biol Chem,* **279**, 38313-24.

PLACHETKA, A., CHAYKA, O., WILCZEK, C., MELNIK, S., BONIFER, C. & KLEMPNAUER, K. H. (2008). C/EBPbeta induces chromatin opening at a cell-type-specific enhancer. *Mol Cell Biol,* **28**, 2102-12.

POSTIGO, A. A., DEPP, J. L., TAYLOR, J. J. & KROLL, K. L. (2003). Regulation of Smad signaling through a differential recruitment of coactivators and corepressors by ZEB proteins. *Embo j,* **22**, 2453-62.

POWNALL, M. E., WELM, B. E., FREEMAN, K. W., SPENCER, D. M., ROSEN, J. M. & ISAACS, H. V. (2003). An inducible system for the study of FGF signalling in early amphibian development. *Dev Biol,* **256**, 89-99.

PRINCE, V. & LUMSDEN, A. (1994). Hoxa-2 expression in normal and transposed rhombomeres: independent regulation in the neural tube and neural crest. *Development,* **120**, 911-23.

PSYCHOYOS, D. & STERN, C. D. (1996a). Fates and migratory routes of primitive streak cells in the chick embryo. *Development,* **122**, 1523-34.

PSYCHOYOS, D. & STERN, C. D. (1996b). Restoration of the organizer after radical ablation of Hensen's node and the anterior primitive streak in the chick embryo. *Development,* **122**, 3263-73.

PUIGSERVER, P. & SPIEGELMAN, B. M. (2003). Peroxisome proliferator-activated receptor-gamma coactivator 1 alpha (PGC-1 alpha): transcriptional coactivator and metabolic regulator. *Endocr Rev,* **24**, 78-90.

QIAO, Q., LI, Y., CHEN, Z., WANG, M., REINBERG, D. & XU, R. M. (2011). The structure of NSD1 reveals an autoregulatory mechanism underlying histone H3K36 methylation. *J Biol Chem,* **286**, 8361-8.

QIAO, Y., ZHU, Y., SHENG, N., CHEN, J., TAO, R., ZHU, Q., ZHANG, T., QIAN, C. & JING, N. (2012). AP2gamma regulates neural and epidermal development downstream of the BMP pathway at early stages of ectodermal patterning. *Cell Res,* **22**, 1546-61.

QUINLAN, R., GRAF, M., MASON, I., LUMSDEN, A. & KIECKER, C. (2009). Complex and dynamic patterns of Wnt pathway gene expression in the developing chick forebrain. *Neural Dev,* **4**, 35.

RADA-IGLESIAS, A., BAJPAI, R., SWIGUT, T., BRUGMANN, S. A., FLYNN, R. A. & WYSOCKA, J. (2011). A unique chromatin signature uncovers early developmental enhancers in humans. *Nature,* **470**, 279-283.

REIJNTJES, S., BLENTIC, A., GALE, E. & MADEN, M. (2005). The control of morphogen signalling: regulation of the synthesis and catabolism of retinoic acid in the developing embryo. *Dev Biol,* **285**, 224-37.

REIJNTJES, S., GALE, E. & MADEN, M. (2004). Generating gradients of retinoic acid in the chick embryo: Cyp26C1 expression and a comparative analysis of the Cyp26 enzymes. *Dev Dyn,* **230**, 509-17.

RENGARAJ, D., LEE, B. R., LEE, S. I., SEO, H. W. & HAN, J. Y. (2011). Expression patterns and miRNA regulation of DNA methyltransferases in chicken primordial germ cells. *PLoS One,* **6**, e19524.

REVERSADE, B., KURODA, H., LEE, H., MAYS, A. & DE ROBERTIS, E. M. (2005). Depletion of Bmp2, Bmp4, Bmp7 and Spemann organizer signals induces massive brain formation in Xenopus embryos. *Development,* **132**, 3381-92.

REX, M., ORME, A., UWANOGHO, D., TOINTON, K., WIGMORE, P. M., SHARPE, P. T. & SCOTTING, P. J. (1997). Dynamic expression of chicken Sox2 and Sox3 genes in ectoderm induced to form neural tissue. *Developmental Dynamics: An Official Publication of the American Association of Anatomists,* **209**, 323-332.

REYMOND, A., MERONI, G., FANTOZZI, A., MERLA, G., CAIRO, S., LUZI, L., RIGANELLI, D., ZANARIA, E., MESSALI, S., CAINARCA, S., GUFFANTI, A., MINUCCI, S., PELICCI, P. G. & BALLABIO, A. (2001). The tripartite motif family identifies cell compartments. *Embo j,* **20**, 2140-51.

REYNOLDS, K., MEZEY, E. & ZIMMER, A. (1991). Activity of the beta-retinoic acid receptor promoter in transgenic mice. *Mech Dev,* **36**, 15-29.

RIBES, V., LE ROUX, I., RHINN, M., SCHUHBAUR, B. & DOLLE, P. (2009). Early mouse caudal development relies on crosstalk between retinoic acid, Shh and Fgf signalling pathways. *Development,* **136**, 665-76.

RIBISI, S., JR., MARIANI, F. V., AAMAR, E., LAMB, T. M., FRANK, D. & HARLAND, R. M. (2000). Ras-mediated FGF signaling is required for the formation of posterior but not anterior neural tissue in Xenopus laevis. *Dev Biol,* **227**, 183-96.

RICHARD-PARPAILLON, L., HELIGON, C., CHESNEL, F., BOUJARD, D. & PHILPOTT, A. (2002). The IGF pathway regulates head formation by inhibiting Wnt signaling in Xenopus. *Dev Biol,* **244**, 407-17.

RIDDLE, R. D., ENSINI, M., NELSON, C., TSUCHIDA, T., JESSELL, T. M. & TABIN, C. (1995). Induction of the LIM homeobox gene Lmx1 by WNT7a establishes dorsoventral pattern in the vertebrate limb. *Cell,* **83**, 631-40.

RIGOURD, V., CHELBI, S., CHAUVET, C., REBOURCET, R., BARBAUX, S., BESSIERES, B., MONDON, F., MIGNOT, T. M., DANAN, J. L. & VAIMAN, D. (2009). Re-evaluation of the role of STOX1 transcription factor in placental development and preeclampsia. *J Reprod Immunol,* **82**, 174-81.

RING, B. Z., CORDES, S. P., OVERBEEK, P. A. & BARSH, G. S. (2000). Regulation of mouse lens fiber cell development and differentiation by the Maf gene. *Development,* **127**, 307-17.

ROBERTS, C., PLATT, N., STREIT, A., SCHACHNER, M. & STERN, C. D. (1991). The L5 epitope: an early marker for neural induction in the chick embryo and its involvement in inductive interactions. *Development,* **112**, 959-70.

RODDA, S., SHARMA, S., SCHERER, M., CHAPMAN, G. & RATHJEN, P. (2001). CRTR-1, a developmentally regulated transcriptional repressor related to the CP2 family of transcription factors. *J Biol Chem,* **276**, 3324-32.

RODRIGUEZ-GALLARDO, L., CLIMENT, V., GARCIA-MARTINEZ, V., SCHOENWOLF, G. C. & ALVAREZ, I. S. (1997). Targeted over-expression of FGF in chick embryos induces formation of ectopic neural cells. *Int J Dev Biol,* **41**, 715-23.

RODRIGUEZ ESTEBAN, C., CAPDEVILA, J., ECONOMIDES, A. N., PASCUAL, J., ORTIZ, A. & IZPISUA BELMONTE, J. C. (1999). The novel Cer-like protein Caronte mediates the establishment of embryonic left-right asymmetry. *Nature,* **401**, 243-51.

ROOSE, J., KORVER, W., DE BOER, R., KUIPERS, J., HURENKAMP, J. & CLEVERS, H. (1999). The Sox-13 gene: structure, promoter characterization, and chromosomal localization. *Genomics,* **57**, 301-5.

ROSENQUIST, G. C. (1972). Endoderm movements in the chick embryo between the early short streak and head process stages. *J Exp Zool,* **180**, 95-103.

ROSENQUIST, G. C. (1981). Epiblast origin and early migration of neural crest cells in the chick embryo. *Developmental Biology,* **87**, 201-211.

RUBIN, S. M., GALL, A. L., ZHENG, N. & PAVLETICH, N. P. (2005). Structure of the Rb C-terminal domain bound to E2F1-DP1: a mechanism for phosphorylation-induced E2F release. *Cell,* **123**, 1093-106.

RUDNICK, D. (1935). Regional restriction of potencies in the chick during embryogenesis. *Journal of Experimental Zoology,* **71**, 83-99.

SAINT-JEANNET, J. P. & DAWID, I. B. (1994). A fate map for the 32-cell stage of Rana pipiens. *Dev Biol,* **166**, 755-62.

SAINT-JEANNET, J. P., HUANG, S. & DUPRAT, A. M. (1990). Modulation of neural commitment by changes in target cell contacts in Pleurodeles waltl. *Dev Biol,* **141**, 93-103.

SAKAMOTO, K., YAN, L., IMAI, H., TAKAGI, M., NABESHIMA, Y., TAKEDA, S. & KATSUBE, K. (1997). Identification of a chick homologue of Fringe and C-Fringe 1: involvement in the neurogenesis and the somitogenesis. *Biochem Biophys Res Commun,* **234**, 754-9.

SASAI, N., KUTEJOVA, E. & BRISCOE, J. (2014). Integration of signals along orthogonal axes of the vertebrate neural tube controls progenitor competence and increases cell diversity. *PLoS Biol,* **12**, e1001907.

SASAI, Y., LU, B., PICCOLO, S. & DE ROBERTIS, E. M. (1996). Endoderm induction by the organizer-secreted factors chordin and noggin in Xenopus animal caps. *Embo j,* **15**, 4547-55.

SASAI, Y., LU, B., STEINBEISSER, H. & DE ROBERTIS, E. M. (1995). Regulation of neural induction by the Chd and Bmp-4 antagonistic patterning signals in Xenopus. *Nature,* **376**, 333-6.

SASAI, Y., LU, B., STEINBEISSER, H., GEISSERT, D., GONT, L. K. & DE ROBERTIS, E. M. (1994). Xenopus chordin: a novel dorsalizing factor activated by organizer-specific homeobox genes. *Cell,* **79**, 779-90.

SATO, F., KAWAMOTO, T., FUJIMOTO, K., NOSHIRO, M., HONDA, K. K., HONMA, S., HONMA, K. & KATO, Y. (2004). Functional analysis of the basic helix-loop-helix transcription factor DEC1 in circadian regulation. Interaction with BMAL1. *Eur J Biochem,* **271**, 4409-19.

SATO, S. M. & SARGENT, T. D. (1989). Development of neural inducing capacity in dissociated Xenopus embryos. *Dev Biol,* **134**, 263-6.

SCHLICHTER, U., BURK, O., WORPENBERG, S. & KLEMPNAUER, K. H. (2001). The chicken Pdcd4 gene is regulated by v-Myb. *Oncogene,* **20**, 231-9.

SCHLOSSER, G. (2010). Making Senses: Development of Vertebrate Cranial Placodes. Academic Press.

SCHMIDT, J., FRANCOIS, V., BIER, E. & KIMELMAN, D. (1995). Drosophila short gastrulation induces an ectopic axis in Xenopus: evidence for conserved mechanisms of dorsal-ventral patterning. *Development,* **121**, 4319-28.

SCHMIDT, M., PATTERSON, M., FARRELL, E. & MUNSTERBERG, A. (2004). Dynamic expression of Lef/Tcf family members and beta-catenin during chick gastrulation, neurulation, and early limb development. *Dev Dyn,* **229**, 703-7.

SCHOENWOLF, G. C., GARCIA-MARTINEZ, V. & DIAS, M. S. (1992). Mesoderm movement and fate during avian gastrulation and neurulation. *Dev Dyn,* **193**, 235-48.

SCHOENWOLF, G. C. & SMITH, J. L. (1990). Mechanisms of neurulation: traditional viewpoint and recent advances. *Development,* **109**, 243-70.

SCHULTE-MERKER, S., LEE, K. J., MCMAHON, A. P. & HAMMERSCHMIDT, M. (1997). The zebrafish organizer requires chordino. *Nature,* **387**, 862-3.

SCHWEITZER, R., VOGAN, K. J. & TABIN, C. J. (2000). Similar expression and regulation of Gli2 and Gli3 in the chick limb bud. *Mechanisms of Development,* **98**, 171-174.

SEIFERT, R., JACOB, M. & JACOB, H. J. (1993). The avian prechordal head region: a morphological study. *J Anat,* **183 (Pt 1)**, 75-89.

SEINO, Y., MIKI, T., KIYONARI, H., ABE, T., FUJIMOTO, W., KIMURA, K., TAKEUCHI, A., TAKAHASHI, Y., OISO, Y., IWANAGA, T. & SEINO, S. (2008). Isx participates in the

maintenance of vitamin A metabolism by regulation of beta-carotene 15,15'-monooxygenase (Bcmo1) expression. *J Biol Chem,* **283**, 4905-11.

SELLECK, M. A. & STERN, C. D. (1991). Fate mapping and cell lineage analysis of Hensen's node in the chick embryo. *Development,* **112**, 615-26.

SEMINA, E. V., FERRELL, R. E., MINTZ-HITTNER, H. A., BITOUN, P., ALWARD, W. L., REITER, R. S., FUNKHAUSER, C., DAACK-HIRSCH, S. & MURRAY, J. C. (1998). A novel homeobox gene PITX3 is mutated in families with autosomal-dominant cataracts and ASMD. *Nat Genet,* **19**, 167-70.

SERVETNICK, M. & GRAINGER, R. M. (1991). Changes in neural and lens competence in Xenopus ectoderm: evidence for an autonomous developmental timer. *Development,* **112**, 177-88.

SHAMIM, H. & MASON, I. (1998). Expression of Gbx-2 during early development of the chick embryo. *Mech Dev,* **76**, 157-9.

SHARPE, C. & GOLDSTONE, K. (2000a). The control of Xenopus embryonic primary neurogenesis is mediated by retinoid signalling in the neurectoderm. *Mech Dev,* **91**, 69-80.

SHARPE, C. & GOLDSTONE, K. (2000b). Retinoid signalling acts during the gastrula stages to promote primary neurogenesis. *Int J Dev Biol,* **44**, 463-70.

SHARPE, C. R. (1991). Retinoic acid can mimic endogenous signals involved in transformation of the Xenopus nervous system. *Neuron,* **7**, 239-47.

SHARPE, C. R. & GURDON, J. B. (1990). The induction of anterior and posterior neural genes in Xenopus laevis. *Development,* **109**, 765-74.

SHENG, G., DOS REIS, M. & STERN, C. D. (2003). Churchill, a zinc finger transcriptional activator, regulates the transition between gastrulation and neurulation. *Cell,* **115**, 603-613.

SHENG, G. & STERN, C. D. (1999). Gata2 and Gata3: novel markers for early embryonic polarity and for non-neural ectoderm in the chick embryo. *Mech Dev,* **87**, 213-6.

SHIH, J. & FRASER, S. E. (1996). Characterizing the zebrafish organizer: microsurgical analysis at the early-shield stage. *Development,* **122**, 1313-22.

SHUKLA, A., MALIK, M., CATAISSON, C., HO, Y., FRIESEN, T., SUH, K. S. & YUSPA, S. H. (2009). TGF-beta signalling is regulated by Schnurri-2-dependent nuclear translocation of CLIC4 and consequent stabilization of phospho-Smad2 and 3. *Nat Cell Biol,* **11**, 777-84.

SIMEONE, A., AVANTAGGIATO, V., MORONI, M. C., MAVILIO, F., ARRA, C., COTELLI, F., NIGRO, V. & ACAMPORA, D. (1995). Retinoic acid induces stage-specific antero-posterior transformation of rostral central nervous system. *Mech Dev,* **51**, 83-98.

SIMPSON, E. H., JOHNSON, D. K., HUNSICKER, P., SUFFOLK, R., JORDAN, S. A. & JACKSON, I. J. (1999). The mouse Cer1 (Cerberus related or homologue) gene is not required for anterior pattern formation. *Dev Biol,* **213**, 202-6.

SIVAK, J. M., PETERSEN, L. F. & AMAYA, E. (2005). FGF signal interpretation is directed by Sprouty and Spred proteins during mesoderm formation. *Dev Cell,* **8**, 689-701.

SKROMNE, I. & STERN, C. D. (2001). Interactions between Wnt and Vg1 signalling pathways initiate primitive streak formation in the chick embryo. *Development,* **128**, 2915-2927.

SMITH, J. C., PRICE, B. M., GREEN, J. B., WEIGEL, D. & HERRMANN, B. G. (1991). Expression of a Xenopus homolog of Brachyury (T) is an immediate-early response to mesoderm induction. *Cell,* **67**, 79-87.

SMITH, S. M. & EICHELE, G. (1991). Temporal and regional differences in the expression pattern of distinct retinoic acid receptor-beta transcripts in the chick embryo. *Development,* **111**, 245-52.

SMITH, W. C. & HARLAND, R. M. (1992). Expression cloning of noggin, a new dorsalizing factor localized to the Spemann organizer in Xenopus embryos. *Cell,* **70**, 829-40.

SMITH, W. C., KNECHT, A. K., WU, M. & HARLAND, R. M. (1993). Secreted noggin protein mimics the Spemann organizer in dorsalizing Xenopus mesoderm. *Nature,* **361**, 547-9.

SMITH, W. C., MCKENDRY, R., RIBISI, S., JR. & HARLAND, R. M. (1995). A nodal-related gene defines a physical and functional domain within the Spemann organizer. *Cell,* **82**, 37-46.

SPEMANN, H. (1921). Die Erzeugung tierischer Chimären durch heteroplastische Transplantation zwischen Triton cristatus und taeniatus. *Roux Arch EntwMech Org,* **100**, 599-638.

SPEMANN, H. & MANGOLD, H. (1924). Über Induktion von Embryonalanlagen durch Implantations artfremder Organisatoren. *Roux's Arch. EntwMech. Org.,* **100**, 599-638.

SPRATT, N. T. (1952). Localization of the prospective neural plate in the early chick blastoderm. *Journal of Experimental Zoology,* **120**, 109-130.

SPRATT, N. T., JR. (1947). Regression and shortening of the primitive streak in the explanted chick blastoderm. *J Exp Zool,* **104**, 69-100.

SRIVASTAVA, D., CSERJESI, P. & OLSON, E. N. (1995). A subclass of bHLH proteins required for cardiac morphogenesis. *Science,* **270**, 1995-9.

STAVRIDIS, M. P., COLLINS, B. J. & STOREY, K. G. (2010). Retinoic acid orchestrates fibroblast growth factor signalling to drive embryonic stem cell differentiation. *Development,* **137**, 881-90.

STAVRIDIS, M. P., LUNN, J. S., COLLINS, B. J. & STOREY, K. G. (2007). A discrete period of FGF-induced Erk1/2 signalling is required for vertebrate neural specification. *Development,* **134**, 2889-94.

STEIN, S. & KESSEL, M. (1995). A homeobox gene involved in node, notochord and neural plate formation of chick embryos. *Mech Dev,* **49**, 37-48.

STEIN, S., NISS, K. & KESSEL, M. (1996). Differential activation of the clustered homeobox genes CNOT2 and CNOT1 during notogenesis in the chick. *Dev Biol,* **180**, 519-33.

STEIN, S., ROESER, T. & KESSEL, M. (1998). CMIX, a paired-type homeobox gene expressed before and during formation of the avian primitive streak. *Mech Dev,* **75**, 163-5.

STERN, C. D. (1990). The marginal zone and its contribution to the hypoblast and primitive streak of the chick embryo. *Development,* **109**, 667-82.

STERN, C. D. (1993). Transplantation in avian embryos. *In:* STERN, C. D. & HOLLAND, P. W. H. (eds.) *Essential Development Biology: A Practical Approach.* Oxford: IRL Press at Oxford University Press.

STERN, C. D. (1998). Detection of multiple gene products simultaneously by in situ hybridization and immunohistochemistry in whole mounts of avian embryos. *Current Topics in Developmental Biology,* **36**, 223-243.

STERN, C. D. (2004a). Gastrulation in the chick. *In:* STERN, C. D. (ed.) *Gastrulation: from cells to embryo.* Cold Spring Harbor Press.

STERN, C. D. (2004b). Neural Induction. *In:* STERN, C. D. (ed.) *Gastrulation: from cells to embryo.* Cold Spring Harbor Press.

STERN, C. D. (2005). Neural induction: old problem, new findings, yet more questions. *Development,* **132**.

STERN, C. D. (2008). Grafting Hensen's node. *Methods in Molecular Biology (Clifton, N.J.),* **461**, 265-276.

STERN, C. D. & CANNING, D. R. (1990). Origin of cells giving rise to mesoderm and endoderm in chick embryo. *Nature,* **343**, 273-5.

STERN, C. D. & IRELAND, G. W. (1981). An integrated experimental study of endoderm formation in avian embryos. *Anatomy and Embryology,* **163**, 245-263.

STEVANOVIC, M., LOVELL-BADGE, R., COLLIGNON, J. & GOODFELLOW, P. N. (1993). SOX3 is an X-linked gene related to SRY. *Hum Mol Genet,* **2**, 2013-8.

STOREY, K. G., CROSSLEY, J. M., DE ROBERTIS, E. M., NORRIS, W. E. & STERN, C. D. (1992). Neural induction and regionalisation in the chick embryo. *Development (Cambridge, England),* **114**, 729-741.

STOREY, K. G., GORIELY, A., SARGENT, C. M., BROWN, J. M., BURNS, H. D., ABUD, H. M. & HEATH, J. K. (1998). Early posterior neural tissue is induced by FGF in the chick embryo. *Development,* **125**, 473-484.

STOREY, K. G., SELLECK, M. A. & STERN, C. D. (1995). Neural induction and regionalisation by different subpopulations of cells in Hensen's node. *Development (Cambridge, England),* **121**, 417-428.

STOWER, M. J. (2012). *Early steps in neural induction.* Doctoral thesis, UCL (University College London).

STREIT, A. (2002). Extensive cell movements accompany formation of the otic placode. *Developmental Biology,* **249**, 237-254.

STREIT, A. (2004). Early development of the cranial sensory nervous system: from a common field to individual placodes. *Developmental Biology,* **276**, 1-15.

STREIT, A. (2008). The cranial sensory nervous system: specification of sensory progenitors and placodes. *StemBook.* Cambridge (MA): Harvard Stem Cell Institute.

STREIT, A., BERLINER, A. J., PAPANAYOTOU, C., SIRULNIK, A. & STERN, C. D. (2000). Initiation of neural induction by FGF signalling before gastrulation. *Nature,* **406**, 74-78.

STREIT, A., FAISSNER, A., GEHRIG, B. & SCHACHNER, M. (1990). Isolation and biochemical characterization of a neural proteoglycan expressing the L5 carbohydrate epitope. *J Neurochem,* **55**, 1494-506.

STREIT, A., LEE, K. J., WOO, I., ROBERTS, C., JESSELL, T. M. & STERN, C. D. (1998). Chordin regulates primitive streak development and the stability of induced neural cells, but is not sufficient for neural induction in the chick embryo. *Development,* **125**, 507-19.

STREIT, A., SOCKANATHAN, S., PÉREZ, L., REX, M., SCOTTING, P. J., SHARPE, P. T., LOVELL-BADGE, R. & STERN, C. D. (1997). Preventing the loss of competence for neural induction: HGF/SF, L5 and Sox-2. *Development (Cambridge, England),* **124**, 1191-1202.

STREIT, A. & STERN, C. D. (1999a). Establishment and maintenance of the border of the neural plate in the chick: involvement of FGF and BMP activity. *Mech Dev,* **82**, 51-66.

STREIT, A. & STERN, C. D. (1999e). Mesoderm patterning and somite formation during node regression: differential effects of chordin and noggin. *Mech Dev,* **85**, 85-96.

STREIT, A. & STERN, C. D. (2001). Combined whole-mount in situ hybridization and immunohistochemistry in avian embryos. *Methods (San Diego, Calif.),* **23**, 339-344.

STREIT, A. & STERN, C. D. (2008). Operations on primitive streak stage avian embryos. *Methods in Cell Biology,* **87**, 3-17.

STREIT, A., STERN, C. D., THÉRY, C., IRELAND, G. W., APARICIO, S., SHARPE, M. J. & GHERARDI, E. (1995). A role for HGF/SF in neural induction and its expression in Hensen's node during gastrulation. *Development (Cambridge, England),* **121**, 813-824.

STREIT, A., TAMBALO, M., CHEN, J., GROCOTT, T., ANWAR, M., SOSINSKY, A. & STERN, C. D. (2013). Experimental approaches for gene regulatory network construction: the chick as a model system. *Genesis,* **51**, 296-310.

STREIT, A., YUEN, C. T., LOVELESS, R. W., LAWSON, A. M., FINNE, J., SCHMITZ, B., FEIZI, T. & STERN, C. D. (1996). The Le(x) carbohydrate sequence is recognized by antibody to L5, a functional antigen in early neural development. *J Neurochem,* **66**, 834-44.

SUBRAMANIAM, N., TREUTER, E. & OKRET, S. (1999). Receptor interacting protein RIP140 inhibits both positive and negative gene regulation by glucocorticoids. *J Biol Chem,* **274**, 18121-7.

SUZUKI, A., CHANG, C., YINGLING, J. M., WANG, X. F. & HEMMATI-BRIVANLOU, A. (1997a). Smad5 induces ventral fates in Xenopus embryo. *Dev Biol,* **184**, 402-5.

SUZUKI, A., UENO, N. & HEMMATI-BRIVANLOU, A. (1997b). Xenopus msx1 mediates epidermal induction and neural inhibition by BMP4. *Development,* **124**, 3037-44.

SUZUKI, H. R., PADANILAM, B. J., VITALE, E., RAMIREZ, F. & SOLURSH, M. (1991). Repeating developmental expression of G-Hox 7, a novel homeobox-containing gene in the chicken. *Dev Biol,* **148**, 375-88.

SWEETMAN, D., SMITH, T. G., FARRELL, E. R. & MUNSTERBERG, A. (2005). Expression of csal1 in pre limb-bud chick embryos. *Int J Dev Biol,* **49**, 427-30.

SWINDELL, E. C., THALLER, C., SOCKANATHAN, S., PETKOVICH, M., JESSELL, T. M. & EICHELE, G. (1999). Complementary Domains of Retinoic Acid Production and Degradation in the Early Chick Embryo. *Developmental Biology,* **216**, 282-296.

TAKAHASHI, K. & YAMANAKA, S. (2006). Induction of pluripotent stem cells from mouse embryonic and adult fibroblast cultures by defined factors. *Cell,* **126**, 663-76.

TAKAHASHI, S., EBIHARA, A., KAJIHO, H., KONTANI, K., NISHINA, H. & KATADA, T. (2011). RASSF7 negatively regulates pro-apoptotic JNK signaling by inhibiting the activity of phosphorylated-MKK7. *Cell Death Differ,* **18**, 645-55.

TAKANAGA, H., TSUCHIDA-STRAETEN, N., NISHIDE, K., WATANABE, A., ABURATANI, H. & KONDO, T. (2009). Gli2 is a novel regulator of sox2 expression in telencephalic neuroepithelial cells. *Stem Cells,* **27**, 165-74.

TAKEMOTO, T., UCHIKAWA, M., KAMACHI, Y. & KONDOH, H. (2006). Convergence of Wnt and FGF signals in the genesis of posterior neural plate through activation of the Sox2 enhancer N-1. *Development,* **133**, 297-306.

TAKEMOTO, T., UCHIKAWA, M., YOSHIDA, M., BELL, D. M., LOVELL-BADGE, R., PAPAIOANNOU, V. E. & KONDOH, H. (2011). Tbx6-dependent Sox2 regulation determines neural or mesodermal fate in axial stem cells. *Nature,* **470**, 394-8.

TAKIZAWA, T., OCHIAI, W., NAKASHIMA, K. & TAGA, T. (2003). Enhanced gene activation by Notch and BMP signaling cross-talk. *Nucleic Acids Research,* **31**, 5723-5731.

THIERRY-MIEG, D. & THIERRY-MIEG, J. (2006). AceView: a comprehensive cDNA-supported gene and transcripts annotation. *Genome Biol,* **7 Suppl 1**, S12 1-14.

TING, S. B., WILANOWSKI, T., CERRUTI, L., ZHAO, L. L., CUNNINGHAM, J. M. & JANE, S. M. (2003). The identification and characterization of human Sister-of-Mammalian Grainyhead (SOM) expands the grainyhead-like family of developmental transcription factors. *Biochem J,* **370**, 953-62.

TONEGAWA, A. & TAKAHASHI, Y. (1998). Somitogenesis controlled by Noggin. *Dev Biol,* **202**, 172-82.

TOTZKE, G., ESSMANN, F., POHLMANN, S., LINDENBLATT, C., JANICKE, R. U. & SCHULZE-OSTHOFF, K. (2006). A novel member of the IkappaB family, human IkappaB-zeta, inhibits transactivation of p65 and its DNA binding. *J Biol Chem,* **281**, 12645-54.

TRAPNELL, C., PACHTER, L. & SALZBERG, S. L. (2009). TopHat: discovering splice junctions with RNA-Seq. *Bioinformatics,* **25**, 1105-11.

TRAPNELL, C., ROBERTS, A., GOFF, L., PERTEA, G., KIM, D., KELLEY, D. R., PIMENTEL, H., SALZBERG, S. L., RINN, J. L. & PACHTER, L. (2012). Differential gene and transcript expression analysis of RNA-seq experiments with TopHat and Cufflinks. *Nat Protoc,* **7**, 562-78.

TSAI, W. W., WANG, Z., YIU, T. T., AKDEMIR, K. C., XIA, W., WINTER, S., TSAI, C. Y., SHI, X., SCHWARZER, D., PLUNKETT, W., ARONOW, B., GOZANI, O., FISCHLE, W., HUNG, M. C., PATEL, D. J. & BARTON, M. C. (2010). TRIM24 links a non-canonical histone signature to breast cancer. *Nature,* **468**, 927-32.

TUMMALA, R., ROMANO, R. A., FUCHS, E. & SINHA, S. (2003). Molecular cloning and characterization of AP-2 epsilon, a fifth member of the AP-2 family. *Gene,* **321**, 93-102.

UCHIKAWA, M., ISHIDA, Y., TAKEMOTO, T., KAMACHI, Y. & KONDOH, H. (2003). Functional analysis of chicken Sox2 enhancers highlights an array of diverse regulatory elements that are conserved in mammals. *Developmental Cell,* **4**, 509-519.

UCHIKAWA, M., KAMACHI, Y. & KONDOH, H. (1999). Two distinct subgroups of Group B Sox genes for transcriptional activators and repressors: their expression during embryonic organogenesis of the chicken. *Mech Dev,* **84**, 103-20.

UCHIKAWA, M., TAKEMOTO, T., KAMACHI, Y. & KONDOH, H. (2004). Efficient identification of regulatory sequences in the chicken genome by a powerful combination of embryo electroporation and genome comparison. *Mech Dev,* **121**, 1145-58.

UEDA, M., WATANABE, K., SATO, K., AKIBA, Y. & TOYOMIZU, M. (2005). Possible role for avPGC-1alpha in the control of expression of fiber type, along with avUCP and avANT mRNAs in the skeletal muscles of cold-exposed chickens. *FEBS Lett,* **579**, 11-7.

UMBHAUER, M., PENZO-MENDEZ, A., CLAVILIER, L., BOUCAUT, J. & RIOU, J. (2000). Signaling specificities of fibroblast growth factor receptors in early Xenopus embryo. *J Cell Sci,* **113 (Pt 16)**, 2865-75.

UNTERGASSER, A., CUTCUTACHE, I., KORESSAAR, T., YE, J., FAIRCLOTH, B. C., REMM, M. & ROZEN, S. G. (2012). Primer3--new capabilities and interfaces. *Nucleic Acids Res,* **40**, e115.

UWANOGHO, D., REX, M., CARTWRIGHT, E. J., PEARL, G., HEALY, C., SCOTTING, P. J. & SHARPE, P. T. (1995). Embryonic expression of the chicken Sox2, Sox3 and Sox11 genes suggests an interactive role in neuronal development. *Mechanisms of development,* **49**, 23-36.

VAKAET, L. (1962). Some new data concerning the formation of the definitive endoblast in the chick embryo. *J Embryol Exp Morphol,* **10**, 38-57.

VAKAET, L. (1970). Cinephotomicrographic investigations of gastrulation in the chick blastoderm. *Arch Biol (Liege),* **81**, 387-426.

VALENZUELA, D. M., ECONOMIDES, A. N., ROJAS, E., LAMB, T. M., NUNEZ, L., JONES, P., LP, N. Y., ESPINOSA, R., 3RD, BRANNAN, C. I., GILBERT, D. J. & ET AL. (1995). Identification of mammalian noggin and its expression in the adult nervous system. *J Neurosci,* **15**, 6077-84.

VAN DER ZEE, M., STOCKHAMMER, O., VON LEVETZOW, C., NUNES DA FONSECA, R. & ROTH, S. (2006). Sog/Chordin is required for ventral-to-dorsal Dpp/BMP transport and head formation in a short germ insect. *Proc Natl Acad Sci U S A,* **103**, 16307-12.

VAN GRUNSVEN, L. A., TAELMAN, V., MICHIELS, C., VERSTAPPEN, G., SOUOPGUI, J., NICHANE, M., MOENS, E., OPDECAMP, K., VANHOMWEGEN, J., KRICHA, S., HUYLEBROECK, D. & BELLEFROID, E. J. (2007). XSip1 neuralizing activity involves the co-repressor CtBP and occurs through BMP dependent and independent mechanisms. *Dev Biol,* **306**, 34-49.

VARGESSON, N. & LAUFER, E. (2001). Smad7 Misexpression during Embryonic Angiogenesis Causes Vascular Dilation and Malformations Independently of Vascular Smooth Muscle Cell Function. *Developmental Biology,* **240**, 499-516.

VAUDIN, P., DELANOUE, R., DAVIDSON, I., SILBER, J. & ZIDER, A. (1999). TONDU (TDU), a novel human protein related to the product of vestigial (vg) gene of Drosophila melanogaster interacts with vertebrate TEF factors and substitutes for Vg function in wing formation. *Development,* **126**, 4807-16.

VEAL, E., EISENSTEIN, M., TSENG, Z. H. & GILL, G. (1998). A cellular repressor of E1A-stimulated genes that inhibits activation by E2F. *Mol Cell Biol,* **18**, 5032-41.

VELASCO, G., GRKOVIC, S. & ANSIEAU, S. (2006). New insights into BS69 functions. *J Biol Chem,* **281**, 16546-50.

VERSCHUEREN, K., REMACLE, J. E., COLLART, C., KRAFT, H., BAKER, B. S., TYLZANOWSKI, P., NELLES, L., WUYTENS, G., SU, M. T., BODMER, R., SMITH, J. C. & HUYLEBROECK, D. (1999). SIP1, a novel zinc finger/homeodomain repressor, interacts with Smad proteins and binds to 5'-CACCT sequences in candidate target genes. *J Biol Chem,* **274**, 20489-98.

VIRE, E., BRENNER, C., DEPLUS, R., BLANCHON, L., FRAGA, M., DIDELOT, C., MOREY, L., VAN EYNDE, A., BERNARD, D., VANDERWINDEN, J. M., BOLLEN, M., ESTELLER, M., DI CROCE, L., DE LAUNOIT, Y. & FUKS, F. (2006). The Polycomb group protein EZH2 directly controls DNA methylation. *Nature,* **439**, 871-4.

VOEGEL, J. J., HEINE, M. J., ZECHEL, C., CHAMBON, P. & GRONEMEYER, H. (1996). TIF2, a 160 kDa transcriptional mediator for the ligand-dependent activation function AF-2 of nuclear receptors. *Embo j,* **15**, 3667-75.

VOGELMANN, J., VALERI, A., GUILLOU, E., CUVIER, O. & NOLLMANN, M. (2011). Roles of chromatin insulator proteins in higher-order chromatin organization and transcription regulation. *Nucleus,* **2**, 358-69.

VOICULESCU, O., BERTOCCHINI, F., WOLPERT, L., KELLER, R. E. & STERN, C. D. (2007). The amniote primitive streak is defined by epithelial cell intercalation before gastrulation. *Nature,* **449**, 1049-52.

VOICULESCU, O., BODENSTEIN, L., LAU, I. J. & STERN, C. D. (2014). Local cell interactions and self-amplifying individual cell ingression drive amniote gastrulation. *Elife,* **3**, e01817.

VOICULESCU, O., PAPANAYOTOU, C. & STERN, C. D. (2008). Spatially and temporally controlled electroporation of early chick embryos. *Nature Protocols,* **3**, 419-426.

WADDINGTON, C. H. (1932). Experiments on the development of chick and duck embryos, cultivated in vitro. *Philosophical Transactions of the Royal Society of London Series B-Containing Papers of a Biological Character,* **221**, 179-230.

WADDINGTON, C. H. (1933). Induction by the primitive streak and its derivatives in the chick. *Journal of Experimental Biology,* **10**, 38-U4.

WADDINGTON, C. H. (1934). Experiments on embryonic induction. *J. exp. Biol.,* **11**, 211-227.

WADDINGTON, C. H. (1936). Organizers in Mammalian Development. *Nature,* **138**, 125.

WADDINGTON, C. H. (1937). Experiments on determination in the rabbit embryo. *Arch Biol,* **48**, 273-290.

WADDINGTON, C. H. & NEEDHAM, J. (1936). Evocation and individuation and competence in amphibian organizer action. *Proc. Kon. Akad. Wetensch. Amsterdam,* **39**, 887-891.

WADDINGTON, C. H. & SCHMIDT, G. A. (1933). Induction by heteroplastic grafts of the primitive streak in birds. *Zeitschr Wiss Biol Abt D Roux Arch Ent Vncklungsmech Organ,* **128**, 522-563.

WAGNER, M., HAN, B. & JESSELL, T. M. (1992). Regional differences in retinoid release from embryonic neural tissue detected by an in vitro reporter assay. *Development,* **116**, 55-66.

WAHL, M. B., DENG, C., LEWANDOSKI, M. & POURQUIÉ, O. (2007). FGF signaling acts upstream of the NOTCH and WNT signaling pathways to control segmentation clock oscillations in mouse somitogenesis. *Development,* **134**, 4033-4041.

WALHOUT, A. J., TEMPLE, G. F., BRASCH, M. A., HARTLEY, J. L., LORSON, M. A., VAN DEN HEUVEL, S. & VIDAL, M. (2000). GATEWAY recombinational cloning: application to the cloning of large numbers of open reading frames or ORFeomes. *Methods Enzymol,* **328**, 575-92.

WANG, X. J. & ZHANG, D. D. (2009). Ectodermal-neural cortex 1 down-regulates Nrf2 at the translational level. *PLoS One,* **4**, e5492.

WANG, Y., LIN, L., LAI, H., PARADA, L. F. & LEI, L. (2013). Transcription factor Sox11 is essential for both embryonic and adult neurogenesis. *Dev Dyn,* **242**, 638-53.

WANG, Z., GERSTEIN, M. & SNYDER, M. (2009). RNA-Seq: a revolutionary tool for transcriptomics. *Nat Rev Genet,* **10**, 57-63.

WARNATZ, H. J., SCHMIDT, D., MANKE, T., PICCINI, I., SULTAN, M., BORODINA, T., BALZEREIT, D., WRUCK, W., SOLDATOV, A., VINGRON, M., LEHRACH, H. & YASPO, M. L. (2011). The BTB and CNC homology 1 (BACH1) target genes are involved in the oxidative stress response and in control of the cell cycle. *J Biol Chem,* **286**, 23521-32.

WARNER, S. J., HUTSON, M. R., OH, S. H., GERLACH-BANK, L. M., LOMAX, M. I. & BARALD, K. F. (2003). Expression of ZIC genes in the development of the chick inner ear and nervous system. *Dev Dyn,* **226**, 702-12.

WEBB, S. E. & MILLER, A. L. (2007). Ca2+ signalling and early embryonic patterning during zebrafish development. *Clin Exp Pharmacol Physiol,* **34**, 897-904.

WEI, Y. & MIKAWA, T. (2000). Formation of the avian primitive streak from spatially restricted blastoderm: evidence for polarized cell division in the elongating streak. *Development,* **127**, 87-96.

WEISKIRCHEN, R., PINO, J. D., MACALMA, T., BISTER, K. & BECKERLE, M. C. (1995). The cysteine-rich protein family of highly related LIM domain proteins. *J Biol Chem,* **270**, 28946-54.

WHARTON, K. A., RAY, R. P. & GELBART, W. M. (1993). An activity gradient of decapentaplegic is necessary for the specification of dorsal pattern elements in the Drosophila embryo. *Development,* **117**, 807-22.

WHITE, J. A., GUO, Y.-D., BAETZ, K., BECKETT-JONES, B., BONASORO, J., HSU, K. E., DILWORTH, F. J., JONES, G. & PETKOVICH, M. (1996). Identification of the Retinoic Acid-inducible All-trans-retinoic Acid 4-Hydroxylase. *Journal of Biological Chemistry,* **271**, 29922-29927.

WILANOWSKI, T., TUCKFIELD, A., CERRUTI, L., O'CONNELL, S., SAINT, R., PAREKH, V., TAO, J., CUNNINGHAM, J. M. & JANE, S. M. (2002). A highly conserved novel family of mammalian developmental transcription factors related to Drosophila grainyhead. *Mech Dev,* **114**, 37-50.

WILSON, P. A. & HEMMATI-BRIVANLOU, A. (1995). Induction of epidermis and inhibition of neural fate by Bmp-4. *Nature,* **376**, 331-333.

WILSON, P. A., LAGNA, G., SUZUKI, A. & HEMMATI-BRIVANLOU, A. (1997). Concentration-dependent patterning of the Xenopus ectoderm by BMP4 and its signal transducer Smad1. *Development,* **124**, 3177-84.

WILSON, S. I. & EDLUND, T. (2001). Neural induction: toward a unifying mechanism. *Nature Neuroscience,* **4**, 1161-1168.

WILSON, S. I., GRAZIANO, E., HARLAND, R., JESSELL, T. M. & EDLUND, T. (2000). An early requirement for FGF signalling in the acquisition of neural cell fate in the chick embryo. *Curr Biol,* **10**, 421-9.

WILSON, S. I., RYDSTROM, A., TRIMBORN, T., WILLERT, K., NUSSE, R., JESSELL, T. M. & EDLUND, T. (2001). The status of Wnt signalling regulates neural and epidermal fates in the chick embryo. *Nature,* **411**, 325-30.

WINNIER, G., BLESSING, M., LABOSKY, P. A. & HOGAN, B. L. (1995). Bone morphogenetic protein-4 is required for mesoderm formation and patterning in the mouse. *Genes Dev,* **9**, 2105-16.

WU, L., SUN, T., KOBAYASHI, K., GAO, P. & GRIFFIN, J. D. (2002). Identification of a family of mastermind-like transcriptional coactivators for mammalian notch receptors. *Mol Cell Biol,* **22**, 7688-700.

YANG, C., YANG, Y., BRENNAN, L., BOUHASSIRA, E. E., KANTOROW, M. & CVEKL, A. (2010). Efficient generation of lens progenitor cells and lentoid bodies from human embryonic stem cells in chemically defined conditions. *Faseb j,* **24**, 3274-83.

YANG, S. H., KALKAN, T., MORISSROE, C., MARKS, H., STUNNENBERG, H., SMITH, A. & SHARROCKS, A. D. (2014). Otx2 and Oct4 drive early enhancer activation during embryonic stem cell transition from naive pluripotency. *Cell Rep,* **7**, 1968-81.

YAO, L., ZHANG, D. & BERND, P. (1994). The onset of neurotrophin and trk mRNA expression in early embryonic tissues of the quail. *Developmental Biology,* **165**, 727-730.

YE, J., COULOURIS, G., ZARETSKAYA, I., CUTCUTACHE, I., ROZEN, S. & MADDEN, T. L. (2012). Primer-BLAST: a tool to design target-specific primers for polymerase chain reaction. *BMC Bioinformatics,* **13**, 134.

YING, Q. L., WRAY, J., NICHOLS, J., BATLLE-MORERA, L., DOBLE, B., WOODGETT, J., COHEN, P. & SMITH, A. (2008). The ground state of embryonic stem cell self-renewal. *Nature,* **453**, 519-23.

YOH, S. M., LUCAS, J. S. & JONES, K. A. (2008). The Iws1:Spt6:CTD complex controls cotranscriptional mRNA biosynthesis and HYPB/Setd2-mediated histone H3K36 methylation. *Genes Dev,* **22**, 3422-34.

YOKOUCHI, Y., VOGAN, K. J., PEARSE, R. V., 2ND & TABIN, C. J. (1999). Antagonistic signaling by Caronte, a novel Cerberus-related gene, establishes left-right asymmetric gene expression. *Cell,* **98**, 573-83.

YOKOYAMA, S., HASHIMOTO, M., SHIMIZU, H., UENO-KUDOH, H., UCHIBE, K., KIMURA, I. & ASAHARA, H. (2008). Dynamic gene expression of Lin-28 during embryonic development in mouse and chicken. *Gene Expr Patterns,* **8**, 155-60.

YOO, Y. G., KONG, G. & LEE, M. O. (2006). Metastasis-associated protein 1 enhances stability of hypoxia-inducible factor-1alpha protein by recruiting histone deacetylase 1. *Embo j,* **25**, 1231-41.

YOSHIDA, C., YOSHIDA, F., SEARS, D. E., HART, S. M., IKEBE, D., MUTO, A., BASU, S., IGARASHI, K. & MELO, J. V. (2007). Bcr-Abl signaling through the PI-3/S6 kinase pathway inhibits nuclear translocation of the transcription factor Bach2, which represses the antiapoptotic factor heme oxygenase-1. *Blood,* **109**, 1211-9.

YU, J., VODYANIK, M. A., SMUGA-OTTO, K., ANTOSIEWICZ-BOURGET, J., FRANE, J. L., TIAN, S., NIE, J., JONSDOTTIR, G. A., RUOTTI, V., STEWART, R., SLUKVIN, II & THOMSON, J. A. (2007). Induced pluripotent stem cell lines derived from human somatic cells. *Science,* **318**, 1917-20.

ZHANG, D., YAO, L. & BERND, P. (1996). Expression of neurotrophin trk and p75 receptors in quail embryos undergoing gastrulation and neurulation. *Developmental Dynamics,* **205**, 150-161.

ZHANG, D., YOON, H. G. & WONG, J. (2005). JMJD2A is a novel N-CoR-interacting protein and is involved in repression of the human transcription factor achaete scute-like homologue 2 (ASCL2/Hash2). *Mol Cell Biol,* **25**, 6404-14.

ZHANG, H. & BRADLEY, A. (1996). Mice deficient for BMP2 are nonviable and have defects in amnion/chorion and cardiac development. *Development,* **122**, 2977-86.

ZHANG, S. J., BUCHTHAL, B., LAU, D., HAYER, S., DICK, O., SCHWANINGER, M., VELTKAMP, R., ZOU, M., WEISS, U. & BADING, H. (2011). A signaling cascade of nuclear calcium-CREB-ATF3 activated by synaptic NMDA receptors defines a gene repression module that protects against extrasynaptic NMDA receptor-induced neuronal cell death and ischemic brain damage. *J Neurosci,* **31**, 4978-90.

ZHANG, T., ZHU, Q., XIE, Z., CHEN, Y., QIAO, Y., LI, L. & JING, N. (2013). The zinc finger transcription factor Ovol2 acts downstream of the bone morphogenetic protein pathway to regulate the cell fate decision between neuroectoderm and mesendoderm. *J Biol Chem,* **288**, 6166-77.

ZHANG, W. & BIEKER, J. J. (1998). Acetylation and modulation of erythroid Kruppel-like factor (EKLF) activity by interaction with histone acetyltransferases. *Proc Natl Acad Sci U S A,* **95**, 9855-60.

ZHANG, X., GAN, L., PAN, H., GUO, S., HE, X., OLSON, S. T., MESECAR, A., ADAM, S. & UNTERMAN, T. G. (2002). Phosphorylation of serine 256 suppresses transactivation by FKHR (FOXO1) by multiple mechanisms. Direct and indirect effects on nuclear/cytoplasmic shuttling and DNA binding. *J Biol Chem,* **277**, 45276-84.

ZHAO, X., SIRBU, I. O., MIC, F. A., MOLOTKOVA, N., MOLOTKOV, A., KUMAR, S. & DUESTER, G. (2009). Retinoic acid promotes limb induction through effects on body axis extension but is unnecessary for limb patterning. *Curr Biol,* **19**, 1050-7.

ZHAO, Y., HERMESZ, E., YAROLIN, M. C. & WESTPHAL, H. (2000). Genomic structure, chromosomal localization and expression of the human LIM-homeobox gene LHX5. *Gene,* **260**, 95-101.

ZHU, L., MARVIN, M. J., GARDINER, A., LASSAR, A. B., MERCOLA, M., STERN, C. D. & LEVIN, M. (1999). Cerberus regulates left-right asymmetry of the embryonic head and heart. *Curr Biol,* **9**, 931-8.

ZIMMERMAN, L. B., DE JESÚS-ESCOBAR, J. M. & HARLAND, R. M. (1996). The Spemann organizer signal noggin binds and inactivates bone morphogenetic protein 4. *Cell,* **86**, 599-606.

ZIMMERMANN, K., AHRENS, K., MATTHES, S., BUERSTEDDE, J. M., STRATLING, W. H. & PHI-VAN, L. (2002). Targeted disruption of the GAS41 gene encoding a putative

transcription factor indicates that GAS41 is essential for cell viability. *J Biol Chem,* **277**, 18626-31.

ZUSMAN, S. B., SWEETON, D. & WIESCHAUS, E. F. (1988). short gastrulation, a mutation causing delays in stage-specific cell shape changes during gastrulation in Drosophila melanogaster. *Dev Biol,* **129**, 417-27.

ZUZARTE-LUIS, V., MONTERO, J. A., RODRIGUEZ-LEON, J., MERINO, R., RODRIGUEZ-REY, J. C. & HURLE, J. M. (2004). A new role for BMP5 during limb development acting through the synergic activation of Smad and MAPK pathways. *Dev Biol,* **272**, 39-52.